THE UNIVERSITY OF
SYDNEY

Cortical hyperexcitability in Amyotrophic Lateral Sclerosis: Diagnostic and pathophysiological biomarker

NIMESHAN GEEVASINGA

A THESIS SUBMITTED IN FULFILMENT OF THE REQUIREMENTS FOR

THE DEGREE OF DOCTOR OF PHILOSOPHY

FACULTY OF MEDICINE, WESTERN CLINICAL SCHOOL,

WESTMEAD HOSPITAL

UNIVERSITY OF SYDNEY

DECEMBER 2015

ACKNOWLEDGEMENTS

There are a number of people whom I am indebted too for their help with the research work that I have been undertaking for the last three years, culminating in this thesis. Foremost, I am grateful to my supervisor and mentor Prof Steve Vucic, who has supported and shone the light, to guide me down this path. His wisdom, countless hours of dedication and motivation in these projects, have enabled me to fulfill my research ambitions. He has always been accessible, and forever accommodating throughout my PhD candidature. To my co-supervisors Prof Matthew Kiernan and Prof Garth Nicholson, I am forever grateful for the wise words and the guidance in these last three years. Each, of whom are immense figures in the field of Neurology, having such role models and supervisors, has motivated me to fulfill my lifetime ambition of completing a PhD. To the staff at Westmead Hospital I am very grateful for the assistance and support. The contributions to the research work by my colleague, Dr Parvathi Menon will also be acknowledged. She selflessly spent hours guiding me through my initial few months of the PhD and then continued to be a source of support. For the patients and the normal volunteers who have invested their time with this research work, I am very thankful. Nothing can measure the time that they have put in, over the last three years, to enable me to undertake this work. I thank the funding bodies who have supported my research, the Motor Neuron Disease Research Institute of Australia and National Health and Medical Research Council, whom jointly co-funded the postgraduate scholarship as well as the Pfizer Grant. Finally I must thank those that are the reason, as to why I wake up every morning with a smile, my lovely girls Imaya and Oviya. Whose presence in my life, has given me the strength to pursue my research ambitions, and whose presence alone, provides a meaning in life that nothing can compare to. To my wife and my parents, I am forever grateful for the support and time that they have invested, not only in my research ambitions, but associated clinical endeavors.

Let us keep looking in spite of everything. Let us keep searching. It is indeed the best method of finding, and perhaps thanks to our efforts, the verdict we will give such a patient tomorrow will not be the same we must give this patient today - Charcot.

ABSTRACT

Amyotrophic lateral sclerosis (ALS) is a progressive and degenerative disease of the motor system clinically defined by the presence of upper and lower motor neuron (UMN/LMN) signs. With the currently utilised diagnostic criteria the revised El Escorial and the Awaji criteria, there is a diagnostic delay of up to 14 months, whereby patients may miss the optimum 'therapeutic window'. To improve upon the diagnostic criteria in ALS we initially undertook a meta-analysis to evaluate the currently utilized criteria, the revised El Escorial (rEEC) and the Awaji criteria. The included primary studies in the meta-analysis were single centre by design, the majority being retrospective in nature and lacking in specificity data. Having identified a modest improvement in the Awaji criteria we designed the first multicenter prospective study looking at both these diagnostic criteria. Whilst the Awaji criteria yet again proved to me more sensitive than the rEEC criteria, the lack of an objective UMN biomarker resulted in a delay in some patients being diagnosed with ALS. This was explored with the addition of a novel threshold tracking transcranial magnetic stimulation (TMS) technique to measure cortical hyperexcitability, as a biomarker of UMN dysfunction, in a cross-sectional study. Adding cortical hyperexcitability as a biomarker of UMN dysfunction, resulted in a greater proportion of ALS patients reaching a definitive diagnosis. Subsequent to this finding, we then designed a multicenter prospective study, undertaken according to the STARD criteria (Standards for Reporting Diagnostic accuracy studies). These studies highlighted that threshold tracking TMS objectively identified abnormalities in ALS at an early stage of the disease process. Given that cortical hyperexcitability appeared to be an early and specific biomarker of UMN dysfunction, we then utilized the threshold tracking TMS technique to gather insights into the most common cause of familial ALS, the c9orf72 repeat expansion. Cortical abnormalities were evident in the familial ALS cohort

and were identical to the sporadic ALS cohort. But interestingly, asymptomatic carriers of the c9orf72 gene expansion did not have any signs of cortical dysfunction, thereby suggesting that patients may not be born with an abnormal motor cortex dysfunction, but rather may be predisposed to developing ALS secondary to the underlying genetic abnormality, potentially triggered by environmental factors. We also explored peripheral changes in c9orf72 familial ALS, highlighting that peripheral dysfunction, as measured by axonal excitability was similar to the sporadic ALS cohort. Having established that cortical hyperexcitability was a robust biomarker of UMN dysfunction, we then studied atypical ALS phenotypes such as the clinically UMN predominant variant, primary lateral sclerosis (PLS), reliably differentiating PLS from mimic disorders such as hereditary spastic paraparesis (HSP). In the lower motor neuron variant of ALS, termed flail leg syndrome, cortical hyperexcitability was only evident in patients with upper motor neuron signs. Taken together, these findings suggest that cortical hyperexcitability is a potentially robust diagnostic and pathophysiological biomarker in sporadic, familial and some atypical ALS variants.

CONTENTS

PUBLICATIONS

Chapter 1

Geevasinga, N., Loy, C. T., Menon, P., Carvalho, M., Swash, M., Schrooten, M., Van Damme P., Gawel, M., Sonoo, M., Noto, Y., Kuwabara, S., Kiernan, M., Macaskill, P & Vucic, S. **Awaji criteria improves diagnostic sensitivity in amyotrophic lateral sclerosis.** (submitted to Clinical Neurophysiology).

I was involved in the study design, literature review, data analysis and manuscript preparation/review

Chapter 2

Geevasinga, N., Menon, P., Scherman, D. B., Simon, N., Yiannikas, C., Henderson, R., Kiernan, M & Vucic S. **Utility of diagnostic criteria for amyotrophic lateral sclerosis: A multicenter prospective study.** (submitted to Neurology).

I was involved in the study design, data analysis and manuscript preparation/review

Chapter 3

Geevasinga, N., Menon, P., Yiannikas, C., Kiernan, M. C & Vucic S. **Diagnostic utility of cortical excitability studies in amyotrophic lateral sclerosis.** Eur J Neurol. 2014; 21(12):1451-7.

I was involved in the study design, data analysis, manuscript preparation/review and responding to reviewer's comments.

Chapter 4

Menon, P., *Geevasinga, N.*, Yiannikas, C., Howells, J., Kiernan, M. C & Vucic S. **Sensitivity and specificity of threshold tracking transcranial magnetic stimulation for diagnosis of amyotrophic lateral sclerosis: a prospective study.** Lancet Neurol. 2015; 14(5):478-84

I was involved in patient recruitment, studying patients, data analysis, manuscript preparation/review and responding to reviewer's comments.

Chapter 5

Geevasinga, N., Menon, P., Nicholson, G.A., Ng, K., Howells, J., Kril, J. J., Yiannikas, C., Kiernan, M. C & Vucic S. **Cortical function in asymptomatic carriers and patients with c9orf72 ALS.** JAMA Neurol. 2015; 72(11):1268-74.

I was involved in the study design, data analysis, manuscript preparation/review and responding to reviewer's comments.

Chapter 6

Geevasinga, N., Menon, P., Howells, J., Nicholson, G. A., Kiernan, M. C & Vucic, S. **Axonal ion channel dysfunction in c9orf72 familial amyotrophic lateral sclerosis.** JAMA Neurol. 2015; 72(1):49-57.

I was involved in the study design, data analysis, manuscript preparation/review and responding to reviewer's comments.

Chapter 7

Geevasinga, N., Menon, P., Sue, C. M., Kumar, K. R., Ng, K., Yiannikas, C., Kiernan, M. C & Vucic, S. **Cortical excitability changes distinguish the motor neuron disease phenotypes from hereditary spastic paraplegia.** Eur J Neurol. 2015; 22(5):826-31.
I was involved in the study design, data analysis, manuscript preparation/review and responding to reviewer's comments.

Chapter 8

Menon, P., *Geevasinga, N*., Yiannikas, C., Kiernan, M. C., Vucic, S. **Cortical contributions to the flail leg syndrome: Pathophysiological insights.** Amyotrophic lateral sclerosis and Frontotemporal Degeneration (accepted for publication, in press)
I was involved in patient recruitment, studying patients, data analysis/interpretation and manuscript review.

ABSTRACT PRESENTATIONS

Chapter 1

- Oral presentation at the ***American Academy of Neurology***, Washington DC, USA, 2015

Chapter 2

- Oral presentation at the ***New Zealand Association of Neurologists annual meeting***, Auckland, New Zealand, 2015.

Chapter 3

- Oral presentation at the ***International ALS symposium***, Brussels, Belgium, 2014.
- Oral presentation at the ***International Neurophysiology conference***, Berlin, Germany, 2014

Chapter 4

- Oral presentation at the ***New Zealand Association of Neurologists annual meeting***, Auckland, New Zealand, 2015.

Chapter 5

- Oral presentation at the ***International ALS symposium***, Brussels, Belgium, 2014.
- Oral presentation at the ***Australia and New Zealand Association of Neurologists annual meeting***, Adelaide, Australia, 2014.

Chapter 7

- Poster presentation at the ***Australia and New Zealand Association of Neurologists annual meeting***, Adelaide, Australia, 2014.

AWARDS

1. The 'ANZAN Jim Lance young investigator award' at Australian and New Zealand Association of Neurologists Annual Meeting, Auckland, 2015, for the presentation titled **'Novel diagnostic algorithm for ALS'** (Chapters 1, 2 and 4).

2. Shortlisted for the best 'Clinical Poster' at the International MND Symposium, Orlando, USA, 2015, **'Novel diagnostic algorithm for ALS'** (Chapter 1, 2 and 4)

3. MND Victoria 'Nina Buscombe Travel Award 2014' for presentation at the International MND Symposium, Belgium 2014, for presentation **'Cortical Excitability In Familial C9orf72 ALS Patients'** (Chapter 5) and **'Diagnostic Utility Of Threshold Tracking Transcranial Magnetic Stimulation In ALS – STARD Study'** (Chapter 4).

4. Winner of the monthly 'Westmead Postgraduate seminar' at Westmead Hospital, Westmead. Titled **'Diagnostic utility of cortical excitability in ALS/MND' (**Chapter 3).

5. Selected and shortlisted for NSW 'RACP Trainee Research Presentations', 2013. Titled '**Diagnostic utility of threshold tracking TMS in ALS: Comparative study to Awaji criteria**' (Chapter 3).

LITERATURE REVIEW

Introduction

Amyotrophic lateral sclerosis (ALS), commonly referred to as Motor Neuron Disease (MND) is a rapidly progressive and invariably fatal neurodegenerative disorder of motor neurons in the spinal cord, brainstem, and motor cortex. To this day, there exists no cure for this progressive disorder. The condition was first described in the mid-19th century by the French neurologist Jean Martin Charcot (1). The incidence of ALS has been estimated at two per hundred thousand (2), with a median survival of 3-5 years (3, 4). In Australia an estimated two people die from ALS every day (5). The diagnosis of amyotrophic lateral sclerosis (ALS) relies on the identification of a combination of upper (UMN) and lower motor neuron (LMN) signs. The Awaji criteria are the currently utilized diagnostic criteria to aid in the diagnosis of ALS (6). ALS results in the rapid development of physical disability, which can subsequently impact on the quality of life, placing tremendous strain on carers, families and the health care system.

Demographics

The mean age of disease onset is estimated at 65 years in population-based studies (7). ALS can affect people of all ages but the age-adjusted incidence rate varies greatly in different age groups. The incidence is very low in the first four decades (1.5/100,000/year) and then increases abruptly around age 40, reaching its peak between ages 60 and 79 (10–15/100,000/year), thereafter decreasing (7). The presence of a peak in the age-specific incidence curve suggests that the disease may result from a time dependent exposure to genetic and environmental risk factors.

Clinical features and neurophysiological features

The majority of ALS patients (65-75%) present with asymmetrical weakness and wasting of the limb muscles, typically spreading along the neuraxis to affect contiguous motor neurons (8-10). Preferential wasting and weakness of thenar muscles, termed the 'split-hand phenomenon' is a specific clinical feature of ALS (11-13). Furthermore there appears to be selective involvement of the abductor pollicis brevis, sparing the flexor pollicis longus, although both muscles have an identical nerve (median) and myotomal innervation, termed the 'split-hand plus sign' (14).

Bulbar-onset disease can occur in 20% of ALS cases and presents with progressive dysphagia and dysarthria (15). Late in the course of the disease, respiratory symptoms develop in the vast majority of ALS patients, ultimately being the most common cause of their demise (10, 16, 17), but only rarely is respiratory dysfunction the presenting feature (18, 19). In addition to motor symptoms, mild frontal lobe-type cognitive abnormalities are evident in 30-50% (20-23) and frank dementia in 3.5% of ALS patients (20). Extraocular and sphincter muscles, innervated by motor neurons not receiving direct projections from the motor cortex, are characteristically spared in ALS (24, 25).

Neurophysiological studies, in the form of routine nerve conduction studies (NCS), disclose a marked reduction of compound muscle action potential (CMAP) amplitudes, although this is typically evident in advanced stages of ALS and reflects axonal loss (26). In addition, a mild reduction in motor conduction velocity (not less than 70% of the lower limit of normal), along with a mild prolongation of distal motor and F-wave latencies (<30% of upper limit of normal) may also be evident in ALS and is secondary to degeneration of large diameter, fast-

conducting fibres (26-28). Sensory NCSs are typically normal in ALS and when evident may suggest an alternative diagnosis (28, 29).

Needle electromyography (EMG) forms an essential part of the diagnostic algorithm and is essential in identifying LMN loss (28). The most frequently recognized abnormalities on EMG are fasciculations and spontaneous "denervation" discharges (fibrillation potentials and positive sharp waves (PSWs), indicative of ongoing motor neuron loss [Figure 1A, B] (28, 29). However, fibrillation potentials and PSWs are not universally identified in all weak muscles and may not develop until one third of the motor neurons have deteriorated (28). Collateral sprouting of surviving motor axons results in large-amplitude, long-duration motor unit potentials (MUPs), also referred to as chronic neurogenic changes [Figure 1C] (28, 29).

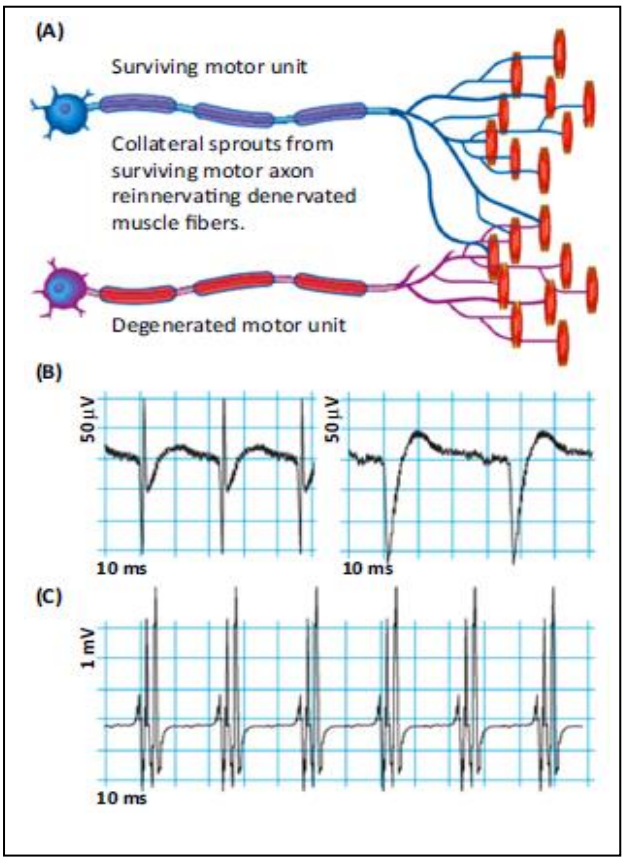

Figure 1. Ongoing degeneration of motor neurons accompanied by collateral sprouting of surviving motor neurons results in the classical electromyography findings including (B) ongoing denervation (fibrillation potentials and positive sharp waves) accompanied by (C) chronic neurogenic changes (large amplitude, long-duration, polyphasic motor unit action potentials with reduced voluntary recruitment). From Vucic S, Rothstein, J. D. Kiernan, M. C. *Advances in treating amyotrophic lateral sclerosis: insights from pathophysiological studies.* Trends Neurosci. 2014.

Surviving motor units may fire spontaneously, as fasciculations. Fasciculations are a classical feature of ALS and usually become widespread as the disease progresses, however it is rarely the initial presenting symptom (15). Fasciculations are often seen commonly in muscles with normal strength, and their incorporation into the Awaji criteria has improved the diagnostic sensitivity (6, 30). Bilateral tongue fasciculations in the presence of progressive weakness are pathognomonic for ALS and are highly specific (31). Insights from axonal excitability studies have revealed changes in axonal membrane conductances, in particular increased persistent sodium (Na^+) and reduced potassium (K^+) conductances, which may then contribute to the generation of fasciculations (32-35). Fasciculations are generated at the nerve terminals, though some arise at more proximal regions including at the level of the motor neuron (36, 37). As ALS progresses, fasciculations develop a complex morphology with increased duration, amplitude and degree of polyphasia (28).

One of the challenges in diagnosing ALS is objectively identifying upper motor neuron dysfunction (38). Clinical evidence of UMN dysfunction may be elusive in ALS and obscured by motor neuron loss (38). Transcranial magnetic stimulation (TMS) techniques may provide a useful clinical tool in identifying UMN dysfunction in a clinical setting (39). The TMS parameters routinely measured in ALS patients include; motor threshold, Motor evoked potential (MEP) amplitude, central motor conduction time (CMCT) and cortical silent period (CSP) duration (*see* TMS section). Abnormalities of the TMS parameters may aid in the identification of UMN dysfunction, thereby permitting an earlier diagnosis of ALS (29, 40-46)

Diagnosis of ALS

The diagnosis of ALS relies on the identification of a combination of upper and lower motor neuron signs in multiple body regions, along with evidence of ongoing disease progression. Importantly, ALS mimic disorders may need to be excluded prior to establishing a definitive diagnosis of ALS (47, 48). Routine nerve conduction studies are utilised in a clinical setting to exclude mimic ALS disorders, such as autoimmune demyelinating neuropathies, diseases of the neuromuscular junction or muscle disorders (49).

Diagnostic criteria: In order to facilitate the diagnosis of ALS, specific diagnostic criteria were developed. The first of the diagnostic criteria was the El Escorial criteria (EEC), proposed at a World Federation of Neurology meeting in El Escorial, Spain [Table 1] (50). The EEC had two stipulations to aid in the diagnosis of ALS; (i) That all other *mimic disorders* needed to be excluded after relevant clinical, laboratory, neuroimaging and neurophysiological evaluation and (ii) Presence of both, *LMN and UMN signs* with a progressive spread of symptoms/signs over time, thereby confirming that the disease universally progresses in all individuals. The EEC divided the body into four regions; 'brainstem', 'cervical', 'thoracic' and 'lumbosacral'. For a given region to be graded as abnormal, concomitant upper and lower motor neuron signs had to be present. Lower motor neuron (LMN) clinical features include fasciculations, muscle wasting/atrophy and weakness, whilst upper motor neuron (UMN) clinical features include hyper-reflexia, spasticity/increased tone, and the presence of pathological reflexes (extensor plantar responses, and Hoffman's sign). To fulfill the diagnosis of ALS by the EEC, patients needed to exhibit dysfunction in at least two of these regions (Table 1).

El Escorial Criteria
Clinically definite ALS
• Evidence of UMN plus LMN signs in the bulbar region and in at least two spinal regions, or
• The presence of UMN plus LMN signs in three spinal regions
Clinically probable ALS
• Evidence of UMN plus LMN signs in at least two regions with some UMN signs rostral to LMN signs
Possible ALS
• UMN plus LMN signs in only one region, or
• UMN signs alone in two or more regions, or
• LMN signs found rostral to UMN
Regions: Bulbar, Cervical, Thoracic, and Lumbosacral

Table 1. The classification of ALS under the El Escorial criteria (50). A minimum criteria of El Escorial 'Probable' classification was necessary for diagnostic confirmation and entry into clinical trials. LMN – Lower motor neuron, UMN - Upper motor neuron.

While the El Escorial criteria were highly specific, the main limitation pertained to reduced sensitivity, leading to a reconsideration of the criteria in 1998, termed the Airlie House or revised El Escorial criteria (49). The revised El Escorial criteria introduced a "***clinically probable-laboratory supported***" diagnostic category (Table 2), enabling the assessment of LMN dysfunction by utilising objective neurophysiological biomarkers.

Revised El Escorial Criteria
Clinically definite ALS
• Evidence of UMN plus LMN signs in the bulbar region and in at least two spinal regions, or
• The presence of UMN signs in two spinal regions and LMN signs in three spinal regions
Clinically probable ALS
• Evidence of UMN plus LMN signs in at least two regions with some UMN signs rostral to LMN signs
Probable laboratory supported ALS
• Clinical evidence of UMN and LMN signs in only one region, or
• UMN sings alone in one region and LMN signs defined by EMG criteria in at least two muscles of different root and nerve origin, in two limbs
Possible ALS
• UMN plus LMN in only one region, or
• UMN signs alone in two or more regions, or
• LMN signs found rostral to UMN
Regions: Bulbar, Cervical, Thoracic, and Lumbosacral

Table 2. The classification of ALS under the revised El Escorial criteria (49). With this criteria there was the addition of the 'Probable laboratory supported' criteria permitting utilisation of electrophysiology to identify subclinical lower motor neuron (LMN) abnormalities. UMN - Upper motor neuron

Although the revised El Escorial criteria (rEEC) resulted in an increased sensitivity, significant diagnostic delays remained, which approximated 14 months (51). Consequently, a neurophysiologically based diagnostic criteria, termed the Awaji criteria were proposed in 2006 (6). The Awaji criteria proposed that neurophysiological features of LMN dysfunction, including chronic and ongoing neurogenic changes (fibrillation potentials/positive sharp waves) were equivalent to clinical LMN signs. In addition, fasciculations were deemed to be a biomarker of LMN dysfunction when combined with chronic neurogenic changes. In order for a region to be classified as being abnormal, the neurophysiological abnormalities had to

be identified in two muscles innervated by a different nerve and nerve root for the spinal region (upper or lower limbs) or one muscle for the bulbar and thoracic region. The assessment of UMN function remained clinically based.

Awaji Criteria
The diagnosis of ALS requires *the presence of*
(1) evidence of lower motor neuron (LMN) degeneration by clinical, electrophysiological or neuropathological examination
(2) evidence of upper motor neuron (UMN) degeneration by clinical examination; and
(3) progressive spread of symptoms or signs within a region or to other regions, as determined by history, physical examination, or electrophysiological tests
The diagnosis of ALS requires *the absence of*
(1) electrophysiological or pathological evidence of other disease processes that might explain the signs of LMN and/or UMN degeneration, and
(2) neuroimaging evidence of other disease processes that might explain the observed clinical and electrophysiological signs
Diagnostic categories
Clinically definite ALS is defined by clinical or electrophysiological evidence by the presence of LMN as well as UMN signs in the bulbar region and at least two spinal regions or the presence of LMN and UMN signs in three spinal regions
Clinically probable ALS is defined on clinical or electrophysiological evidence by LMN and UMN signs in at least two regions with some UMN signs necessarily rostral to (above) the LMN signs
Clinically possible ALS is defined when clinical or electrophysiological signs of UMN and LMN dysfunction are found in only one region; or UMN signs are found alone in two or more regions; or LMN signs are found rostral to UMN signs.
Neuroimaging and clinical laboratory studies will have been performed and other diagnoses must have been excluded.
Regions: Bulbar, Cervical, Thoracic, and Lumbosacral

Table 3. The classification of ALS under the Awaji criteria (6). These changes allowed the combining of clinical and electrophysiological findings within a given region, and accepted ‘fasciculations’ as a marker of ongoing nerve injury.

The diagnostic utility of the Awaji criteria was assessed in retrospective and prospective studies, most of which established an increased sensitivity when compared to rEEC (30, 52-59), although one study reported a lower sensitivity (60). This unexpected finding was attributed to the omission of a "probable-laboratory supported" diagnostic category. Two study-level meta-analyses reported an improved diagnostic performance of the Awaji criteria, with higher sensitivity and diagnostic odds ratios (30, 61). The diagnostic benefits, however, appeared to be most prominent in ALS patients with bulbar-onset disease. Interestingly, one study reported that 20% of patients classified as "probable laboratory-supported" on the rEEC were downgraded to Awaji "possible" (61), although this latter study was criticised for utilising incomplete data sets (62). A potential limitation of both previous meta-analyses was the lack of specificity data.

The most recent emendation to the diagnostic criteria was proposed in 2015 by the World Federation of Neurology MND/ALS sub group committee (63). The 2015 criteria proposed that the 'possible' category be deemed diagnostic of ALS, once mimic disorders were excluded after extensive clinical, neurophysiological and neuroimaging assessment.

Variant forms of ALS

Adding to the complexity of diagnosis ALS and understanding the underlying pathophysiology, is the existence of atypical phenotypes. These atypical phenotypes vary from the clinically pure upper motor neuron ***primary lateral sclerosis (PLS)*** phenotype, to the predominant LMN phenotypes encompassing the ***flail-arm*** and ***flail leg*** syndrome variants of ALS.

Primary lateral sclerosis is a pure upper motor neuron presentation of ALS. The term PLS was first coined by Erb in 1875 (64), with earlier pathological findings described by Charcot in 1865 (65). The incidence of PLS is estimated at 1-4% of ALS cases (66-69). The first diagnostic criteria were proposed by Pringle and colleagues, who proposed that UMN dysfunction be present for at least 3 years prior to development of LMN signs (70) [Table 4].

Clinical	Insidious onset of spastic paresis, usually beginning in the lower extremities, but occasionally involving bulbar or upper extremities
	Adult onset, usually in the fifth decade or later, with an absence of a family history
	Gradually progressive course (no step-wide deterioration)
	Duration of approximately 3 years
	Clinical findings limited to those associated with corticospinal dysfunction
	Symmetrical distribution, ultimately developing severe spastic spinobulbar paresis
Laboratory (to aid in exclusion of other diagnoses)	Normal routine blood tests, including normal serum chemistry including normal vitamin B12 levels, negative serologic tests for syphilis, negative Lyme and HTLV-1 serology
	Normal CSF parameters, including the absence of oligoclonal bands
	Absent denervation potentials on Needle EMG or at most, *occasional* fibrillation and increased insertional activity in a few muscles (late and minor)
	Absence of compressive lesions of cervical spine or foramen magnum (spinal MRI scanning)
	Absence of high signal lesions on MRI similar to those seen in MS
Additionally features suggestive of PLS	Preserved bladder function
	Absent or very prolonged latency on cortical motor evoked responses in the presence of normal peripheral stimulus-evoked maximum compound muscle action potentials
	Focal atrophy of the precentral gyrus on MRI
	Decreased glucose consumption in the pericentral region on PET scan

Table 4. The diagnostic criteria in PLS, proposed by Pringle and colleagues in 1992 (70).

The original PLS criteria exhibited a poor specificity, with up to a third of ALS patients being misdiagnosed with PLS, resulting in prognostication and management issues (66). Consequently, Gordon and colleagues proposed a modification of the criteria in 2006 (66) [Table 5]. The main modification was the requirement that UMN dysfunction be present in isolation for at least 4 years from symptom onset. In addition, subtypes of PLS were proposed to highlight the heterogeneity of the disease process and to aid in diagnosis. The salient features are outlined in Table 5.

Autopsy proven PLS	Clinically diagnosed PLS with degeneration in motor cortex and corticospinal tracts, no loss of motor neurons, no gliosis in anterior horn cells, and no Bunina or Ubiquinated inclusions.
Clinically pure PLS	Evident upper motor neuron signs, no focal muscle atrophy or visible fasciculation, and no denervation in EMG 4 years from symptom onset. Age at onset after 40. Secondary and mimicking conditions excluded by laboratory and neuroimaging.
UMN-dominant ALS	Symptoms less than 4 years, or disability due predominantly to UMN signs but with minor EMG denervation or LMN signs on examination, not sufficient to meet diagnostic criteria for ALS.
PLS plus	Those with predominant UMN signs who also have clinical, laboratory, or pathologic evidence of dementia, parkinsonism, or sensory tract abnormalities. Note: If cerebellar signs, urinary incontinence, or orthostatic hypotension are evident, multiple system atrophy could be considered.
Symptomatic lateral sclerosis	Clinically diagnosed PLS with evident possible cause (HIV, paraneoplastic syndrome).

Table 5. The diagnostic criteria in upper motor neuron predominant ALS, proposed by Gordon and colleagues in 2006 (66).

Primary lateral sclerosis exhibits a more favorable prognosis with regards to survival, although disability remains a critical feature (66, 67). The mean age of onset is in the early 50's, with males and females equally affected (66). Lower limb onset is typically evident with subsequent spread of symptoms to upper limb and bulbar regions, although there is a rare hemiplegic variant termed the Mills syndrome (71). Bulbar dysfunction, along with preserved bladder and sensory function may distinguish PLS from mimic disorders. Development of lower motor neuron dysfunction or bulbar palsy, may herald an adverse prognosis (66, 72). Importantly, the development of cognitive impairment and aphasia may be also be associated with an adverse prognosis in PLS (73).

Neuroimaging studies have reported marked cortical atrophy within the precentral and parietal region in PLS patients (70, 74-76), signifying significant cortical neuronal loss. In addition, abnormalities of the corticospinal tract have also been identified in PLS signifying degeneration of the UMN (77). Underscoring the marked UMN dysfunction, are findings of motor cortex inexcitability and markedly prolonged central motor conduction time on TMS testing (70, 78).

Neuropathological studies have reported widespread degeneration of Betz cells and corticospinal tracts, potentially forming the basis of the clinical, radiological and physiological findings (69, 79-81). Ubiquinated inclusions with and without Bunina bodies along with skein like lesions have also been reported within the precentral, frontal and temporal cortices (67, 79, 80, 82, 83). Importantly, the anterior horn cell population remains preserved, although ubiquitin-positive inclusions have been reported (69).

Progressive muscular atrophy (PMA) is thought to comprise approximately 10% of patients with motor neuron disease (84). Primary muscular atrophy presents with predominantly LMN dysfunction, although at least one-third of cases can develop UMN dysfunction (85, 86). The flail leg (FL) syndrome, also termed leg amyotrophic diplegia and pseudopolyneuritic variant of ALS, is an unusual PMA phenotype first described in the early 20th century (87). Clinically, the FL syndrome is characterized by a predominantly lower motor neuron phenotype, with weakness and wasting confined to the distal lower limbs for at least 12 months (88)[Table 6]. Upper motor neuron (UMN) signs are typically absent, or if evident are subtle (84, 87, 88). Although the prognosis for FL syndrome is favorable with a median survival of 90 months (84, 88), there appears to be a heterogeneity, with patients exhibiting a greater degree of UMN dysfunction having a shorter survival that mirrors the classical ALS phenotype (89).

Inclusion criteria	Lower motor neuron disorder of the lower limbs
	Characterized by progressive distal onset weakness and wasting
	Flail leg pattern of weakness with evidence of pathological deep tendon reflexes (without hypertonia or clonus)
Exclusion criteria	Functionally significant weakness or wasting in upper limbs, bulbar and respiratory musculature within 12 months after onset of lower limb symptoms
	Hypertonia or clonus in lower limbs
	Wasting or weakness beginning proximally in legs without distal involvement at presentation

Table 6: The inclusions and exclusion criteria for the flail leg syndrome as proposed by Wijesekera and colleagues (88).

Pathophysiology of ALS

Although the mechanisms underlying ALS pathogenesis remains to be fully elucidated, emerging evidence suggests the importance of genetic factors and dysfunction of vital molecular pathways and processes (Figure 2). A genetic etiology has been identified in up to 20% of sporadic and 70% of familial ALS cases, with at least 20 genes and genetic loci implicated in ALS pathogenesis (90-96). Importantly, these genetic breakthroughs have shed significant insights into the mechanisms underlying the development of ALS with clear diagnostic and therapeutic implications.

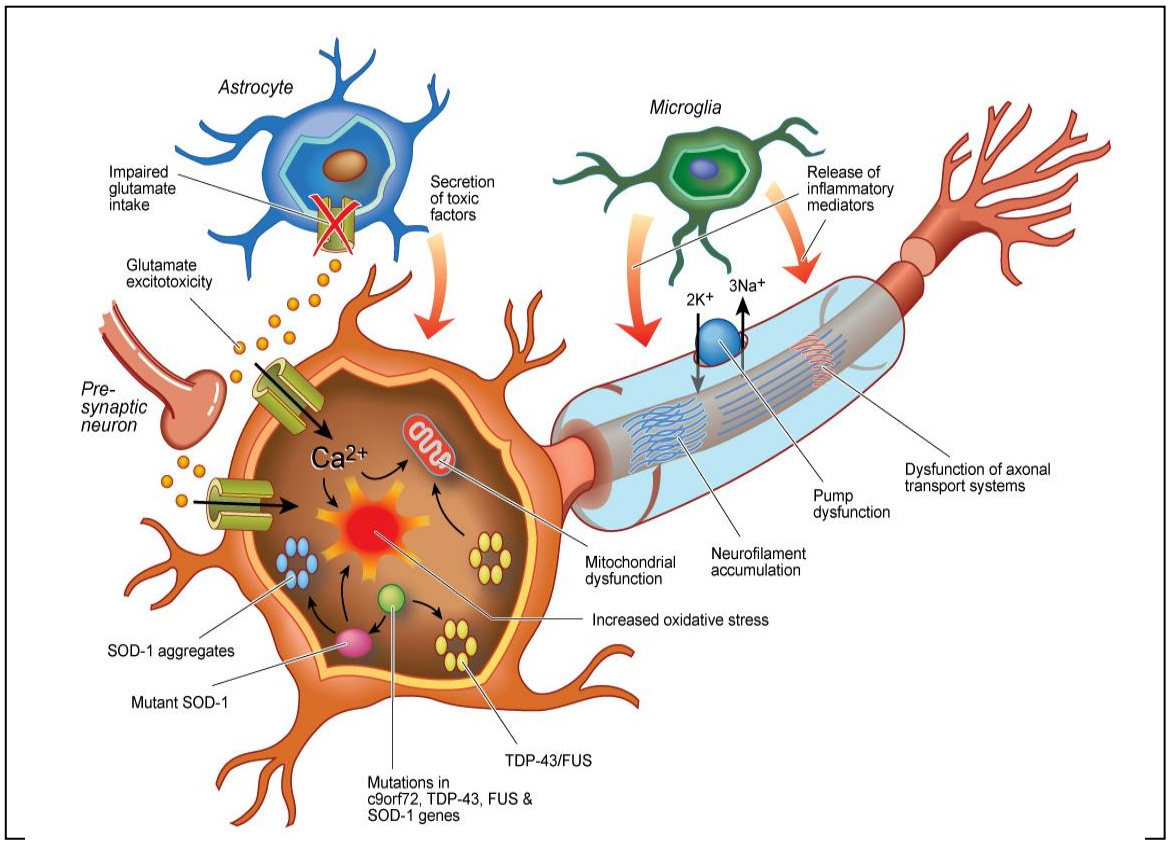

Figure 2: The pathophysiological mechanisms underlying neurodegeneration in amyotrophic lateral sclerosis (ALS) is complex and multifactorial. Evidence exists for complex interplay between molecular and genetic pathways. Dysfunction of the astrocytic excitatory amino acid transporter 2 (EAAT2) results in reduced uptake of glutamate from the synaptic cleft potentially leading to glutamate excitotoxicity. Glutamate-induced excitotoxicity results in increased influx of Na^+ and Ca^{2+} ions and ultimately neurodegeneration through activation of Ca^{2+}-dependent enzymatic pathways. In addition, glutamate excitotoxicity results in generation of free radicals which in turn contributes to neurodegeneration. Mutations in the c9orf72, TDP-43 and FUS result in deregulated RNA metabolism that ultimately leads to formation of intracellular aggregates which are harmful to neurons. Of further relevance, mutant SOD-1 enzyme increases oxidative stress, induces mitochondrial dysfunction, forms intracellular aggregates and adversely affect neurofilament and axonal transport processes. Activation of microglia results in secretion of proinflammatory cytokines, producing further toxicity. Figure from Vucic S, Rothstein, J. D. Kiernan, M. C. *Advances in treating amyotrophic lateral sclerosis: insights from pathophysiological studies.* Trends Neurosci. 2014.

C9orf72 hexanucleotide expansion: A major advance in the understanding of ALS pathogenesis occurred with the discovery of the dominantly inherited c9orf72 gene [increased hexanucleotide repeat expansion (GGGGCC)] in the non-coding region of chromosome 9p21, which underlies over 40% of familial ALS cases (97, 98). Importantly, the frequency of the c9orf72 hexanucleotide expansion exhibits significant geographic variations, accounting for nearly 50% of Finnish familial ALS cases with lower frequencies reported in Italian and German populations (97). In keeping with other repeat expansion genetic diseases, apparent anticipation has also been reported in c9orf72 expansions, with the disease onset being 7-10 years earlier in the offspring of affected parents (99). The pathogenic expansion was reportedly non-penetrant in carriers under the age of 35 years, 50% penetrant at age 28 years and almost fully penetrant by 80 years of age (100). In addition to being causative in familial ALS, the c9orf72 hexanucleotide expansion has been reported in 4.1-8.3% of apparently "sporadic" ALS cases (100).

This monumental discovery has radically altered the understanding of ALS pathogenesis, implying that ALS is a multisystem neurodegenerative disorder, rather than a pure neuromuscular disease. Underscoring this notion are findings that the c9orf72 hexanucleotide expansions are also causative for frontotemporal dementia (97, 98, 100). Accumulation of TDP-43 along with p62 positive TDP-43 negative inclusions in the hippocampus and cerebellar neurons, as well neurons located within the cortex, appears to be a pathological hallmark of c9orf72 associated ALS and FTD (101), suggesting the existence of a common pathophysiological pathway.

Clinical presentation: Although the pathognomonic clinical features in c9orf72 familial ALS are dominated by a combination of upper and lower motor neuron signs, with rapid disease progression, phenotypic differences have been observed in c9orf72 associated ALS patients. Specifically, ALS patients exhibiting the c9orf72 expansion are more likely be female, exhibit bulbar-onset disease and report a family history of ALS (99, 100, 102). In addition, patients with the pathogenic expansion exhibit an earlier age of onset and shorter survival (102, 103), with size of the c9orf72 expansion correlating with the age of onset (104). Atypical phenotypes have also been reported in the c9orf72 hexanucleotide expansion including monomelic amyotrophy, progressive muscular atrophy, mixed flaccid/spastic dysarthria and primary lateral sclerosis (102).

Cognitive impairment and frontotemporal dementia are significantly more common in c9orf72 ALS patients (99). Clinically, the frontotemporal dementia is characterized by executive and language dysfunction, irrational behavioral, personality changes, apathy, poor insight, loss of apathy, irritability and disinhibition (105, 106). Deficits in social cognition, emotional processing and theory of the mind have recently been identified in ALS (107).

Importantly, frontotemporal dementia may precede the onset of ALS by up to 4 years, although the converse has also been reported with ALS preceding the onset of FTD (99, 102). Interestingly, c9orf72 FTD is invariably characterized by behavioral symptoms, with semantic dementia and progressive non-fluent aphasia FTD phenotypes infrequently reported (102). In addition, psychotic symptoms such as delusions and hallucinations are more frequent in patients carrying the c9orf72 repeat expansion (99, 108, 109).

Neuroimaging studies disclose symmetrical and bilateral frontotemporal cortical atrophy, with subcortical white matter changes, a finding in keeping with the clinical findings (102, 110). Importantly, the pattern of cortical atrophy evident in the c9orf72 expansion cohorts, was distinct to that evident with progranulin and tau gene mutations (110). Of relevance, hypermetabolism and hypoperfusion of the frontal cortical regions accompanied the cortical atrophy, with the deficits most evident in the anterior and middle cingulate gyrus (102).

Pathophysiological mechanisms underlying c9orf72 gene expansion: The mechanisms by which c9orf72 hexanucleotide expansion causes neurodegeneration in ALS remains to be fully elucidated (97, 98), although three potential pathogenic mechanisms have been proposed, including (i) haploinsufficiency, (ii) repeat RNA-mediated toxicity and (iii) dipeptide protein toxicity related to repeat associated non-ATG (RAN) translation of the expanded c9orf72 gene (111). Evidence for haploinsufficiency is suggested by studies reporting a reduction in the c9orf72 short and long isoforms in ALS patients (97, 98), although a reduction in the corresponding c9orf72 protein is yet to be established. In addition, reduced expression of the c9orf72 transcript in the zebrafish model of ALS resulted in motor axonal degeneration with locomotion deficit, providing additional support for haploinsufficiency as a factor in ALS pathogenesis (112).

Of further relevance, RNA-mediated toxicity has also been proposed as a potential mechanism. Such a process was inferred from observations of intranuclear RNA foci containing c9orf72 hexanucleotide repeats (98), and supported by findings that specific RNA-binding proteins associate with the c9orf72 expansion resulting in formation of intranuclear and cytoplasmic inclusions (113). More recently, studies utilizing induced pluripotent stem-cell differentiated neurons from C9orf72 patients provided additional support for RNA

toxicity and importantly established that the pathological changes were mitigated by antisense oligonucleotide therapeutic approaches (114).

In addition, non-ATG related translation of the c9orf72 expansion (RAN translation) has also been proposed as a potential pathogenic mechanism (115). Specifically, RAN translation results in generation of insoluble di-peptides (anti-C9RANT), which form intraneuronal (nuclear and cytoplasmic) inclusions and appear to be specific for c9orf72 associated ALS/FTD (115). Given that neuronal degeneration and dysfunction may result from accumulation of insoluble proteins, and that C9RANT-positive pathology appears specific for c9orf72 related ALS/FTD, novel therapeutic strategies aimed at modulating such a process may prove useful.

Importantly, the c9orf72 hexanucleotide expansion is associated with characteristic neuropathological features dominated by neuronal cytoplasmic inclusions containing hyperphophylated-TDP43 as well as ubiquitin and p62 [sequestosome 1] (101). These inclusions are evident in the interneurons of the neocortex as well as neurons in the cerebellum and hippocampus, and are similar to neuropathological changes evident in FTD (101, 116, 117). The TDP-43 pathology can be variable in c9orf72 ALS, but the vast majority of cases were classified as type A in one large series (118). The type A (Mackenzie type 1) is characterized by many cortical neuronal cytoplasmic inclusions and dystrophic neuritis, often with intranuclear inclusions and widespread involvement of subcortical areas. The type B (Mackenzie type 3) classification meanwhile have many neuronal cytoplasmic inclusions, but few dystrophic neurites and more limited subcortical pathology (119). Importantly, excessive protein accumulation, secondary to c9orf72 expansions, could

potentially underlie neuronal degeneration by activation of ubiquitin-proteasome system (UPS) or by autophagosome–lysosome pathways (101).

Other genetic mutations

Mutations in other DNA/RNA-processing genes, namely the transactive-region DNA-binding protein gene (TARDBP) (120) and fused in sarcoma (FUS) genes (121) were described prior to the c9orf72 hexanucleotide expansions and represent 4-6% of familial and up to 2% of sporadic ALS (90, 122). To date, approximately 50 mutations have been identified in each gene, and most mutations are dominantly inherited (120, 123). The TARDBP mutations are localized in the highly conserved C-terminal glycine-rich domain (120), while FUS mutations are located in the nuclear localization signal domain that translocates the FUS protein into the nucleus (123). The mutant proteins are redistributed from the nucleus to the cytoplasm, resulting in toxicity.

Multiple pathophysiological mechanisms appear to underlie neuronal degeneration in TARDBP/FUS gene mutations, including gain of toxicity, loss of nuclear function, or formation of large stress granules (111). Transgenic mouse models have provided evidence for a toxic gain of function, whereby increased expression of the mutated TDP-43 proteins leads to neurodegeneration (124-131). The severity of cortical and spinal motor neuron degeneration appears proportional to the TDP-43 protein levels (125), suggesting a potential role for TDP-43 in regulating disease severity. In addition, cytoplasmic accumulation of TDP-43 aggregates has been well established in ALS patients (132), implying a potential role for a TDP-43 loss of nuclear function mechanism in ALS pathogenesis, and recent transgenic mouse models provide support for such a theory (133, 134).

Of further relevance, cytoplasmic accumulation of FUS positive inclusions in ALS patients (121, 123) implies a loss of nuclear function of FUS as a potential mechanism in ALS pathogenesis, being similar to TARDBP mutations. Support for such a notion was provided by studies demonstrating that expression of a FUS variant in transgenic mice, at lower levels than endogenous FUS, leads to selective motor neuron degeneration (135). Conversely, a toxic-gain of function of mutated FUS has also been inferred from studies demonstrating that expression of mutated FUS leads to progressive motor dysfunction, which was rescued by over expression of wild-type FUS (136).

Pathological TDP-43 and FUS mutants appear to exhibit a greater propensity to associate and alter the dynamics of cytoplasmic stress granules (121, 137-140). Importantly, wild-type TDP-43 and FUS proteins associate with cytoplasmic stress granules under physiological conditions in order to temporarily suppress translation of mRNA and stored pre-RNA complexes during periods of cellular stress, thereby safe-guarding the coded RNA information from deleterious chemicals (137, 141, 142). Consequently, alteration of stress granule dynamics induces neuronal degeneration in ALS by sequestration of RNA-binding proteins and repression of RNA translation along with formation of pathological inclusions (137, 143-145).

Mutations in the superoxide dismuates-1 (SOD-1) gene (*see oxidative stress below*), as well as genes responsible for regulating protein ubiquitination [ubiquilin-2, UNC13A] (146, 147), trafficking of endosomes [vesicle-associated membrane protein/synatobrevin-associated protein, charged multivesicular body protein] (148-150), and protein homeostasis [valosin-containing protein, optineurin, p62/SQSTM1] (151-153), have all been associated with ALS. These genetic mutations are dominantly inherited and appear to exert a pathogenic effect by

disrupting the function of vital cellular processes ultimately leading to neurodegeneration (111).

Molecular processes and ALS pathogenesis

In addition to genetic mutations, a host of potentially interdependent molecular processes have been implicated in ALS pathogenesis (Figure 2). Critically, these molecular processes may be linked with underlying genetic mutations and may occur in a complex sequential multi-step process prior to the onset of neurodegeneration (154). In addition, the predisposition to develop ALS may occur at conception, with a prolonged pre-clinical period emerging during which the deleterious molecular processes are activated (155).

Glutamate-mediated excitoxicity: Glutamate-mediated excitoxicity is a critical mechanism in ALS pathogenesis (47, 48, 156-158). Glutamate is the major excitatory neurotransmitter in the central nervous system (159, 160). During axonal depolarization, glutamate is released from presynaptic neurons, the major pool for glutamate, and activates postsynaptic receptors. The excitatory signal is terminated by removal of glutamate from the synaptic cleft by specific glutamate re-uptake transporters located on neurons and astrocytes (161, 162). Within astrocytes, glutamate is converted into glutamine by the enzyme glutamine synthetase, and then returned to the neuron for resynthesis of glutamate (163).

Excessive activation of the postsynaptic glutamate receptors, broadly classified into ionotropic and metabotropic, leads to glutamate-mediated excitoxicity (160). The ionotropic receptors are implicated in the pathogenesis in ALS, by resulting in excessive influx of Na^{+} and Ca^{2+} ions (164). Based on pharmacological studies, glutamate ionotropic receptors are further classified as: (i) ***N-methyl-D-aspartate (NMDA)***, (ii) ***α-amino-3-hydroxy-5-methyl-4-***

isoxazoleproprionic acid (AMPA), and (iii) ***kainite*** receptors. This pharmacological classification is supported by cloning studies that have identified six different families of glutamate ionotropic receptors that conform to the original agonist studies (164). ***N-methyl-D-aspartate*** receptors are permeable to influx of Na^+ and Ca^{2+} and efflux of K^+ (164). An essential feature of NMDA receptors is their voltage-dependent blockade by Mg^{2+} binding within the channel pore, which can be alleviated by depolarization (165). NMDA receptors are involved in excitatory neurotransmission, which is characterized by a slow rise time and decay.

The NMDA receptor complex is composed of different subunits derived from 6 genes; NMDAR1 (eight splice variants described), NMDAR2 (A-D) and NMDAR3 (A, B) (160, 164). While the NMDAR1 subunit forms the basic structure of the receptor (160), the NMDAR2 subunit determines ion channel properties and forms ligand-binding sites (166-168). Functional and pharmacological properties of NMDA receptors are determined through specific combination of NMDAR1 and NMDAR2 subunits (166, 169). In addition, there are regional variations in the expression of NMDA receptor subtypes (166, 169-175), with the NMDAR3B subunit heavily expressed in somatic motor neurons (176, 177).

AMPA receptors mediate a rapid influx of monovalent ions (Na^+, K^+ and chloride), but are impermeable to Ca^{2+} (160). Four AMPA receptor subtypes have been cloned (*Glu*R1-4) and are composed of three transmembrane domains (M1, M3, M4) with a fourth cytoplasmic hairpin loop (M2), contributing to a pore-lining region (164, 178). The AMPA receptor exists as a pentameric structure in vivo, which is formed by the arrangement of subunits to create receptor diversity (160). The GluR2 subunit influences Ca^{2+} permeability of AMPA

receptors, whereby editing defects within the GluR2 subunit render the APMA receptors more permeable to Ca^{2+} ions (160, 164).

Kainate receptors are located in both presynaptic and postsynaptic neuronal membranes, existing as heteromeric pentamer complexes (179). The kainite receptors are thought to modulate slow synaptic responses and are unlikely to contribute to excitoxicity. Kainate receptors are involved in short-term synaptic plasticity, particularly at the mossy fiber synapses and also seem to be involved in long-term plastic phenomena. However, their signal transduction pathways, which are probably dual, need to be clarified and despite their wide distribution their exact role in excitability needs to be elucidated (180).

Glutamate excitotoxicity has been postulated to underlie neuronal degeneration via a trans-synaptic anterograde process mediated by corticomotoneurons, termed the ***dying forward hypothesis*** (24). Transcranial magnetic stimulation studies (TMS) have provided support for this mechanism by identifying cortical hyperexcitability, a biomarker of glutamate excitotoxicity, as an early feature in sporadic and familial (SOD-1) ALS, linked to motor neuron degeneration (41, 42, 96, 181-186) and preceding the clinical onset of ALS (185, 187). In addition, disinhibition of the motor cortex, secondary to degeneration of γ-amino butyric acid (GABA) secreting inhibitory interneurons has been documented in ALS, thereby further contributing to development of cortical hyperexcitability (188, 189).

At a molecular level, significant reduction in the expression and function of the astrocytic glutamate transporter (EAAT2), which mediates glutamate reuptake at synapses, has been reported in superoxide dismutase-1 (SOD-1) mouse model and the motor cortex and spinal cord of ALS patients (156, 190-193). Of further relevance, dysfunction of the EAAT2

transporter appears to be a pre-clinical phenomenon (194, 195), and an increase in expression and activity of EAAT2 increases the lifespan of mutant SOD-1 mice (196). In addition, activation of caspase-1, which normally inhibits the EAAT2 transporter, has been reported in the transgenic SOD-1 mouse model prior to onset of neuronal degeneration (194, 195).

At a postsynaptic level, increased expression of the Ca^{2+} permeable AMPA receptors exhibiting an unedited GluR2 subunit, has been reported in motor neurons in ALS (197-201), potentially explaining the increased sensitivity of motor neurons to excitotoxicity (160, 202). In addition, vulnerable motor neurons lack the intracellular expression of Ca^{2+} buffering proteins parvalbumin and calbindin D28k (203). Increased expression and aberrant activity of the inositol 1,4,5-triphosphate receptor 2 (ITPR2) gene has been reported in ALS (204), which leads to excessive accumulation of Ca^{2+} upon glutamate stimulation (204, 205). Of further relevance, motor neurons in ALS, at least in animal models, appear to be larger, with an increase in distal dendritic branching (206). Consequently, input conductance of motor neurons is increased rendering them more vulnerable to electrical and metabolic stresses, in particular those imparted by glutamate excitotoxicity (207).

Although details of the molecular mechanisms by which glutamate exerts toxicity remain to be clarified, several pathways have been defined. Initially, an influx of Na^+ and Cl^- ions, along with water molecules, leads to acute neuronal swelling that is potentially reversible (208-210). Subsequently, an influx of Ca^{2+} ions occurs via activation of ionotropic receptors such as the NMDA and Ca^{2+}-permeable AMPA receptors, as well voltage-gated Ca^{2+} channels (208, 211). Ultimately, increased intracellular Ca^{2+} concentration ensues with activation of Ca^{2+}-dependent enzymatic pathways leading to neuronal death (202, 209, 212,

213). In addition, glutamate excitotoxicity results in production of free radicals that can further damage intracellular organelles thereby causing cell death (214-216).

The clinical benefit of the anti-glutaminergic agent riluzole in ALS (217-221), provides additional support for the importance of glutamate excitoxicity as a pathogenic mechanism in ALS. In addition, the neuroprotective benefits afforded by retigabine, a K^+ channel activator which antagonizes neuronal hyperexcitability (222), lends further credence to the importance of glutamate excitoxicity in ALS pathogenesis. Although some have argued the glutamate excitoxicity was neuroprotective (223), the finding that riluzole normalizes cortical hyperexcitability argues against a neuroprotective role in ALS patients (224).

Site of disease onset in ALS: The notion that glutamate excitoxicity is an important, and possibly primary, pathogenic mechanism in ALS is of significance when considering the site of disease onset. Three schools of thought have emerged pertaining to the site of disease onset, and include: (i) "the *dying forward*" hypothesis; (ii) "the *dying back*" hypothesis and (iii) "the *independent degeneration*" hypothesis (Figure 3).

The ***dying forward hypothesis*** proposed that ALS was primarily a disorder of the corticomotoneurons, which connect monosynaptically with spinal motor and bulbar neurons (24). Corticomotoneuronal hyperexcitability was postulated to induce anterior horn cell degeneration trans-synaptically via an anterograde glutamate-mediated excitotoxic process (24, 96). This dying forward hypothesis was based on a number of clinical observations including: (i) relative preservation of extraocular and sphincter muscles in ALS, postulated to be due to a paucity of corticomotoneuronal projections onto the motor nuclei innervating these muscles; (ii) absence of an animal model of ALS, ascribed to a lack of direct

corticomotoneuronal-anterior horn cell connections (225, 226); (iii) rarity of pure lower motor neuron forms of ALS, with subclinical upper motor neuron dysfunction invariably detected with TMS studies (227); and (iv) the specificity of the split hand phenomenon in ALS remains best explained by a dying forward mechanism (11, 12, 14, 228-232).

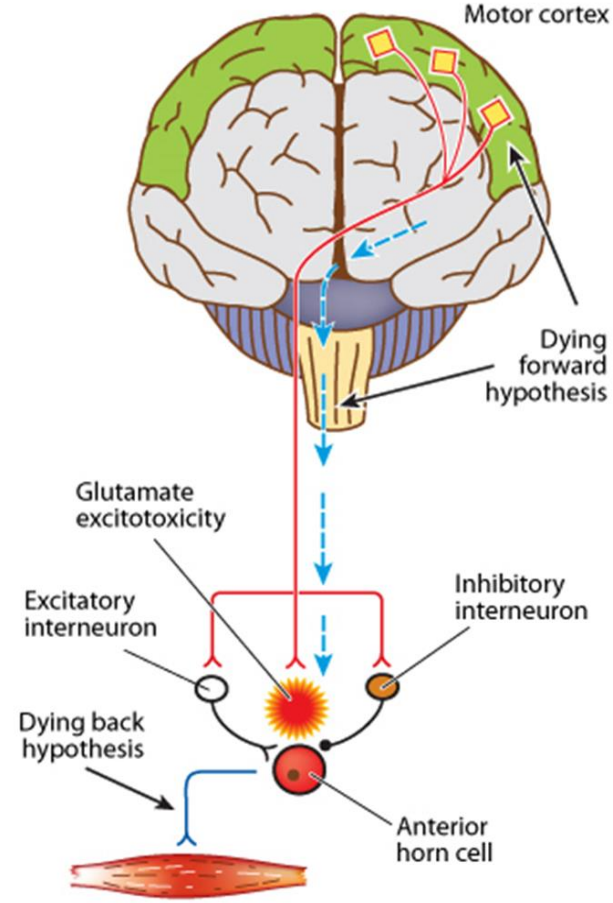

Figure 3: Controversy: Where does ALS begin? Despite Jean Martin Charcot's initial observation of concomitant upper and lower motor neuron pathology in ALS, the issue of where ALS begins has not been resolved. Resolution of this question will enhance the understanding of ALS pathophysiology and be of therapeutic significance.

- ***Dying forward hypothesis*** proposes that ALS is primarily a disorder of corticomotoneurons, which connect monosynaptically with anterior horn cell, mediating anterograde degeneration of motor neurons via glutamate excitotoxicity. This view was held by Charcot.
- ***Dying back hypothesis*** proposes that ALS begins within the muscle cells or at the neuromuscular junction.
- ***Independent degeneration hypothesis*** proposes that upper and lower motor neuron degeneration occurs independently.

Figure from Vucic S, et al. JNNP, 2013

As discussed above, threshold tracking TMS studies have identified cortical hyperexcitability as an early feature in sporadic and familial ALS, linked to the process of motor neuron degeneration (41, 42, 96, 181-185), preceding the development of lower motor neuron dysfunction (185, 187) and following the pattern of dissociated muscle atrophy (14, 187, 232). In keeping with a cortical origin of ALS are findings of concordance between

handedness and site of disease onset (233), the notion that upper motor neurons potentially mediate the site of disease onset and patterns of spread in ALS (234), as well the now accepted view that ALS and frontotemporal dementia (FTD) represent an overlapping continuum of the same disorder (235, 236), an observation underscored by recent genetic discoveries that increased hexanucleotide repeat expansions in the first intron of C9ORF72 gene (9p21) [*see above*] was associated with both ALS and FTD (97, 98).

The notion that cortical hyperexcitability is a compensatory mechanism in response to motor neuron degeneration has also been proposed (45). Given however, that cortical hyperexcitability was not evident ALS mimic disorders patients despite a comparable peripheral disease burden (187, 237-239), argues against a compensatory mechanism. Of further relevance is the identification of cortical hyperexcitability in atypical ALS phenotypes, dominated by a paucity of upper motor neuron signs (240), further underscoring the importance of a dying forward mechanism in ALS pathogenesis.

The ***dying back hypothesis*** proposed that ALS was primarily a disorder of lower motor neurons, with pathogens retrogradely transported from the neuromuscular junction to the cell body where they exert their deleterious effects (241). Support for a dying back process has been largely provided by transgenic mouse model and pathological studies (241-245), although no pathogens have been identified. In addition, the presence of widespread dysfunction within the frontal cortex, including the primary, supplementary and pre-frontal motor cortices in ALS remains difficult to reconcile with any dying back process (246-248). Finally, the absence of central pathology in other lower motor neuron mimic disorders such as Kennedy's disease or poliomyelitis provides a further argument against a dying back process (238, 249).

The ***independent degeneration hypothesis*** suggested that upper and lower motor neurons degenerate independently and concurrently (250). Neuropathological studies documenting an absence of significant correlation between corticomotorneuron and anterior horn cell densities formed the basis of the independent degeneration hypothesis (251, 252), a view held by Charcot's contemporary, WR Gowers (253). These correlative morphological techniques, however, were significantly confounded by the anatomical and functional complexity of the corticomotoneuronal system (254). In particular, there remains considerable variability in the corticomotoneuronal to anterior horn cell ratio, due to synaptic changes, and as such, attempts to correlate upper and lower motor neurons on autopsy studies may not reflect an accurate model in vivo (249). More recently, clinical studies documenting the pattern of disease spread documented an absence of correlation between upper and lower motor neuron signs (255), thereby invoking an independent degeneration mechanism. These clinical observations were accompanied by neurophysiological assessments, and consequently subclinical upper or lower motor neuron dysfunction may have gone undetected.

Other molecular processes and ALS pathogenesis

Mitochondrial dysfunction: In conjunction with glutamate excitotoxicity, mitochondrial dysfunction has also been implicated in ALS pathogenesis (92, 256-262). Mitochondria are intracellular organelles whose main function is to generate energy for the cell in the form of ATP. Glutamate excitotoxicity leads to production of free radicals by mitochondria, secondary to excessive Ca^{2+} accumulation (263), and thereby injury of critical neuronal cellular proteins and DNA. In addition, mitochondria remain sensitive to free radical damage at both the protein and DNA level, resulting in further mitochondrial dysfunction (264). Of

relevance, mitochondrial damage may enhance glutamate excitotoxicity by disrupting the normal voltage-dependent Mg^{2+} mediated block of NMDA receptor channels (160, 209).

Mitochondrial degeneration and dysfunction has been reported in ALS patients and in the transgenic SOD-1 mouse model (258, 261, 265). Specifically, structural abnormalities of muscle mitochondria have been reported in ALS (257, 260, 266). In addition, dysfunction of mitochondrial enzymes involved in energy generation, such as Cytochrome C Oxidase and respiratory chain complexes I and IV, as well as down-regulation of nuclear genes encoding mitochondrial components within the motor cortex have been reported in ALS (259, 260, 266-268). Reduction in protein import, impairment of Ca^{2+} sequestration and an exaggerated depolarizing response of the inner mitochondrial membrane has been reported in the pre-symptomatic stages of ALS (269-273). Ultimately, severe damage to the mitochondrial membrane potential, respiration, and electron transfer chain ensues, resulting in reduced ATP synthesis and neurodegeneration (207).

The neuronal transportation of mitochondria appears to be impaired in ALS (207). Specifically, movement of mitochondria is regulated through Ca^{2+} signaling and synaptic activity (274), and increases in intracellular Ca^{2+} concentration, as may be induced by glutamate excitotoxicity, interrupts mitochondrial movement within the cell (275). Abnormalities of mitochondrial distribution and transport have been reported in ALS, with evidence of reduced distribution in the axons and more frequent pauses in mitochondrial movements (276). Ultimately, this interruption in mitochondrial mobility may result in depletion of energy supply in critical neuronal segments, essential for the maintenance of the resting membrane potential and generation of action potentials, with resultant neuronal degeneration.

From a therapeutic perspective, a recent phase II trial of dexpramipexole, a pharmacological agent that enhances mitochondrial function (277), was shown to be effective in slowing ALS disease progression and reducing mortality over a 24 week period potentially offering hope in ALS (278). Unfortunately, a phase III, multicenter international trial, undertaken to assess the clinical efficacy of dexpramipexole as add on therapy to riluzole in ALS, was shown to be ineffective (279), although a recent post-hoc analysis suggested benefits in a subgroup of riluzole-treated, short-symptom duration, rEEC definite ALS patients (280).

Oxidative stress and the SOD-1 gene: In concert with glutamate excitotoxicity and mitochondrial dysfunction, oxidative stress has also been implicated in the pathogenic process of ALS, although the importance of this mechanism seems limited (262). Mutations in the SOD-1 gene, the first ALS gene reported and mapped to the long arm of chromosome 21 [21 q22.1] implied a role for oxidative stress in ALS pathogenesis (281). To date, over 166 SOD-1 mutations have been reported, underlying 14-23% of familial and 1-7 % of sporadic ALS cases (90). Intra- and interfamilial variation in penetrance, age and site of disease onset, rate of disease progression and survival has been reported for most SOD-1 mutations, with approximately 50% of patients expressing the disease by age 43 and more than 90% by 70 years (282).

The pathophysiological mechanisms by which SOD-1 gene mutations mediates neurodegeneration in ALS remains to be fully elucidated (92). A toxic gain of function, as indicated by aberrant biochemical activity of the SOD-1 enzyme has been implicated as a potential pathogenic mechanism (283). Specifically, SOD-1 mutations may lead to increased production of hydroxyl and free radicals (284), as well as nitration of tyrosine residues on

proteins (285-287). The findings of normal SOD-1 enzyme activity in mutants (288), along with an absence of correlation between dismutase activity and disease severity (289), and lack of beneficial effects of antioxidant therapy in ALS patients (290), potentially argues against a significant role for oxidative stress in SOD-1 related ALS pathogenesis.

In addition, aggregation of mutated SOD-1 peptides which may lead to toxicity and neuronal degeneration has also been proposed as a potential pathogenic mechanism (47). Importantly, disease severity in SOD-1 mutants appear to correlate with instability of the SOD-1 mutant (291). The mechanisms by which confirmation changes in the SOD-1 protein leads to neurodegeneration remains to be determined, although co-aggregation of essential cellular components or induction of aberrant catalysis by misfolded SOD-1 mutants have been proposed as potential processes (292).

Impairment of axonal transport systems (241, 293, 294), endosomal trafficking (148, 149, 241, 295), neuroinflammation (296-298), induction of an excessive endoplasmic reticulum stress response (299, 300), and expression of human endogenous retrovirus-K (301) have all been implicated in ALS pathogenesis, although their role remains to be fully clarified (47, 157).

Non-cell autonomous processes: An emerging concept in ALS pathogenesis pertains to non-cell autonomous processes, whereby neighboring glial cells mediate motor neuron cell death (94, 156, 302). Studies in transgenic mouse models reported that modulation of mutant SOD-1 expressed in microglia, slowed disease progression (302), while astrocytes expressing the mutant SOD-1 gene exerted toxic effects in cultured primary motor neurons (303, 304). Importantly, silencing of astrocytic mutant SOD-1 genes significantly slowed disease

progression (305). Non-neuronal cells appear to be important in regulating disease progression rather than initiating motor neuron disease (296, 302), and an interaction between motor neurons and non-neuronal cells seems to be critical for pathogenesis (306-308).

The pathogenic mechanisms by which non-neuronal cells exert toxicity remain to be elucidated, although multiple mechanisms appear to be responsible (157). Specifically, impairment of passive properties of astrocytes, such as uptake or recycling of neurotransmitters and regulation of extracellular ion homeostasis, along with activation of microglia cells with increased secretion of neurotoxic agents, such as glutamate and pro-inflammatory cytokines, appear to be important mechanisms (94). In addition, non-cell autonomous toxicity may also be mediated by a process termed to as necroptosis, a form of programmed cell death mediated by interaction of vital protein [receptor-interacting protein 1 and the mixed lineage kinase domain-like protein] (309). Importantly, non-cell autonomous processes may serve as important therapeutic targets in ALS.

Assessment of cortical excitability

To further explore and assess the function of the central nervous system in ALS and thereby gaining a better understanding of ALS pathophysiology, we utilised ***transcranial magnetic stimulation***. TMS is a relatively painless neurophysiological technique which can be performed non-invasively by stimulating the human motor cortex, being first described by Barker and colleagues (310).

Principles of magnetic stimulation

Magnetic stimulators consist of a capacitor, thereby acting as a device which can store a charge, when discharged there is a flow of current through a coil which then subsequently generates a magnetic field. This magnetic field in turn, induces an electric field in a nearby conductor (which in respect to our study are the cortical neurons), thereby resulting in current flow and subsequent neural stimulation (311, 312). The position at which the cortical motor neuron is excited by the magnetic stimulation depends on the voltage gradient parallel to the nerve fibre. Neural anatomy in the brain is very complex, the point of neural excitation occurs at bends, branch points or at the transition from cell body to axon (313). Hence, it can be appreciated that the orientation of neurons, relative to the induced magnetic field, is critical in determining which neurons are activated.

In addition to the positioning of the magnetic coil, the physical properties of the coil can also influence neural excitation, such that circular coils induce maximum current at the coil circumference. Hence, when these magnetic circular coils are placed at the vertex, with the coil edge overlying the hand area, there will be preferential stimulation of the primary motor area. If a more focal "figure-of-eight coil" which is formed by two smaller adjacent circular coils is utilised, more focal magnetic fields are generated and hence specific positioning and orientation of the coil over the motor cortex is required to ensure adequate cortical motor neuron activation (311, 312, 314). The direction of current flow that is induced by the magnetic stimulation will dictate which cerebral hemisphere is stimulated, current flowing from a posterior-anterior direction (i.e. inion to nasion) is most effective at stimulating the motor cortex. For a circular coil positioned at the vertex, clockwise current in the coil (viewed from above) preferentially stimulates the right hemisphere (311, 312, 314).

From animal experiments it has been demonstrated that cortical stimulation can result in generation of complex corticomotoneuronal volleys composed of direct [**D]-waves** (due to direct stimulation of the corticospinal axon) and multiple indirect [**I]-waves** arising from trans-synaptic excitation of pyramidal cells via excitatory cortical interneurons (315). The D wave is produced by direct activation of corticospinal axons, whereas the I-waves are produced through secondary activation of neural elements presynaptic to the corticospinal cells (316).

In humans, TMS activates the motor cortex at a depth of approximately 1.5 to 2.1 cm (317) and cervical epidural recordings have confirmed the presence of D and I-waves, at intervals of 1.5-2.5 ms (318, 319). The I-waves are numerically labeled according to the time interval, such that the first I-wave is called I1, the second I2, the third I3 and so on (319). I-waves are best elicited by cortical currents directed in a posterior-anterior direction, whereas D-waves are produced preferentially if the current runs in a lateral to medial direction (320-324). The production of I-waves may not be sequential, such that I3 waves may be recruited prior to other I-waves, if the stimulating conditions are optimal (325). Although numerous models have been proposed to attempt to explain how I-waves are produced within the motor cortex, the mechanisms continue to remain elusive (326).

In a clinical setting, the assessment of cortical excitability and the integrity of corticospinal pathways are best evaluated by measuring the following neurophysiological parameters: (i) motor threshold; (ii) motor evoked potential (MEP) amplitude; (iii) central conduction time; (iv) cortical silent period; and (v) short interval intracortical inhibition and facilitation.

(i) Motor threshold

Motor threshold (MT) reflects the ease with which corticomotoneurons are excited, the International Federation of Clinical Neurophysiology proposed its assessment to be the minimum stimulus intensity required to elicit a small (usually >50 μV) motor evoked potential (MEP) in the target muscle in 50% of trials (327). Recently employed threshold tracking techniques, can measure MT as the stimulus intensity required to elicit and maintain a target MEP response of 0.2 mV (328-330). Motor threshold is thought to reflect the density of corticomotoneuronal projections onto spinal motor neurons, whereby the intrinsic hand muscles exhibit the lowest MTs due to the highest density of projections (331-333), and whereby the MTs are lower in the dominant hand (333), and as such correlate with the ability to perform fine fractionated finger movements (334). Further to reflecting the density of corticomotoneuronal projections, MTs may also be act as a biomarker of cortical neuronal membrane excitability (317, 335, 336). Studies have shown that MTs can be influenced by the glutamatergic neurotransmitter system, through AMPA receptors, and excessive glutamate activity may reduce MTs (337). Inhibition of voltage-dependent Na^+ channels with agents such as carbamazepine increases MT (338-340). Of further relevance, MTs are influenced by the state of wakefulness and by the extent of target muscle activation (311, 341).

Motor threshold findings in ALS have been varied and inconsistent. Some TMS studies have reported an increased MT or even an inexcitable motor cortex (40, 342-348), whereas other studies have shown either normal or reduced MT (41, 45, 183, 185, 349, 350). Interestingly, in longitudinal studies, there is a reduction of MTs early in the disease course, thereafter, the MT increases to the point of cortical inexcitability, correlating with disease progression (350). Early reductions in MTs appear to be most prominent in ALS patients with profuse

fasciculations, preserved muscle bulk and hyper-reflexia (249). The findings of fasciculations preceding other clinical features of ALS by several months, when interpreted with reduced MTs, may suggest a cortical origin of fasciculations (351). Excess glutamergic activity and thereby glutamate excitotoxity, along with reduced GABAergic inhibition may underlie the development of reduced motor thresholds in ALS. The findings of reduced MTs early in the disease process may support an anterograde trans-synaptic process, where cortical hyperexcitability potentially underlies the development of progressive neurodegeneration.

(ii) Motor evoked potential (MEP Amplitude)

The MEP amplitude reflects the summation of complex corticospinal volleys consisting of D and I waves onto the spinal motor neuron (335, 352). At the motor threshold, TMS elicits I-waves at intervals of 1.5 ms, which increase in amplitude with increasing stimulus intensity (352). As the MEP amplitude increases with increasing stimulus intensity, it may then be possible to generate a ***stimulus-response curve*** which follows a sigmoid function (353). The MEP amplitude is thought to reflect the density of corticomotoneuronal projections onto spinal and bulbar motor neurons (354), it may partly assesses the function of cortical neurons that are positioned further away from the center of the TMS field, or assess cortical neurons that are less excitable (312). To accurately to account for LMN dysfunction, the MEP amplitude should be expressed as a percentage of the maximum peripheral CMAP response (327). The sensitivity and thereby the diagnostic utility of the MEP/CMAP ratio in detecting UMN dysfunction, is limited by a large inter-subject variability (312, 355).

The MEP responses may also be modulated other neurotransmitter systems within the central nervous system (354, 356). Specifically, GABAergic neurotransmission via $GABA_A$ receptors suppresses, while glutamatergic and noradrenergic neurotransmission enhances the

MEP amplitude (340). The changes in MEP amplitude may occur independently of MT changes, thereby suggesting that the physiological mechanisms underlying the generation of MEP amplitude and MTs are varied.

Abnormalities of MEPs have been extensively documented in ALS patients (39, 312). Specifically, the MEP amplitude is increased in all forms of ALS, including both sporadic and familial forms of ALS, it appears to be most prominent in early stages of the disease process (183, 185, 240). The MEP amplitude also correlates with surrogate biomarkers of axonal degeneration, thereby suggesting an association between cortical hyperexcitability and motor neuron degeneration (183, 184). This increase in MEP amplitude appears to be specific for ALS, with no similar findings in mimic disorders, despite a comparable degree of LMN dysfunction, arguing against adaptive secondary changes as a result of simple cortical plasticity (237-239, 357).

(iii) Central motor conduction time (CMCT)

The central motor conduction time reflects the time from stimulation of the motor cortex to the arrival of corticospinal volley at the spinal motor neuron (327). A number of factors have been attributed to the contribution of the CMCT including, time to activate the corticospinal cells, conduction time of the descending volley down the corticospinal tract, synaptic transmission and activation of spinal motor neurons (358). The calculation of the CMCT may be done by two methods, the F-wave method (see Methodology) or cervical (or lumbar) nerve root stimulation methods (359, 360). Given that both methods estimate the CMCT (311, 358), and a number of technical, physiological and pathological factors influence CMCT (358), a range of normative CMCT data exists.

The central motor conduction time has been shown to be prolonged in approximately 20% of ALS cases (40, 350, 361), it likely reflects degeneration of the fastest conducting corticomotoneuronal axons, with the possibility of concomitant increased desynchronization of corticomotoneuronal volleys secondary to the axonal loss (46, 349, 362). Some have advocated for utilising the CMCT when clinical features of UMN signs are equivocal (40, 350). The sensitivity of detecting a prolonged CMCT in ALS may be improved by recording from both, the upper and lower limb muscles, or from the cranial muscles with bulbar-onset disease (39, 314, 348).

(iv) Cortical silent period (CSP)

The cortical silent period (CSP) refers to a neurophysiological parameter that results from interruption of voluntary electromyography (EMG) activity in a target muscle, when magnetic stimulation is applied over the contralateral motor cortex (363). The measurement of the CSP duration is from the onset of the MEP response to the resumption of voluntary EMG activity (354, 363). With increases in magnetic stimulus intensity, there is a prolongation of the CSP duration (363-365).

The underlying mechanism of the CSP appears to be complex and multifactorial in nature. It has been shown that the early segment of the CSP is mediated by spinal processes (364, 366), whilst the later segment is mediated by long-lasting inhibitory post-synaptic potentials (IPSP), generated via gamma-aminobutyric acid type B ($GABA_B$) receptors (312, 364, 366, 367), this is supported by pharmacological studies utilising GABAergic compounds (368, 369). The $GABA_B$ receptors are metabotropic receptors that are coupled to Ca^{2+} and K^+ channels via G proteins and second messenger systems, located at the pre-and postsynaptic nerve terminals (370). It is postulated that post-synaptic $GABA_B$ receptors mediate CSP by

activating a specific G-protein, inducing an increase in K^+ efflux, which then results in hyperpolarization of the postsynaptic membrane (370). Conversely, the presynaptic $GABA_B$ receptors mediate inhibition through voltage-gated Ca^{2+} channels, resulting in inhibition of neurotransmitter release (371-373). Furthermore, in addition to the $GABA_B$ receptor modulation, the CSP is also influenced by the density of the corticomotoneuronal projections onto motor neurons, motor attention, the extent of voluntary drive and other neuromodulators, such as dopamine (312, 338, 374, 375).

The CSP abnormalities are well described in ALS (354), specifically a reduced or unchanged CSP duration has been reported in ALS, with the reduction is CSP duration being most prominent early in the disease process (43, 45, 182, 183, 185, 238, 239, 361, 376, 377). Amongst neuromuscular disorders the reduction of CSP duration appears specific for ALS, with a normal CSP reported in Kennedy's disease, acquired neuromyotonia and distal hereditary motor neuronopathy with pyramidal features (237-239, 357). Although the underlying mechanisms of the reduced CSP duration in ALS remain to be fully established, reduced GABAergic inhibition and decreased motor drive, due to a combination of inhibitory interneuronal degeneration or dysfunction of $GABA_B$ receptors, may underlie the reduced CSP duration in ALS.

(v) Paired-pulse techniques

Transcranial magnetic stimulation may also be performed by a paired-pulse technique to assess cortical excitability, in this paradigm a conditioning stimulus modulates and precedes the effects of a second test stimulus. To date there have been several different paired-pulse paradigms developed (39, 312, 354). Neurophysiologically the two parameters that have

been utilised most commonly are the *short interval intracortical inhibition (SICI)* and *intracortical facilitation (ICF)*, frequently utilised in ALS clinical research as methods to determine cortical excitability. Hence, in this thesis the two parameters discussed and utilised are the SICI and ICF.

When a subthreshold conditioning stimulus (set to 70 of RMT) is delivered by a paired-pulse paradigm at pre-determined time intervals before a suprathreshold test stimulus, it is possible to measure the short interval intracortical inhibition (SICI) (329, 378-380). When the technique was first developed, the conditioning and test stimuli remained constant and the effects of the conditioning stimulus were measured by recording changes in the MEP amplitude. When the pulses are delivered between the interstimulus interval (ISI) of 1-5 ms, the test response was inhibited ***(SICI)***. With increasing interstimulus intervals of 7 and 30 ms, there is a facilitation of the test response ***(ICF)*** (312).

Both, SICI and ICF are generated at the level of the motor cortex (352, 380). Epidural recordings have established that SICI is associated with reduction in number and amplitude of late I-waves, mediated by inhibitory cortical interneurons via $GABA_A$ receptors (379, 381). Conversely ICF was associated with an increase in the I-wave amplitude, being reduced by $GABA_A$ receptor agonists (338). $GABA_A$ receptors are ionotropic in that they directly gate Cl^- selective ion channels and possess modulatory binding sites for benzodiazepines, barbiturates, neurosteroids and ethanol (382, 383). The $GABA_A$ receptors consist of five protein subunits arranged around a central pore, each subunit consists of an extracellular N-terminal domain, followed by three membrane spanning domains (M 1-3), of which the M2 domain forms the pore channel, an intracellular loop and a fourth membrane spanning domain (M4) (384). Sixteen different subunits could potentially comprise the

$GABA_A$ receptor, including α1–6, β1–3, γ1–3, δ, ε, π and θ, with the α1β2/3γ2, α2β3γ2, and α3β3γ2 subunit combinations being the most frequent (384-386).

SICI appears to be mediated by $GABA_A$ receptors comprised of the alpha 1 subtype (387). Furthermore both SICI and ICF are also modulated by other cortical neurotransmitter systems including glutamate (39, 224, 388, 389), dopamine (338, 390) and norepinephrine (338), and selective serotonin re-uptake inhibitors (391). Importantly, SICI and ICF appear to be physiologically distinct processes as evident by lower thresholds for activation of SICI and that SICI remains independent of the direction of subthreshold conditioning current flow within the motor cortex, while ICF appears to be preferentially generated by current flowing in a posterior-anterior direction (392).

One of the limiting factors with the original "constant stimulus" technique was marked variability in the MEP amplitude with consecutive stimuli (379, 393). The variability of the MEP responses in part was related to spontaneous fluctuations in the resting threshold of cortical neurons. To overcome this variability, a ***threshold tracking technique*** was developed, whereby a constant target MEP response (0.2 mV) was tracked by a test stimulus (328, 329). By utilizing threshold tracking, two distinct phases of SICI were identified (328, 329, 394, 395), a smaller phase at ISI ≤1 ms and a larger phase at ISI 3 ms. The second phase of the SICI it thought to be related to synaptic neurotransmission through the $GABA_A$ receptors (381, 396-398), however, the precise mechanisms underlying the first phase of SICI remains unresolved. One suggestion was that the first phase of SICI reflected local excitability properties, particularly relative refractoriness of cortical axons, with resultant resynchronization of cortico-cortical and corticomotoneuronal volleys (328, 399).

Synaptic processes therefore, could best explain the development of the initial phase of the SICI, driven by activation of cortical inhibitory circuits that were distinct from the circuits mediating the later SICI phase (394, 395, 400). Hyperexcitability therefore, is defined as a reduction or absence of SICI, with increase in ICF also supporting this notion. These findings of reduced SICI and increased ICF have been well documented in sporadic and familial ALS patients (45, 183, 185, 238, 357, 388, 401-405). Cortical hyperexcitability appears to be an early pathophysiological process in ALS, correlating with measures of peripheral neurodegeneration and preceding the clinical development of familial ALS (183, 185).

The reduction or absence of SICI in ALS have been attributed to degeneration of inhibitory cortical interneurons (406) along with glutamate-mediated excitotoxicity (224, 388). Underscoring this notion is the findings of SICI abnormalities in ALS at low (40% of resting motor threshold (RMT), medium (70% of RMT) and high (90% of RMT) conditioning stimulus intensities (407). One potential therapeutic option in ALS is attempting to preserve the integrity of intracortical inhibitory circuits, and counteracting excitatory cortical circuits.

Axonal Excitability Testing

Threshold tracking techniques can also be utilized to assess peripheral nerve function (408, 409). In the context of axonal function, the term threshold refers to the stimulus current required to produce a specific potential. Utilising threshold tracking, changes in the test stimulus current intensity required to generate a preset amplitude can be adjusted on-line to keep the target amplitude constant (*see Methodology*). The utility of axonal excitability to

probe axonal ion channel function, may provide unique insights into the generation of the peripheral findings that underlie the generation of symptoms in ALS, such as fasciculations and cramps, as well as probe processes responsible for motor neuron degeneration in ALS (35, 410-413). In this thesis, we utilized the threshold tracking protocol, measuring the following parameters of axonal excitability: threshold; strength-duration time constant; rheobase; threshold electrotonus; current/threshold relationship; and recovery cycle.

(i) Threshold

In axonal excitability studies, the term threshold refers to the amount of stimulus current required to activate an axon and thereby produce a compound muscle action potential of a specific amplitude (408, 409). The threshold may be utilised as a surrogate biomarker of membrane potential, whereby membrane hyperpolarization increases and depolarization decreases the membrane threshold. The threshold can be influenced by such instances of hyperventilation or nerve ischemia, and in that instance it may not accurately reflect membrane potential. Therefore, in those circumstances the ambiguity may be resolved by measuring other indices of axonal excitability (414-418).

(ii) Strength duration time constant and rheobase

The strength-duration time constant (τ_{SD}), which is also known as chronaxie, measures the rate at which the threshold current for a target potential declines as the stimulus duration is increased (419-421). The τ_{SD} in human peripheral nerves can be calculated by using the ratio between stimulus-response curves for two different stimulus durations according to the Weiss' formula (422). Rheobase is the threshold current (mA) for stimulus of infinitely long

duration (409). The τ_{SD} and rheobase are properties of the nodal membrane, being dependent on passive membrane properties and persistent Na^+ channel conductances [I_{NaP}] (423).

The persistent Na^+ currents, constitute approximately 1-2% of the total Na^+ current (423-425) and are conducted through voltage-gated Na^+ channels composed of one alpha (α) and four beta (β1-4) subunits (426, 427). The channels are structured, such that the α subunits are organized in four homologous domains (I-IV), each consisting of six transmembrane α helices (S1-S6) and a pore loop located between the S5 and S6 segments that acts as a selectivity filter. The S4 segments of each domain functions as a voltage sensor. The inactivation of Na^+ channels is mediated by a short intracellular loop connecting homologous domains III and IV, which fold into the channel structure and blocks the pore from the inside during sustained membrane depolarization. When there is inactivation of the I_{NaP} , it occurs very slowly or incompletely (428). At least ten distinct Na^+ channel isoforms have been identified to date, Na_v 1.1 to Na_v 1.9 and Na_x (426, 427, 429), with I_{NaP} conducted by the Na_v1.6 isoform which is expressed at the nodes of Ranvier (426, 427, 429, 430).

A full understanding of the I_{NaP} channel is yet to be determined, however it has been proposed that a uniform population of Na^+ channels may generate both transient and persistent Na^+ currents by switching between different gating modes (431). Amino-acid residue phosphorylation within the alpha subunit of voltage-gated Na^+ channels may underlie these gating changes (432, 433).

Changes in the strength duration-time constant and rheobase may be influenced by the resting membrane potential, such that depolarization reduces rheobase and prolongs τ_{SD}, whilst hyperpolarization exerts the opposite effects. Furthermore, changes in nerve geometry, such

as axonal loss or demyelination, may also influence the τ_{SD}, as may discrete changes in nodal Na^+ conductances (434-437). In ALS, the finding of prolonged τ_{SD} may lead to excessive ectopic axonal activity, underlying the generation of fasciculations and cramping, as well as neurodegeneration (34, 183, 184, 413, 437-439). Furthermore, upregulation of I_{NaP} may underlie neurodegeneration by increasing the intracellular concentration of Ca2+ (210, 440, 441).

(iii) Threshold Electrotonus

Threshold electrotonus (TE) describes the changes in threshold produced by long-lasting subthreshold currents and provides insight into into both nodal and internodal membrane conductances (408). This technique measures changes in threshold current produced by a long-duration polarizing current (408, 442) The conditioning currents are subthreshold and in themselves do not trigger an action potential, but rather result in local changes in the membrane potential (408, 409). The TE is usually measured by long duration 1 ms current pulses, which is long compared to the time constant of the nodes of Ranvier, but short compared with the time constants of the internodal membrane and slowly activating ion channels (443). The changes in the threshold current can be measured at varying conditioning-time intervals in response to subthreshold conditioning currents (444, 445). By conventional TE is plotted in a way that, an increase in excitability (threshold reduction) produces an upwards deflection and a decrease in excitability, a downward deflection. The reason this convention was adopted was so changes in threshold electrotonus would resemble the underlying changes in membrane potential. The ‘threshold tracking’ protocol of axonal excitability testing utilizes test stimuli of 1-ms duration to produce the target CMAP response (40% of maximal) and changes in threshold induced by subthreshold polarizing currents of

100 ms in duration, set to + 40% (depolarizing) and − 40% (hyperpolarizing) of the control threshold current (444).

The initial fast response ("F" phase, Figure 4) reflects rapid changes in threshold at the node of Ranvier, resulting from the application of either a depolarizing or hyperpolarizing subthreshold current. This is followed by slower changes in threshold over tens of milliseconds in both depolarizing and hyperpolarizing directions, called the "S1" phase, and reflects the spread of current to the internodal membrane (Figure 4). During the depolarization phase, the S1 phase peaks at 20 ms after the onset of the current pulse, after which threshold begins to return to baseline, the S2 phase. This S2 phase occurs due to activation of nodal and internodal slow K^+ channels (408, 442).

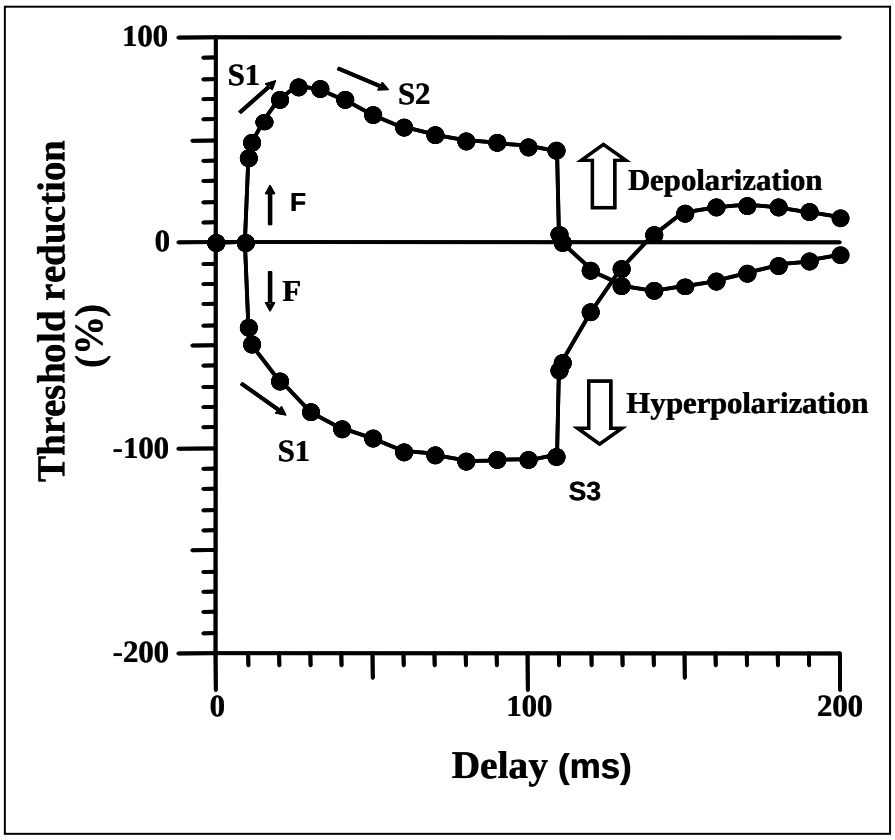

Figure 4. Threshold changes to polarising currents of 100 ms duration set to ± 40% of resting threshold. Changes are plotted with threshold reductions, with depolarisation represented as an upward deflection and hyperpolarization in a downward direction. *Reproduced with permission S.Vucic 2007.*

During the hyperpolarization phase, the S1 phase peaks at 100-150 ms after the onset of the subthreshold conditioning current and then proceeds to return to baseline thereafter, termed the S3 phase (Figure 4). This accommodative phase, the S3 phase, is due to activation of the hyperpolarizing-activated inward rectifying currents (I_H) (408, 409, 446, 447). On termination of the subthreshold conditioning currents, there is an overshoot of threshold with both depolarization and hyperpolarization. With depolarization, slow K^+ channels mediate the overshoot, whilst in hyperpolarization the overshoot is mediate by I_H.

The voltage-gated K^+ channels are members of the voltage-gated ion channel protein superfamily (448), and are composed of four alpha pore-forming subunits and accessory β subunits (449). In human myelinated axons voltage-gated K^+ currents are activated by depolarization, and three types of currents have been identified, including two fast (I_{Kf1} and I_{Kf2}) and one slow current (I_{Ks}). The slow (S) channels underlie the S2 phase of TE, exhibit slower deactivating kinetics and are located at both the node and internode (446, 450-454). The internodal S channels play an important role in the maintenance of the internodal resting membrane potential, thereby contributing to the nodal resting potential and increasing the safety factor of impulse conduction (450, 455).

Alterations in membrane potential result in changes in threshold electrotonus. Specifically, with membrane depolarization there is a reduction in the resistance of the internodal membrane, due to activation of paranodal and internodal K+ channels, resulting in reduction of the S1 phase in both depolarizing and hyperpolarizing directions, thereby causing a "fanning in" appearance of TE (408, 409, 456). Conversely, hyperpolarization closes the

paranodal and internodal K^+ channels, thereby increasing the S1 and S2 phases producing a fanning out appearance (408, 409, 456).

The alterations in TE were first described in ALS, whereby two distinct responses were described; (i) TE recordings with greater threshold reductions during depolarization *(Type 1 response*) and (ii) TE recordings with an unexpectedly rapid increase in threshold during depolarisation (*Type 2 response)* (32, 413). The mechanism underlying this was felt to be a reduction in internodal slow K^+ channel conduction. Abnormalities of TE have now been reported in several conditions including autoimmune neuropathies, such as multifocal motor neuropathy (457), as well as in metabolic and chemotherapy related neuropathies (33, 446, 458-463).

(iv) Current threshold relationship (I/V)

Changes in threshold can also be plotted in response to long duration subthreshold currents (200ms duration) applied in a ramp like fashion, referred to as the current-threshold relationship (I/V plot), with currents applied from +50% (depolarizing) to −100% (hyperpolarizing) of the control threshold in 10% steps (444, 445). Conventionally, threshold increases (hyperpolarization) are plotted to the left and threshold decreases (depolarization) to the right (Figure 5). The I/V relationship estimates rectifying properties of both nodal and internodal axonal segments (408). The I/V gradient induced by depolarizing sub-threshold currents reflects conduction through outward rectifying K^+ channels, while the I/V gradient during hyperpolarizing sub-threshold currents reflects inwardly rectifying conductances [I_H] (408).

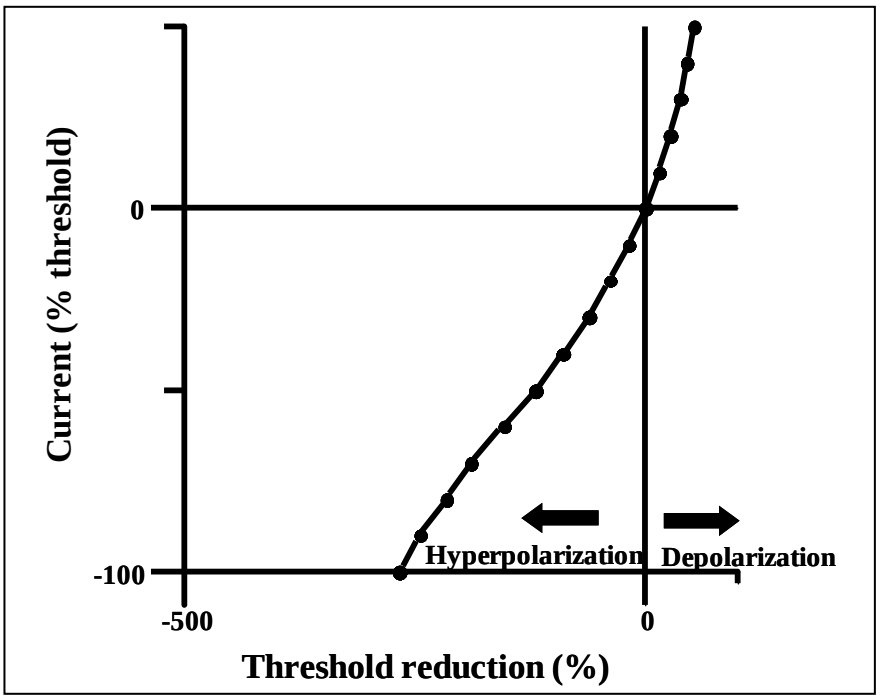

Figure 5. Current-threshold relationship: normalised threshold changes at the end of 200 ms duration currents are plotted, with depolarization represented to the right and hyperpolarization to the left. The conditioning current is varied from +50 % to –100 % of control threshold. *Reproduced with permission S.Vucic 2007.*

Two basic types of current underlie inward rectification (464). The first type, which is the classic inward rectifier, is related to a pure K^+ conducting channel, which is activated at membrane potentials negative to the K^+ equilibrium potential (465, 466). The second type of inward rectification is mediated by a channel that exhibits conductance for both Na^+ and K^+ (467, 468). This current begins to activate at between -45 mV and -60 mV and peaks at -110mV (465, 469). The second I_H current activates and deactivates slowly, and the magnitude of the I_H current is also dependent on extracellular K^+ concentration (468).

A major function of internodal I_H is to limit electrogenic hyperpolarization and the consequent reduction of axonal excitability in response to high-frequency activity (467). Given that high-frequency activity can induce failure of impulse conduction in axons with a reduced safety factor of transmission, the I_H current may be critical in preventing such conduction failure (470). In primary demyelinating neuropathies, motor nerves may have a

predilection to develop activity-dependent conduction failure (471, 472) in contrast to sensory nerves, due to the reduced expression of I_H in motor nerves (473, 474).

(v) The recovery cycle of axonal excitability

Once there is conduction of an action potential, the axons undergo a series of stereotyped excitability changes known as the recovery cycle (Figure 6). Initially, there is a period of total axonal inexcitability, lasting for 0.5-1 ms during which the axon cannot generate an action potential, termed the **absolute refractory period**. Following this period, the axon enters a **relative refractory period (RRP)**, during this period an action potential may be generated by stronger than normal stimulus currents. This period lasts for up to 4ms and may be measured as an increase in current required to generate a potential (termed refractoriness), or as the duration of the RRP, the point where the recovery cycle curve crosses the x-axis (Figure 6).

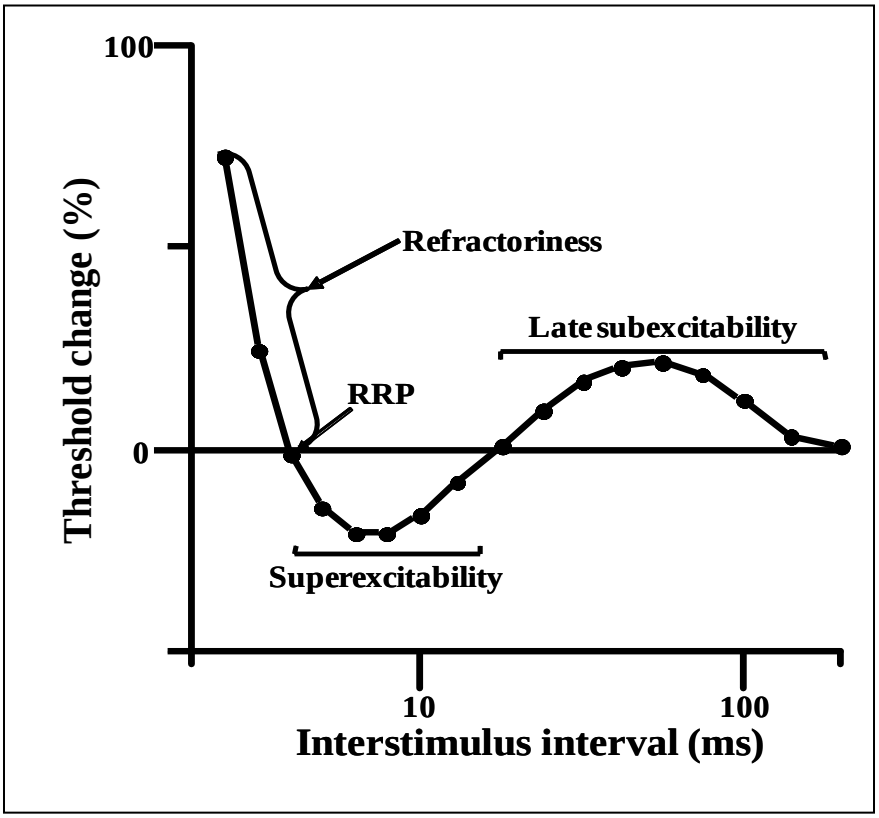

Figure 6. Recovery cycle of excitability is assessed by tracking the changes in threshold that occur following a supramaximal conditioning stimulus of 1-ms duration. RRP refers to the 'relative refractory period'. *Reproduced with permission S.Vucic 2007.*

The absolute refractory period is secondary to inactivation of nodal voltage-gated transient Na^+ channels, while the RRP results from gradual recovery of these channels from inactivation (475). Similar to the persistent Na^+ channels these transient Na^+ channels are of the $Na_v1.6$ isoform, and consist of alpha and beta (β) subunits (427), and exhibit "fast" activation and inactivation kinetics, namely the channels open rapidly with depolarization and inactivate rapidly (427, 476). Transient Na+ currents are first detected at membrane potentials of -55 mV, peaking at ~ -30 mV and underlie the rapid phase of depolarization of the action potential (409).

The changes in membrane potential can influence Na^+ channel kinetics, and subsequently affect refractoriness (409). At normal resting membrane potential, approximately 30% of Na^+ channels are inactivated, with hyperpolarization there is a shift to reduce the degree of "inactivated" Na^+ channels, this then leads to a decrease in refractoriness. Conversely, depolarization increases the extent of Na^+ channel inactivation, subsequently increasing refractoriness (409). Refractoriness is also sensitive to temperature changes, with refractoriness being increased by reductions in limb temperature (477, 478).

Following refractoriness there is a period of increased axonal excitability, termed **superexcitability**, lasting for approximately 15 ms. This period is mediated by re-excitation of the nodal membrane by the discharge of current stored on the internodal membrane following an action potential, also known as the depolarizing long-lasting afterdepolarization (DAP) (409, 479). The amplitude and time course of DAP is limited by activation of paranodal and juxtaparanodal K^+ channels, which serve to reduce the degree of DAP, and thereby superexcitability, by shunting the internodal current (480). Paranodal K^+ channels are kinetically classified into fast (F) channels and intermediate (I) channels (452, 453, 481).

F channels are activated at potentials between -40 and +40 mV, then deactivating very rapidly at potentials between -120 mV and -65 mV (454, 482, 483). In contrast, I channels are first activated by depolarization to around -70 mV, becoming fully activated at around -40 mV and then deactivating slowly (483).

Superexcitability can be influenced by changes in membrane potential, membrane depolarization reduces superexcitability by limiting Na^+ influx and increasing K^+ efflux through paranodal and juxtaparanodal fast K^+ channels (484). Conversely, membrane hyperpolarization increases DAP and therefore superexcitability. Subsequently, superexcitability may be used as an indicator of membrane potential (444).

The final phase of the recovery cycle is referred to as **late sub excitability.** This period denotes a reduction in axonal excitability and lasts for approximately 100ms. This period is defined by activation of nodal slow K^+ channels (467) and is influenced by both the membrane potential and the K^+ equilibrium potential. As such, current induced membrane depolarization, which changes the electrochemical gradient for K+, increases late subexcitability. Conversely, membrane depolarization secondary to increases in extracellular K+ concentration, as occurs with ischemia or renal failure, results in reduction of late subexcitability (456, 458, 460, 485).

In this thesis both cortical excitability and axonal excitability studies will be utilised in sporadic and familial ALS patients, in order to determine the diagnostic utility of cortical and pathophysiological processes underlying neurodegeneration in ALS.

METHODOLOGY

Subjects

The healthy subjects utilized in this study as the 'control' population had no clinical evidence of a peripheral nerve disorder or any history of medical conditions known to affect peripheral nerve function. Before testing was undertaken it was ensured that patients were not on other medications which could influence the parameters of cortical excitability testing (338, 486-488). ALS patients who had a history of other illnesses like diabetes mellitus or other conditions which are known to cause neuropathy were excluded from all axonal excitability studies. All patients were diagnosed and catergorised using the Awaji criteria as 'possible', 'probable', 'probable lab-supported' or 'definite ALS' (6). Where patients were utilized in diagnostic studies, they were followed up over a three year period to confirm disease progression and thereby confirm the diagnosis of ALS. All patients and subjects gave written informed consent to the procedures, which had been approved by the Sydney West Area Health Service Human Research Ethics Committees and the University of Sydney Human Research Ethics committee.

Equipment

The list of equipment which was utilized to perform the studies in this thesis are listed:

Hardware requirements:

1) Personal computer fitted with a 16-bit data acquisition card (National Instruments PCI-MIO-16E-4) that sampled signals at 10 kHz.

2) Isolated linear bipolar constant stimulator (maximal output ± 50 mA) (DS5, Digitimer, Welwyn Garden City, UK)

3) Conventional non-polarisable 5-mm Ag-AgCl surface EMG electrodes (3M Healthcare, MN, USA) for stimulation and recording.

4) Preamplifier and filter (3 Hz-3 kHz) for recording sensory and motor potentials Nicolet-Biomedical EA-2 amplifier (Cardinal Health Viking Select version 11.1.0, Viasys Healthcare Neurocare Group, Madison, USA).

5) Electronic noise was further filtered by using a Hum Bug (Hum Bug 50/60 Hz Noise Eliminator, Quest Scientific Instruments, North Vancouver, Canada)

6) Two high-power magnetic stimulators which were connected via a BiStim device (Magstim Co., Whitland, South West Wales, UK).

7) Circular stimulation coil for transcranial magnetic stimulation (Magstim Company: High Power 90mm Coil -P/N9784-00)

8) Purpose built thermometer for measuring skin temperature.

9) Synergy EMG machine, Neurocare Group, Madison, USA.

10) 26 G concentric EMG needle (Dantec DCN™ Disposable Concentric Needle Electrodes)

Software requirements:

1) Data acquisition and stimulation delivery (both electrical and magnetic) were controlled by a computerised threshold tracking programme, QTRACS software version 16/02/2009 (© Professor Hugh Bostock, Institute of Neurology, Queen Square, London, UK).

Stimulating and Recording Paradigms

The peripheral nerve studies which were described in Chapters 3-8 were undertaken over the median nerve (Figure 7) using conventional non-polarisable 5-mm Ag-AgCl surface EMG electrodes (3M Healthcare, MN, USA). Median nerve stimulation was performed electrically

at the wrist, the cathode was placed at the wrist crease and the anode was placed at the mid-forearm. The compound muscle action potentials (CMAPs) were recorded via surface electrodes with the active recording electrode positioned over the motor point of the abductor pollicis brevis (APB), the reference electrode was placed 4 cm distally over the proximal phalanx of the thumb (444) (Figure 7).

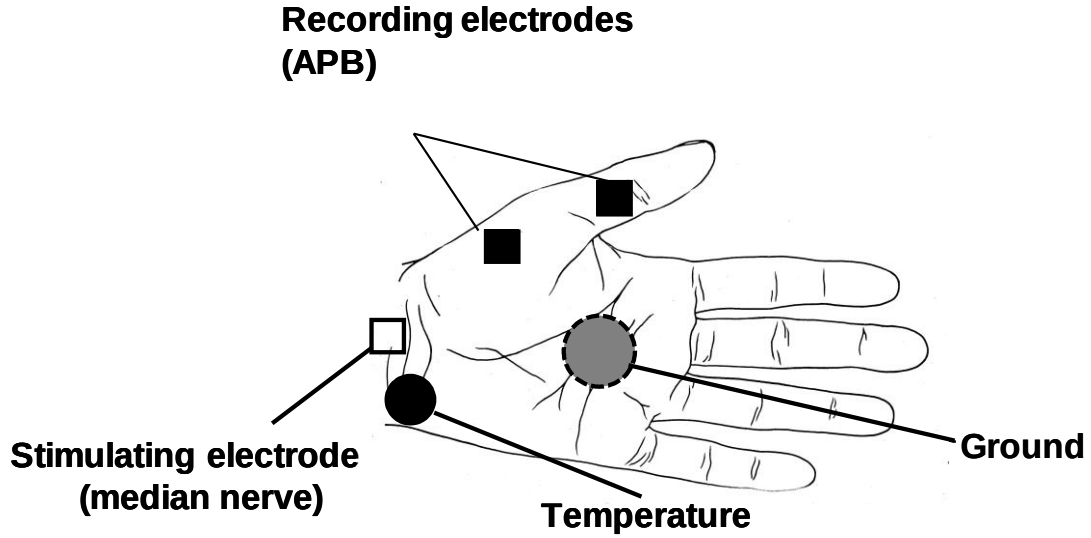

Figure 7. The configuration of the stimulating and recording electrodes for peripheral nerve stimulation. The median motor is stimulated at the wrist with recording over the abductor pollicis brevis muscle (APB). The motor evoked potentials are recorded over APB muscle using the same recording electrode configuration.

Threshold tracking and excitability protocols

Cortical excitability studies

Cortical excitability studies which are described in Chapters 3-5, 7-8 were performed by transcranial magnetic stimulation (TMS), with the motor cortex stimulated utilising a 90 mm circular coil. The coil was oriented to induce a current flow in a posterior-anterior direction in order to preferentially activate the motor cortex. The coil, initially centered over the vertex, was moved in the antero-posterior and medial-lateral directions in order to ascertain the optimal position for evoking responses of maximal amplitude from the target muscle (abductor pollicis brevis (APB)). The magnetic currents were generated by utilising two high-power magnetic stimulators connected via a BiStim device (Magstim Co., Whitland, South West Wales, UK). By utilising two stimulators the conditioning and test stimuli could be independently set and delivered through one coil. The magnetic evoked potentials (MEPs) were recorded using surface electrodes and the peak-to-peak amplitude and onset latency were determined for MEPs.

TMS threshold tracking (Figure 8)**:** A paired pulse cortical stimulation technique was performed using the threshold tracking TMS protocol (329). With this protocol, the output (MEP response) was fixed (at 0.2mV) and changes in the test stimulus intensity required to generate a target response, when preceded by either sub- or suprathreshold conditioning stimuli, were measured.

It has been previously established by Fisher and colleagues in 2002 that the relationship between the logarithm of the MEP amplitude and the stimulus was close to linear over a hundred-fold range of responses, from about 0.02 to 2 mV (489). Based on these findings, a

small target response of 0.2 mV (±20%), which lies in the middle of this linear range, was selected for the present study and subsequently tracked. The resting motor threshold (RMT) was defined as the stimulus intensity required to produce and maintain the target MEP response (0.2 mV peak-to-peak) (329).

Initially, the stimulus response (SR) curve for cortical stimulation was determined by increasing the intensity of the magnetic stimulus to the following levels: 60, 80, 90, 100, 110, 120, 130, 140 and 150% of RMT. Three stimuli were delivered at each level of stimulus intensity. The maximum MEP amplitude (mV) and MEP onset latency (ms) were recorded. Central motor conduction time (CMCT, ms) was calculated according to the F-wave method (490, 491).

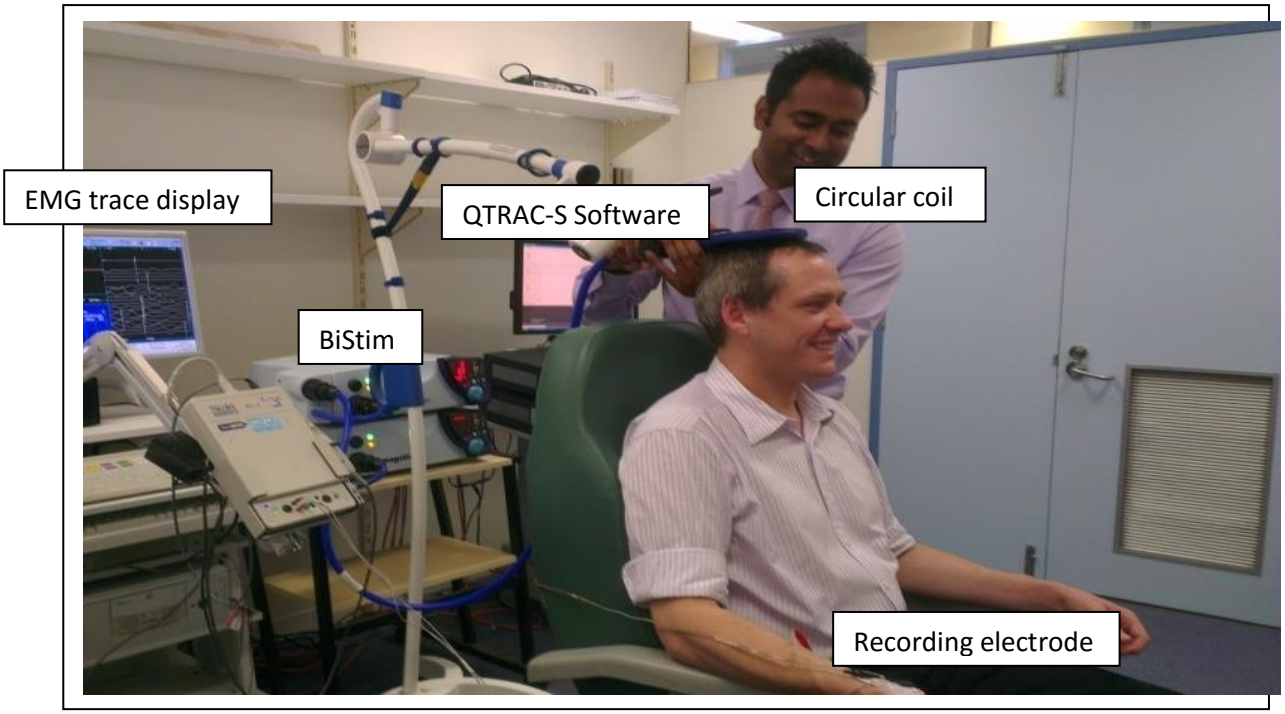

Figure 8. Threshold tracking transcranial magnetic stimulation: equipment and recording configuration.

The cortical silent period (CSP), which was induced by single-pulse TMS was recorded whilst performing a weak voluntary contraction, estimated to be around 10-30 % of maximum voluntary contraction. To aid in assessing the level of muscle contraction, audio feedback was provided to the subject, to help them sustain the contraction at the required force. Similar to the generation of the SR curve, the magnetic stimulus intensity was varied at preset levels. The duration of the silent period was measured from the beginning of the MEP response to the return of EMG activity (492).

A paired-pulse paradigm was developed (329) whereby a subthreshold conditioning stimulus preceded a suprathreshold test stimulus at increasing interstimulus intervals (ISIs) as follows: 1, 1.5, 2, 2.5, 3, 3.5, 4, 5, 7, 10, 15, 20, and 30 ms. The chosen subthreshold conditioning stimulus was set at 70% RMT, which did not evoke a response. Stimuli were delivered sequentially as a series of three channels (Figure 9): channel 1 tracked the stimulus intensity required to produce the unconditioned test response (Figure 10A and B); channel 2 monitored the subthreshold conditioning stimulus so as to ensure that a MEP response was not produced and to ensure the subject remained relaxed; and channel 3 tracked the stimulus required to produce the target MEP when conditioned by a subthreshold stimulus equal in intensity to that on channel 2. Tracking was deemed acceptable when the test stimulus produced two consecutive MEP responses that were within 20% of the target response (0.2 mV) or consistently oscillated about the target. The three channels were applied sequentially. The stimulus deliveries were limited by the charging capacity for the BiStim system and were delivered every 5-10 seconds. The computer advanced to the next ISI only when tracking met the target criteria. The precision of the tracking method was limited by the fact that the intensity of the magnetic stimulus was restricted to integral values from 1% to 100% of maximum stimulator output.

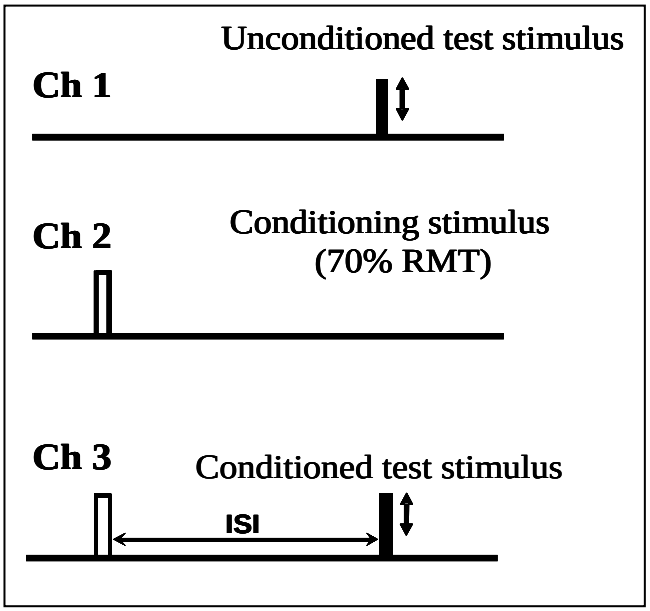

Figure 9. Experimental paradigm and configuration of stimulus patterns used in Chapters 3-5, 7 and 8. Cortical excitability was assessed by measuring changes in stimulus intensity required to generate a target magnetic evoked potential response of 0.2 mV, when recording over the abductor pollicis brevis. Channel 1 = unconditioned test stimulus, measuring resting motor threshold (RMT); Channel 2 = conditioning stimulus, which was set to subthreshold (70% RMT) when assessing short interval intracortical inhibition; Channel 3 = conditioned test stimulus at different interstimulus intervals (ISIs). SICI was measured by increasing ISI from 1-30 ms. *Reproduced with permission S.Vucic 2007*

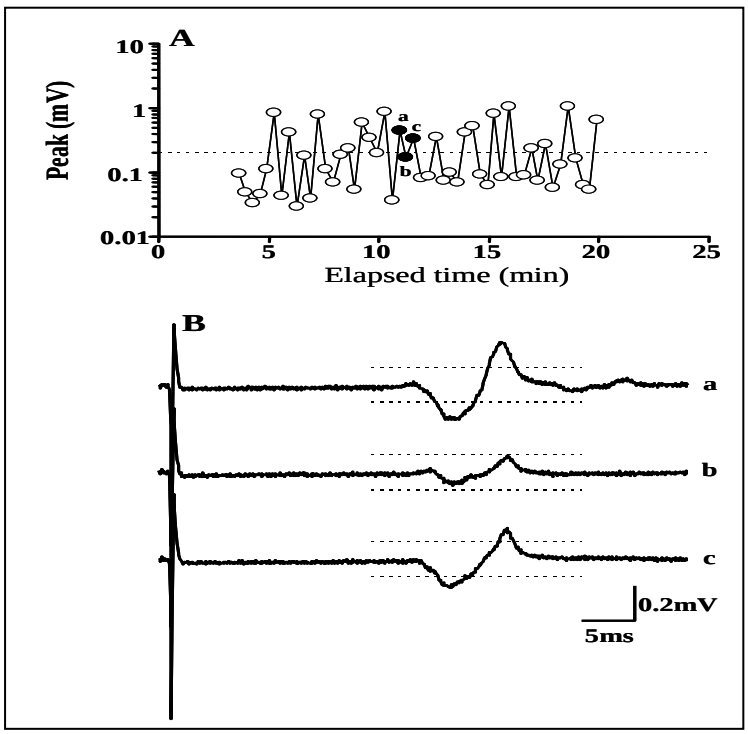

Figure 10. **(A)** Illustration of threshold tracking. The dashed horizontal line represents the target output of 0.2 mV which was "tracked". The circles (clear and filled) represent the magnitude of the motor evoked potential (MEP) amplitude with each stimulus. **(B)** Illustration of three MEP responses of different amplitude. The MEP response is initially larger **(a)**, then smaller **(b)**, and again larger **(c)** then the target output of 0.2 mV in three consecutive stimuli. These are depicted as filled circles in Figure A. The dashed horizontal lines represent the tracking windows, which were set to 0.2 mV (peak-to-peak). *Reproduced with permission S.Vucic 2007*

Intracortical inhibition induced by a conditioning stimulus was measured as the increase in the test stimulus intensity required to evoke the target MEP. Inhibition was calculated off-line by using the following formula (489):

Inhibition = (Conditioned test stimulus intensity – RMT)/RMT * 100
Facilitation was measured as the decrease in the conditioned test stimulus intensity required to evoke the target MEP.

Each of the data points were weighted (QTRACS software version 16/02/2009) such that any measures recorded outside the threshold target window (0.2mV, peak-to-peak) contributed least to the data analysis. A student t-test was used for assessing differences between the two groups. Analysis of variance (ANOVA) was used for multiple comparisons to assess the difference between the conditioned test and unconditioned test stimuli at different ISIs. A probability (P) value of < 0.05 was considered statistically significant.

Axonal excitability

Axonal excitability can be investigated using a threshold tracking technique, where 'threshold' refers to the stimulus current required to produce a target potential (408, 409). Utilising the threshold tracking technique, the resting threshold is measured and nerve excitability is altered by changing the nerve environment, which can be undertaken by applying a conditioning polarizing current (409). This technique subsequently provides information about membrane potential and axonal ion channel function.

In this thesis the threshold tracking software that was used was an automated tracking system, whereby the test stimulus intensity was automatically increased or decreased in percentage

steps after each response, depending on the difference between the recorded and target responses (Figure 11). For measurement of multiple excitability parameters, an automated multiple excitability protocol, TRONDF version 16/02/2009 (© Professor Hugh Bostock, Institute of Neurology, Queen Square, London, UK) was used. This protocol contained a proportional tracking system, in which the change in test stimulus current intensity was proportional to the difference (or error) between the recorded response and target response. Proportional tracking can be more efficient, especially when excitability changes abruptly.

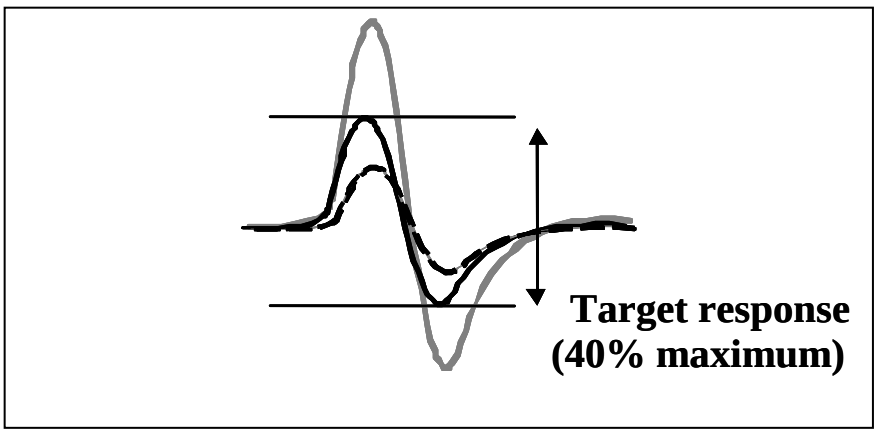

Figure 11. With the threshold tracking technique, the target response is set to 40% of the supramaximal compound muscle action potential (CMAP) amplitude. When the CMAP amplitude is smaller than the target response (dashed black line), the subsequent test stimulus current intensity is increased. When the CMAP amplitude is larger than the target response (grey line), the subsequent test stimulus current intensity is reduced. If the CMAP amplitude is equal to the target response, the subsequent test stimulus intensity remains unchanged. *Reproduced with permission S.Vucic 2007.*

Multiple excitability measures: sequence of recordings

The first step of the protocol is to generate a stimulus-response (SR) curve, using test current impulses of 0.2- and 1-ms (Figure 12A, B). The target response (40% of supramaximal CMAP response) was generated by measuring the peak amplitude (from baseline to negative peak) from utilizing 1ms current intensities. Stimuli were increased in 4% steps, with two responses averaged at each step until three averages were considered maximal. The ratio between the SR curves for two different stimulus durations that produced the same CMAP

response were used to calculate the rheobase, defined as the threshold current for a target response when the stimulus is of infinitely long duration (408, 409), and strength-duration time constant (τ_{SD}; Figure 12D) of motor axons of different thresholds using Weiss' formula (408, 409, 420).

Threshold electrotonus which refers to the threshold changes that occur in response to subthreshold depolarizing and hyperpolarizing pulses, was measured by altering nerve excitability using prolonged sub-threshold polarizing currents of 100 ms duration, set to + 40% (depolarizing) and - 40% (hyperpolarising) of controlled threshold current (408, 409). There were a total of three stimulus combinations that were tested sequentially: test stimulus alone (measured control threshold current); test stimulus + depolarizing current; test stimulus + hyperpolarizing current. Threshold was tested at 26 time points before, during and after the 100 ms polarizing pulse. The stimulus combinations were repeated until three valid estimates were recorded within 15% of target response (444).

A current-threshold relationship (I/V) was obtained by tracking the changes in threshold of 1ms test pulses that occurred following sub-threshold polarizing currents of 200-ms duration which were altered in ramp fashion from +50% (depolarizing) to -100% (hyperpolarizing) of controlled threshold in 10% steps. Stimuli with conditioning currents were alternated with test stimuli until three valid threshold estimates were recorded. The I/V relationship estimates rectifying properties of both nodal and internodal segments of the axon (467, 493). The I/V gradient during depolarizing sub-threshold currents reflects conduction through outward rectifying K^+ channels, while the I/V gradient during hyperpolarizing sub-threshold currents reflects inwardly rectifying conductances activated by hyperpolarization (444, 465).

Finally, the recovery of axonal membrane excitability, referred to as the recovery cycle, was assessed by tracking the changes in threshold that occurred following a supramaximal conditioning stimulus of 1 ms duration. Eighteen conditioning-test stimulus intervals were studied, decreasing from 200 to 2 ms. Three stimulus combinations were recorded: (i) unconditioned test stimulus (1 ms duration); (ii) supramaximal conditioning stimulus alone; (iii) conditioning and test stimuli in combination. The response in (ii) was subtracted on-line from response in (iii) so as to eliminate contamination of the measured CMAP response by the supramaximal conditioning response at short interstimulus intervals. Each stimulus combination was repeated until 4 valid estimates were obtained (444).

Following the completion of the recovery cycle, a profile of nerve excitability was generated using a customized plotting program (QTRACP version 16/02/2009), consisting of six different plots (Figure 12A-F). The 95% confidence limits were calculated as mean ± $t_{0.05}$ SD (where $t_{0.05\ is}$ the value of Student's t-test which the probability of a larger value is 0.05) such that 95% of individual observations would fall within the limits if the variables were distributed normally. For data plotted on logarithmic axes (Figure 12A, F), the logarithm of the variable was assumed to be normally distributed, and the mean plotted is the geometric mean. Differences in excitability parameters were analysed using Student's t-test. A probability (P) value of < 0.05 was considered statistically significant. All results are expressed as mean ± standard error of the mean.

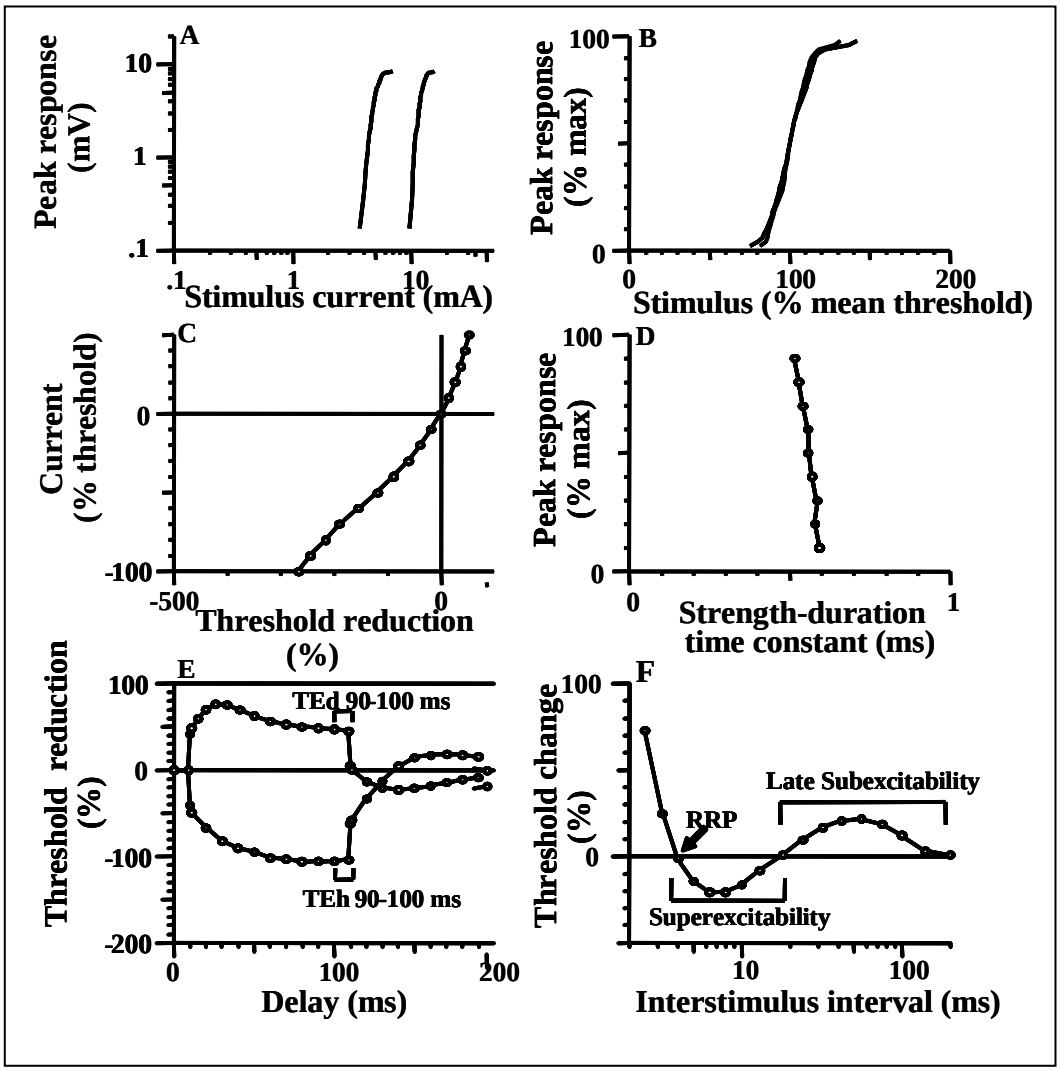

Figures 12. To highlight the axonal excitability parameters, six plots that were recorded from the abductor pollicis brevis muscle in single subject are displayed. **(A)** Absolute stimulus-response relationship. **(B)** Normalised stimulus-response relationship. **(C)** Current-threshold relationship. **(D)** Strength-duration time constant. **(E)** Threshold electrotonus. The conditioning-test interval corresponding to hyperpolarising threshold electrotonus at 90-100 ms (The 90-100 ms) and depolarising threshold electrotonus at the same time interval (Ted 90-100 ms) are depicted. **(F)** Recovery cycle, demonstrating the time point at which the relative refractory period (RRP) is measured, as well as superexcitability and late subexcitability. *Reproduced with permission S.Vucic 2007.*

Data analysis

Values for the multiple excitability parameters were automatically generated upon completion of the axonal excitability protocol. Stimulus intensity (mA) was measured as the current required to elicit a target response set to 40% of maximal CMAP for a stimulus of 1 ms duration. Strength-duration time constant (ms), which reflects nodal persistent Na^+

conductances (494), was calculated for nine motor axonal populations, starting from axons contributing to CMAP responses between 5-15% up to the maximum of 85-95%, increasing in 10% batches (444). Rheobase (mA), which is defined as the threshold current for a target response when the stimulus is of infinitely long duration, was also calculated. Stimulus-response slope was calculated from the normalized SR curves by subtracting the stimulus that evoked a 25% maximal CMAP response from that which evoked a 75% response and dividing the result by the stimulus evoking a 50% response.

Threshold electrotonus parameters were calculated from data in Figure 12E. TEd (peak) refers to the peak threshold reduction produced by a subthreshold depolarizing current. The reduction in threshold was measured at three time points relative to onset of the subthreshold depolarizing current, i.e. at 10-20 ms, TEd (10-20 ms), 40-60 ms TEd (40-60 ms), and at 90-100 ms TEd (90-100 ms). Threshold changes were also measures at similar latencies following a subthreshold hyperpolarizing current and are referred to as TEh (10-20 ms) and TEh (90-100 ms). S2 accommodation was calculated as the difference between the peak threshold reduction in the depolarizing direction and the plateau value, i.e. TEd (peak) – TEd (90-100 ms). The peak threshold increase at the end of depolarizing current and peak threshold reduction at the end of hyperpolarizing current were averaged over 20 ms, being referred to as TEd (undershoot) and TEh (overshoot).

From the I/V graph, the following parameters were recorded; (i) resting I/V slope, calculated from polarizing currents between +10% to -10%, minimal I/V slope, calculated by fitting a straight line to each three adjacent points in turn, and (iii) hyperpolarizing I/V slope, calculated from polarizing current between 0-100%.

For the recovery cycle of axonal excitability the following parameters were measured; (i) relative refractory period (RRP, ms), defined as the first intercept at which the recovery curve crosses the x-axis; (ii) superexcitability, expressed as a percentage reduction in threshold current, was calculated as the minimum mean of three adjacent point at conditioning-test intervals of 5-15 ms and (iii) late subexcitability (%), as the maximum mean of three adjacent points at interstimulus intervals > 15 ms.

For the axonal excitability parameters, there already exist normative values for the median nerve motor axons (413, 444).

Clinical Scores in Amyotrophic Lateral Sclerosis

A neurological history and physical examination were undertaken in all ALS patients. All ALS patients were clinically staged using the amyotrophic lateral sclerosis functional rating scale-revised (ALSFRS-R) (495) . The ALSFRS-R is a questionnaire-based, 12-item functional rating scale administered to the patient or, if the patient cannot communicate effectively to an informant, such as the carer. The ALSFRS-R incorporates assessment of bulbar function, fine motor function, gross motor function and respiratory function. Functional scores in each domain are graded from 0 (complete dependence for that function) to 4 (normal function), resulting in a total ALSFRS-R score ranging from 0 to 48 (normal).

Muscle strength in all patients was assessed using the Medical Research Council (MRC) rating scale (496) with the following group of muscles tested bilaterally yielding a total MRC score of 90: shoulder abduction; elbow flexion; elbow extension; wrist dorsiflexion; finger

abduction; thumb abduction; hip flexion; knee extension; ankle dorsiflexion. The MRC scale is a five point scale ranging from 0 (no movement) to 5 (normal strength).

The degree of upper motor neuron (UMN) dysfunction was assessed by an UMN score incorporating the following parameters: jaw jerk, facial reflex, upper and lower limb deep tendon reflexes and plantar responses with the score ranging from 0 [no UMN dysfunction] to 16 [severe UMN dysfunction] (497).

Chapter 1

AWAJI CRITERIA IMPROVES DIAGNOSTIC SENSITIVITY IN AMYOTROPHIC LATERAL SCLEROSIS

Summary

One of the limitations of the current diagnostic criteria in amyotrophic lateral sclerosis (ALS) is the delay in diagnosis. To determine the utility of the currently employed diagnostic criteria in diagnosing ALS and to propose a novel modification so as to enhance sensitivity, we utilised an individual patient data (IPD) analysis. Our literature review identified 13 studies that compared the diagnostic accuracy of the Awaji and revised El Escorial (rEEC) criteria. Individual patient data was available from 8 studies, which was included in the analysis. Predefined subgroup analysis was undertaken in bulbar and limb onset disease. The sensitivity of a novel updated Awaji criteria, incorporating a 'probable-laboratory supported" category, was also undertaken. Individual patient data was available from 1086 patients, consisting of 881 ALS and 205 mimic disorder patients. Summary sensitivities based on random effects logistic regression modelling disclosed a higher sensitivity of the Awaji criteria (0.70, 95% Confidence Interval [CI] 0.51-0.83) and updated Awaji criteria (0.73, 95% CI 0.56-0.85) when compared to rEEC (0.58, 95% CI 0.48-0.68). Paired analysis revealed higher sensitivities of the Awaji criteria in 4 studies and updated Awaji criteria in 7 studies when compared to rEEC. A generalized estimating equation model confirmed a higher sensitivity of the Awaji and updated Awaji criteria ($P<0.0001$). Using individual patient data analysis, the present study established a higher sensitivity of the Awaji criteria when compared to rEEC. The updated Awaji criteria enhanced the diagnostic sensitivity in ALS, particularly in limb-onset disease, and should be taken into account as diagnostic criteria in clinical practice and future therapeutic trials.

Introduction

There is no diagnostic test for Amyotrophic lateral sclerosis (ALS), a rapidly progressive and fatal neurodegenerative disorder of the motor neurons(48). Rather, diagnosis of ALS relies on identification of a combination of upper (UMN) and lower motor neuron (LMN) signs across specific body regions (6, 48, 498). Clinically based diagnostic criteria were designed to be highly specific for ALS, although their sensitivity is limited, particularly in early stages of ALS (51, 247, 499). Consequently, significant diagnostic delays are inevitable, leading to delay in the institution of neuroprotective therapies and recruitment into therapeutic trials, perhaps beyond the therapeutic window period.

The neurophysiologically based Awaji criteria were developed (6) for use in conjunction with the clinical criteria as set out in the revised El-Escorial Criteria (rEEC) in an attempt to reduce diagnostic delays. The Awaji criteria proposed that neurophysiological features of LMN dysfunction, including chronic and ongoing neurogenic changes (fibrillation potentials/positive sharp waves) were equivalent to clinical LMN signs. In addition, fasciculations were deemed to be a biomarker of LMN dysfunction when combined with chronic neurogenic changes. Subsequently, the diagnostic utility of the Awaji criteria was assessed in retrospective and prospective studies, most of which established an increased sensitivity when compared to rEEC (30, 52-59), although one study reported a lower sensitivity, a finding attributed to the omission of a "probable-laboratory supported" diagnostic category (60).

The diagnostic accuracy of the Awaji criteria was also assessed in two study-level meta-analyses, and these reported an improved diagnostic performance of the Awaji criteria, with higher sensitivity and diagnostic odds ratios (30, 61). The diagnostic benefits, however,

appeared to be most prominent in ALS patients with bulbar-onset disease. Interestingly, one study reported that 20% of patients classified as "probable laboratory-supported" on the rEEC were downgraded to Awaji "possible"(61). Importantly, both study-level meta-analyses were limited by a high heterogeneity of the pooled sensitivity estimates, potentially impacting on the outcome.

In order to maximise the statistical power of the analysis, and explore variation at an individual patient level, we aimed to perform a systematic review using individual patient data. In particular, we aimed to (1) summarise diagnostic accuracy of the rEEC, Awaji, and the updated Awaji criteria, (2) explore reasons for heterogeneity in diagnostic accuracy for each criteria using patient and study level covariates, (3) compare diagnostic accuracy of the rEEC versus the Awaji and updated Awaji criteria, and (4) explore differences in accuracy for the diagnostic criteria, when applied to the bulbar and limb-onset subgroups.

Methods

Selection and eligibility criteria

All studies assessing the diagnostic accuracy of rEEC and the Awaji criteria in ALS were considered eligible for analysis. The accepted diagnosis of ALS was defined by good clinical practice as described in the studies, requiring disease progression deemed to be consistent with that evident in ALS. Clinical progression was used as the reference standard.

Search strategy, study selection and data extraction

Potentially eligible studies were identified through an electronic search of bibliographic databases (MEDLINE through Ovid, PubMed and Web of Science) from 2006, the year of the consensus meeting that gave rise to the Awaji recommendations, to March 2015. The

following terms were used in the search field tag and combined "***awaji.tw OR Escorial.tw OR sensitivity.tw OR specificity.tw OR criteria.tw OR accuracy.tw OR electrodiagn$.tw OR neurophysiol$.tw OR electromyograp$.tw OR EMG diagnosis.tw***", combined with "***amyotrophic lateral sclerosis.tw OR motor neuron disease.tw***." No language restrictions were placed on the search strategy. Reference lists from identified studies were cross-checked for additional studies. Senior authors from the identified studies were contacted to obtain raw data and unpublished data was solicited from the corresponding authors. Selection of studies and data extraction was performed independently by two authors (NG and SV) and checked for accuracy. Disagreement between the independent reviewers was resolved by consensus and with a third reviewer (PM).

Quality assessment

Study quality was assessed by 2 reviewers (NG, SV) using the 'Quality Assessment of Diagnostic Accuracy Studies-2' (QUADAS-2) checklist (500). The QUADAS-2 is an 11 item questionnaire, with each item scored as yes, no, or unclear. A representative patient population included consecutive subjects with suspected ALS/motor neuron disease, who were assessed in different centers. An "adequate reference standard" required evidence of clinical disease progression over an adequate follow-up period consistent with ALS. We required that the index tests (rEEC and Awaji criteria) were applied at the same assessment in each study.

Statistical analysis and data synthesis

Definition of disease status

In order to assess the diagnostic performance of the rEEC and Awaji criteria, disease status was assigned to subjects as 'probable' or 'definite' ALS. For rEEC, "probable ALS-laboratory supported" was also regarded as positive for ALS. The 'possible' and 'negative' classifications were regarded as negative for diagnosis of ALS. The Updated Awaji criteria extended the Awaji criteria, by including patients with 2 regions of lower motor neuron involvement (clinical and/or needle EMG) and one region of UMN involvement in the disease group.

Summarising test accuracy for the three sets of diagnostic criteria

Sensitivity and specificity were calculated for each study, using published and unpublished individual patient data. Study specific sensitivity and specificity were displayed in a forest plot using Cochrane Revman 5. Since the ALS criteria were designed to be highly specific, only four out of the eight studies included a non-disease group and three out of four of these studies reported a specificity of 100%. The fourth study reported a specificity of 80% but this was only based on 5 individuals (4/5). Consequently, the standard bivariate analysis (501) that simultaneously models sensitivity and specificity was not feasible. Hence, all further analyses focused on sensitivity only. Random effects logistic regression, fitting a study as a random effect, was used to obtain summary sensitivity and corresponding 95% Confidence Interval for each criterion (SAS 9.4, SAS Corp, Cary NC, USA).

Exploring reasons for heterogeneity in diagnostic accuracy for each set of criteria using patient and study level covariates

We explored variation in sensitivity by adding each study and individual- level factor in the random effects logistic model for each diagnostic criterion. Study-level factors examined were: whether study populations had been pre-screened, whether the study was prospective and whether assessment of upper motor neuron signs was stipulated. Individual-level factors examined were: age, sex, duration of illness, and bulbar vs limb onset. Each model included only one variable because of the limited number of studies.

Compare diagnostic accuracy of the rEEC criteria versus the Awaji and Updated Awaji criteria

Comparison of test accuracy within each study was performed using the exact form of McNemar's test, to take account of pairing of test results within patients. Extending the random effects logistic regression model to include nested random effects for patients within studies to allow for pairing of criteria results, did not converge due to data sparsity. As an alternative we used a Generalised Estimating Equation (GEE) model to test for association between sensitivity and diagnostic criteria. The model has a binomial error distribution, clustering by study, repeated measures (criteria results) for each patient, and patients nested within studies.

Explore differences in accuracy for the diagnostic criteria sets, when applied to the bulbar and limb-onset subgroups

Given *a priori* clinical interest in the difference between bulbar and limb onset subgroups, we used random effects logistic regression to estimate summary sensitivity for these subgroups. To compare diagnostic accuracy of the rEEC criteria versus the Awaji (and Updated Awaji)

criteria for these subgroups, we extended the GEE modelling to include covariates for criteria, region of onset, and an interaction (product) term for criteria and region of onset to test for effect modification.

Results

Included Studies

From the literature review 13 studies were identified that compared the diagnostic accuracy between rEEC criteria and the Awaji criteria (52-60, 502-505). Corresponding authors from 6 studies provided data on individual patients (53, 55, 59, 60, 502, 504), while patient information on individual subjects was extracted from 2 published manuscripts (54, 57) (Table 1.1). Individual patient data from the remaining 5 studies was not available for the following reasons: (i) loss of data due to technical reasons (503) (ii) lack of correspondence, (52, 56, 505) (iii) inability to provide suitable individual patient data for analysis (58). Consequently, individual patient data was available on a total of 1086 patients.

Quality assessment

On quality assessment of the included studies, all studies included a representative spectrum of ALS patients. The majority of studies recruited or reviewed patient data in a consecutive manner. The reference standard utilised to confirm the diagnosis of ALS was sufficient in all studies, with most studies utilising clinical and electrophysiological measures, and all studies also using "progression" during a follow up period to confirm the diagnosis of ALS. All studies applied the rEEC and Awaji criteria at the same time, hence there was no time lag between applying the two sets of diagnostic criteria.

Study	Site	Sample size	Study design	Age in years, Mean, (SD), [Range]	Disease duration in months, Mean, (SD), [Range]	Bulbar onset (%)	Neurophysiological protocol, (N-number of muscles)	Case ascertainment
Boekestein et al[9]	Netherlands	213 (120 NM)	Retrospective	58	NA	27	Yes (B, C, T, and LS regions), N>6	Unclear
Chen et al[13]	USA	70 (16 NM)	Retrospective	62.4 (12.6) [37-89]	21.6 (23.7) [2-109]	31	No (at least 3 of 4 regions: B, C, T, and LS regions), N=Unclear	Independent (other physician)
De Carvalho et al[8]	Portugal	55	Prospective	61.8 (15.2) [20-83]	12.8 (9.8) [2-36]	27	Yes (B, C, T, and LS regions) plus diaphragm, N>10	Consensus (2 investigators)
Gawel et al[15]	Poland	160	Retrospective	55.9 (11.6) [18-81]	15.3 (14.9) [2-44]	25	Yes (B, C, T, and LS), N>3	Other physician
Geevasinga et al[28]	Australia	146 (64 NM)	Prospective	56.9 (9.8) [28-86]	15.6 (17.1) [2-108]	40	Yes (B, C, T, and LS Regions), N=11 (mean number of muscles)	Consensus (2 investigators)
Higashihara et al[16]	Japan	129 (5 NM)	Retrospective	64.4 (10.2) [31–87]	13.2 (9.1) [2-52]	30	Yes (B, C, T, and LS), N=3-8	Independent (2 investigators)
Noto et al[29]	Japan	113	Retrospective	66.5 (9.8) [34-86]	13.9 (11) [2-59]	42	Yes (B, C, T, and LS regions), N=4-8	Single investigator
Schrooten et al[10]	Belgium	200	Prospective	61.0 (12.8)	12.4 (13.7) [<1-108]	25	Yes (C, LS at least 2 muscles; B, T at least 1 muscle), N>6	Independent computer algorithm

Table 1.1. Characteristics of the included studies, including demographic and study methodological details. All studies were performed at single centers in the countries listed. The sample size includes patients with ALS as well as NM - neuromuscular controls (who were used to calculate specificity data). For neurophysiological protocol, B = Bulbar, C = Cervical, T = Thoracic, LS – Lumbosacral; refer to the regions assessed by needle electromyography and N – refers to the number of muscles assessed at the time of the neurophysiological assessment.

Test accuracy for the three sets of diagnostic criteria

Meta-analysis was based on a cohort of 881 ALS patients from eight studies that included a total pool of 1086 patients, 205 of whom were non-ALS neuromuscular control subjects. The summary sensitivity and corresponding 95% confidence interval for the diagnostic criteria were derived from separate random effects logistic regression models. The sensitivity estimates were higher for the Awaji [0.70 (95% Confidence Interval [CI] 0.51-0.83)] and updated Awaji 0.73 (95% CI 0.56-0.85) criteria when compared to rEEC [0.58 (95% CI 0.48-0.68), Table 1.2]. It should be stressed however, that the Awaji criteria downgraded the diagnosis to a "possible" category in 26 (21%) patients classified as "probable laboratory supported" by the rEEC. Based on these summary estimates, the Awaji criteria was able to identify an additional 12% of ALS patients while the updated Awaji criteria identified an additional 15% of patients.

	Number of patients (for calculating sensitivity)	**rEEC**	**Awaji criteria**	**Updated Awaji criteria**
Overall	881	0.58 (0.48-0.68)	0.70 (0.51-0.83)	0.73 (0.56-0.85)
Bulbar onset subgroup*	234	0.55 (0.42-0.68)	0.72 (0.51-0.86)	0.73 (0.55-0.86)
Limb onset subgroup*	546	0.62 (0.42-0.78)	0.73 (0.44-0.91)	0.76 (0.50-0.91)

Table 1.2. Summary sensitivity (95% Confidence Intervals) for the three diagnostic criteria. rEEC= revised El Escorial Criteria *Not all patients included in the overall analysis had data for region of onset.

Compare diagnostic accuracy of the rEEC criteria versus the Awaji and Updated Awaji criteria

Sensitivity of the Awaji criteria was significantly higher using the exact form of McNemar's test when compared to rEEC in four studies (53, 55, 502, 504), while in one study the rEEC exhibited a higher sensitivity (60) [Table 1.3]. In the remaining three studies, the observed sensitivity was higher for Awaji compared with rEEC criteria, but this difference was not statistically significant (54, 57, 59). Only four studies included a non-disease group, with three studies (54, 57, 504) reporting a specificity of 100% and one study (60) a specificity of 80%.

Of further relevance, the observed sensitivity of the updated Awaji criteria, based on the McNemar's analyses for individual studies, was also higher when compared to rEEC criteria in all eight studies, and significantly higher in five of these studies (53-55, 502, 504) [Table 1.3]. GEE modelling provided strong evidence of an association ($P<0.0001$) between sensitivity and criteria, for both Awaji versus rEEC and updated Awaji versus rEEC criteria.

Bulbar-onset disease: The Awaji criteria exhibited a significantly greater sensitivity using the exact form of McNemar's test when compared to rEEC in three studies (53, 55, 502) [Table 1.4]. In contrast, there were no significant differences in the sensitivity between Awaji and rEEC criteria in four other studies (57, 59, 60, 504). The updated criteria did not lead to a significant improvement in sensitivity over the existing Awaji criteria in bulbar onset ALS patients (Table 1.4).

Study	Number	Sensitivity		P-Value	Sensitivity	P-Value
		rEEC (%)	Awaji criteria (%)	McNemar	Updated Awaji criteria (%)	McNemar
Boekestein et al[9]	213	65/93 (70)	66/93 (71)	1.0	72/93 (77)	**0.016**
Chen et al[13]	70	39/54 (72)	40/54 (74)	1.0	40/54 (74)	1.0
De Carvalho et al[8]	55	33/55 (60)	52/55 (95)	**<0.0001**	52/55 (95)	**<0.0001**
Gawel et al[15]	160	87/160 (54)	86/160 (54)	1.0	91/160 (57)	0.22
Geevasinga et al[23]	146	29/82 (35)	38/82 (46)	**0.023**	39/82 (48)	**0.0063**
Higashihara et al[16]	129	57/124 (46)	48/124 (39)	**0.035**	61/124 (49)	0.13
Noto et al[21]	113	69/113 (61)	80/113 (71)	**0.035**	86/113 (76)	**<0.0001**
Schrooten et al[10]	200	132/200 (66)	170/200 (85)	**<0.0001**	170/200 (85)	**<0.0001**

Table 1.3. Comparison of the diagnostic utility of revised El Escorial criteria (rEEC), Awaji criteria and updated Awaji criteria with a 'probable laboratory supported' category (*see* Methods) in the entire ALS cohort irrespective of site of disease onset. The updated Awaji criteria were compared against the rEEC. Total number of patients (N) refers to all patients in the included studies (ALS and neuromuscular patients). The specificity (*not shown*) of the rEEC, Awaji and updated Awaji criteria was available for four studies, being 100% in three

Study	Number	Sensitivity		P-Value	Sensitivity	P-Value
		rEEC (%)	Awaji criteria (%)	McNemar	Updated Awaji (%)	McNemar
Chen et al[13]	17	11/17 (65)	12/17 (71)	1.0	12/17 (71)	1.0
De Carvalho et al[8]	16	5/16 (31)	14/16 (88)	**0.0039**	14/16 (88)	**0.0039**
Gawel et al[15]	37	27/37 (73)	26/37 (70)	0.317	27/37 (73)	NA
Geevasinga et al[23]	33	12/33 (36)	13/33 (39)	1.0	14/33 (42)	0.63
Higashihara et al[16]	31	15/31 (48)	14/31 (45)	1.0	16/31 (52)	1.0
Noto et al[21]	51	30/51 (59)	42/51 (82)	**0.0005**	42/51 (82)	**0.0005**
Schrooten et al[10]	49	32/49 (65)	45/49 (92)	**0.0005**	45/49 (92)	**0.0005**

Table 1.4. Comparison of the diagnostic utility of revised El Escorial criteria (rEEC), Awaji criteria and the updated Awaji criteria in bulbar onset amyotrophic lateral sclerosis (ALS) patients. The updated Awaji criteria were compared against the rEEC. Total number of patients (N) refers to all ALS patients included in the study. The specificity (*not shown*) of rEEC, Awaji and updated Awaji criteria was available in 2 studies and was 100%[16,31]. The exact form of McNemar's test was undertaken in each study utilising individual patient data. $P < 0.05$ was regarded as statistically significant. NA- not applicable - no discordant pairs.

Of relevance, the summary sensitivities, based on random effects logistic regression modelling, were higher for the Awaji and updated Awaji criteria when compared with rEEC criteria (Table 1.2). Specifically, the sensitivity of the Awaji criteria was 0.72 (95% CI 0.51-0.86), updated Awaji criteria 0.73 (0.55-0.86), and rEEC 0.55 (95% CI 0.42-0.68). GEE modelling provided evidence of effect modification for both the rEEC versus Awaji criteria comparison (p=0.009) and the rEEC versus updated Awaji criteria (p=0.033), indicating that the improvement in sensitivities was greater in the bulbar-onset subgroup.

Limb-onset disease: Using the exact form of McNemar's test, it was evident that the Awaji criteria exhibited a significantly higher sensitivity in limb onset disease in three studies when compared to rEEC (53, 55, 504). There were no differences in two studies (59, 502), while in one study the rEEC criteria appeared to be more sensitive (60) [Table 1.5]. The updated Awaji criteria improved the sensitivity in one study (502), while the sensitivity was maintained in five studies (53, 55, 57, 59, 504). Importantly, in the study reporting a higher sensitivity of the rEEC (60), the updated Awaji criteria increased the sensitivity such that there was no longer a significant difference in sensitivity when compared to rEEC (Table 1.5). Although the summary estimates of sensitivity were higher for the Awaji criteria 0.73 (95% CI 0.44-0.91) when compared to rEEC (0.62, 95% CI 0.42-0.78, Table 1.2), the updated Awaji criteria modestly enhanced the sensitivity to 0.76 (95% CI 0.50-0.91) in limb-onset ALS.

Study	Number	Sensitivity		P-Value	Sensitivity	P-Value
		rEEC (%)	Awaji (%)	McNemar	Awaji LS (%)	McNemar
Chen et al[13]	30	28/30 (93)	28/30 (93)	NA	28/30 (93)	NA
De Carvalho et al[8]	39	28/39 (72)	38/39 (97)	**0.002**	38/39 (97)	**0.002**
Gawel et al[15]	123	60/123 (49)	60/123 (49)	1.0	64/123 (52)	0.22
Geevasinga et al[23]	49	17/49 (35)	25/49 (51)	**0.0078**	25/49 (51)	**0.0078**
Higashihara et al[16]	93	42/93 (45)	34/93 (37)	**0.039**	45/93 (48)	0.25
Noto et al[21]	62	39/62 (63)	38/62 (61)	1.0	44/62 (71)	**0.0063**
Schrooten et al[10]	150	100/150 (67)	125/150 (84)	**<0.0001**	125/150 (84)	**<0.0001**

Table 1.5. Comparison of the diagnostic utility of revised El Escorial criteria (rEEC), Awaji criteria and the updated Awaji criteria in limb onset amyotrophic lateral sclerosis (ALS) patients. The updated Awaji criteria were compared against the rEEC. Total number of patients (N) refers to all ALS patients included in the study. The specificity (*not shown*) of rEEC, Awaji and updated Awaji criteria was available in 2 studies and was 100%[16,31]. The exact form of McNemar's test was undertaken in each study utilising individual patient data. NA- not applicable - no discordant pairs.

In order to investigate the factors underlying the heterogeneity of sensitivity of the three diagnostic criteria between the studies, the effects of patient and study level covariates were assessed. For patient-level covariates, disease duration exerted a significant effect on the sensitivity of diagnostic criteria. Specifically, the effects appeared to be non-linear, with the highest sensitivity occurring between 6-11 months post-symptom onset (Table 1.6). Although the non-linear pattern was evident in all criteria, it was statistically significant in the Awaji (χ^2=17.8, df 3, P=0.0005) and updated Awaji criteria (χ^2=17.8, df 3, P=0.015), but not the rEEC (χ^2=6, df 3, P=0.11).

Among study-level factors, stipulating the methods by which the upper motor neuron signs were assessed was associated with a lower estimate of sensitivity for all criteria including rEEC (P=0.032), Awaji criteria (P=0.068) and updated Awaji criteria (P=0.089), although this was only statistically significant for the rEEC criteria. There was no association between sensitivity and any other study-level or individual-level factors.

		rEEC			**Awaji criteria**			**Updated Awaji criteria**		
Disease duration (months)	***N***	**Odds ratio**	**95% CI**	**Estimated sensitivity**	**Odds ratio**	**95%CI**	**Estimated sensitivity**	**Odds ratio**	**95% CI**	**Estimated sensitivity**
< 6	140	1	referent	0.49	1	referent	0.63	1	referent	0.67
6 -11	254	1.63	(0.94, 2.80)	0.61	1.83	(0.98, 3.41)	0.76	1.80	(0.96, 3.36)	0.78
12-35	312	1.37	(0.81, 2.31)	0.51	1.26	(0.70, 2.26)	0.69	1.24	(0.69, 2.24)	0.72
≥36	82	1.05	(0.51, 2.16)	0.51	0.92	(0.42, 2.01)	0.61	0.78	(0.36, 1.70)	0.61

Table 1.6. The effects of disease duration on the sensitivity of the three diagnostic ALS criteria.

Discussion

Utilising individual patient data available from 1086 individuals across 8 published studies, the present study established a greater sensitivity of the Awaji criteria when compared to the revised El Escorial diagnostic criteria. Specifically, the Awaji criteria exhibited a higher or comparable sensitivity in most studies, with the summary sensitivity of Awaji criteria being 70% compared to 58% for the rEEC, translating to a 12% increase in the diagnostic utility. Importantly, this increase in sensitivity was predominantly evident in bulbar-onset ALS patients. Addition of the "probable-laboratory supported" category to Awaji criteria increased the sensitivity, particularly in limb-onset disease, translating to an extra 3% of patients correctly diagnosed with ALS.

Diagnostic utility of the Awaji criteria

In the absence of a definitive test, the diagnosis of ALS remains clinically based, relying on the identification of a combination of upper and lower motor neuron dysfunction. This has represented a major diagnostic challenge leading to significant delays in diagnosis, particularly in younger patients (<45 years) (51, 506). Consequently, critical delays of patient recruitment into clinical trials have ensued, perhaps delaying treatment beyond the therapeutic window period. The consensus Awaji criteria were developed in order to enable an earlier clinical diagnosis of ALS by introducing an objective biomarkers of LMN dysfunction (6). Although a number of studies have reported a greater sensitivity of the Awaji criteria when compared rEEC (52, 53, 55, 56, 58, 502, 504), some have reported equivalent sensitivities (54, 57, 59), while one study documented a lower sensitivity for the Awaji criteria (60). The studies were critiqued for being of varying quality, single center design and for specific methodological limitations (507). A prospective, multicenter study conducted in accordance with the Statement for Reporting Studies of Diagnostic Accuracy

protocol would represent an ideal approach in comparing the utility of the different ALS diagnostic criteria.

A meta-analysis approach could provide unique insights into the utility of the ALS diagnostic criteria. Two study-level meta-analyses reported a higher sensitivity of the Awaji criteria (30, 61), with sensitivity being greater for bulbar-onset ALS. Importantly, there was high heterogeneity among studies, perhaps reflecting statistical or methodological diversity (508, 509). Individual patient data meta-analysis provides the least biased and most reliable information on the effects size of different diagnostic criteria as it allows the pairing of criteria results within an individual to be taken into account (508). Although bivariate IPD meta-analysis was not feasible, due to sparsity of specificity data, analysis of sensitivity was undertaken confirming a higher sensitivity of the Awaji criteria when compared to rEEC, in keeping with study-based meta-analyses (30, 61), with the sensitivity benefit most evident in bulbar-onset ALS.

In limb-onset ALS, the Awaji criteria have been reportedly less sensitive (59-61, 502), a finding attributed to the omission of the "probable laboratory supported" diagnostic category (59, 60, 509). Importantly, 21% of ALS patients in the current IPD analysis that were classified as "probable laboratory-supported ALS" on the rEEC were downgraded to a "possible" diagnostic category on the Awaji criteria. Consequently, recruitment into clinical trials could be potentially prevented, although it should be acknowledged that some therapeutic trials now accept 'Awaji possible' patients. The current IPD analysis suggested that the updated Awaji criteria, incorporating a probable laboratory supported category, exhibited a higher sensitivity when compared to rEEC, and this increase appeared to be evident in bulbar and in limb-onset ALS (Tables 1.2-1.4).

Patient and study level covariates were assessed in order to gain further insights into the mechanisms underlying the heterogeneity in previous literature-based meta-analyses (30, 61). Disease duration appeared to exert a non-linear effect, whereby the sensitivity was highest in patients within 6-11 months post-symptom onset. The effect of disease duration on sensitivity could be related to atypical phenotypes in patients with a protracted disease duration (≥36 months), or limited disease burden in patients with a shorter disease duration (<6 months).

Study level factors impacted on the varied sensitivity across studies for the three sets of diagnostic criteria. Stipulating whether UMN signs were assessed within a cohort significantly influenced the diagnostic sensitivity of the three criteria. This relationship could be explained by the well-recognised difficulty in identifying UMN dysfunction in ALS using clinical criteria (38), thereby impacting on diagnostic sensitivity. Objective assessment of UMN dysfunction by threshold tracking transcranial magnetic stimulation (TMS) techniques has been reported to increase the sensitivity of the Awaji criteria at an early stage in the disease process (510). We recommend that future revisions of the Awaji criteria should consider incorporating objective biomarkers of UMN dysfunction, such as short interval intracortical inhibition (510).

Chapter 2

UTILITY OF DIAGNOSTIC CRITERIA FOR AMYOTROPHIC LATERAL SCLEROSIS: A MULTICENTER PROSPECTIVE STUDY

Summary

While the Awaji criteria in the previous chapter were more sensitive when compared to the El Escorial criteria, during the process of the literature review, it was noted that there were no prospective multicentre studies evaluating these diagnostic criteria. Furthermore there was a lack of specificity data in most of the studies that had been undertaken. Subsequently we designed the first prospective multicentre study, across three east coast centres in Australia, to evaluate the El Escorial and Awaji criteria. In total we recruited 416 patients (233 ALS and 183 non-ALS mimic disorders) between January 1 2012 and August 31 2015, to compare the diagnostic accuracy of Awaji and rEEC criteria in a population of suspected ALS. The sensitivity of the Awaji criteria (57%, 50.0-63.3%) was significantly higher when compared to the rEEC (45%, 38.7-51.7%, P<0.001), translating to a 12% gain in sensitivity. The specificity of the both criteria were identical 99.5% (95% CI 96-100%), thereby indicating the number needed to test in order to diagnose one extra case of ALS was 1.8 (1.5-2) for Awaji criteria and 2.4 (2-2.6) for rEEC. Importantly, the Awaji criteria exhibited a higher sensitivity across subgroups, including patients with bulbar (P<0.001) and limb-onset (P<0.001) disease. The inclusion of the "possible" diagnostic category as a positive finding significantly enhanced the sensitivity of the Awaji criteria and rEEC, particularly in early stages of the disease (<12 months form symptom onset), whilst specificity remain unchanged. Our study established a higher sensitivity of Awaji criteria when compared to rEEC, with diagnostic benefits evident in bulbar and limb-onset disease. Inclusion of "possible" ALS as a positive finding significantly enhanced the sensitivity of both criteria, while maintaining specificity, and should be considered in clinical practice and future therapeutic trials.

Introduction

Amyotrophic lateral sclerosis (ALS) is a fatal neurodegenerative disorder of the human motor system, with a median survival of 3-5 years (47, 48). The diagnosis of ALS remains phenotypically based, relying on the identification of upper (UMN) and lower motor neuron (LMN) signs within body regions, with the level of diagnostic certainty dependent on the extent of upper and lower motor neuron dysfunction (6, 498, 511). In the absence of a pathognomonic test, consensus diagnostic criteria were developed in order to provide a more definite diagnosis of ALS and thereby facilitate in patient management and recruitment into clinical trials.

The first consensus diagnostic criteria were developed in El Escorial (Spain) at an international workshop organized by the World Federation of Neurology in 1990 (511). The clinically based El Escorial criteria mandated that the diagnosis of ALS should be based on identifying the presence of upper and lower motor neuron signs, with four levels of diagnostic certainty. In 1998, the El Escorial criteria were revised (revised El Escorial [rEEC], also known as the Airlie House criteria) in order to improve the diagnostic sensitivity, whereby an additional "clinically probable-laboratory supported" category was added and defined as the presence of upper and lower motor neuron signs in one region or isolated upper motor neuron signs in 1 region, with features of lower motor neuron dysfunction evident in 2 regions on neurophysiological testing (498). Although both sets of criteria were specific for ALS, the sensitivity remained an issue, particularly in the early stages of the disease process resulting in diagnostic delays and recruitment into therapeutic trials perhaps, beyond the therapeutic window period (51, 247, 499, 512).

In an attempt to reduce the diagnostic delay, a neurophysiologically based Awaji criteria was developed in 2006 (6). These criteria proposed that neurophysiological features of LMN dysfunction, including chronic neurogenic and ongoing changes (fibrillation potentials/positive sharp waves) were equivalent to clinical features of LMN dysfunction. In addition, fasciculations were deemed equivalent to the presence of fibrillation potentials/positive sharp waves. Upper motor neuron dysfunction, however, remained clinically based.

The diagnostic utility of the Awaji criteria was compared to the revised El Escorial criteria by a number of single centre retrospective and prospective studies, most of which reported an increased sensitivity when compared to rEEC (30, 52-59). One study (60) reported a lower sensitivity of the Awaji criteria and another study suggested that in approximately 20% of ALS patients, the diagnostic category was downgraded (61), a finding largely attributed to the omission of the "probable-laboratory supported" diagnostic category. Importantly, the diagnostic benefit appeared to be most prominent in bulbar-onset ALS (30, 61). In addition, whilst ALS diagnostic criteria are regarded to be specific, there is a paucity of specificity (30, 61) data preventing objective conclusions about the reliability of the ALS diagnostic criteria.

Given the uncertainties around the currently available diagnostic ALS criteria, a multicentre prospective study could be of importance in further clarifying their utility. Consequently, the aim of the current prospective multicenter study was to compare the sensitivity and specificity of the ALS diagnostic criteria (revised El Escorial versus Awaji) and to establish their utility in a clinical setting.

Methods

All patients were prospectively and consecutively recruited from four large ALS centers on the East Coast of Australia in keeping with the inclusion criteria. Inclusion criteria were as follows: (i) Suspected diagnosis of ALS by the referring physician; (ii) Pure motor disorder with clinical features of upper and lower motor dysfunction in separate body regions, where LMN dysfunction developed caudal to UMN dysfunction, with evidence of disease progression over 6 months from initial assessment; or (iii) Neuromuscular disorder defined as muscle weakness and wasting for at least 6 months in at least one body region, irrespective of whether sensory symptoms were present. At time of assessment, the assessor was blinded to the eventual diagnosis, namely whether the diagnosis of ALS or a mimic disorder.

Exclusion criteria included (i) pure UMN syndrome in which laboratory and neuroimaging studies suggested a diagnosis other than ALS, such as hereditary spastic paraplegia or progressive forms of multiple sclerosis; (ii) diagnosis of a non-neuromuscular neurological disorder to explain the patient's symptoms, such as cerebellar or extrapyramidal syndromes; (iii) non-neurological disorders causing the symptoms; (iv) inability or refusal to provide informed consent. All patients provided written informed consent to the procedures approved by the Western Sydney Local Health District and South East Sydney Area Health Service Human Research Ethics Committees.

Once recruited, all patients underwent a clinical assessment and detailed investigations to diagnose mimic disorders. The investigations were as follows: routine biochemistry, hematology, vasculitic screen (ANA, ENA, ANCA), immunoelectrophoeresis, angiotensin converting enzyme levels, metabolic screen (vitamin B12, folate, B6, thyroid function tests), infective screen (HIV, syphilis serology, HTLV 1 and II), genetic testing (Kennedys disease-

for male patients, oculopharyngeal muscular dystrophy testing, spinal muscular atrophy), anti-ganglioside antibodies (GM1, anti-MAG), voltage-gated K^+ channels, acetylcholine receptor and muscle specific tyrosine kinase antibodies. In addition, magnetic resonance imaging of brain and spinal cord was undertaken to exclude structural lesion.

Patients were clinically staged using the amyotrophic lateral sclerosis functional rating score (ALSFRS-R) (513). The disease duration (months) from time of symptom onset and site of disease onset were recorded. Muscle strength was assessed by the Medical Research Council (MRC) score, with the following muscle groups assessed: shoulder abduction, elbow flexion and extension, wrist dorsiflexion, finger abduction and thumb abduction, hip flexion, knee extension and ankle dorsiflexion bilaterally, yielding a maximal score of 90. Upper motor neuron function was assessed and graded by a dedicated UMN score (497).

Nerve conduction study and needle electromyography (EMG) was performed according to established techniques by experienced neurophysiologists (514). In all patients, at least three body regions were sampled (bulbar, cervical, and lumbosacral), and special attention was given to fasciculations. Two physicians (NG and PM) graded the sensitivity of the revised El Escorial (498) and Awaji (6) criteria in all patients. At time of initial assessment the authors were blinded to the eventual diagnosis. Statistical analysis was performed by a separate rater (SV).

Statistics

The primary outcome measure was the diagnostic utility (sensitivity and specificity) of the consensus criteria (rEEC versus Awaji) in differentiating ALS from non-ALS mimic disorders. The secondary outcome measures included the diagnostic utility of the criteria in

ALS subgroups, defined by site of disease onset (bulbar versus limb), functional disability (ALSFRS-R > 38 less severe; <38 more severe disease) and disease duration at time of assessment (< 12 months early; >12 months longer disease). The sensitivity, specificity, and number needed to test (NNT) were determined for each criteria (rEEC and Awaji criteria). Pearson Chi square test or McNemar test were utilised to assess differences between the criteria. A probability value <0.05 was considered statistically significant. Results were expressed as median (interquartile range).

Results

Clinical features

Between January 1 2012 and August 31 2015, we enrolled 416 patients (253 males, 163 females median age 61 years, [49-69]) with suspected ALS from four neuromuscular clinics on the East Coast of Australia who met the inclusion criteria. After a detailed clinical, laboratory, neurophysiological and radiological assessment and follow-up for at least 6 months, 233 patients were eventually diagnosed with ALS (142 males, 91 females, median age 62 years [52-69]), while 212 patients were diagnosed with an ALS mimic disorder (Table 2.1).

The degree of functional impairment in the ALS patients, as indicated by the ALSFRS-R score, was mild (Table 2.1). Muscle strength, as measured by the MRC score, was comparable between the groups, as was the median age at time of assessment (Table 2.1). In contrast, UMN signs were more prominent in ALS patients, while the disease duration was significantly shorter in ALS (Table 2.1). During the course of the study 42 (18%) ALS patients died, with median survival from symptom onset being 28 (20-39) months. At last follow-up, the median disease duration in the surviving patients was 35 (26-53.5) months.

	ALS	Non-ALS neuromuscular mimic disorders
Median Age (years)	62 (52-69)	58 (44-69)
Gender (Male: Female)	142:91	111:72
Disease duration (months)	12 (6-20.5)	60 (33-192)
ALSFRS-R	42 (36.8-44)	N/A
MRC total score	82 (75.8-88)	88 (82-90)
MRC upper limb score	56 (49-60)	60 (56-60)
MRC lower limb score	29 (26-30)	29 (26-30)
UMN score	12 (8-14)	0 (0-0)

Table 2.1. Demographic and clinical details of 416 patients with suspected amyotrophic lateral sclerosis (ALS). In total, 233 patients were diagnosed with ALS and 183 diagnosed with non-ALS neuromuscular mimic disorders, including chronic inflammatory demyelinating neuropathy (63), acquired neuromyotonia (22), myopathy (22), Kennedy's disease (13), myasthenia gravis (13), axonal neuropathy (13), multifocal motor neuropathy (10), spinal muscular atrophy (6), Hirayama's disease (6), distal hereditary motor neuronopathy with pyramidal features (5), FOSMN syndrome (4), cervical radiculopathy (3), Lead toxicity (1), post-polio syndrome (1). All patients were assessed using the amyotrophic lateral functional rating score-revised (ALSFRS-R), Medical Research Council (MRC) score, N/A – not applicable, and an upper motor neuron (UMN) score. All data is expressed as median (interquartile range).

Comparison of diagnostic criteria

The sensitivity of the Awaji criteria, as defined by the proportion of patients categorized as definite or probable ALS, at time of initial assessment was 57% (95% confidence interval [CI] 50.0-63.3%) and was significantly higher when compared to rEEC (45%, 95% CI 38.7-51.7%; Pearson Chi-Square 124.3, df 2, $P < 0.001$, Table 2.2). The specificity for the Awaji and revised El Escorial criteria were 99.5% (95% CI 96-100%), with the number needed to test in order to diagnose one extra case of ALS, in a population composed of neuromuscular diseases, being 1.8 (1.5-2) for the Awaji criteria and 2.4 (2-2.6) for the rEEC.

	Awaji criteria % (95% confidence interval)	Revised El Escorial criteria % (95% confidence interval)	P Value
Total ALS population			
Sensitivity (def/prob)	57 (50.0-63.3)	45 (38.7-51.7)	< 0.001
NNT	1.8 (1.5-2)	2.4 (2-2.6)	
Sensitivity (+possible)	83.4 (78.0-87.9)*	79.6 (73.9-84.5)*	0.28
Bulbar-onset ALS			
Sensitivity (def/prob)	52.2 (39.8-64.4)	42 (30.2-54.5)	< 0.001
NNT	1.9 (1.6-2.5)	2.5 (1.9-3.4)	
Sensitivity (+possible)	75.8 (63.6-85.5)[!]	67.7 (55.2-78.5)[x]	
Limb-onset ALS			
Sensitivity (def/prob)	58.9 (50.9-66.5)	43.1 (31.2-51.4)	< 0.001
NNT	1.7 (1.5-2)	2.3 (2-3.3)	
Sensitivity (+possible)	87.5 (81.4-92)[!]	85 (78.6-90.7)[s]	
ALSFRS-R			
Sensitivity (def/prob) (>38)	49.1 (41.1-57.1)	36.8 (29.4-44.7)	< 0.05
Sensitivity (def/prob) (<38)	77.3 (65.3-86.7)#	67.6 (55-78.8)#	0.15
ALSFRS-R			
Sensitivity (+possible) (>38)	78.9 (71.8-84.9)	71.6 (64-78.4)	0.13
Sensitivity (+possible) (<38)	90.9 (81.3-96.6)	86.2 (75.3-93.5)	0.39
Disease duration (months)			
Sensitivity (def/prob) (<12 months)	62.4 (53.6-70.7)	47 (38.2-55.9)	< 0.05
Sensitivity (def/prob) (>12 months)	48.9 (38.1-59.8)	41.4 (30.9-52.4)	0.32
Disease duration (months)			
Sensitivity (+possible) (<12 months)	84.2 (76.9-90)[$]	79.7 (71.7-75)[$]	0.34
Sensitivity (+possible) (>12 months)	78.9 (68.7-86.6)[$]	75 (64.6-83.6)[$]	0.66

Table 2.2. The Awaji criteria exhibited a significantly higher sensitivity when compared to the revised El Escorial criteria (rEEC) in the entire cohort of amyotrophic lateral sclerosis (ALS) as well as patients with bulbar and limb-onset disease, with a reduced number needed to test (NNT). The specificity of both criteria were identical at 99.5%. Inclusion of the ALS "possible" diagnostic category as a positive finding [sensitivity (+possible)], significantly enhanced the sensitivity of both the Awaji and revised El Escorial criteria in ALS and subgroups as follows; *P < 0.001 (Awaji [definite/probable] versus Awaji [add possible]); $^{!}$P <0.001 (Bulbar and limb-onset ALS Awaji [definite/probable] versus Awaji [add possible]); ^{X}P < 0.01 (Bulbar-onset ALS, rEEC [definite/probable] versus rEEC [add possible]; ^{S}P < 0.001 (Limb-onset ALS, rEEC [definite/probable] versus rEEC [add possible]; $^{\#}$P< 0.05 (Awaji and rEEC sensitivity significantly higher in patients with worse functional deficits); $^{\$}$ P< 0.001 (Addition of possible category significantly increased sensitivity for Awaji and rEEC in patient with shorter and longer disease duration).

The identification of early onset disease, 'possible or suspected ALS' was more robust in the Awaji criteria, upgrading 31 (24%) of patients in the El Escorial criteria to Awaji 'definite or probable', conversely only 2 (2%) patients classified as ALS possible/suspected on the Awaji criteria were upgraded by the rEEC. In addition, 12 (5.1%) patients were classified as "probable-laboratory supported" on the rEEC, resulting in 10 patients classified as definite/probable on the Awaji criteria with only 2 patients downgraded to a "possible" diagnostic category.

The diagnostic utility of the Awaji and revised El Escorial criteria were further assessed by considering the "possible" diagnostic category as a positive finding. The sensitivity of the Awaji [83.4%, 78.0-87.9%, P < 0.001] and revised El Escorial criteria [79.6%, 73.9-84.5%, P < 0.001] increased, and interestingly the sensitivity of the Awaji criteria and rEEC were now comparable (Table 2.2). Importantly, the specificity for both the Awaji and revised El Escorial criteria remained unchanged [99.5% (95% CI 96-100%)]. As expected the number needed to test in order to diagnose an extra ALS case was reduced to 1.2 (1.1-1.3) for the Awaji criteria and 1.3 (1.2-1.4) for the rEEC.

Comparison of diagnostic utility in ALS subgroups

Subgroup analysis, based on site of disease onset, disclosed that the sensitivity of the Awaji criteria (52.2% [39.8-64.4]) were significantly higher for bulbar onset disease when compared to the rEEC (42% [30.2-54.5], Pearson Chi-Square 39.5, df 1, $P < 0.001$, Table 2.2). Importantly, the number of bulbar onset ALS patients needed to be tested in order to diagnose one extra case of ALS was 1.9 (1.6-2.5) by the Awaji criteria and 2.5 (1.9-3.4) by the rEEC. In addition, the sensitivity of the Awaji criteria (58.9% [50.9-66.5]) were significantly higher in limb-onset patients when compared to rEEC (43.1% [31.2-51.4], Pearson Chi-Square 86.4, df 2, $P < 0.001$, Table 2.2), with the NNT for Awaji criteria being 1.7 (1.5-2) and for rEEC 2.3 (2-3.3).

The inclusion of the "possible" diagnostic category as a positive finding significantly enhanced the sensitivity of both criteria while the specificity remained unchanged. Specifically, in bulbar-onset ALS the sensitivity of the Awaji criteria was significantly increased to 75.8% (63.6-85.5%, $P < 0.001$) and rEEC to 67.7% (55.2-78.5%, $P < 0.01$, Table 2.2). In limb-onset ALS a more impressive increase in sensitivity was evident for both the Awaji criteria (87.5% [81.4-92%], $P < 0.001$) and rEEC (85% [78.6-90.7%], $P < 0.001$).

The degree of functional disability, as indicated by ALSFRS-R score, also influenced the sensitivity of both the Awaji and rEEC criteria. Specifically, the sensitivity of the Awaji criteria in patients with greater functional disability (ALSFRS-R < 38) was 77.3% (65.3-86.7%, Table 2.2), and was significantly higher when compared to patients with less severe disease (49.1%, 41.1-57.1%, $P < 0.05$). In addition, the rEEC criteria also exhibited a higher sensitivity in patients with more severe disease (67.6%, 55-78.8%) compared to patients with less functional impairment (36.8%, 29.4-44.7%, $P < 0.05$). The Awaji criteria, however, was

significantly more sensitive when compared to rEEC in less severe disease ($P< 0.05$), while comparable sensitivities between the criteria were evident in the more severe disease subgroup ($P=0.15$). Taken together, these findings suggest that while both sets of criteria are less efficient at diagnosing patients in the earlier stages of the disease process, the Awaji criteria may exhibit a greater sensitivity at the early stages.

The inclusion of the "possible" diagnostic category as a positive finding significantly enhanced the sensitivity for both criteria. Specifically, the sensitivity of the Awaji criteria was significantly increased to 90.9% (81.3-96.6%, $P < 0.05$) in patients with more severe disease and to 78.9% (71.8-84.9%, $P < 0.001$) in the less severe group. Likewise, the sensitivity of the rEEC was increased to 86.2% (75.3-93.5%, $P < 0.05$) in the more severe cohort and to 71.6% (64-78.4%, $P < 0.001$) in the group that was functionally more severe. Importantly, the specificity for both criteria was maintained.

The disease duration at time of assessment significantly impacted on the sensitivity of the Awaji criteria when compared to rEEC. Specifically, the sensitivity of the Awaji criteria was significantly higher than rEEC in patients with shorter disease duration (< 12 months, Table 2.2), while the sensitivity was comparable in patients with longer disease duration at time of assessment. Importantly, the sensitivity of both criteria were significantly increased by incorporating the "possible" diagnostic category, and this benefit was evident in patients with shorter and longer disease duration (Table 2.2, Figure 2.1).

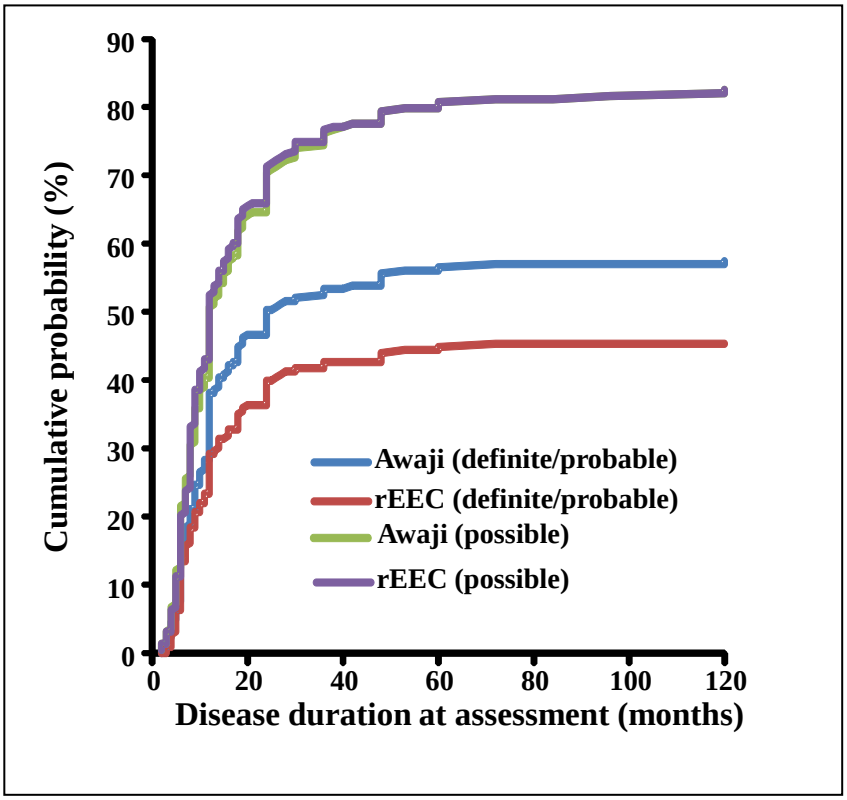

Figure 2.1. Cumulative probability of reaching a diagnosis of amyotrophic lateral sclerosis (ALS) for different diagnostic categories at the time of initial assessment plotted as a function of disease duration (months) at first assessment.

Discussion

An accurate and expeditious diagnosis of ALS is critical for patient management as it enables institution of appropriate management strategies, including commencement of riluzole and multidisciplinary care, at an earlier stage of the disease process as well as providing diagnostic certainty for patients and families that will enable adequate future planning. In addition, an early and accurate diagnosis facilitates recruitment of patients into clinical trials, at a stage of the disease process where neuroprotective therapies may be most effective - the putative therapeutic window period. In the absence of a pathognomonic test, the diagnosis of ALS has relied on consensus criteria, namely the El Escorial/Airlie House (498, 511) and the Awaji (6) criteria, which have exhibited a varied sensitivity (30, 61). Moreover, specificity data were infrequently reported (54, 57, 60, 504), thereby further limiting the interpretation of diagnostic utility of the criteria.

The current prospective multicenter study, incorporating a total of 435 ALS and non-ALS neuromuscular mimic disorder patients, established a higher sensitivity of the Awaji criteria when compared to rEEC. Importantly, the increase in sensitivity was evident in both bulbar and limb-onset ALS, as well as patients with less severe disease (ALSFRS-R>38) and with shorter disease duration (< 12 months). Of relevance, application of the Awaji criteria resulted in a 12% gain in sensitivity, which was lower than previously reported (30, 52-54). Given the large sample size (N=233) and a multidisciplinary prospective design, it seems plausible to conclude that the present findings reflect more accurately the diagnostic accuracy of the criteria in a clinical setting. This notion is underscored by marked heterogeneity of sensitivities in previous studies, with some reporting a higher sensitivity of the Awaji criteria (52, 53, 55, 56, 58, 502, 504), others documenting equivalent sensitivities (54, 57, 59), while one study established a lower sensitivity for the Awaji criteria (60).

The Awaji criteria has been critiqued for the omission of the "probable laboratory supported" diagnostic category, which has been suggested as a likely explanation for the lower sensitivity of Awaji criteria in limb-onset disease (59, 60, 509). Specifically, it has been reported that the Awaji criteria downgraded approximately 20% of ALS classified as "probable-laboratory supported" on the rEEC. In the present study, 10 (4.3%) patients were classified as probable-laboratory supported, of which 2 were downgraded to the Awaji "possible" category. Importantly, the sensitivity of the Awaji criteria was significantly higher when compared to rEEC in limb-onset ALS, thereby arguing against a significant diagnostic impact of omitting the "probable laboratory supported" diagnostic category from the Awaji criteria.

In an attempt to increase the sensitivity of the diagnostic criteria, a number of trials have permitted the inclusion of ALS patients classified within the "possible" diagnostic category (278, 515). Of relevance, the latest revision proposed a further liberalization of the El Escorial criteria, whereby "possible" ALS was considered a positive finding (63). While such a revision would ultimately increase the sensitivity, the issue of whether specificity is maintained remains to be determined. Importantly the present findings confirm a significant increase in sensitivity by incorporating the "possible" diagnostic category for both Awaji and Revised El Escorial criteria. This increase in sensitivity was evident across ALS subgroups, as defined by site of disease onset, function deficits and disease duration (Table 2.2). Importantly, the specificity remained unchanged, thereby suggesting that liberalisation of the criteria could significantly enhance the diagnosis of ALS, which could be of particular relevance in the early stages of the disease, ultimately enabling earlier recruitment of patients into clinical trials where neuroprotective therapies are likely to be most effective.

The utility of diagnostic criteria may be limited in the restricted or atypical ALS phenotypes. Specifically, in clinically pure lower motor neuron phenotypes, such as flail arm syndrome or progressive muscular atrophy (63). Identification of subclinical UMN dysfunction with TMS techniques has been shown to facilitate the diagnosis in the flail leg syndrome (240). In addition, a recent revision of the El Escorial criteria suggested that identification of LMN dysfunction in isolation could be deemed as consistent with ALS, in the setting of excluding mimic disorders (63). While this modification would potentially diagnose the LMN variants of ALS, the specificity needs to be confirmed. Given that the modification was published after the commencement of the current study, assessment of specificity in a blinded fashion was not possible and future blinded prospective studies should investigate the issue of sensitivity.

A potential limitation of the diagnostic criteria remains the reliance on clinically identifying upper motor neuron dysfunction. Specifically, the identification of upper motor neuron signs in ALS may be difficult for a variety of reasons (38), potentially impacting on the sensitivity of criteria. Objective assessment of UMN function by threshold tracking transcranial magnetic stimulation (TMS) techniques has been documented to significantly increase the sensitivity of the Awaji and revised El Escorial criteria, reliably differentiating ALS from potential mimic disorders and reducing the diagnostic delay by months (237, 510). Consequently, incorporation of the threshold tracking TMS technique into future revisions of diagnostic criteria could further enhance the diagnosis of ALS.

Chapter 3

DIAGNOSTIC UTILITY OF CORTICAL DYSFUNCTION IN ALS

Summary

Whilst the previous chapter highlighted that the Awaji criteria could be improved by the incorporation of a 'possible' criteria, the lack of an objective biomarker of upper motor neuron (UMN) dysfunction continued to be problematic. Given that cortical hyperexcitability appears to be an early feature in ALS, with potential as a diagnostic biomarker, the present study assessed the diagnostic utility of threshold tracking transcranial magnetic stimulation (TMS) technique as an aid to the Awaji criteria in establishing of an earlier diagnosis of ALS. Prospective studies were undertaken on a cohort of 82 patients with suspected ALS and results were compared to 34 healthy controls. A measure of cortical hyperexcitability, short-interval intracortical inhibition (SICI) was significantly reduced in ALS patients ($P<0.0001$), with a comparable reduction evident in the Awaji groups ($SICI_{AWAJI\ POSSIBLE}$ 1.3±1.3%; $SICI_{AWAJI\ PROBABLE/DEFINITE}$ 1.4±1.7%). Central motor conduction time was significantly prolonged ($P<0.001$), while the motor evoked potential amplitude ($P<0.05$) and intracortical facilitation ($P<0.05$) were increased. The frequency of TMS abnormalities was similar across Awaji subgroups, and addition of TMS abnormalities as a diagnostic category enabled reclassification of 88% of Awaji possible patients to Awaji probable/definite. Cortical dysfunction, as measured by the threshold tracking TMS, potentially facilitates an earlier diagnosis of ALS when combined with the Awaji criteria.

Introduction

Amyotrophic lateral sclerosis (ALS) is a rapidly progressive and fatal neurodegenerative disorder of motor neurons (48). Clinically, ALS is characterized by the presence of a combination of upper (UMN) and lower motor (LMN) neuron signs, which form the diagnostic basis for ALS (498). Diagnostic criteria, based on the identification of upper and lower motor neuron dysfunction may be insensitive, especially in the early stages of ALS, potentially resulting in a diagnostic delay (51) and ultimately institution of neuroprotective therapies and recruitment into clinical trials (247).

The Awaji criteria were developed in order to facilitate an earlier diagnosis of ALS (6). These consensus criteria proposed that neurophysiological findings of chronic neurogenic changes could be equated to clinical features of LMN dysfunction. In addition, the presence of fasciculation potentials was deemed to be a marker of denervation. The sensitivity of the Awaji criteria was reported to be significantly increased, while the specificity appeared to be preserved (30, 52-57). Quantitative dysfunction of UMNs, however, was not captured by the Awaji criteria, thereby potentially precluding the diagnosis of ALS prior to development of widespread neurogenic changes or when the presenting phenotype is atypical such as such as the flail-arm variant (240).

Upper motor neuron function may be assessed by transcranial magnetic stimulation (TMS) techniques. Specifically, resting motor threshold (RMT), motor evoked potential (MEP) amplitude, and cortical silent period (CSP) duration are all biomarkers of UMN function, elicited by single pulse TMS techniques, and may be abnormal in ALS (39). Of further relevance, short interval intracortical inhibition (SICI) is elicited by paired-pulse TMS

techniques, whereby a subthreshold conditioning stimulus suppresses the response produced by a subsequent test stimulus when the interstimulus interval is between 1-7 ms (329, 378).

Importantly, cortical dysfunction appears to be an early feature in ALS, distinguishing ALS from mimic disorders, and supporting an earlier diagnosis of ALS when compared to the El-Escorial criteria (237). The diagnostic utility of TMS when compared to the Awaji criteria in identifying ALS, however, remains to be determined. Consequently, the present study assessed the diagnostic potential of the threshold tracking TMS technique in ALS, particularly whether the finding of cortical hyperexcitability is more sensitive at establishing an earlier diagnosis of ALS than the Awaji criteria.

Methods

Clinical phenotype

Studies were undertaken prospectively on a cohort of 82 patients (52 males and 30 females, mean age 60) with suspected ALS. All patients were followed for up to three years, during which period the diagnosis of ALS was confirmed. At the time of initial clinical assessment all patients underwent TMS studies. None of the patients with ALS were receiving medications, which could potentially interfere with the neurophysiological results. Informed consent to the procedures was provided by all patients, with the study approved by the Sydney West Area Health Service and Human Research Ethics Committees.

Patients were clinically staged using the Amyotrophic Lateral Sclerosis Functional Rating Scale-Revised (ALSFRS-R) (495) and categorised according to site of disease onset as limb or bulbar-onset. In addition, muscle strength was assessed using the Medical Research Council (MRC) score (516), with the following muscle groups assessed bilaterally yielding a

total MRC score of 90: shoulder abduction; elbow flexion; elbow extension; wrist dorsiflexion; finger abduction; thumb abduction; hip flexion; knee extension; ankle dorsiflexion. Upper motor neuron (UMN) dysfunction was clinically assessed utilizing the UMN score (497).

Neurophysiological studies

Peripheral studies

Prior to undertaking cortical excitability studies, all patients were assessed by nerve conduction studies and needle electromyography. The degree of peripheral disease burden was assessed in the median nerve, whereby the median nerve was stimulated electrically at the wrist using 5-mm Ag-AgCl surface electrodes (ConMed, Utica, USA). The resultant compound muscles action potential (CMAP) was recorded from the APB muscle and the onset latency and peak-peak amplitude were measured. Subsequently, the neurophysiological index (NI) was derived according to a previously reported formula (26).

Needle EMG was performed using a concentric electrode (26G, Alpine Biomed ApS), and at least 3 regions were assessed (cranial, cervical and lumbosacral). The median number of muscles studied per patient was 12 (IQR 7-14). Evidence of ongoing activity (positive sharp waves and fibrillation potentials), fasciculations and chronic neurogenic changes were recorded.

Cortical excitability

Cortical excitability was assessed by utilising the threshold tracking TMS technique according to a previously reported technique (329). Briefly, the MEP response was fixed at 0.2mV (±20%), and changes in test stimulus intensity required to generate the target

response, when preceded by a subthreshold conditioning stimuli, were measured. The following TMS parameters were recorded; short interval intracortical inhibition (SICI), intracortical facilitation (ICF), resting motor threshold (RMT), central motor conduction time (CMCT), MEP amplitude (%CMAP response) and cortical silent period (CSP) duration.

Statistical analysis

Cortical excitability in ALS patients were compared to control data obtained from 34 healthy subjects (17 men; 17 women, mean-age 56 years). Student's t-test or a Wilcoxon-Signed rank test was used for assessing differences between means. Analysis of variance was used for multiple comparisons. A P value<0.05 was considered statistically significant. Results are expressed as mean ± standard error of the mean (SEM) or median with interquartile range (IQR).

Results

Clinical features

At the time of TMS testing 61% of patients were classified as Awaji possible while 39% were classified as probable/definite (Table 3.1). During the follow-up period of up to 3 years, 95% of patients progressed to be classified as probable or definite ALS. The median disease duration at time of TMS testing from symptom onset was 11 months (IQR 6-18 months). Forty percent of patients exhibited bulbar-onset disease while 60% reported limb-onset disease. During the follow-up period, 21% of patients died with median survival being 14 months (3-36).

The degree of functional impairment was mild at time of assessment, with the median ALSFRS-R score being 42 (IQR 38-45) and similar in the Awaji groups ($Awaji_{POSSIBLE}$ 43 [39-45]; $Awaji_{PROBABLE/DEFINITE}$ 41 [37-45], Z= -0.75, P=0.23). The median MRC sum score was 84 (IQR 79-88), while the median MRC score from the APB was 4 (IQR 4-5). The median UMN score was 12 (9-13), indicating the presence of significant clinical UMN dysfunction in the ALS cohort.

	ALS (N = 82)	**ALS Possible (N = 50)**	**ALS Probable/Definite (N = 32)**	**Bulbar-onset (N = 33)**	**Limb-onset (N = 49)**
Age (years, mean , SEM)	60 (1.5)	61 (2.0)	59 (2.0)	61 (2.5)	59 (1.8)
Sex	52M, 30F	28M, 22F	24M, 8F	22M, 11F	30M, 19F
Disease duration (months, IQR)	11 (6-18)	10 (6-24)	11 (6-12)	11 (8-20)	9 (6-18)
APB (median, IQR)	4 (4-5)	5 (4-5)	4 (4-5)	5 (4-5)	4 (4-5)
ALSFRS (median, IQR)	42 (38-45)	43 (39-45)	42 (37-45)	42 (38-44)	43 (39-46)
MRC UL score (median, IQR)	57 (51-60)	58 (55-60)	52 (45-57)	58 (55-60)	56 (50-59)
MRC LL score (median, IQR)	30 (26-30)	30 (27-30)	29 (23-30)	30 (30-30)	29 (23-30)
MRC SUM score (median, IQR)	84 (79-88)	86 (82-89)	79 (67-84)	88 (84-90)	81 (76-86)
UMN Score	12 (0.6)	9.6 (0.8)	10.5 (1.0)	11.5 (0.8)	8.7 (0.8)

Table 3.1. Clinical features summarized for 82 patients with suspected amyotrophic lateral sclerosis (ALS). All patients were clinically staged by the amyotrophic lateral sclerosis functional rating scale-revised (ALSFRS-R) and Medical Research Council (MRC) score, in the upper limb (UL), lower limbs (LL) and abductor pollicis brevis (APB) muscle. Upper motor neuron (UMN) score was utilised o assess the degree of clinical UMN dysfunction. All data are expressed as mean±standard error of the mean (SEM) or median (interquartile range, IQR).

Neurophysiological studies

The CMAP amplitude (ALS 7.2±0.5 mV, controls 9.5±0.5 mV, P<0.0001) and NI (ALS 1.2 ± 0.1; controls 2.3±0.1, P<0.0001) were significantly reduced in ALS patients. Sub-group analysis disclosed a comparable reduction of CMAP amplitude ($CMAP_{POSSIBLE}$ 6.9 ±0.5 mV; $CMAP_{PROBABLE/DEFINITE}$ 6.9±0.9 mV) and NI ($NI_{POSSIBLE}$ 1.3±0.2; $NI_{PROBABLE/DEFINITE}$ 1.1±0.2) in the Awaji subgroups, indicating a comparable degree of peripheral disease burden.

Cortical excitability

Paired-pulse threshold tracking TMS studies disclosed a significant reduction of SICI in ALS (Fig. 3.1). Specifically, averaged SICI was significantly reduced in ALS (ALS1.3±1.1%; controls 10.3±1.1%, P<0.0001, Fig. 3.2A), with a similar reduction evident in the Awaji groups ($SICI_{POSSIBLE}$; 1.3±1.3%, $SICI_{PROBABLE/DEFINITE}$ 1.4±1.7%; controls 10.3±1.1%, F=14.9, P<0.0001, Fig. 3.2B). In addition, a comparable reduction of SICI was evident in ALS patients with and without out UMN signs ($SICI_{UMN\ score\ 0}$ 2.0±1.9; $SICI_{UMN\ score\ >0}$ 1.5±1.3). Of relevance, peak SICI at interstimulus interval (ISI) 1 and 3 ms were significantly reduced in ALS (Fig. 3.1), with a comparable reduction of peak SICI at 1 ms ($SICI_{POSSIBLE}$ 1.0±0.8%; $SICI_{PROBABLE/DEFINITE}$ 1.7±1.7%; $SICI_{CONTROL}$ 6.1±1.3%, F=5.6, P<0.01, Fig. 3.2C) and 3 ms ($SICI_{POSSIBLE}$ 2.4±1.9%; $SICI_{PROBABLE/DEFINITE}$ 4.7±2.5%; $SICI_{CONTROL}$ 15.4±1.6%, F=13.8, P <0.001, Fig. 3.2D) being evident in the Awaji groups.

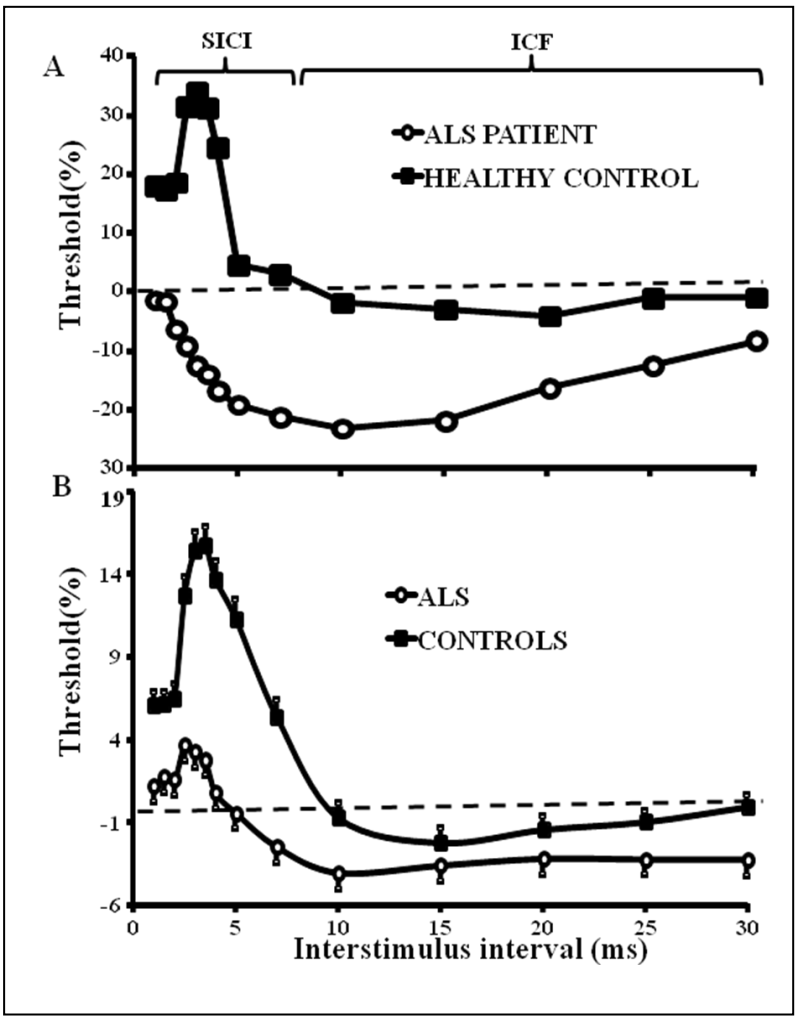

Figure 3.1. Short-interval intracortical inhibition (SICI) was significantly reduced in amyotrophic lateral sclerosis (ALS) patients compared to controls.

Intracortical facilitation follows SICI and was significantly increased in ALS ($P<0.05$, Fig. 3.1). Importantly, a comparable increase of ICF was evident in the Awaji groups (ICF $_{\text{POSSIBLE}}$ -3.6±0.8%; ICF $_{\text{PROBABLE/DEFINITE}}$ -4.4±1.6%).

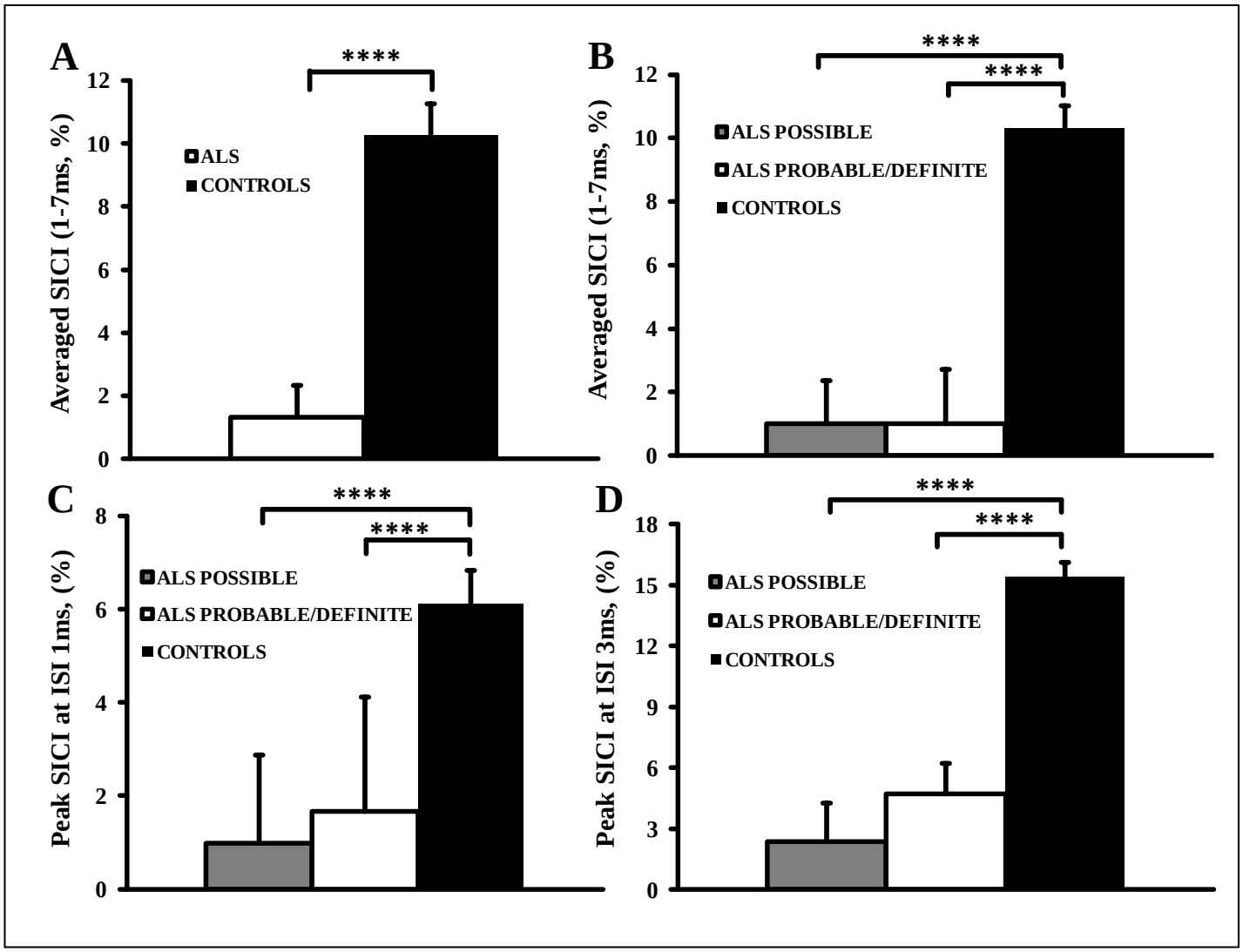

Figure 3.2. **(A)** Averaged short-interval intracortical inhibition (SICI), between interstimulus interval (ISI) 1-7 ms, was significantly reduced in amyotrophic lateral sclerosis (ALS). (**B)** The reduction of averaged SICI was comparable in Awaji subgroups. Peak SICI at ISI **(C) 1** ms and **(D)** 3 ms was significantly reduced in Awaji subgroups. ****P<0.0001.

Single pulse TMS disclosed a significant increase in MEP amplitude in ALS patients (ALS 33.3±2.8%; controls 25.5±2.5%, Fig. 3.3A, P<0.05). Although the increase in MEP amplitude was evident in both Awaji subgroups, it was only significant in the Awaji possible/definite group (Fig. 3.3B). In addition, the CSP duration was significantly reduced in ALS (ALS 178.1±5.1 ms; controls 214.9±3.6 ms, Fig. 3.3C, P<0.0001), and was comparable in the Awaji groups (P=0.13, Fig. 3.3D).

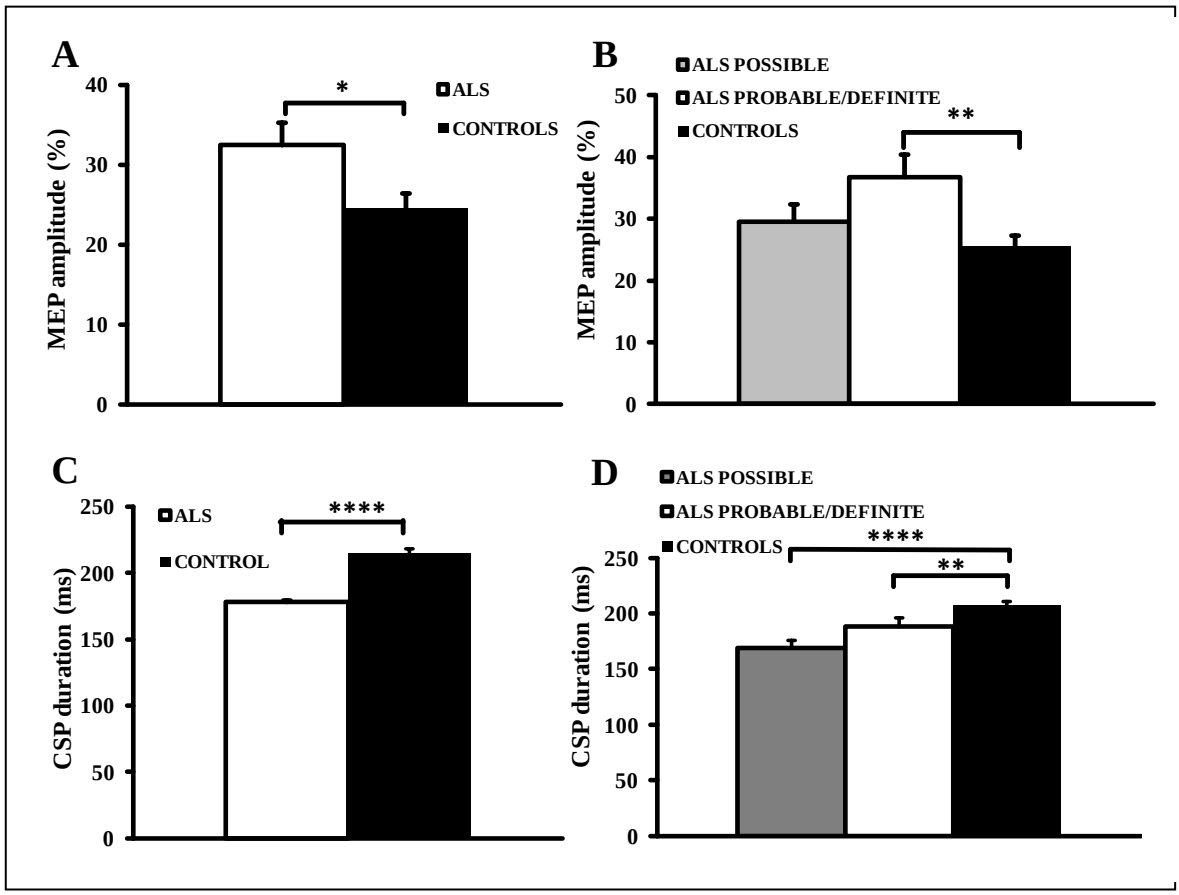

Figure 3.3. Motor evoked potential (MEP) was significantly increased in **(A)** amyotrophic lateral sclerosis (ALS), although this increase **(B)** was only evident in the Awaji probable/definite group. (**C)**. Cortical silent period (CSP) duration was significantly reduced in ALS. **(D)** The reduction in CSP duration was evident in both Awaji groups. *P<0.05;**P<0.01;****P<0.0001

The motor cortex was inexcitable in 23% of ALS patients. In total, 63% of these patients were classified as Awaji possible and 37% as probable/definite. In the remaining 77% of patients, the RMT was significantly reduced (ALS cohort 56.7±1.2%; controls 61.0±1.4%, P<0.05), with the reduction being similar in both Awaji groups (P=0.13). The CMCT was significantly prolonged in ALS patients (ALS 6.6±0.2 ms; controls 5.3±0.2 ms, Fig. 3.4A, P<0.001), and the prolongation was similar in both Awaji groups ($CMCT_{POSSIBLE}$ 6.7±0.3 ms; $CMCT_{PROBABLE/DEFINITE}$ 6.4±0.3 ms, Fig. 3.4B).

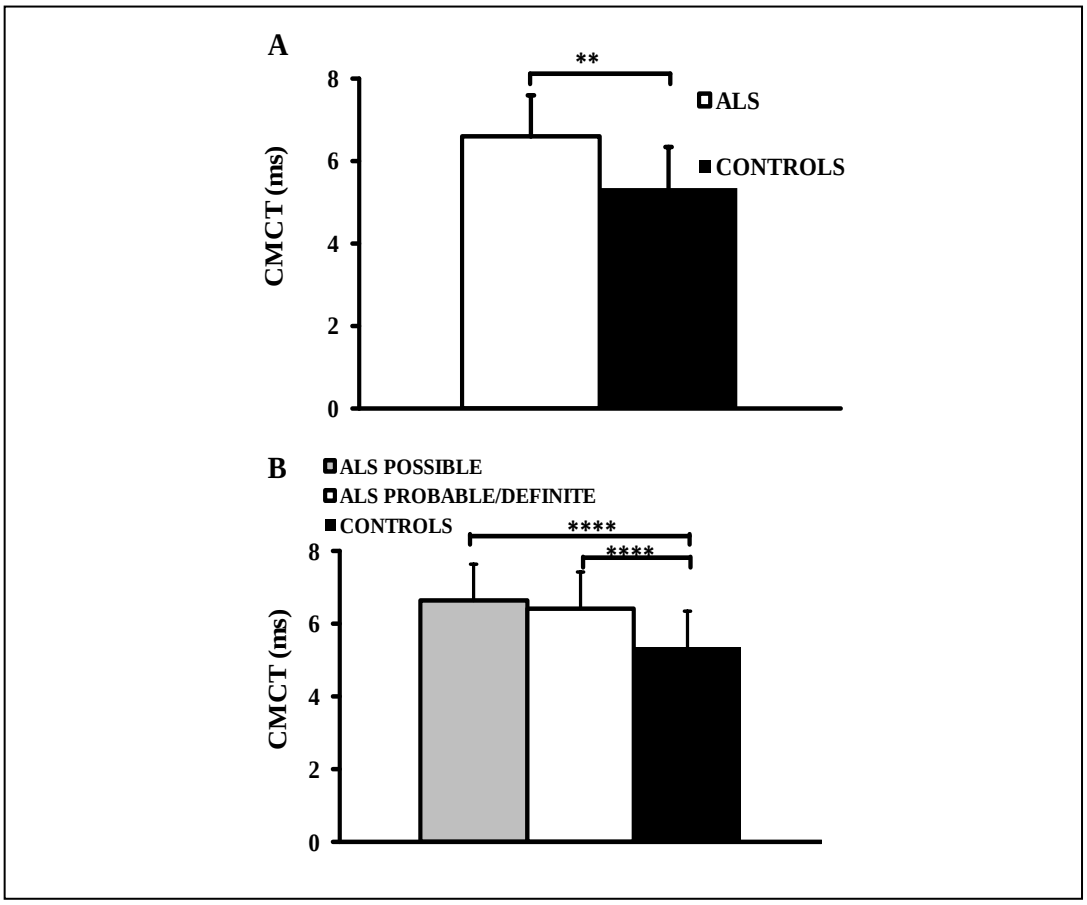

Figure 3.4. (A) Central motor conduction time (CMCT) was significantly prolonged in amyotrophic lateral sclerosis (ALS), and **(B)** was evident in Awaji possible (grey bar) and probable/definite (white bar) ALS when compared to controls (black bar). **P<0.001; ****P<0.0001.

Clinical correlations

Combining clinical, neurophysiological and cortical excitability parameters, it was evident that RMT significantly correlated with the CMAP amplitude (R= -0.40, P<0.01) and NI (R= -0.34, P<0.01). In addition, the MEP amplitude was significantly correlated with the CMAP amplitude (R=0.61, P<0.0001). Taken together, the findings seem to suggest that cortical hyperexcitability may be an early feature in ALS, in keeping with previous studies (39).

Diagnostic utility of threshold tracking TMS

In order to assess the diagnostic utility of threshold tracking TMS, a previously established cut-off value for averaged SICI < 5.5% (237) along with prolonged CMCT and inexcitability of motor cortex, were utilised as biomarkers of cortical dysfunction. TMS abnormalities were evident in 77% of ALS patients, with frequency of abnormalities being similar across Awaji groups (Chi square 1.36, P=0.112). Of relevance, 54% of Awaji possible patients exhibited cortical hyperexcitability, while 27% exhibited an inexcitable motor cortex and 56% prolonged CMCT. Importantly, the frequency of TMS abnormalities was similar in bulbar and limb-onset disease patients (Awaji POSSIBLE BULBAR-ONSET 80%; Awaji POSSIBLE LIMB-ONSET 78%, P=0.595). The addition of TMS abnormalities (reduced SICI, prolonged CMCT or inexcitable cortex) as a diagnostic category resulted in 88% of Awaji possible patients being reclassified as Awaji probable/definite.

Discussion

The current prospective study has established that the findings of cortical dysfunction, as indicated by TMS abnormalities, may be a useful diagnostic biomarker in early symptomatic ALS. Cortical dysfunction was heralded by significant reduction in short-interval intracortical inhibition, resting motor threshold and cortical silent period duration, along with an increase in the MEP amplitude and intracortical facilitation. Importantly, cortical dysfunction appeared to be an early feature in ALS, with cortical hyperexcitability evident in 54% and motor cortex inexcitability in 27% of patients classified as Awaji possible ALS. In addition, prolonged CMCT was evident in 56% of Awaji possible patients. Interestingly even in ALS patients who did not exhibit UMN signs, there was evidence of cortical dysfunction. Importantly, 88% of Awaji possible patients could be re-classified as Awaji probable/definite if TMS abnormalities, including prolonged CMCT, inexcitable motor

cortex or reduced SICI, were used as additional diagnostic parameters. Taken together, these findings suggest that the presence of UMN dysfunction could potentially hasten the diagnosis of ALS when compared to the Awaji criteria.

Diagnosis of amyotrophic lateral sclerosis

In the absence of a pathognomonic test, the diagnosis of ALS has relied on identification of a combination of upper and lower motor signs with evidence of disease progression (498). The clinical criteria have proved insensitive in establishing ALS, especially in the early stages of disease process, thereby resulting in critical delays in institution of appropriate management strategies. Recently developed Awaji criteria (6) have increased the diagnostic sensitivity for ALS without compromising specificity (52-55), although the increase in diagnostic accuracy was attributable to patients with bulbar-onset disease (30, 502). Importantly, UMN dysfunction was assessed clinically in the Awaji criteria and as such in patients with equivocal or absent UMN signs, the diagnosis of ALS may be delayed.

An objective measure of UMN dysfunction could potentially enable an earlier diagnosis of ALS. TMS techniques have been proposed as an objective tool for establishing UMN dysfunction in ALS (39). A modest prolongation of CMCT has been previously established in ALS, and probably reflects degeneration of the fastest conducting corticomotoneuronal fibres as well as increased desynchronization of corticomotoneuronal volleys (46, 517). Of relevance, it has been suggested that the sensitivity of prolonged CMCT could be improved by recording from cranial muscles in patients with bulbar-onset disease (314). The findings in the present study underscore the diagnostic utility of CMCT in ALS, whereby prolongation of CMCT appears to be a sensitive and early biomarker of UMN dysfunction, evident in Awaji possible patients irrespective of site of disease-onset.

Reduction or absence of SICI is an early and robust biomarker of cortical dysfunction in ALS (39). Degeneration of inhibitory cortical interneurons along with glutamate-mediated excitoxicity appears to underlie SICI abnormalities in ALS (224, 406). Importantly, reduction of SICI is specific for ALS among the group of neuromuscular mimic disorders (237), while subclinical reduction of SICI is evident in atypical ALS phenotypes (240). Absence or reduction of SICI may also lead to an earlier diagnosis of ALS when compared to El Escorial criteria (237). The findings in the present study underscore the potential utility of SICI as a diagnostic biomarker in early ALS, being evident in 56% of Awaji possible patients and enabling a more definitive diagnosis of ALS when combined with other TMS parameters.

Diagnostic utility of threshold tracking TMS in ALS

Enrollment of ALS patients into clinical trials remains a major challenge (499), in part related to the use of stringent clinical inclusion criteria which rely on identifying UMN and LMN signs in multiple body regions (498). The reliance on such stringent clinical criteria may exclude ALS patients in early stages of the disease process from enrollment into clinical trials, the very group in which therapeutic agents may be most efficacious.

The Awaji diagnostic criteria were developed in order to enhance the diagnostic accuracy of ALS (6). While numerous studies have reported increased sensitivity and preserved specificity of the Awaji criteria when compared to El Escorial criteria (30, 52-57), a recent study reported a lower sensitivity of the Awaji criteria (60). The discordance between the studies was attributed to the requirement for finding UMN signs in at least 2 regions in order that the Awaji probable criteria are attained. Consequently, utilization of TMS techniques may objectively document UMN dysfunction, enabling an earlier diagnosis of ALS, commencement of neuroprotective therapies and recruitment into clinical trials.

Chapter 4

THE SENSITIVITY AND SPECIFICITY OF THRESHOLD-TRACKING TRANSCRANIAL MAGNETIC STIMULATION FOR THE DIAGNOSIS OF AMYOTROPHIC LATERAL SCLEROSIS: A PROSPECTIVE STUDY

Summary

The earlier study, described in Chapter 3 looked at the diagnostic utility of the threshold tracking TMS in ALS. However, the study design was not undertaken according to the 'Standards of reporting of diagnostic accuracy' (STARD) criteria, which are the 'gold criteria' for diagnostic clinical studies. Subsequently a prospective multicenter study was undertaken on patients referred to three neuromuscular centers in Sydney, Australia between January 1 2010 and March 1 2014. The study was performed in accordance with the STARD criteria. The inclusion criteria included: (i) Definite, probable, or possible ALS as defined by the Awaji criteria; (ii) Pure motor disorder with clinical features of upper and lower motor dysfunction in at least one body region progressing over a 6 month follow-up period; (iii) Neuromuscular disorder mimicking ALS (non-ALS). All subjects underwent threshold tracking TMS at recruitment, with the reference standard being the Awaji criteria. The primary outcome measure was the sensitivity and specificity of TMS in differentiating ALS from non-ALS. Receiver operator curve analysis, a plot of sensitivity and the false-positive rate, was utilized to derive the sensitivity and specificity of TMS. The investigators who performed the index test were blinded to the results of the reference test and all other investigations. In total, 333 patients were studied and 281 patients satisfied the inclusion criteria. Eventually, 209 patients were diagnosed with ALS and 68 with NALS. The threshold tracking TMS technique reliably differentiated ALS from NALS with sensitivity of 73.08% (95% CI: 66.51-78.98%) and specificity of 80.88% (69.53-89.40%) at an early stage in the disease process with mean disease duration at time of testing being 16.7±1.1 months. The threshold tracking TMS technique reliably distinguishes ALS from non-ALS, and could represent a useful diagnostic investigation when combined with the Awaji criteria to prove upper motor neuron dysfunction at early stages of ALS.

Introduction

Amyotrophic lateral sclerosis (ALS) is a rapidly progressive and invariably fatal neurodegenerative disorder of the upper and lower motor neurons (48). The diagnosis of ALS relies on the identification of concurrent upper (UMN) and lower motor neuron (LMN) dysfunction, with the level of diagnostic certainty dependent on the extent of UMN and LMN dysfunction (6, 48, 498). The clinically based ALS diagnostic criteria were deemed insensitive, particularly in early stages of the disease or in the setting of atypical phenotypes, potentially resulting in significant diagnostic delays (51). Consequently, the institution of adequate management strategies, including commencement of neuroprotective therapies such as riluzole, and recruitment into therapeutic trials may be delayed, perhaps beyond the therapeutic window period (247).

Despite rapidly evolving interest in ALS clinical trial methodology, the process of diagnosis remains complex. Attempts to better define a diagnosis of ALS led to the first international workshop that aimed to reach consensus agreement, at El Escorial in 1990 (511). Since then, there have been multiple revisions and new approaches (498), including the most recent neurophysiologically based Awaji criteria (6). The Awaji criteria proposed that neurophysiological features of LMN dysfunction, as indicated by chronic neurogenic changes and fibrillation potentials/positive sharp waves along with fasciculations were equivalent to clinical features of LMN dysfunction. Although the Awaji criteria exhibited a higher sensitivity compared to the revised El Escorial criteria (30, 52-56, 58, 60), the diagnostic benefit appeared most prominent in patients with bulbar-onset disease (30). In addition, the clinically probable laboratory-supported diagnostic category was abolished in the Awaji criteria thereby necessitating the identification of UMN signs in two regions in order to establish a diagnosis of ALS. Given the difficulties in identifying UMN signs in ALS (38),

the sensitivity of the Awaji criteria could be reduced when compared to the revised El Escorial criteria (60).

The functional integrity of the upper motor neuronal system in ALS can be objectively assessed by transcranial magnetic stimulation (TMS) techniques (39). Multiple lines of evidence, utilising animal and human studies have established a TMS focus on the upper motor neuron, with neuronal activation mediated by ion channels and synaptic processes acting via multiple neurotransmitter systems (39, 518). A recently developed threshold tracking TMS technique (329), which overcomes the motor evoked potential amplitude variability evident with conventional TMS techniques, has established cortical hyperexcitability as a specific and early feature of ALS, reliably differentiating ALS from mimic neuromuscular disorders (237). Importantly, it has been postulated that cortical hyperexcitability may evolve to normal or hypoexcitability during the course of disease (39). While diagnostic threshold tracking TMS values have been reported (237), the study was not performed in accordance with the Standards for Reporting of Diagnostic Accuracy (STARD) criteria and was limited to a single center. As such, the generalizability of the results could not be definitively evaluated (519). Consequently, the aim of the present study was to determine the diagnostic accuracy of the threshold tracking TMS technique in differentiating ALS from mimic neuromuscular disorders. In order to avoid potential bias and to ensure a wider applicability of the findings, patients were recruited across multiple neuromuscular clinics in accordance with the STARD criteria.

Methods

Patients

All patients underwent detailed clinical assessment and grading prior to enrolment, including electrodiagnostic investigations. Recruitment of patients was performed prospectively and consecutively in keeping with the inclusion criteria. The Awaji diagnostic criteria was used as the reference standard (6). The study population comprised patients with suspected ALS, although none of the patients were diagnosed with ALS prior to recruitment. Inclusion criteria included: (i) Definite, probable, or possible ALS as defined by the Awaji criteria (6); (ii) Pure motor disorder with clinical features of upper and lower motor dysfunction in separate body regions, where LMN dysfunction developed caudal to UMN dysfunction, with evidence of disease progression over 6 months follow-up period from initial assessment; (iii) Neuromuscular disorders mimicking ALS, defined as muscle weakness and wasting for at least 6 months. At time of assessment, it was not known whether these patients would be classified in the "non-ALS" group.

Exclusion criteria included (i) pure UMN syndrome in which laboratory and neuroimaging studies suggested a diagnosis other than "possible" ALS; (ii) history of acute migraine headaches in the 4 weeks preceding recruitment, since migraine may increase cortical excitability; (iii) treatment with medications that could affect TMS parameters; (iv) history of head trauma, movement disorder, epilepsy, stroke or transient ischemic attack; (v) presence of pacemaker or other cardiac devices, cochlear implants and previous brain surgery such as clipping of a cerebral aneurysm; and (vi) unable to tolerate TMS testing or (vi) marked wasting of the thenar eminence precluding recording of motor responses. All patients provided written informed consent to the procedures approved by the Western Sydney Local

Health District and South East Sydney Area Health Service Human Research Ethics Committees.

Once recruited, ALS patients were clinically staged using the amyotrophic lateral sclerosis functional rating score (ALSFRS-R) (513). The disease duration (months) from time of symptom onset and site of disease onset were recorded. Muscle strength was assessed by the Medical Research Council (MRC) score, with the following muscle groups assessed: shoulder abduction, elbow flexion and extension, wrist dorsiflexion, finger abduction and thumb abduction, hip flexion, knee extension and ankle dorsiflexion bilaterally, yielding a maximal score of 90. Upper motor neuron function was assessed and graded by a dedicated UMN score(497).

Index test

Cortical excitability

Threshold tracking TMS was performed by two examiners (PM, and NG), with neurology training and neurophysiological expertise. These examiners were blinded to the results of the reference test at time of assessment, as well as the clinical history and all aspects of the assessment. Data analysis was performed by a separate rater (SV) with expertise in analysing the results of the index test and reference standard.

The TMS investigation was undertaken in all patients according to a previously reported technique (329), using a 90 mm circular coil. Briefly, the motor evoked potential (MEP) amplitude was fixed and changes in the test stimulus intensity required to generate a target response of 0.2 mV (±20%), when preceded by a sub-threshold conditioning stimulus, was measured (329). The motor evoked potential (MEP) response was recorded over the right

abductor pollicis brevis muscle in all patients. Resting motor threshold (RMT) was defined as the stimulus intensity required to maintain this target MEP response. ***Paired-pulse threshold tracking*** was undertaken to determine short interval intracortical inhibition (SICI) and intracortical facilitation (ICF), while ***single pulse TMS*** was utilized to determine the MEP amplitude (mV), cortical silent period (CSP) duration (ms) and central motor conduction time (CMCT) according to a previously reported technique (329). In patients with severe wasting of the thenar eminence, as assessed clinically or with nerve conduction studies disclosing a median nerve compound muscle section potential of < 1mV, cortical excitability testing was not undertaken.

Statistical Analysis

The primary outcome measure was the diagnostic sensitivity and specificity of TMS in differentiating ALS from non-ALS. The secondary outcome measures included the diagnostic utility of TMS in ALS subgroups based on Awaji criteria (definite/probable or possible), site of disease onset (bulbar versus limb), phenotype (presence or absence of UMN signs), and therapy (riluzole versus non-riluzole). Receiver operator curve analysis was utilized to assess the diagnostic utility of the index test. The ***sensitivity***, ***specificity***, ***positive likelihood ratio***, ***negative likelihood ratio and diagnostic odds ratio*** were determined for the index test. In addition, the number needed to test in order to diagnose one extra case of ALS with TMS, when applied to a group of patient with neuromuscular disorders, was calculated according to the formula reported by Bandolier (http://www.medicine.ox.ac.uk/bandolier/band27/b27-2.html). Multiple regression analysis was utilized to assess whether the outcome variables (SICI reduction and motor cortex inexcitability) were influenced by independent variables. A probability value <0.05 was considered statistically significant. Results were expressed as mean ± standard error of mean or median (interquartile range).

Results

Clinical features (Table 4.1)

A prospective study was undertaken between January 1, 2010 and March 1, 2014, with subjects recruited from three neuromuscular centers in Sydney, Australia. The study was conducted in accordance with the STARD criteria (Fig 4.1), and the index test and reference standard (Awaji criteria) were applied to all subjects at time of recruitment. No adverse events were recorded from performance of the index test. In total, 333 patients (206 males, 127 females, mean age 57.6±0.8years) satisfied the inclusion criteria. At recruitment, 209 patients were suspected of suffering with ALS. Of these, 52% were classified as Awaji definite/probable, 22% as Awaji possible, while 26% of patients did not meet Awaji criteria at initial assessment, although most progressed during the follow-up period leading to re-classification to Awaji definite/probable group (96%). Two patients failed to progress appreciably and remained Awaji negative eventually being diagnosed with primary muscular atrophy. A total of 6.3 % (N=21, Fig. 4.1) of patients could not undergo TMS testing due to marked hand weakness. All patients tolerated the study well, and none of the patients stopped testing due to intolerance. Sixty-eight patients were diagnosed as non-ALS (Table 4.1, Fig. 4.1) and served as pathological controls. The non-ALS cohort was significantly younger than the ALS patients, potentially representing a limitation of the current study.

	ALS (N=209)	Non-ALS (N=68)
Mean age at assessment (years)	59.9 (0.9)	48.4 (1.9)
Male:Female	125:84	45:23
Mean disease duration (months)	16.7 (1.1)	102 (13.6)
ALSFRS-R	41 (38-44)	
Median Total MRC score	82 (79-88)	86.5 (84-88)
Median upper limb MRC score	57 (51-60)	57 (56-60)
Median lower limb MRC score	30 (26-30)	30 (28-30)
Upper motor neuron score	12 (10-13)	0

Table 4.1. Demographic features in amyotrophic lateral sclerosis (ALS) and non-ALS neuromuscular mimic disorders. The muscle strength, as measured by the Medical Research Council (MRC) score, was comparable between groups. The amyotrophic lateral sclerosis functional rating score (ALSFRS-R) indicated a milder level of dysfunction in the ALS cohort. All data are expressed as mean (standard error of mean) or median (interquartile range).

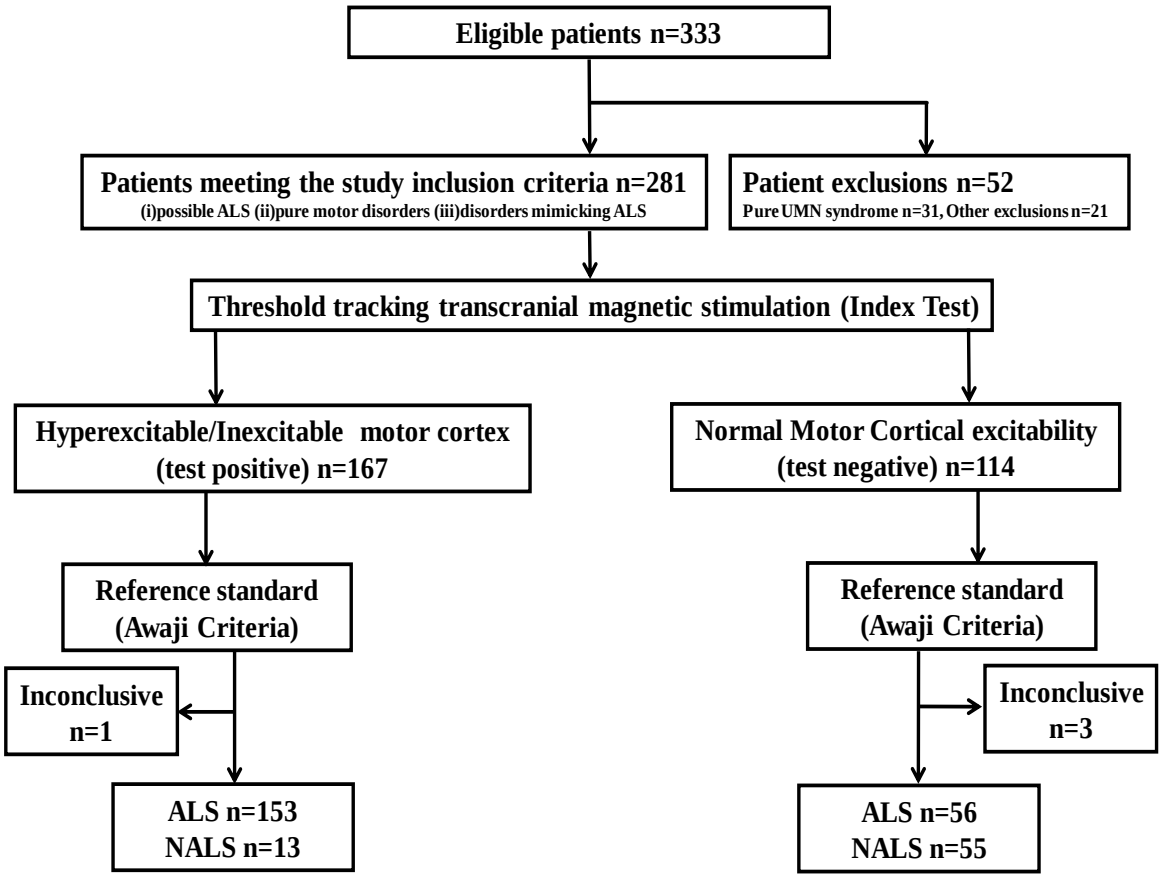

Figure 4.1. Flow diagram illustrating the study which was performed in accordance with the Standards for Reporting of Diagnostic Accuracy (STARD) criteria. Of the 56 ALS patients exhibiting a negative index test, defined as SICI > 5.5% and absence of motor cortex inexcitability, 45% were classified as Awaji possible or not meeting criteria, while 55% were classified as Awaji definite/probable ALS. The Awaji criterion was part of the inclusion criteria

Primary outcome measures

Threshold tracking TMS reliably differentiated ALS from NALS disorders (Fig. 4.2). Receiver operating characteristic curve analysis was utilised to assess the diagnostic utility of threshold tracking TMS. Importantly, reduction of averaged SICI [ISI 1-7 ms] appeared to be the most robust parameter at differentiating ALS from non-ALS with area under curve of 0.80 (95% confidence interval [CI], 0.75-0.85, Table 4.2, Fig. 4.3), indicating a “very good”

diagnostic utility. The remainder of the TMS parameters exhibited a lower diagnostic utility, as indicated by lower area under curve, and included reduced peak SICI at ISI 3 ms (0.78, 0.72-0.84), reduced CSP duration (0.73, 0.64-0.79), increased ICF (0.62, 0.54-0.68), increased MEP amplitude (0.56, 0.50-0.65), reduced RMT (0.51, 0.50-0.58) and prolonged CMCT (0.50, 0.50-0.54).

Consequently, a positive index test was defined as either a reduction of averaged SICI (< 5.5% as previously reported (237)) or inexcitable motor cortex defined as RMT > 95% of maximal stimulator output (504)). Utilising these diagnostic parameters, the threshold tracking TMS technique exhibited a sensitivity of 73.21% (95% CI: 66.66-79.08%), specificity of 80.88% (69.53-89.40), positive likelihood ratio of 3.83 (95% CI: 2.33-6.29) and negative likelihood ratio of 0. 33 (95%CI: 0.26-0.43). In addition, the diagnostic odds ratio was 11.66 (95% CI: 5.87-22.76), while the number needed to test in order to diagnose one extra case of ALS, in a population composed of neuromuscular diseases, was 1.8 (1.5-2.8, Table 4.2).

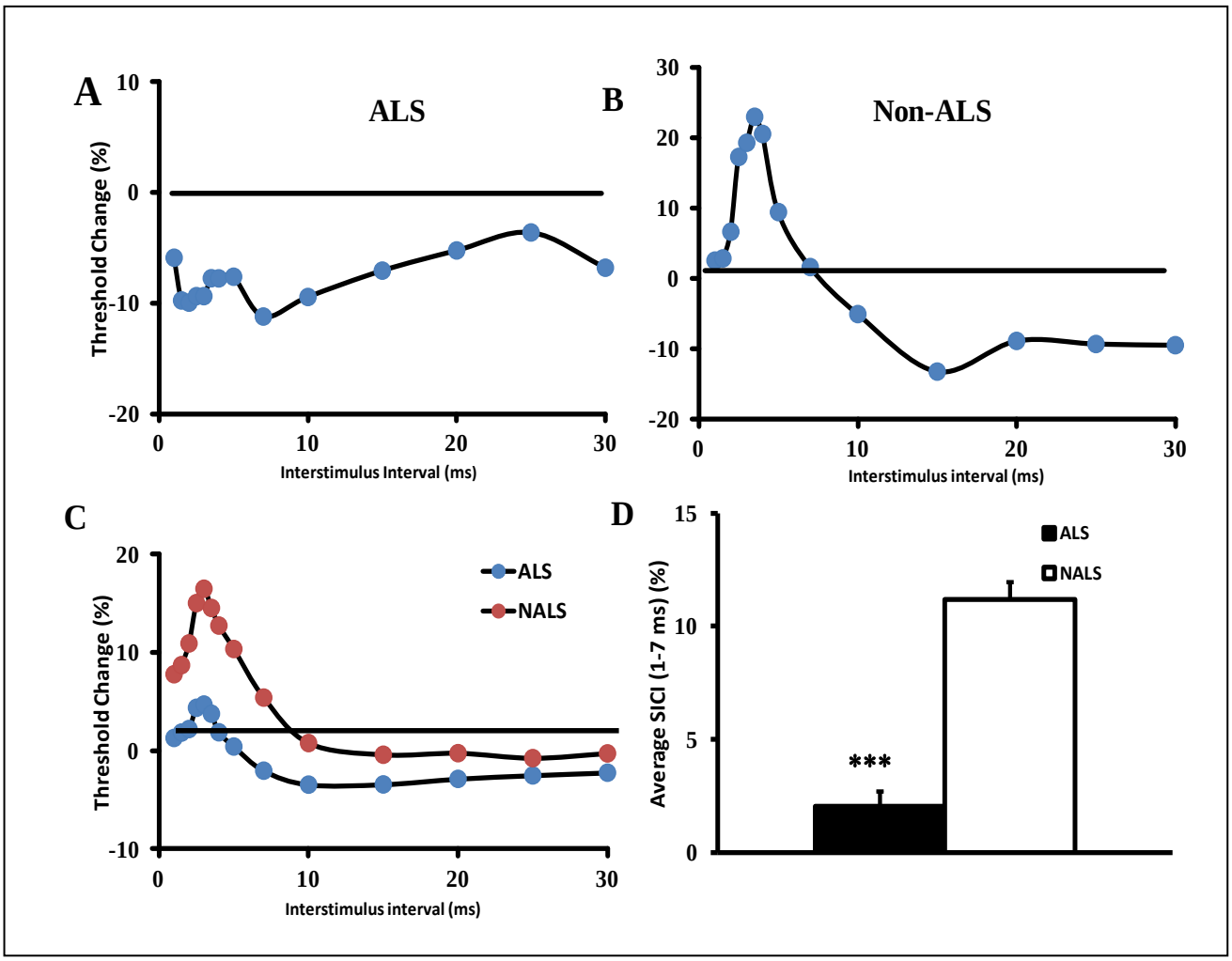

Figure 4.2. Short interval intracortical inhibition (SICI) was significantly reduced in amyotrophic lateral sclerosis (ALS) when compared to non-ALS mimic neuromuscular disorders (NALS). **(A, B)** Illustrative cases demonstrating differences in SICI between an ALS and a non-ALS patient. **(C, D)** Group data confirmed a significant reduction of averaged SICI, between interstimulus intervals (ISI) 1-7 ms. ***P < 0.001.

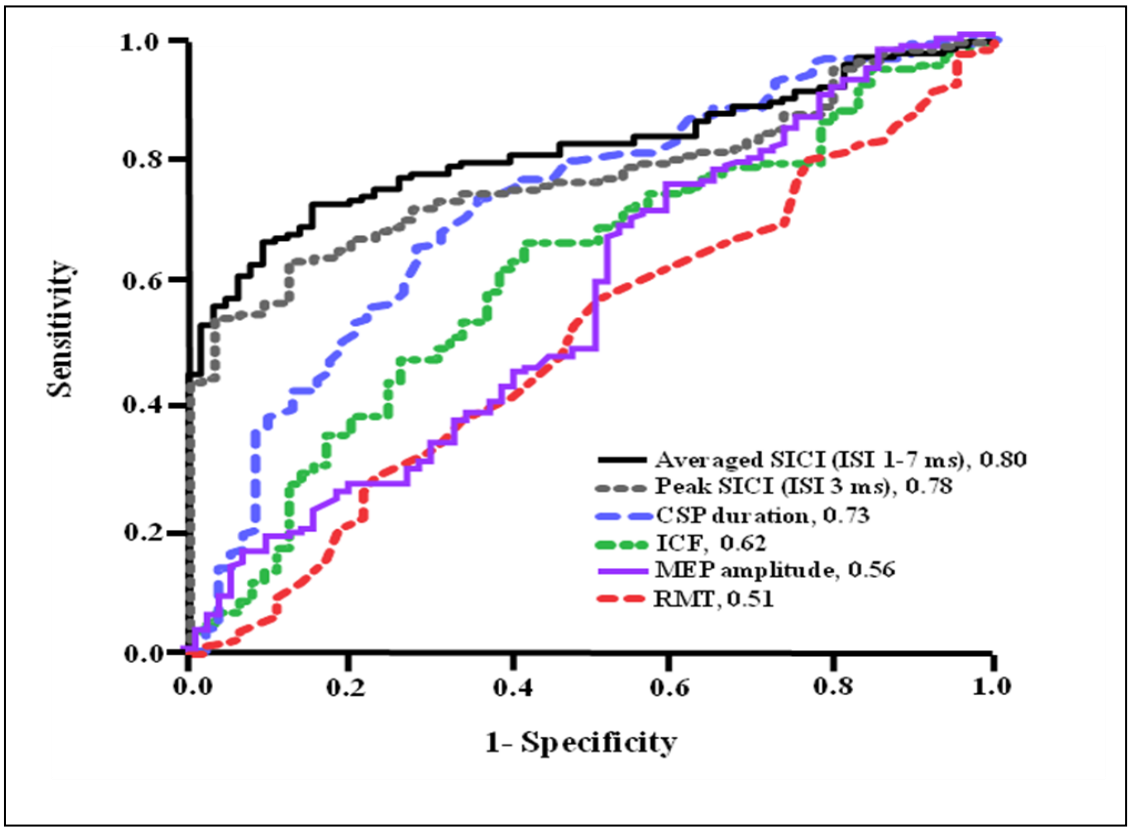

Figure 4.3. Receiver operator characteristic curves for the threshold tracking transcranial magnetic stimulation parameters. The area under the curve (AUC) was highest for averaged short interval intracortical inhibition (SICI) between interstimulus intervals (ISI) 1-7 ms. In addition, the AUC was high for peak SICI at ISI 3 ms, followed by cortical silent period (CSP) duration. The diagnostic utility for intracortical facilitation (ICF), motor evoked potential (MEP) amplitude and resting motor threshold (RMT) was inadequate.

Clinical Group	Sensitivity (%) (95% CI)	Specificity (%) (95% CI)	+LR (95% CI)	-LR (95% CI)	DOR (95%CI)	NNT (95% CI)
ALS	73.21 (66.66- 79.08)	80.88 (69.53-89.40)	3.83 (2.33- 6.29)	0.33 (0.26- 0.43)	11.66 (5.87-22.76)	1.8 (1.5-2.8)
ALS definite	71.30 (61.79-89.40)	80.88 (69.53-89.40)	3.73 (2.25-6.17)	0.35 (0.26-0.49)	10.51 (5.0-21.9)	1.9 (1.3-3.2)
ALS Possible/NMC	73.47 (63.59-81.88)	80.88 (69.53-89.40)	3.84 (2.32-6.36)	0.33 (0.23-0.47)	11.72 (5.52-24.87)	1.8 (1.4-3.0)
ALS Bulbar-onset	68.25 (55.31-79.41)	80.88 (69.53-89.40)	3.57 (2.13-5.99)	0.39 (0.27-0.57)	9.10 (4.10-20.33)	2.0 (1.5-4.0)
ALS Limb-onset	71.62 (63.63-78.72)	80.88 (69.53-89.40)	3.75 (2.27-6.17)	0.35 (0.26-0.46)	10.68 (5.29-21.55)	1.90 (1.5-3.0)

Table 4.2: The diagnostic utility of threshold tracking transcranial magnetic stimulation (TMS) in amyotrophic lateral sclerosis (ALS). Importantly, the diagnostic utility of threshold tracking TMS, as indicated by the sensitivity, specificity, positive likelihood ratios (+LR), negative likelihood ratios (-LR), diagnostic odds ratios (DOR) and number needed to test in order to diagnose one extra case of ALS, was comparable between different subgroups, including patients not meeting the Awaji criteria (NMC). The 95% confidence intervals (CI) are expressed in parenthesis.

Secondary outcome measures (Table 4.2)

Subgroup analysis disclosed a comparable area under curve between definite/probable (0.79, 95% CI 0.72-0.86) and possible/not meeting criteria (0.83, 95% CI 0.76-0.89) patients. Given the overlapping 95% CIs, the findings underscore a comparable diagnostic utility of the index test in ALS, including in the early stages of the disease process. In addition, the sensitivity ($ALS_{DEFINITE/PROBABLE}$ 71.30% [61.79-89.40]; $ALS_{POSSIBLE/not\ meeting\ criteria}$ 73.47% [63.59-81.88%], P=0.75) and specificity ($ALS_{DEFINITE/PROBABLE}$ 80.88% [69.53-89.40%]; $ALS_{POSSIBLE/\ not\ meeting\ criteria}$ 80.88% [69.53-89.40%]) of threshold tracking TMS was comparable between groups. The mean time between TMS assessment and progression to an ALS diagnosis, as defined by Awaji "definite/probable" category, was 15.8±2.0 months. An extra 34% of ALS patients could be diagnosed at initial assessment when utilising the threshold tracking TMS abnormalities compared solely to applying the Awaji criteria.

Further, the sensitivity of the threshold tracking TMS technique was similar between ALS patients classified as "not meeting criteria" and the Awaji possible group ($ALS_{\text{not meeting criteria}}$ 72.22% [58.35-83.54%]; $ALS_{POSSIBLE}$ 77.08% [62.68-87.95%], P=0.42). There was no significant difference in sensitivity of threshold tracking TMS technique between patients with [UMN score≥3] (74.0%, 66.28-80.56%) and without (65.22%, 42.47-83.58%, P=0.38) UMN signs [UMN score<3].

The diagnostic utility of the threshold tracking TMS technique was similar between bulbar and limb-onset ALS patients. Specifically, the sensitivity ($ALS_{BULBAR\text{-}ONSET}$ 68.25% [55.31-79.41%]; $ALS_{LIMB\text{-}ONSET}$ 71.62 % [63.63-78.72%], P = 0.76) and diagnostic odds ratio ($ALS_{BULBAR\text{-}ONSET}$ 9.10, 4.10-20.33; $ALS_{LIMB\text{-}ONSET}$ 10.68, 5.29-21.55) were comparable between groups.

Riluzole therapy may increase SICI (224) and may limit the diagnostic utility of threshold tracking TMS. In total, 64% of the ALS patients were receiving riluzole therapy at time of threshold tracking TMS. The sensitivity was comparable between patients on riluzole (69.03% [59.64-77.39%]) and those yet to be commenced on riluzole (65.08% [52.03-76.66%], P=0.54).

Multiple regression analysis

In order to determine whether the outcome variables, namely SICI reduction and motor cortex inexcitability, were influenced by independent variables including ALSFRS-R, MRC total score, UMN score, disease duration, site of disease onset, gender, and treatment status, a multiple regression analysis was utilised. There was no significant correlation between

outcome variables and the independent factors, thereby arguing against any significant effects of the independent variables on the outcome parameters.

Discussion

Findings in the present prospective study, undertaken in accordance with the STARD criteria, establish diagnostic utility of the threshold tracking TMS technique in ALS. Reduction of averaged SICI appeared to be the most robust diagnostic biomarker, and when combined with motor cortex inexcitability, exhibited high sensitivity and specificity with the number needed to test with TMS in order to diagnose one extra case of ALS being only 1.8. Importantly, the diagnostic utility of threshold tracking TMS was comparable between Awaji diagnostic categories and was similar in bulbar and limb onset patients, but was not influenced by riluzole therapy. Taken together, the present study underscores the importance of the threshold tracking TMS technique as a diagnostic aid in ALS, providing an objective biomarker of UMN dysfunction and potentially leading to an earlier diagnosis of ALS, by an average of 15.8 months, when combined with clinical and conventional neurophysiological measurements.

Diagnosis of ALS

In the absence of a pathognomonic test, the diagnosis of ALS remains reliant on identifying a combination of upper and lower motor neuron dysfunction (47, 498). Given the diagnostic limitations of the clinical criteria, neurophysiologically based Awaji criteria were developed in order to increase the diagnostic sensitivity for ALS (6). Although a number of studies have reported increased sensitivity of the Awaji criteria, when compared to the revised El Escorial criteria (52, 53, 55, 56, 58), others have failed to detect any significant differences (54, 502) and one study reported a decreased sensitivity as UMN signs could not be elicited

(60). These discordant findings may relate to difficulties in detecting UMN signs, which remain clinically based in the Awaji criteria. Identification of UMN signs in ALS may be limited by complex physiological factors, including the extent of muscle wasting along with dysfunction of descending motor pathways and local spinal circuits that underlie development of UMN signs (38). Separately, secondary adaptive changes within the neuromuscular system may further complicate assessment.

Consequently, direct assessment of UMN function by TMS techniques could potentially overcome the limitations imparted by the disease process leading to an objective diagnostic biomarker of UMN dysfunction. In the present study, the threshold tracking TMS technique reliably differentiated ALS from mimic disorders at an early stage in the disease process. Importantly, TMS abnormalities were evident in ~ 70% of ALS patients categorised as Awaji possible or "not meeting criteria". Reduction of SICI, a biomarker of motor cortical inhibitory function first reported by Kujirai and colleagues (378), appeared to be the most robust diagnostic parameter supporting previous studies (237, 504). The present study design supports a wider applicability of the current findings and potentially avoids bias, underscoring the diagnostic utility of threshold tracking TMS in ALS.

It should be acknowledged that the threshold tracking TMS remains a specialised technique requiring specific technology (special hardware and customised software termed QTRACS), expertise and training. Consequently, while the tolerability of the index test remains good, the practicability of widespread application of the test are limited, and as such there remains uncertainty about the diagnostic reliability of threshold tracking TMS when performed in less experienced centers or those using different methodology, such as the constant stimulus TMS technique. Of further relevance, while the intra-rater variability was established (329), inter-

rater variability remains to be determined. In addition, it could also be argued that subtle differences between cohort characteristics could influence the results. This seems unlikely given that the outcome variables were not influenced by any of the demographic, functional and treatment factors in a multiple regression analysis.

The Awaji criteria appears to be less sensitive in patients with limb-onset disease when compared to bulbar-onset disease (30), potentially leading to diagnostic delays, as recently reported (506). Importantly, the present study provides evidence for diagnostic utility of the threshold tracking TMS technique irrespective of site of disease onset. A potential limitation may occur in ALS patients with severe hand wasting, which may preclude TMS testing as evident in 6.3% of the current cohort. Assessment of cortical excitability from lower limb muscles, or less affected intrinsic hand muscles, may increase the diagnostic yield of threshold tracking TMS.

A major challenge in ALS management remains a delay in definite diagnosis (47). Riluzole has been established as the only effective neuroprotective therapy for ALS, prolonging patient survival by 3-6 months (220). Importantly, riluzole appears to be less effective in advanced stages of the disease (520), underscoring the need for an earlier diagnosis. Reliance on inclusion criteria that are based on identifying UMN and LMN dysfunction in multiple body regions utilizing clinical and conventional neurophysiological approaches (6, 498) may result in low recruitment rates into therapeutic trials, especially in the early stages of the disease process where neuroprotective therapies may be most effective (247). Consequently, addition of the threshold tracking TMS technique to the diagnostic algorithm may lead to an earlier diagnosis, thereby enhancing recruitment of ALS patients into therapeutic trials when combined with clinical and conventional methodologies.

Chapter 5

CORTICAL FUNCTION IN ASYMPTOMATIC CARRIERS AND PATIENTS WITH C9ORF72 ALS

Summary

Having established in Chapters 3 and 4 that cortical hyperexcitability was an early and useful biomarker of upper motor neuron (UMN) dysfunction, we aimed to explore the pathophysiological processes underlying the most common genetic form of ALS, the c9orf72 gene expansion. The pathophysiological mechanism, by which the c9orf72 gene expansion leads to neurodegeneration remains to be elucidated. Cortical hyperexcitability is potentially an important pathophysiological process in sporadic and familial ALS (FALS). To investigate whether cortical hyperexcitability formed the pathophysiological basis of c9orf72 FALS, we utilized the threshold tracking TMS in a prospective single-centre study at a large neuromuscular centre. Clinical and functional assessment, along with TMS studies were undertaken on 15 c9orf72 FALS patients and 11 asymptomatic c9orf72 expansion carriers who were longitudinally followed for up to 3 years. The results were compared to 73 sporadic ALS patients and 74 healthy controls. Cortical excitability variables, including short interval intracortical inhibition, were measured in c9orf72 FALS patients and results compared to asymptomatic c9orf72 carriers, sporadic ALS patients and healthy controls. Short-interval intracortical inhibition (SICI) was significantly reduced in c9orf72 FALS (1.2 ± 1.8%) and sporadic ALS patients (1.6 ± 1.2%) compared to asymptomatic c9orf72 expansion carriers (10.2 ± 1.8%, $F=16.1$, $P < 0.0001$) and healthy controls (11.8 ± 1.0%, $F=16.1$, $P < 0.0001$). The reduction of SICI was accompanied by an increase in intracortical facilitation ($P < 0.01$) and motor evoked potential amplitude ($P < 0.05$) as well as reduction in resting motor threshold ($P < 0.05$) and cortical silent period duration ($P < 0.0001$). This study establishes cortical hyperexcitability as an intrinsic feature of symptomatic C9orf72 expansion-related ALS, but not in asymptomatic expansion carriers.

Introduction

Identification of increased hexanucleotide repeat expansion (GGGGCC) in the c9orf72 gene (97, 98), which appears to underlie over 40% of familial and 8% of "sporadic" ALS cases (97, 98, 100) has radically altered the understanding of ALS pathogenesis, broadening the clinical heterogeneity of ALS. The c9orf72 hexanucleotide expansion underlies both ALS and frontotemporal dementia [FTD] (97, 98), while subtle cognitive abnormalities may be evident in up to 50% of ALS patients and FTD may develop in 15% of ALS patients (521).

The precise pathophysiological mechanisms by which c9orf72 gene expansion mediates neurodegeneration in ALS has not been established (97, 98), although a number of pathogenic mechanisms have been proposed, including haploinsufficiency (97, 98, 112), RNA-mediated toxicity (113, 522) and dipeptide repeat protein toxicity related to non-ATG (RAN) translation of the expanded c9orf72 gene (111, 115). Motor neuronal hyperexcitability was suggested as a potential pathophysiological mechanism in c9orf72 ALS, a process mediated by inactivation of K^+ channels (523). Importantly, blockade of neuronal hyperexcitability by ***retigabine***, a K^+ channel activator, exerted neuroprotective benefits, identifying a putative therapeutic target in ALS (523).

In ALS patients, motor neuronal hyperexcitability may be assessed by transcranial magnetic stimulation (TMS) techniques (39). Previous TMS studies in sporadic and familial ALS patients, linked to mutations in the superoxide dismuates-1 (SOD-1) gene, have established cortical hyperexcitability as an early feature in ALS and linked to the process of neurodegeneration, while the level of cortical excitability was normal in asymptomatic SOD-1 mutation carriers (183, 185, 237, 238). These studies highlighted the pathogenic importance of cortical hyperexcitability in ALS, and suggested that the onset of ALS was

potentially triggered by one or more factors acting in concert with genetic mutations. Consequently, the present study utilized threshold tracking TMS techniques to assess cortical function in asymptomatic c9orf72 expansion carriers, with results compared to c9orf72 FALS and sporadic ALS patients, in order to clarify the underlying pathophysiological mechanisms in this form of familial ALS.

Methods

Patients

Subjects were recruited from the ALS genetic database and from the multidisciplinary ALS clinics. Studies were undertaken on 15 familial ALS patients (7 females and 8 males, mean age 60 years, age range 41-78 years), with confirmed c9orf72 hexanucleotide expansion, defined as possible or probable/definite ALS according to the Awaji criteria (6). In addition, studies were also undertaken on 11 asymptomatic c9orf72 mutation carriers (10 females and 1 male, mean age 49 years, age range 26-78 years), that were followed for up to 3 years. Seventy-three sporadic ALS patients were also assessed (45 males and 28 females, age range 28-86, mean age 60).

The ALS patients were clinically reviewed on a regular basis through the multidisciplinary ALS clinics. All patients were clinically staged using the Amyotrophic Lateral Sclerosis Functional Rating Scale-Revised (ALSFRS-R) (495) and categorised according to site of disease onset as limb or bulbar-onset ALS. In addition, the disease duration (months) at the time of testing was recorded and muscle strength was assessed using the Medical Research Council (MRC) rating scale, with the following muscle groups assessed bilaterally yielding a total MRC score of 90: shoulder abduction; elbow flexion; elbow extension; wrist

dorsiflexion; finger abduction; thumb abduction; hip flexion; knee extension; ankle dorsiflexion.

The degree of upper motor neuron (UMN) dysfunction was assessed by a specific UMN score (497). None of the patients with ALS were receiving medications, which could potentially interfere with the neurophysiological results. Informed consent to the procedures was provided by all patients, with the study approved by the Sydney West Area Health Service and Human Research Ethics Committees.

Neurophysiological studies

Cortical excitability was assessed by utilizing a threshold tracking TMS technique according to a previously reported method (329). The MEP response was recorded over the abductor pollicis brevis (APB) muscle. The following parameters were recorded in all participants: (i) Short interval intracortical inhibition (%), between interstimulus interval (ISI) 1-7 ms; (ii) intracortical facilitation (ISI 10-30 ms); (iii) resting motor threshold (RMT, %); (iv) Motor evoked potential (MEP) amplitude (%); (v) cortical silent period (CSP) duration (ms); and (vi) central motor conduction time (CMCT, ms).

In the same sitting nerve conduction studies and needle electromyography was undertaken on all participants. The compound muscle action potential (CMAP) was recorded from the APB muscle and the CMAP onset latency and peak-peak amplitude were measured. Subsequently, the neurophysiological index (NI) was derived according to a previously reported formula (26).

Recordings of the compound muscle action potential (CMAP) and MEP responses were amplified and filtered (3 Hz-3 kHz) using a Niolet-Biomedical EA-2 amplifier (Cardinal Health Viking Select version 11.1.0, Viasys Healthcare Neurocare Group, Madison, Wisconsin, USA) and sampled at 10 kHz using a 16-bit data acquisition card (National Instruments PCI-MIO-16E-4). Data acquisition and stimulation delivery were controlled by QTRACS software. Temperature was monitored with a purpose built thermometer at the stimulation site.

Statistical analysis

Cortical excitability was compared to 74 healthy controls (37 males, 37 females, mean age 53.1 years, age range 23-83 years). Data were assessed for normality using the Shapiro-Wilk test. Student's t-test and Wilcoxon-Signed rank test were used to assess differences between means. Analysis of variance (ANOVA) with post-Hoc testing using a Bonferroni correction (parametric data), or Kruskal-Wallis test (non-parametric data) were used for multiple comparisons. A P value < 0.05 was considered statistically significant. A potential caveat in this study relates to the fact that healthy controls were significantly younger than c9orf72 expansion-related and sporadic ALS patients. Pearson's or Spearmen's correlations were used to assess the relationship between parameters. Results are expressed as mean ± standard deviation (SD) or median with interquartile range (IQR).

Results

Clinical features

The clinical phenotype and level of functional impairment was similar between the 15 clinically affected FALS patients and sporadic ALS patients (Table 5.1). Specifically, the mean ALSFRS-R score in c9orf72 FALS patients was 39.4 ± 10.1, indicating a moderate degree of impairment, and was comparable to sporadic ALS patients (41.2 ± 5.4, P = 0.25). In addition, the mean MRC total score in the c9orf72 FALS patients was 82.6 ± 7.1, re-affirming a moderate degree of functional impairment, and was comparable to the MRC total score in sporadic ALS patients (80.7± 11.5, P=0.09). The median UMN score was similar in the c9orf72 FALS (14, 10-14, SD 6) and sporadic ALS patients (12, 10-14, SD 5, P =0.32) signifying presence of upper motor neuron signs in both cohorts.

At the time of TMS testing, the median disease duration in the FALS patients was 8 months (5-12 months, SD 12.6 months) and was comparable to sporadic ALS patients (10.5, 6-18 months, SD 18.1 months). Forty percent of the FALS patients exhibited bulbar-onset disease, while 60% reported limb-onset disease, which was identical to that evident in the sporadic ALS patients. All of the patients were receiving riluzole at time of assessment.

In contrast, the physical examination in all the asymptomatic c9orf72 hexanucleotide expansion carriers, including the pre-symptomatic carrier, was normal. Specifically, there were no upper motor neuron features, such as increased muscle tone, hyper-reflexia, extensor plantar responses, positive Hoffman sign or the presence of a jaw-jerk in any of the subjects at the time of testing.

Symptomatic c9orf72 expansion carrier	Age (years)/Sex	ALS onset	Disease duration (months)	ALS-FRS	UMN score	MRC sum score
1	78F	Limb	3	44	14	70
2	41M	Bulbar	14	45	15	81
3	64F	Bulbar	10	44	0	90
4	73F	Limb	6	42	12	83
5	45M	Limb	6	48	14	90
6	66F	Limb	38	13	12	83
7	58M	Bulbar	10	36	14	75
8	70M	Limb	12	42	0	87
9	75M	Limb	36	34	14	86
10	50M	Bulbar	4	46	4	90
11	68M	Limb	8	42	12	74
12	44F	Limb	7	39	14	81
13	56F	Limb	4	44	14	83
14	72F	Bulbar	24	30	8	85
15	44M	Limb	7	47	14	88
Mean	60.3		12.4	39.5	10.7	83.2
SEM	3.3		2.9	2.2	1.3	1.6
Sporadic ALS Patients						
Mean	60.1		15.0	41	10	80
SEM	1.5		2.4	0.6	0.6	1.4
Asymptomatic c9orf72 expansion carrier						
Mean	49.5			48	0	90
SEM	5.0					
Controls						
Mean	53.1			48	0	90
SEM	1.3					

Table 5.1: Clinical details for the clinically affected c9orf72 FALS cohort with mean data for asymptomatic carriers, sporadic ALS cohort and healthy controls. The patients were clinically assessed using the amyotrophic lateral sclerosis functional rating scale revised (ALSFRS-R), with a maximum score of 48 when there is no disability. Muscle strength was clinically assessed using the Medical Research Council (MRC) sum score (upper limbs and lower limbs). Upper motor neuron (UMN) score was utilised to assess the degree of clinical UMN dysfunction, with a possible maximum score of 16. Disease duration refers to the period from symptom onset to date of TMS testing.

Neurophysiological studies

Prior to undertaking cortical excitability studies the peripheral disease burden was assessed. The CMAP amplitude (FALS 6.3 ± 2.3 mV; SALS 7.0 ± 4.0 mV; controls 9.9 ± 4.3 mV, F=6.6, P<0.0001) and neurophysiological index (FALS 1.5 ± 1.2; SALS 1.2 ± 0.9; controls 2.3 ± 0.9, F=10.3, P<0.0001) were significantly reduced in FALS and sporadic ALS patients when compared to controls. In contrast, there was no significant difference in the CMAP amplitude and NI between asymptomatic c9orf72 hexanucleotide expansion carriers and controls ($CMAP_{asymptomatic\ carriers}$ 9.2 ± 3.3 mV; $CMAP_{controls}$ 9.9 ± 4.3 mV, P=0.33; $NI_{asymptomatic\ carriers}$ 1.8 ± 1.3; $NI_{controls}$ 2.3 ±0.9, P=0.20).

Cortical excitability

Short-interval intracortical inhibition, as reflected by an increase in the conditioned stimulus intensity required to track a constant target MEP of 0.2 mV, was significantly reduced in FALS and sporadic ALS patients (Fig. 5.1A). Averaged SICI, between ISIs 1 to 7 ms, was significantly reduced in FALS and ALS patients when compared to controls (FALS 1.2 ± 7.0 %; SALS 1.6 ± 10.3 %; controls 11.8 ± 8.6 %, F=16.1, P<0.0001, Fig. 5.1B), as was SICI at ISI 1ms (FALS 0.3 ± 7.0 %; SALS 1.7 ± 6.8 %; controls 6.8 ± 10.3 %, F=4.9, P<0.005, Fig. 5.2A) and ISI 3 ms (FALS 4.1 ± 9.3 %; SALS 3.5 ± 13.7 %; controls 17.2 ± 12.9 %, F=18.1, P<0.0001, Fig. 5.2B). In contrast, there was no significant difference in the averaged SICI (asymptomatic carriers 10.2 ± 6.0 %; controls 11.8 ± 8.6 %, P=0.2, Fig. 5.1B), SICI at ISI 1ms (asymptomatic carriers 5.6 ± 6.6 %; controls 6.8 ± 10.3 %, P=0.2, Fig. 5.2A), and ISI 3ms (asymptomatic carriers 15.5 ± 9.6 %; controls 17.2 ± 12.9 %, P=0.1, Fig. 5.2B) between asymptomatic c9orf72 carriers and controls.

Following SICI, a period of intracortical facilitation (ICF) develops between ISI of 10-30 ms. Intracortical facilitation was increased in FALS and sporadic ALS patients (FALS -3.2 ± 4.3 %; SALS -4.1 ± 6.0 %, F=3.3, P < 0.05) when compared to controls (-1.4 ± 6.9 %). In contrast, ICF was comparable between the asymptomatic expansion carriers (-1.2 ± 2.0 %, P=0.40) and controls.

Single pulse TMS disclosed a significant increase in the MEP amplitude, expressed as a percentage of CMAP response, in both the FALS and sporadic ALS patients when compared to controls (FALS 45.2 ± 25.5 %; SALS 32.2 ± 23.1 %; controls 23.4 ± 13.8 %, Fig. 5.3A, F=3.5, P < 0.01). In contrast, the MEP amplitude in asymptomatic expansion carriers was similar to controls (asymptomatic expansion carriers 24.4 ± 12.9 %, controls 23.4 ± 13.8 %, P=0.42). In addition, the CSP duration was significantly reduced in FALS and sporadic ALS patients (FALS 186.1 ± 40.7 ms; SALS 173.8 ± 41.9 ms; controls 214.1 ± 33.6 ms, F=10.8, P<0.0001, Fig. 5.3B), but not in the asymptomatic expansion carriers (211.4 ± 44.1 ms, P=0.40).

Of further relevance, the RMT was significantly reduced in the c9orf72 FALS patients (52.2 ± 8.1%) when compared to sporadic ALS, asymptomatic carriers and control cohorts (SALS 57.2 ± 11.1%; asymptomatic carriers 58.5 ± 16.6 %; controls 60.3 ± 12.0%, F=3.4, P<0.05). In addition, the CMCT was significantly increased in FALS and sporadic ALS patients (FALS 5.9 ± 1.9 ms; SALS 6.6 ± 1.7 ms; controls 5.5 ± 2.6 ms, F=4.4, P<0.01, Fig. 5.3D). In contrast, the CMCT was not significantly increased in asymptomatic carriers (asymptomatic carriers 5.2 ± 2.0 ms; controls 5.5 ± 2.6 ms, P=0.3).

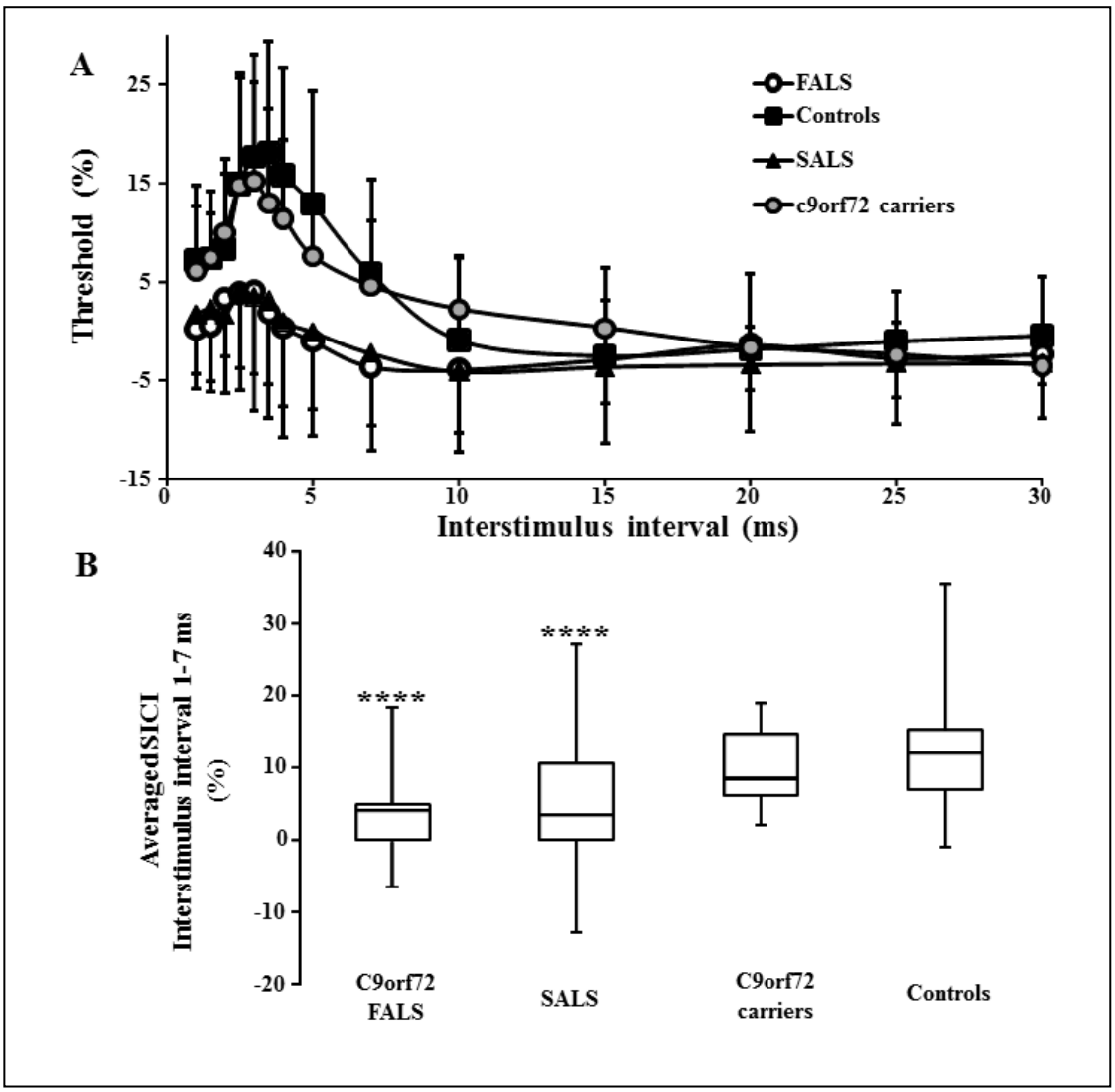

Figure 5.1. Averaged SICI is reduced in c9orf72 FALS
(A) Short-interval intracortical inhibition (SICI) was significantly reduced in c9orf72 familial amyotrophic lateral sclerosis (FALS) patients when compared to asymptomatic c9orf72 expansion carriers and controls. The reduction of SICI was comparable to that evident in in sporadic ALS patients (SALS) patients. **(B)** Averaged SICI, between interstimulus intervals (ISI) 1-7ms, was significantly reduced in FALS and SALS patients. ****P<0.0001.

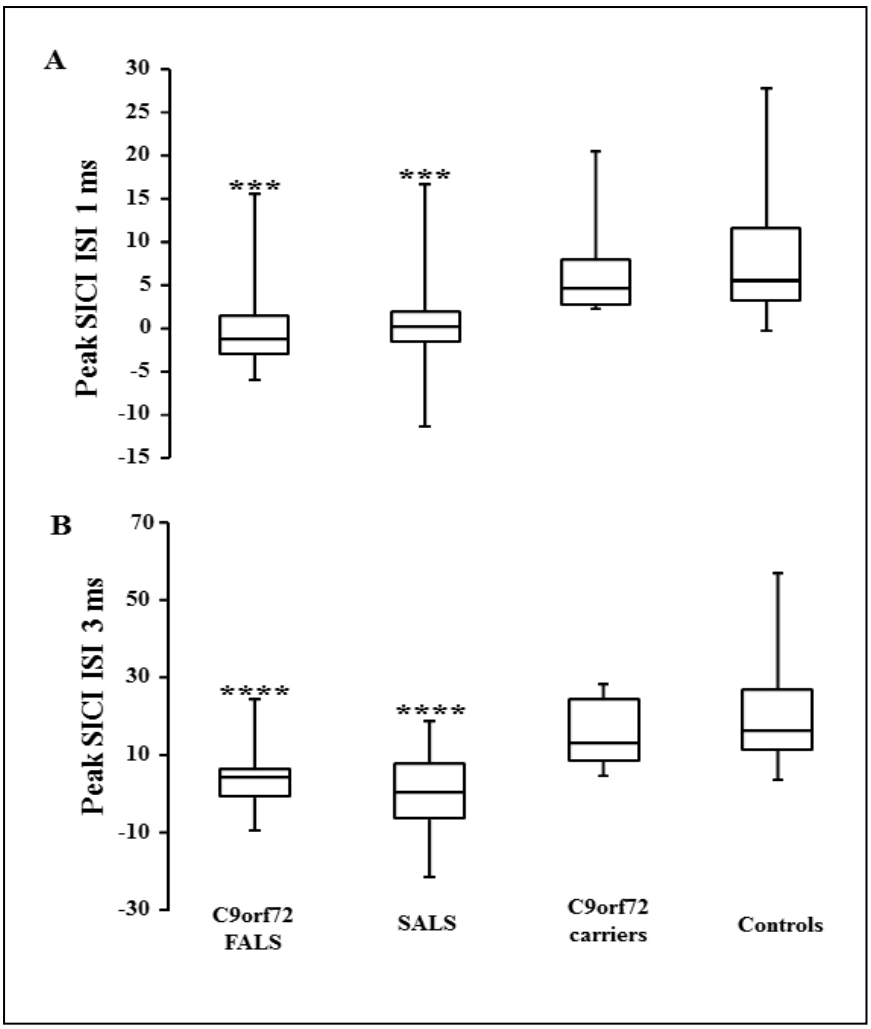

Figure 5.2. The peak components of SICI are reduced in c9orf72 FALS
(A) Peak short interval intracortical inhibition (SICI) at interstimulus interval (ISI) 1 ms and **(B)** 3 ms was significantly reduced in the familial amyotrophic lateral sclerosis (FALS) and sporadic ALS (SALS) patients compared to asymptomatic c9orf72 expansion carriers and controls. ***P<0.001, ****P<0.0001.

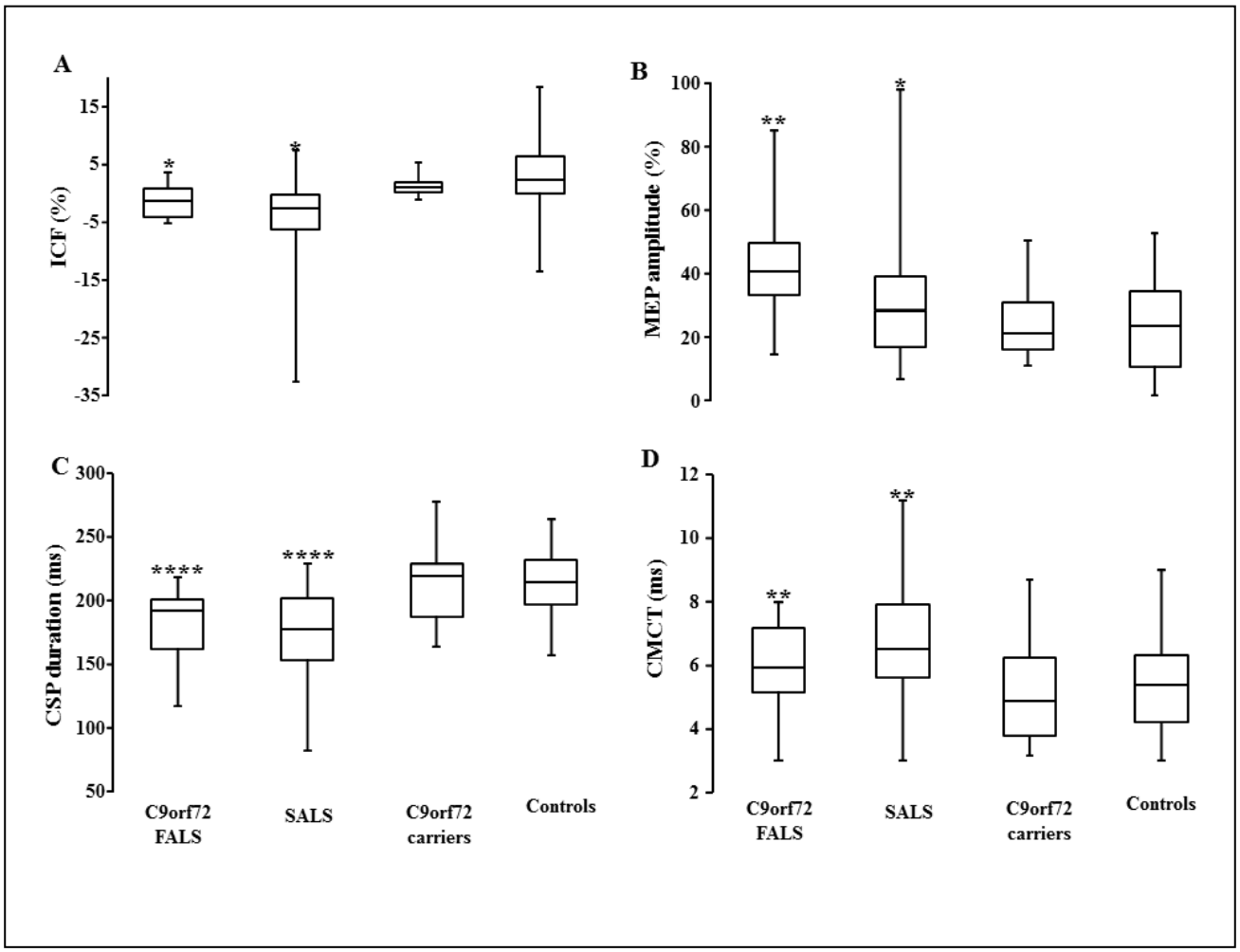

Figure 5.3. Cortical hyperexcitability is a feature of c9orf72 FALS
(A) Intracortical facilitation (ICF) follows was significantly increased in familial amyotrophic lateral sclerosis (FALS) and sporadic ALS (SALS) patients. **(B)** Motor evoked potential (MEP) was significantly increased in FALS and SALS patients when compared to asymptomatic c9orf72 expansion carriers and controls. **(C)** The cortical silent period (CSP) duration was significantly reduced in FALS and SALS patients when compared to asymptomatic c9orf72 expansion carriers and controls. **(D)** Central motor conduction time (CMCT) was significantly increased in FALS and SALS patients.*P< 0.05, **P<0.01, ***P< 0.001, ****P<0.0001. All P-values were corrected for multiple comparisons using post-Hoc Bonferroni testing.

Correlation studies

Combining, clinical, peripheral neurophysiological and cortical excitability findings, it was evident that in the c9orf72 familial ALS cohort the averaged SICI (ISI 1-7 ms) significantly correlated with the CMAP amplitude ($R = -0.55$, $P < 0.05$), MRC upper limb score ($Rho = -0.80$, $P < 0.01$) and the MRC APB score ($Rho = -0.46$, $P < 0.05$). In addition, intracortical facilitation significantly correlated with the CMAP amplitude ($R = -0.67$, $P < 0.05$) as did the

cortical silent period duration (R= -0.59, P < 0.05) and the resting motor threshold (R=0.53, P < 0.05). Taken together, these findings suggest the features of cortical hyperexcitability was most prominent when muscle strength and motor amplitudes were relatively preserved.

Discussion

The findings in the present study have confirmed cortical hyperexcitability as an intrinsic feature of c9orf72 expansion related ALS as well as apparently sporadic FALS. Cortical hyperexcitability was associated by a marked reduction of short-interval intracortical inhibition and cortical silent period duration, combined with an increase in MEP amplitude and intracortical facilitation. In contrast, cortical excitability was normal in the asymptomatic c9orf72 expansion carriers, and was significantly different when compared to familial and sporadic ALS cohorts. The potential mechanisms underlying these findings and their pathophysiological implications for ALS are further discussed.

Cortical hyperexcitability and ALS pathogenesis

The pathophysiological mechanisms underlying the development of motor neuron degeneration in ALS appears to be multifactorial, with a complex interaction between genetic factors and dysfunction of vital molecular pathways (47). Identification of the dominantly inherited c9orf72 gene as an important genetic aetiology of ALS (97, 98), has altered the understanding of ALS pathogenesis, building on the concept of ALS as a multisystem neurodegenerative disorder (524) and emphasising the importance of cortical mechanisms in ALS pathophysiology. This notion was further underscored by neuropathological studies demonstrating cortical intraneuronal inclusions that were evident in both c9orf72 associated ALS and frontotemporal dementia [FTD] (101).

Cortical hyperexcitability was a feature of c9orf72 FALS in the present study, being comparable to findings in the sporadic ALS cohort and evidenced by marked reduction of short interval intracortical inhibition. Short interval intracortical inhibition is mediated by activation of cortical inhibitory circuits, acting via $GABA_A$ receptors, as well as glutaminergic neurotransmission (39, 224, 379). Consequently, the reduction of SICI could have been mediated by degeneration and dysfunction of inhibitory cortical interneurons (406, 525), as well as glutamate mediated excitoxicity. A significant reduction in the CSP duration and resting motor thresholds, along with an increase in the MEP amplitude, further support the presence of cortical hyperexcitability in the c9orf72 ALS patients.

The findings of cortical hyperexcitability in the present c9orf72 FALS cohort was similar to previous studies in familial ALS patients attributed to different genetic mutations (185, 405). As such, cortical hyperexcitability appears to represent a uniform pathophysiological process in ALS, irrespective of the underlying genetic status. Of relevance, recent mathematical modeling has inferred a six-step process in ALS (154), with a prolonged prodromal period, perhaps extending to the perinatal period (155). Cortical hyperexcitability could represent one of the final steps in ALS pathogenesis, perhaps developing just prior to, or at onset of neuronal degeneration, a notion supported by findings of significant correlations between features of cortical hyperexcitability and motor amplitude and muscle strength. Recent animal studies lend credence to this assumption, identifying neuronal hyperexcitability at a pre-clinical stage, upstream of the spinal motor neuron (158, 526).

Further supporting a multistep process in ALS, is the finding of normal cortical excitability in the asymptomatic c9orf72 expansion carriers, similar to findings in SOD-1 mutation carriers (185). Consequently, the development of neuronal hyperexcitability in familial ALS appears

to be dependent on additional factors other than the inheritance of genetic mutations. Identifying and modulating these "triggering" factors could be therapeutically significant for ALS. In addition, the findings of normal cortical excitability in the asymptomatic familial ALS cohorts would argue against therapeutic benefits of prophylactic riluzole.

It could be argued that cortical hyperexcitability was an adaptive process in response to peripheral neurodegeneration, and could serve as a neuroprotective strategy. Underscoring this notion are recent animal studies suggesting that an increase in neuronal excitability may be neuroprotective (223). While this notion could not be absolutely discounted in ALS patients, it seems unlikely given that riluzole, an anti-glutaminergic agent that prolongs survival (217, 220), reduces cortical hyperexcitability (224). Of further relevance, reduction of neuronal hyperexcitability by pharmacological agents such as retigabine appear to be neuroprotective (523), while normalizing astrocyte function by "knocking-down" the expression of mutated genes, and thereby normalizing glutamate homeostasis, appear neuroprotective (304). In addition, features of cortical hyperexcitability were not evident in non-ALS neuromuscular cohorts despite a comparable degree of peripheral neurodegeneration (237, 238, 357), further arguing against the notion that cortical hyperexcitability represents a simple compensatory mechanism. Rather, cortical hyperexcitability may serve as a final common pathway in ALS, mediating neuronal degeneration via a trans-synaptic glutamate process, and the identification and modulation of factors that trigger cortical hyperexcitability may prove therapeutically useful.

Chapter 6

AXONAL ION CHANNEL DYSFUNCTION IN C9ORF72 FAMILIAL AMYOTROPHIC LATERAL SCLEROSIS

Summary

Having established that cortical hyperexcitability played a pivotal role in familial ALS (FALS) in the previous chapter, the next study evaluated the role of the peripheral nervous system in FALS. Specifically, in sporadic amyotrophic lateral sclerosis (SALS) phenotypes there has been documentation of peripheral nerve axonal excitability abnormalities, characterised by upregulation of persistent Na^+ conductances and reduced K^+ current, linked to the development of clinical features such as fasciculations as well as neurodegeneration. We wanted to investigate whether abnormalities of axonal ion channel function, particularly upregulation of persistent Na^+ conductances and reduced K^+ currents, form the pathophysiological basis of c9orf72 FALS. Subsequently a prospective single-centre study at a large neuromuscular centre was undertaken**.** Clinical and functional assessment, along with motor nerve excitability studies were undertaken in 10 clinically affected c9orf72 FALS patients, 9 asymptomatic c9orf72 mutation carriers and 21 sporadic ALS (SALS) patients. Axonal excitability variables were measured in c9orf72 ALS patients and results compared to matched SALS patients and healthy controls. Strength-duration time constant (τ_{SD}) was significantly increased in the c9orf72 FALS and SALS patients (c9orf72 0.50±0.02 ms; SALS 0.52±0.02 ms, $P < 0.01$) when compared to controls (0.44 ± 0.01). In contrast, there were no significant changes of τ_{SD} in asymptomatic c9orf72 mutation carriers ($P=0.42$). An accompanying increase in depolarising threshold electrotonus at 90-100 ms (TEd90-100 ms) was also evident in the c9orf72 FALS ($P<0.05$) and SALS cohorts ($P < 0.01$). Mathematical modelling suggested that an increase in persistent Na^+ conductances along with reduced K^+ currents, best explained the changes in axonal excitability. Importantly, these abnormalities in axonal excitability correlated with the motor amplitude (τ_{SD}, $R= -0.38$, $P<0.05$; TEd 90-100 ms, $R = -0.44$, $P<0.01$), muscle weakness (TEd 90-100 ms, $R = -0.32$, $P < 0.05$) and the ALS

functional rating scale (TEd 90-100 ms, R= -0.34, P<0.05). Findings from the present study establish that upregulation of persistent Na^+ conductances and reduced K^+ currents were evident in both c9orf72 FALS and SALS cohorts, and these changes in axonal excitability were associated with motor neuron degeneration.

Introduction

Amyotrophic lateral sclerosis (ALS) is a rapidly progressive and universally fatal neurodegenerative disorder of the motor neurons (48). A genetic etiology has been identified in up to 60% of familial and 20% of apparently sporadic ALS cohorts, with at least 21 genes and genetic loci implicated in ALS pathogenesis (90). Recently, an increased hexanucleotide repeat expansion (GGGGCC) in the first intron of the c9orf72 gene on chromosome 9p21 was reported to be the most common of the genetic mutations in ALS, underling approximately 40% of familial and 20% of sporadic ALS cases (97, 98), although subsequent studies have established a c9orf72 mutation frequency of 4-8% (100).

The c9orf72 phenotype may be characterised by ALS and frontotemporal dementia with psychiatric features, although the penetrance and expression of the genotype may vary within and between cohorts (97, 98, 105, 527). The c9orf72 associated ALS phenotype is clinically characterised by co-existence of upper (UMN) and lower motor neuron (LMN) signs encompassing multiple body regions, with an earlier age of onset and shorter survival (103). Importantly, LMN signs are characterized by fasciculations, muscle wasting and weakness, clinically indistinguishable from the LMN features in sporadic ALS cohorts.

The pathophysiological mechanisms by which c9orf72 gene hexanucleotide expansion leads to development of neurodegeneration and thereby the clinical features of ALS, particularly

fasciculations, remains to be established (97, 98). Widespread axonal ion channel dysfunction, including upregulation of persistent Na^+ conductances and reduction of slow and fast K^+ channel conductances, has been extensively documented in sporadic ALS, resulting in motor axonal hyperexcitability (33-35, 413, 528-533). Importantly, such changes in motor axonal excitability were postulated to underlie motor neuron degeneration and the development of clinical features of ALS, particularly fasciculations (33-35, 413, 438, 528-531). In addition, motor axonal hyperexcitability, as reflected by upregulation of persistent Na^+ conductances, was also reported in familial ALS cohorts secondary to mutations in the superoxide dismuate-1 (SOD-1) gene and linked to the process of neurodegeneration.

Threshold tracking techniques may provide unique insights into nodal and internodal axonal membrane properties by sequentially assessing multiple excitability parameters (444, 446, 456). The strength-duration time constant (τ_{SD}), a measure of the rate at which the threshold current for a target potential declines as stimulus duration increases (34, 419, 423, 534-536), appears to be a biomarker of persistent Na^+ conductances (409). This notion is underscored by computer modelling studies of the human motor axon establishing that the τ_{SD} reflects the behaviour of persistent Na^+ conductances (423). In addition, depolarising and hyperpolarising threshold electrotonus, along with superexcitability and late subexcitability, appear to be robust biomarkers of fast and slow K^+ conductances respectively (409). Consequently, the present study utilised axonal excitability techniques in an attempt to determine whether upregulation of persistent Na^+ conductances and reduction of K^+ currents was a feature of c9orf72 FALS, and whether such changes in axonal excitability were linked to the processes of neurodegeneration, potentially informing the pathophysiological basis of c9orf72 FALS. In addition, the present study also aimed to determine whether axonal ion channel dysfunction was evident in asymptomatic c9orf72 mutation carriers.

Methods

Studies were undertaken on 10 clinically affected familial c9orf72 ALS patients as defined by the Awaji criteria (6 males, 4 females, mean age 63 years age range 41-78 years) and 9 asymptomatic c9orf72 mutation carriers (1 male, 8 females, mean age 45 years, age range 24-60 years). For comparison, 21 sporadic ALS patients were studied (16 males, 5 females, mean age 55 years age range 32-73). All ALS patients (sporadic and familial) were clinically staged using the ALS-functional Rating Scale-Revised (ALSFRS-R) (537). In addition, muscle strength was assessed by utilising the Medical Research Council (MRC) score with the following muscle groups assessed bilaterally yielding a total MRC score of 90: shoulder abduction; elbow flexion; elbow extension; wrist dorsiflexion; finger abduction; thumb abduction; hip flexion; knee extension; ankle dorsiflexion (532, 538). The degree of upper motor neuron (UMN) dysfunction was assessed by a specific UMN score incorporating the following parameters: brisk jaw jerks (1 point), brisk facial reflex (1 point), pathologically brisk biceps, triceps, supinator, finger, knee and ankle reflexes (1 point for each, assessed bilaterally) and extensor plantar responses (1 point each and assessed bilaterally). The UMN score ranged from 0 [no UMN dysfunction] to 16 [severe UMN dysfunction] (497). Cognitive screening was undertaken only in the c9orf72 FALS patients and asymptomatic mutation carriers utilising the Addenbrooke's Cognitive Examination - Revised (ACE-R) (539). Patients and carriers suffering with diabetes mellitus or chronic renal failure were excluded from the study. None of the subjects were taking medications that could affect the results. All subjects gave informed consent to the procedures, which were approved by the South East Sydney Area Health Service Human Research Ethics Committee.

Following clinical staging and phenotyping, the median nerve was stimulated at the wrist and the resultant CMAP recorded from the abductor pollicis brevis (APB) using surface

electrodes. The active recording electrode was placed over the motor point of APB and the reference was placed 4 cm distally, at the base of the thumb. Skin temperature was monitored close to the site of stimulation for the duration of each study. Prior to excitability studies, CMAP amplitude and onset latency, F-wave latency and frequency were all measured. The neurophysiological index (NI), a marker of peripheral disease burden in ALS, was derived according to a previously reported formula (540):

NI = CMAP amplitude (mV)* F-wave frequency/Distal motor latency (ms),

where F-wave frequency was expressed as the proportion of F responses recorded in 20.

Axonal excitability

All ALS patients underwent axonal excitability studies on the median motor nerve according to a previously described protocol (444). The median nerve was stimulated at the wrist using 5 mm non-polarizable Ag-AgCl electrodes (ConMed, Utica, USA) with the cathode positioned over the skin crease and anode ~ 10 cm proximally over the lateral forearm. Stimulation was computer controlled and converted to current using an isolated linear bipolar constant current simulator (maximal output ± 50 mA; DS5, Digitimer, Welwyn Garden City, UK). The CMAP responses were recorded from the APB muscle with the active (G1) electrode positioned over the motor point and the reference (G2) electrode placed at the proximal phalanx 4 cm away.

Test current pulses were applied at 0.5s intervals and combined with either sub-threshold polarizing currents or suprathreshold conditioning stimuli according to previously described protocols (444). The CMAP amplitude was measured from baseline to negative peak, with the target set to 40% of maximum for all tracking studies. Proportional tracking was utilized

to determine the changes in threshold current required to produce and maintain a target response (408).

Electrical stimuli were increased in incremental steps to generate the motor stimulus-response (SR) curve. Subsequently, the strength-duration time constant (τ_{SD}), a biomarker of persistent Na^+ conductance, and rheobase, defined as the threshold current for a stimulus of infinitely long duration, were measured according to Weiss' formula (34, 408, 422, 534).

Following the determination of the stimulus strength-duration relationship, threshold electrotonus (TE) was determined using sub-threshold polarizing currents of 100 ms duration, set to +/- 40% of controlled threshold current (408, 409, 444). Test stimuli of 1 ms duration were used to produce and maintain a target response of 40% of maximum CMAP amplitude. Three stimulus combinations were tested sequentially: test stimulus alone (measured control threshold current); test stimulus + depolarizing current; test stimulus + hyperpolarizing current. Threshold was tested at 26 time points before, during, and after the 100 ms polarizing pulse. The stimulus combinations were repeated until three valid estimates were recorded within 15% of target response (444). The following TE changes were recorded with sub-threshold depolarizing currents: TEd (10-20 ms); TEd (40-60 ms); and TEd (90-100 ms). In addition, changes in membrane threshold to hyperpolarizing currents at 10-20 ms, TEh (10-20 ms) and at 90-100 ms, TEh (90-100 ms) were also measured.

The current-threshold relationship (I/V), a biomarker of inward and outward rectifying membrane currents (409), was assessed by tracking threshold changes following sub-threshold polarizing currents of 200-ms duration which were altered in ramp fashion from +50% (depolarizing) to -100% (hyperpolarizing) of controlled threshold in 10% steps.

Conditioning stimuli were alternated with test stimuli until three valid threshold estimates were recorded. The following parameters were recorded: (i) resting I/V slope, calculated from polarizing currents between +10% to -10%; and (ii) hyperpolarizing I/V slope, calculated from polarizing current between -80% to -100%.

Lastly, the recovery cycle of axonal excitability was recorded according to a well-established protocol (444, 445). The following parameters were measured; (i) relative refractory period (RRP, ms), defined as the first intercept at which the recovery curve crosses the x-axis and a biomarker of transient Na^+ channel function (409); (ii) superexcitability (%), defined as the minimum mean threshold change of three adjacent points and a biomarker of paranodal fast K^+ channel conduction (409); (iii) late subexcitability (%), defined as the largest increase in threshold following the superexcitability period and a biomarker of nodal K^+ channel conduction (409).

Recordings of CMAP responses were amplified and filtered (3 Hz-3 kHz) using a Nicolet-Biomedical EA-2 amplifier (Cardinal Health Viking Select version 11.1.0, Viasys Healthcare Neurocare Group, Madison, Wisconsin, USA) and sampled at 10 kHz using a 16-bit data acquisition card (National Instruments PCI-MIO-16E-4). Data acquisition and stimulation delivery were controlled by QTRACS software (TROND-F, version 16/02/2009, © Professor Hugh Bostock, Institute of Neurology, Queen Square, London, UK).

Mathematical modelling of axonal excitability changes

To model the axonal excitability changes evident in c9orf72 FALS and sporadic ALS patients, mathematical simulations were undertaken using an established model of the human motor axon (541-545). Nodal transient and persistent Na^+ currents were modelled using data

from voltage-clamp and latent addition studies in human axons (546, 547). This model incorporates: slow and fast K^+ currents at both the node and internode; the hyperpolarization-activated current I_h at the internode; and leak and pump currents at both the node and internode (Howells *et al.*, 2012). The discrepancy between the model and the group data was calculated as the weighted sum of the squares of the error terms: $(x_m - \bar{x})^2$, where x_m is the model threshold and $\bar{x}$ is the mean threshold for the group data. The weights were 0.5 for the strength-duration time constant and 1 for each of the other threshold measurement types (i.e. threshold electrotonus, current-threshold relationship and the recovery cycle). The model was first adjusted to fit the normal control data using an interactive least squares procedure which minimized the discrepancy between model and data (548).

Statistical analysis

Axonal excitability studies were compared to 34 age-matched controls (13 males; 21 females, mean age 51.1±2.2 years), with the Student t-test utilised for assessing differences between means in patients, carriers and controls. All of the axonal excitability data was normally distributed as assessed by the Shapiro-Wilk test. Pearson's correlation coefficients were used to examine the relationship between parameters. Since measures of excitability may vary with age and temperature, parameters were compensated for age, temperature and sex if required before statistical analysis, using the relations established previously in control subjects (549). The ACE-R score was non-parametrically distributed and a Mann-Whitney test was utilised to compare differences between c9orf72 FALS and asymptomatic mutation carriers. A probability (P) value of <0.05 was considered statistically significant, and the probability values were corrected for multiple comparisons. Results were expressed as mean ± standard error of the mean or median [interquartile range].

Results

Clinical phenotype

The clinical features for the 10 clinically affected FALS patients, 9 asymptomatic c9orf72 mutation carriers and 21 sporadic ALS patients are summarized in Table 6.1. At the time of assessment, the c9orf72 FALS and sporadic ALS patients presented with the classical "ALS" phenotype. Bulbar-onset disease was evident in 40% of c9orf72FALS and 29% of sporadic ALS patients, while limb-onset disease was reported in 60% of c9orf72 FALS and 71% of sporadic ALS patients. At the time of assessment, the mean age of onset was unexpectedly higher in the c9orf72 FALS cohort (FALS $_{c9orf72}$ 63 ± 3.8 years; sporadic ALS 55 ± 2.5 years, P = 0.08), while the disease duration from symptom onset was comparable between the FALS and sporadic ALS patients (FALS $_{c9orf72}$ 14.3 ± 3.9 months; sporadic ALS 12.5 ± 2 months, P = 0.35).

Clinical features	c9orf72 FALS	SALS	AMC
Mean age at assessment [years]	63 (3.8)	55 (2.5)	45 (5.4)
Sex (M:F)	6:4	16:5	1:8
Mean disease duration (months)	14.3 (3.9)	12.5 (2.0)	-
Site of disease onset	Bulbar:40% Limb :60%	Bulbar:29% Limb:71%	
ALSFRS-R	39 (3.2)	41.6 (1.4)	48
Mean MRC upper limb score	54 (2.2)	53.8 (1.8)	60
Mean MRC lower limb score	28 (0.7)	28 (0.8)	30
Mean MRC total	82 (2.3)	82 (1.5)	90

Table 6.1. Clinical details for the 10 s9orf72 familial amyotrophic lateral sclerosis (FALS) patients, 21 sporadic ALS patients (SALS) and 9 asymptomatic c9orf72 mutation carriers (AMC). Disease duration refers to the period from symptom onset to date of testing. The patients were clinically graded using the amyotrophic lateral sclerosis functional rating scale revised (ALSFRS-R), with a maximum score of 48 when there is no disability. Muscle strength was clinically assessed using the Medical Research Council (MRC), with an upper limb, lower limb and total score being generated (*see* Methods).

The mean ALSFRS-R score in the c9orf72 FALS was 39±3.2, and was comparable to the sporadic ALS patients (41.6 ± 1.4, P = 0.22), indicating a similar degree of functional impairment. In addition, the degree of muscle weakness was similar between the groups as reflected by the upper limb (FALS $_{c9orf72}$ 54 ± 2.2; sporadic ALS 53.8 ± 1.8, P = 0.25, maximal score of 60 when normal strength), lower limb FALS $_{c9orf72}$ 28 ± 0.7; sporadic ALS 28 ± 0.8, P = 0.20, maximal score 30 when muscle strength normal) and total MRC scores (FALS $_{c9orf72}$ 82 ± 2.3; sporadic ALS 82 ± 1.5, P = 0.48, maximal score 90 when muscle strength normal). In addition, there was a comparable degree of upper motor neuron dysfunction in both the c9orf72 FALS and sporadic ALS patients (FALS $_{c9orf72\ UMN\ score}$ 10.7 ± 1.8; sporadic ALS $_{UMN\ score}$ 10 ± 0.6). While frontotemporal dementia was not evident in the current c9orf72 ALS cohort, there was a mild reduction of the ACE-R score suggesting the presence of subtle cognitive dysfunction in c9orf72 FALS patients (ACE-R$_{ACE\text{-}R\ c9orf72}$ 86 [76-92]; ACE-R $_{asymptomatic\ mutation\ carriers}$ 97 [95-98], P <0.05).

Neurological examination was normal in all the asymptomatic c9orf72 mutation carriers. Specifically, there was no clinical evidence of upper or lower motor neuron dysfunction at time of assessment. To date, all of the asymptomatic mutation carriers have remained well.

Neurophysiology

The mean CMAP amplitudes were significantly reduced in the c9orf72 FALS and sporadic ALS patients when compared to normal controls (FALS $_{c9orf72}$ 3.4 ± 0.3 mV; sporadic ALS 5.6 ± 0.8 mV; controls 8.8 ± 0.4 mV, F = 17.9, P < 0.01). Importantly, there were no significant differences in CMAP amplitudes between the c9orf72 FALS and sporadic ALS cohorts (P = 0.112). In addition, the neurophysiological index was also significantly reduced in the c9orf72 FALS and sporadic ALS patients when compared to controls (FALS $_{c9orf72}$ 1.1

± 0.2; sporadic ALS 1.2 ± 0.2; controls 2.5 ± 0.1, P < 0.01). While these findings indicate a significant degree of LMN dysfunction in the C9orf72 FALS and SALS cohorts, there was a trend for the CMAP amplitude to be lower in the c9orf72 FALS patients, despite a comparable clinical disease burden. This discordant finding could be potentially explained by a greater sensitivity of neurophysiological techniques in detecting LMN dysfunction (550). Of further relevance, clinical and electrical evidence of fasciculations were evident in all the C9orf72 FALS and SALS patients.

In contrast, there was no significant differences in the CMAP amplitude (c9orf72 mutation carriers 7.0 ± 0.6 mV; controls 8.8 ± 0.4 mV) and neurophysiological index (asymptomatic c9orf72 mutation carriers, 2.5 ± 0.3; controls 2.5 ± 0.1) between the c9orf72 mutation carriers and normal controls, re-affirming the structural integrity of the peripheral nerves at time of assessment in asymptomatic controls.

***Strength duration time-constant and rheobas*e**

Strength-duration time constant is a biomarker of persistent Na^+ conductances at the node of Ranvier (34, 421, 423, 534-536). The mean τ_{SD} was significantly increased in the c9orf72 FALS (0.5 ± 0.02 ms, P < 0.05, Fig. 6.1A, B) and sporadic ALS patients (0.52 ± 0.02 ms, P < 0.01, Fig. 6.1A, B) when compared to controls. In contrast, there were no significant differences in τ_{SD} between asymptomatic c9orf72 mutation carriers and controls (asymptomatic c9orf72 mutation carriers, 0.45 ± 0.04; controls 0.44 ± 0.01, P = 0.42, Fig. 6. 1A, B). Of further relevance, rheobase was significantly reduced in both c9orf72 FALS (1.61 ± 0.5 mA, P < 0.001, Fig 6.1A, C) and sporadic ALS patients (1.35 ± 0.10 mA; controls 2.27 ± 0.23 mA, P < 0.001, Fig 6.1A, C). In contrast, rheobase was slightly increased in the

asymptomatic c9orf72 mutation carriers (2.64 ± 0.72 mA, Fig 1A, C), but again this increase was not significant.

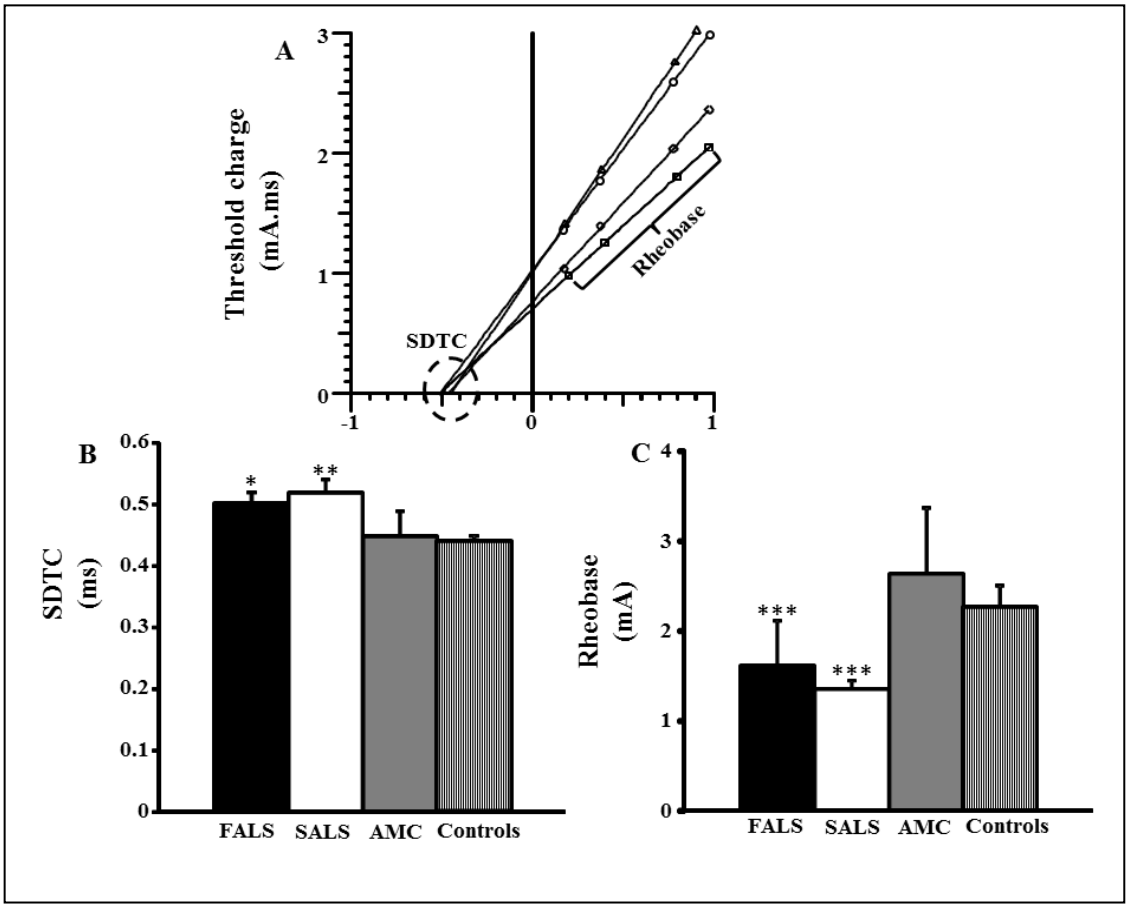

Figure 6.1. Strength-duration time constant in amyotrophic lateral sclerosis. The strength-duration time constant (τ_{SD}) reflects nodal persistent Na^+ channel conductances. **(A)** The τ_{SD} was significantly increased in c9orf72 familial amyotrophic lateral sclerosis patients [FALS] (clear triangles) and sporadic amyotrophic lateral sclerosis (SALS, clear circles) when compared to asymptomatic c9orf72 mutation carriers (AMC, clear diamonds) and controls (clear squares). **(B)** Mean SDTC was significantly increased in FALS and SALS patients. (C) Rheobase was significantly reduced in FALS and SALS patients. *P < 0.05; **P< 0.01; ***P< 0.001.

Threshold electrotonus

Threshold electrotonus (TE) provides insight into nodal and internodal membrane conductances. Previously, two types of abnormalities of TE have been described in SALS, namely the type I abnormality, in which there is a greater change in response to a sub-threshold depolarizing pulse, and the type II abnormality, in which there is a sudden decrease in membrane excitability marked by an abrupt increase in threshold (530). In the present study, the type I abnormality was evident in 40% of the c9orf72 FALS patients and 29% of sporadic ALS patients, while the type II abnormality was not evident. Further, neither the type I nor type II abnormalities were evident in the asymptomatic c9orf72 mutation carriers.

Group data analysis disclosed the presence of significant difference in TE between FALS and sporadic ALS patients, asymptomatic c9orf72 mutation carriers and controls (Fig. 6.2A). Specifically, TEd (90-100 ms) was significantly increased in both the c9orf72 FALS (51.0 ± 1.9%, $P < 0.05$, Fig 6.2B) and sporadic ALS (50.3 ± 1.4%, $P < 0.01$, Fig. 6.2B) patients when compared to controls (45.6 ± 0.6%). Although there was a greater threshold change to hyperpolarizing sub-threshold conditioning pulses in the c9orf72 FALS and sporadic ALS patients (FALS $_{c9orf72}$ -128.7 ± 8.7%; sporadic ALS -122.5 ± 0.6%; controls -117.5 ± 3.2%, $P = 0.13$, Fig. 6.2), this difference was not significant.

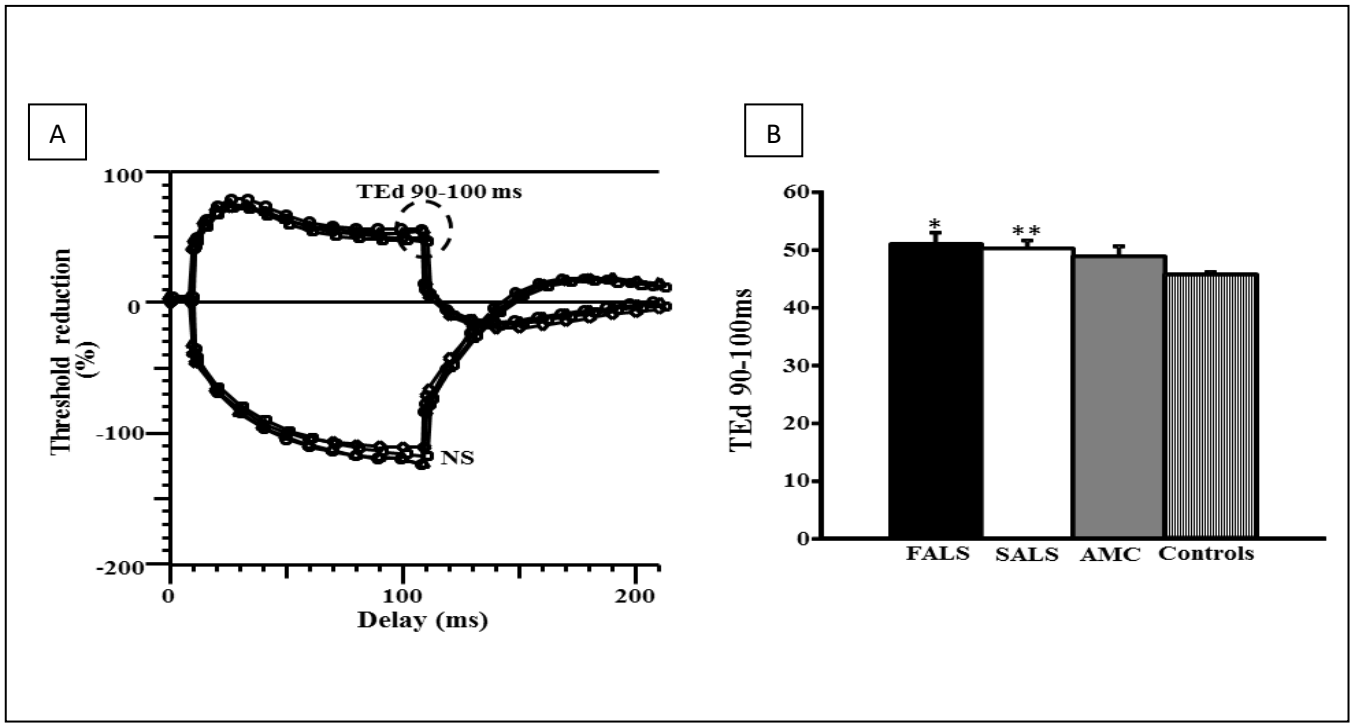

Figure 6.2. **Threshold electrotonus measures in amyotrophic lateral sclerosis**. Threshold electrotonus reflects changes in membrane excitability in response to long duration polarizing currents. Threshold reduction with depolarization is represented in an upward direction and hyperpolarization in a downward direction. **(A)** Depolarising threshold electrotonus was significantly increased in c9orf72 familial amyotrophic lateral sclerosis patients (FALS) (clear triangles) and sporadic ALS (SALS, clear circles) when compared to asymptomatic c9orf72 mutation carriers (AMC, filled diamonds) and controls (clear squares). In contrast, hyperpolarising threshold electrotonus was not significant (NS) between groups. **(B)** Mean TED90-100 ms was significantly increased in c9orf72 FALS and SALS. *P < 0.05; **P < 0.01.

Current/threshold (I/V) relationship

The I/V relationship estimates the inward and outward rectifying properties of nodal and internodal axonal segments, with the hyperpolarising I/V gradient reflecting conductances via inward rectifying currents (408, 551). The hyperpolarizing I/V gradient was significantly increased in c9orf72 FALS (0.42 ± 0.02, P < 0.05) and sporadic ALS patients (sporadic ALS, 0.41 ± 0.02, P < 0.05) when compared to asymptomatic mutation carriers (0.34 ±0.03) and controls (0.36 ± 0.01).

Recovery cycle of excitability

The RRP duration was not significantly different when compared to controls ($FALS_{c9orf72}$, 3.7 ± 0.2 ms, P = 0.06; sporadic ALS, 3.8 ± 0.3 ms, P = 0.08; asymptomatic c9orf72 mutation carriers, 3.2 ± 0.1 ms, P = 0.36; controls, 3.3 ± 0.1 ms). In addition, there were no significant differences in superexcitability and late subexcitability between groups.

Correlation with clinical parameters and disease duration

Combining measures of axonal excitability, clinical assessment and disease severity, it was evident that τ_{SD} (R = -0.38, P < 0.05, Fig. 6.3A) and TEd [90-100 ms] (R = -0.44, P < 0.01, Fig. 6.3B) in c9orf72 FALS and sporadic ALS patients correlated with the CMAP amplitude, thereby suggesting that the increase in τ_{SD} and TEd [90-100 ms] were potentially linked to axonal degeneration. In addition, the TEd [90-100 ms] was significantly correlated with the ALSFRS-R (R =-0.34, P < 0.05) and MRC upper limb score (R = -0.32, P < 0.05). Taken together, these findings suggest that abnormalities of axonal excitability, particularly increased τ_{SD} and TEd [90-100 ms], are late features of c9orf72 FALS, and linked to the process of neurodegeneration.

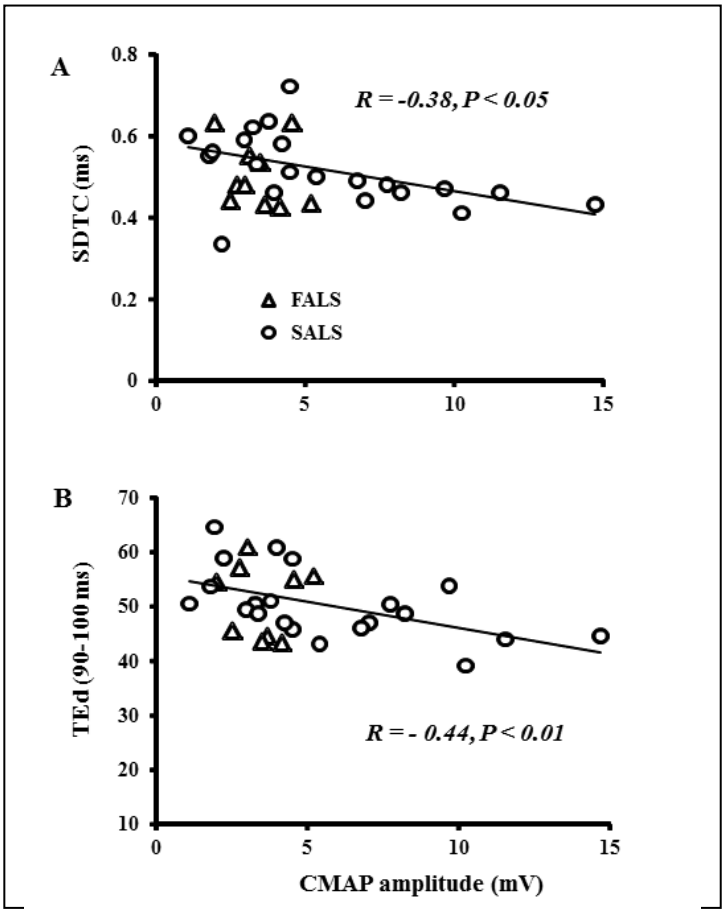

Figure 6.3. Correlation of axonal excitability parameters with motor amplitudes. **(A)** The strength-duration time constant (SDTC) and (**B)** depolarising threshold electrotonus at 90-100 ms (TEd 90-100 ms) significantly correlated with the compound muscle action potential (CMAP) amplitude, thereby suggesting that SDTC and TEd 90-100 ms were linked with the process of axonal degeneration.

Mathematical modelling of abnormal excitability properties

To assist in interpreting the changes observed in axonal excitability, a mathematical model of the human motor axon was adjusted to provide a close match to the control group (Figs. 6.4 and 6.5). The model was then used to explore which membrane parameter changes could reproduce the changes seen in the combined FALS and sporadic ALS patient recordings. The axonal excitability data in c9orf72 FALS and sporadic ALS was best modeled by a 30% reduction in the nodal slow K^+ conductance along with an increase in persistent Na^+ conductances and increase in I_h current, reducing the overall discrepancy by 81.7%. The modelled changes resulted in a net depolarization of resting membrane potential (RMP) of 0.8 mV.

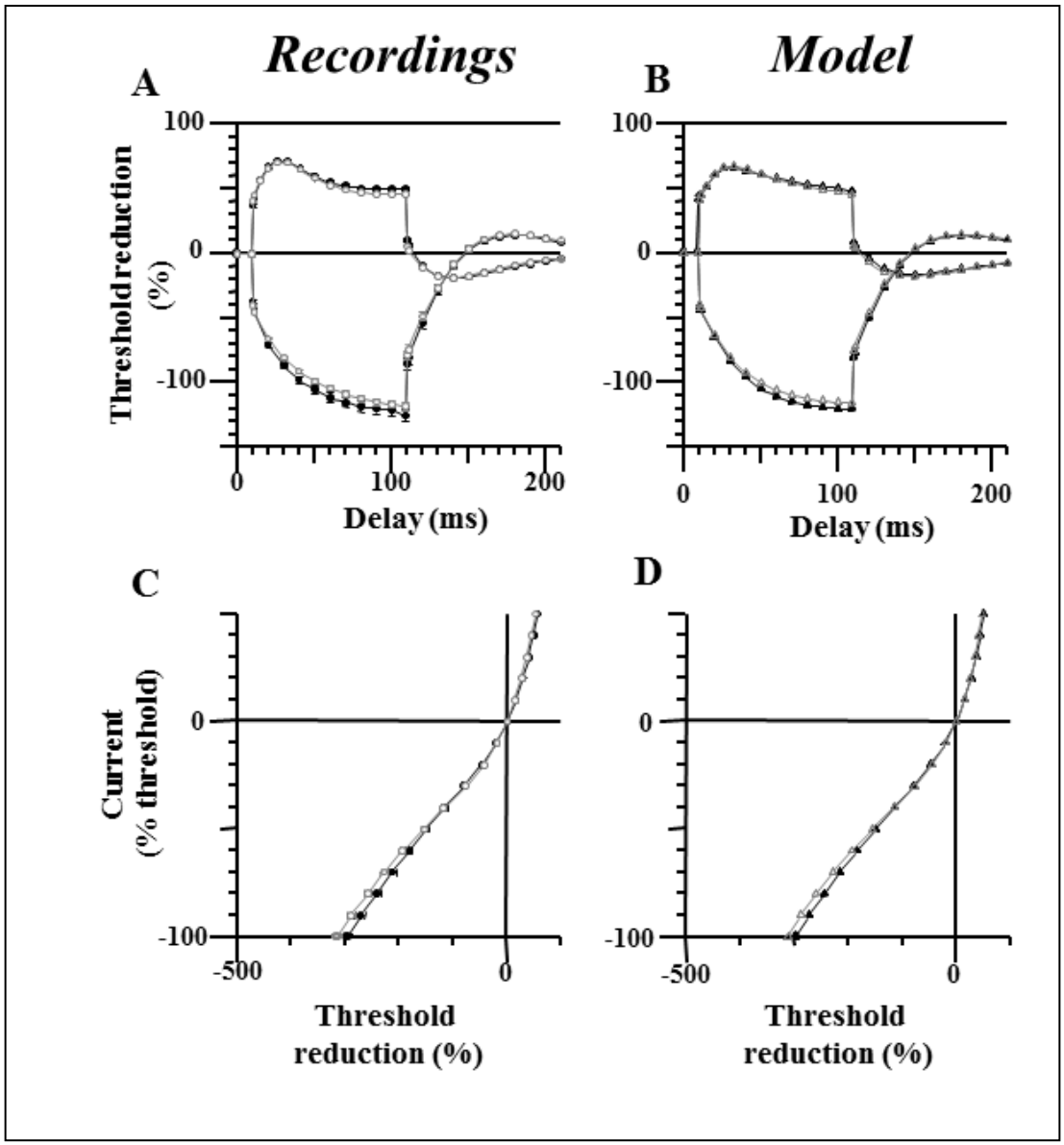

Figure 6.4. Mathematical modelling of axonal excitability parameters in ALS. Comparison of group data (controls, open circles; combined c9orf72 and sporadic ALS, filled circles) and mathematical model (open triangles, normal model; c9orf72 and sporadic ALS model, filled triangles). **A.** Threshold electrotonus group data. **B.** Modelled threshold electrotonus. **C.** Current-threshold relationship. **D.** Modelled current-threshold relationship.

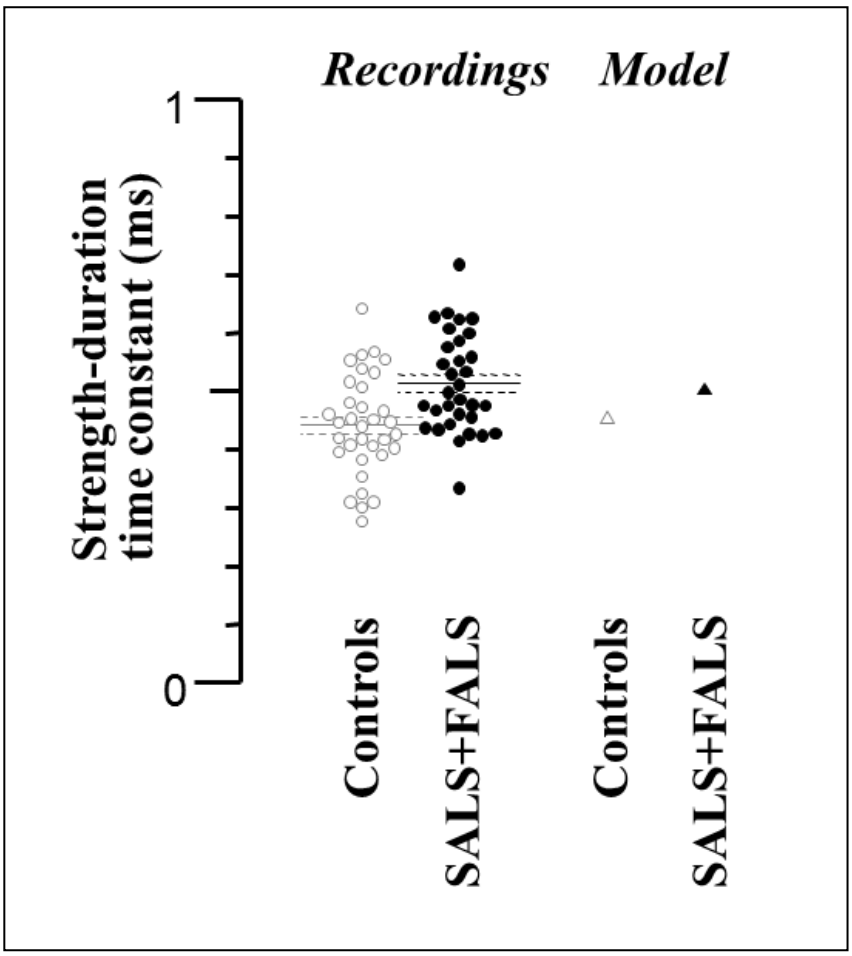

Figure 6.5. Mathematical modelling of strength-duration time constant in ALS. Comparisons of recorded and modelled strength-duration time constant (τ_{SD}) data. The τ_{SD} was significantly increased in c9orf72 familial amyotrophic lateral sclerosis (FALS) and sporadic ALS (SALS) patients. Modelled strength-duration time constant for normal and combined SALS and FALS datasets.

Discussion

The present study has established a pattern of axonal excitability abnormalities in c9orf72 FALS that resembled changes observed in sporadic ALS patients. Specifically, the strength-duration time constant was significantly longer and depolarising threshold electrotonus at 90-100 ms significantly greater in the c9orf72 FALS and sporadic ALS cohorts. Mathematical modelling suggested that the changes in axonal excitability were best explained by a reduction of slow nodal K^+ currents along with an increase in persistent Na^+ conductances, inward rectification and Na^+ pump activity. Importantly, the abnormalities of axonal excitability correlated with functional (ALSFRS-R and MRC upper limb score) and neurophysiological (CMAP amplitude) biomarkers of peripheral disease burden. In contrast, axonal excitability was normal in asymptomatic c9orf72 mutation carriers. Taken together, the findings from the present series have identified a potential role for a reduction of slow nodal K^+ currents and an upregulation of persistent Na^+ conductances in the pathophysiology of c9orf72 associated FALS.

Axonal ion channel dysfunction in c9orf72 FALS

Strength-duration time constant, or *chronaxie*, is a measure of the rate at which the threshold current declines as stimulus duration increases (423). The τ_{SD} is a biomarker of persistent Na^+ conductances (34, 35, 408, 409, 419, 421, 529, 534-536, 552), a notion supported by computer modelling of the human motor axon (423). Prolongation of τ_{SD} has previously been established as a feature of sporadic ALS, attributed to upregulation of persistent Na^+ conductances (34, 35, 413, 529). Importantly, upregulation of persistent Na^+ conductances has been linked to the development of axonal degeneration in ALS (35, 413, 438), including the split-hand pattern of degeneration (533), as well as motor axonal hyperexcitability and generation of fasciculations (34, 35, 413, 529, 532, 533). In addition, prolongation of τ_{SD}

was also reported in SOD-1 FALS and correlated with biomarkers of peripheral disease burden (184), thereby suggesting that upregulation of persistent Na^+ conductances contributed to development of clinical features and neurodegeneration in SOD-1 FALS, a finding in keeping with transgenic SOD-1 mouse model studies (523).

The present study establishes that prolongation of τ_{SD}, and thereby upregulation of persistent Na^+ conductances, was a pathophysiological feature of c9orf72 FALS, a notion supported by mathematical modelling of axonal excitability. The correlation between prolongation of τ_{SD} and biomarkers of peripheral disease burden (including the CMAP amplitude) suggests that persistent Na^+ conductances may contribute to motor neuron degeneration in c9orf72 FALS. Importantly, findings from the present study imply the existence of a common pathogenic pathway in ALS, irrespective of the underlying genotype.

In addition to prolongation of τ_{SD}, there were significant changes in depolarising threshold electrotonus. Specifically, the type I abnormality of threshold electrotonus, in which there was a greater change in response to a sub-threshold depolarizing pulse, was evident in the c9of72 FALS cohort, but not asymptomatic mutation carriers. In addition, the mean TEd [90-100ms] was significantly increased in c9orf72 FALS and sporadic ALS, correlating with peripheral biomarkers of peripheral disease burden, and thereby suggesting that reduction of slow K^+ currents contributed to development of axonal hyperexcitability and clinical features in c9orf72 FALS. Importantly, mathematical modelling indicated that reduction of slow K^+ currents in a large part accounted for the changes observed in axonal excitability, suggesting an important role for slow K^+ channels in c9orf72 pathophysiology. This notion is further underscored by recent patch-clamp studies reporting that retigabine, a K^+ channel activator, reduces axonal hyperexcitability and improves motor neuron survival in pluripotent stem

cells derived from c9orf72 FALS patients, thereby implying a therapeutic potential for retigabine (523). Of further relevance, a similar degree of reduction in slow K^+ currents in the c9orf72FALS and sporadic ALS patients underscores the existence of common pathogenic pathways.

It could also be argued that the observed reduction in slow K^+ conductances contributed to the increase in τ_{SD} through depolarisation of the RMP. Such a hypothesis cannot be discounted given that modelling studies suggested that reduction in slow K^+ plays a bigger role in reducing the discrepancy in the measure of τ_{SD} than the increase in fraction of persistent Na^+ channels. Given that axonal excitability parameters, such as superexcitability and threshold electrotonus which are reduced with RMP depolarisation (456), remained unchanged argues against the notion that membrane depolarization solely accounted for the increase in τ_{SD}.

In contrast to previous studies in sporadic ALS patients (35, 413), paranodal fast K^+ channel function appears to be preserved in c9orf72 FALS patients and the current SALS cohort. Specifically, superexcitability and TEd [10-20ms], both biomarkers of paranodal fast K^+ channels (409), were not significantly altered in the c9orf72 FALS and sporadic ALS cohorts. Importantly, paranodal fast K^+ channel dysfunction appears to evolve with disease progression and seems most pronounced immediately prior to motor axonal loss (553). Consequently, the discordant findings between the current and previous ALS cohorts may relate to differences in the extent and stage of motor axonal loss, reflecting the membrane properties of surviving motor axons at the time of assessment.

An increase in the hyperpolarising I/V gradient was also evident in the c9orf72 FALS and sporadic ALS cohorts and is best explained by an increase in inward rectifying currents (I_h). The increase in I_h most likely represents an adaptive response to the increased demands on surviving motor axons, perhaps secondary to axonal hyperexcitability due to reduction in slow K^+ currents and upregulation of persistent Na^+ conductances.

In contrast to abnormalities of axonal excitability evident in the c9orf72 FALS and SALS patients, there were no significant changes in asymptomatic c9orf72 mutation carriers. This finding is in keeping with previous studies in SOD-1 asymptomatic mutation carriers (184), implying that factors other than inheritance of the genetic mutation may be required to trigger the disease process.

Clinical implications

The mechanisms by which axonal ion channel dysfunction leads to neurodegeneration and adverse survival in ALS (554) remains to be elucidated, although it has been postulated that an influx of Na^+ ions results in reverse operation of the Na^+/Ca^{2+}-exchanger, intra-axonal accumulation of Ca^{2+} and ultimately activation of Ca^{2+}-dependent enzyme pathways leading to motor neuron degeneration (210, 555-558) . In addition, reduction of slow K^+ currents and upregulation of persistent Na^+ conductances would increase the depolarizing drive, thereby leading to axonal hyperexcitability and development of cramps and fasciculations, both prominent symptoms in ALS (15, 36, 48, 559-562).

Chapter 7

CORTICAL EXCITABILITY CHANGES DISTINGUISH THE MOTOR NEURON DISEASE PHENOTYPES FROM HEREDITARY SPASTIC PARAPLEGIA

Summary

Having established that cortical hyperexcitability is an important pathogenic mechanism in ALS, we wanted to explore whether cortical hyperexcitability is a common process across the ALS/MND phenotypes, including amyotrophic lateral sclerosis (ALS) and primary lateral sclerosis (PLS). Separately, the clinical distinction between PLS and "mimic disorders" such as hereditary spastic paraparesis (HSP) may be difficult, potentially delaying diagnosis. Consequently, the aim of the present study was to determine the nature and spectrum of cortical excitability changes across the ALS/MND phenotypes, and to determine whether the presence of cortical dysfunction distinguishes PLS from HSP. Cortical excitability studies were undertaken on a cohort of 14 PLS, 82 ALS and 13 HSP patients with mutations in the *spastin* gene. Cortical hyperexcitability, as heralded by reduction of short interval intracortical inhibition (PLS 0.26%, -3.8 to 1.4%; ALS -0.15%, -3.6 to 7.0%, $P<0.01$) and cortical silent period duration (CSP_{PLS} 172.2±5.4 ms; CSP_{ALS} 178.1±5.1ms, $P<0.001$) along with an increase in intracortical facilitation, were evident in ALS and PLS phenotypes, appearing more frequently in the former. Inexcitability of the motor cortex was more frequent in PLS (PLS 71%, ALS 24%, $P<0.0001$). Cortical excitability was preserved in HSP. Cortical dysfunction appears to be an intrinsic process across the MND phenotypes, with cortical inexcitability predominating in PLS and cortical hyperexcitability predominating in ALS. Importantly, cortical excitability was preserved in HSP, thereby suggesting that the presence of cortical dysfunction could help differentiate PLS from HSP in a clinical setting.

Introduction

Motor neuron disease (MND) encompasses a group of neurodegenerative disorders exhibiting a heterogeneous clinical phenotype (48). The commonest phenotype is amyotrophic lateral sclerosis (ALS), a rapidly progressive neurodegenerative disorder affecting both the upper and lower motor neurons (48, 563). In contrast, the upper motor neuron (UMN) phenotype, termed primary lateral sclerosis (PLS), is characterized by a slowly progressive UMN syndrome with absence of LMN features (66, 70, 564, 565). Given the phenotypic variability, the issue as to whether common pathophysiological processes underlie the varied MND phenotypes remains to be elucidated.

Corticomotoneuronal hyperexcitability and disinhibition has been implicated in ALS pathogenesis, with neuronal degeneration mediated by an anterograde glutamate-mediated excitotoxic process (24). Transcranial magnetic stimulation (TMS) techniques have established cortical hyperexcitability as an early and specific feature of ALS, linked to the process of motor neuron degeneration (39, 183, 185, 237). In contrast, TMS studies in PLS have been limited (70, 76, 78), disclosing cortical inexcitability and prolongation of central motor conduction time (70, 76, 78). Whether corticomotoneuronal hyperexcitability and disinhibition are features of PLS remains unknown, and resolution of this issue may shed light on whether PLS forms a pathophysiological continuum with ALS. Consequently, the present study utilized threshold tracking TMS techniques (329) in order to dissect out the underlying pathophysiological processes in the varied MND phenotypes, with a particular aim of delineating the nature and spectrum of cortical dysfunction between ALS, PLS and the mimic disorder pure hereditary spastic paraplegia (HSP), and to determine whether the presence of cortical dysfunction could differentiate PLS from HSP.

Methods

Clinical assessment:

Studies were undertaken on 14 primary lateral sclerosis patients (8 males and 6 females, mean age 62, range 48-75 years) that were diagnosed according to previously established criteria (66, 70). Specifically, the PLS diagnostic criteria utilized in the present cohort included: (i) presence of UMN signs with absence of focal muscle atrophy, fasciculations and EMG evidence of denervation for at least 3, but preferably 4 years after symptom onset; (ii) age of onset > 40 years; and (iii) exclusion of mimic disorders by laboratory and neuroimaging investigations (66, 70). Clinical and cortical excitability findings were compared to a cohort of 13 genetically confirmed hereditary spastic paraplegia (HSP) patients (6 males and 7 females, mean age 56, range 24-72 years) secondary to mutations in the *spastin* gene (SPG42p21-22), 82 ALS patients (48 males, 34 females, mean age 60 years, range 40-85 years, Table 7.1) diagnosed according to the Awaji criteria (6) and in part previously reported (504), as well as 37 healthy controls (18 males and 19 females, mean age 58, range 46-73 years). Informed consent to the procedures was provided by all patients, with the study approved by the Sydney West Area Health Service and Human Research Ethics Committees.

Patients were clinically staged using the Amyotrophic Lateral Sclerosis Functional Rating Scale-Revised [ALSFRS-R] (495) or the Spastic Paraplegia Rating Scale [SPRS](566). Muscle strength was assessed by the Medical Research Council (MRC) score (496) , with the following muscle groups assessed bilaterally yielding a total MRC score of 90: shoulder abduction; elbow flexion; elbow extension; wrist dorsiflexion; finger abduction; thumb abduction; hip flexion; knee extension; ankle dorsiflexion. The degree of upper motor neuron (UMN) dysfunction was assessed by an UMN score incorporating the following parameters:

jaw jerk, facial reflex, upper and lower limb deep tendon reflexes and plantar responses with the score ranging from 0 [no UMN dysfunction] to 16 [severe UMN dysfunction] (497). In all patients, the site of disease onset was recorded as either limb or bulbar.

All patients were initially assessed by nerve conduction studies and needle electromyography. The degree of peripheral disease burden was assessed by stimulating the median nerve electrically at the wrist using 5-mm Ag-AgCl surface electrodes (ConMed, Utica, USA). The resultant compound muscles action potential (CMAP) was recorded from the abductor pollicis brevis (APB), as was the neurophysiological index (NI) according to a previously reported formula (26).

Brain and spinal cord magnetic resonance imaging (MRI) studies excluded mimic disorders such as structural, metabolic or demyelinating lesions in the current PLS cohort. High T2 signal intensity in the corticospinal tract (internal capsule) was evident in one PLS patient. Nerve conduction study and needle electromyography excluded lower motor neuron dysfunction. Basic biochemistry, full blood count, vasculitic screen (ANA, ENA, ANCA), immunoelectrophoeresis, angiotensin converting enzyme levels, vitamin B12, folate, and B6 levels, thyroid function studies, coeliac disease serology, very-long-chain fatty acids, infective serology (human immunodeficiency virus, human T-lymphotrophic virus I and II, syphilis) and paraneoplastic screen were normal or negative. In addition, cerebrospinal fluid analysis was unremarkable in all PLS patients as was genetic testing for the *spastin* gene mutation.

Cortical excitability was assessed by utilizing a threshold tracking TMS technique according to a previously reported method (329). Specifically, TMS studies were undertaken by

applying a 90 mm circular coil connected to two high-power magnetic stimulators connected via a BiStim device (Magstim Co., Whitland, South West Wales, UK). The coil position was adjusted such that an optimal stimulating site was determined as indicated by a point on the vertex, at which a maximal motor evoked potential (MEP) amplitude was evoked by the smallest TMS current. The MEP response was recorded over the abductor pollicis brevis (APB) muscle.

Short interval intracortical inhibition and intracortical facilitation were assessed by the paired-pulse threshold tracking TMS technique as previously reported (329). Briefly, the MEP amplitude was fixed and changes in the test stimulus intensity required to generate a target response of 0.2 mV (± 20%), when preceded by sub-threshold conditioning stimuli, were measured. Resting motor threshold (RMT) was defined as the stimulus intensity required to maintain the target MEP response of 0.2 mV (±20%).

Short-interval intracortical inhibition was determined over the following interstimulus intervals (ISIs): 1, 1.5, 2, 2.5, 3, 3.5, 4, 5, and 7 ms, while ICF was measured at ISIs of 10, 15, 20, 25 and 30 ms. Stimuli were delivered sequentially as a series of three channels: **channel 1**: stimulus intensity, or threshold (% maximal stimulator output) required to produce the unconditioned test response (i.e., RMT); **channel 2**: sub-threshold conditioning stimulus (70% RMT); and **channel 3** tracks the stimulus (% maximal stimulator output) required to produce the target MEP when conditioned by a sub-threshold stimulus equal in intensity to 70% of RMT.

Single pulse TMS technique was utilized to determine the MEP amplitude (mV), MEP onset latency (ms) and central motor conduction time. The MEP amplitude was recorded with the

magnetic stimulus intensity set to 150% of the RMT, and four responses were recorded and averaged at this stimulus intensity. The resultant MEP amplitude was normalized by being expressed as a percentage of the compound muscle action potential (CMAP) response. The cortical silent period (CSP) was recorded while performing a weak voluntary contraction, approximately 30% of maximum voluntary contraction, and calculated from commencement of the MEP response to return of electromyography activity (329, 366). The central motor conduction time (CMCT) was derived by utilizing the F-wave method according to the previously following formula (567).

Recordings of the CMAP and MEP responses were amplified and filtered (3 Hz-3 kHz) using a Nicolet-Biomedical EA-2 amplifier (Cardinal Health Viking Select version 11.1.0, Viasys Healthcare Neurocare Group, Madison, Wisconsin, USA) and sampled at 10 kHz using a 16-bit data acquisition card (National Instruments PCI-MIO-16E-4). Data acquisition and stimulation delivery were controlled by QTRACS software. Temperature was monitored with a purpose built thermometer at the stimulation site.

Statistical analysis

All data was assessed for normality using the Shapiro-Wilk test. Student's t-test and Mann-Whitney U test were utilized to assess differences between groups, while Chi square testing (χ^2) was used for assessing differences between categorical variables. Analysis of variance (ANOVA), with a Bonferroni correction or Kruskal-Wallis test, was used for multiple comparisons. No statistical analysis was performed for cortical excitability changes in the 4 PLS patients, but rather the values are expressed as a function of the 95% confidence interval as calculated from normative data (*see* above). A P value < 0.05 was considered statistically

significant. All data are expresses as mean ± standard error of the mean (SEM) or median [interquartile range (IQR)].

Results

Clinical phenotypes

The PLS phenotype was characterized by a progressive spastic paraparesis with generalized hyper-reflexia affecting the bulbar, cervical and lumbosacral regions as indicated by a median UMN score of 14 (14-15). Importantly, UMN bulbar dysfunction, as characterized by a spastic dysarthria, slow tongue movement and absence of tongue atrophy and fasciculations, was evident in 64% of the PLS cohort. The mean age of symptom onset was 58±3.3 years, with the mean disease duration being 85.5 ± 14 months. The median ALSFRS-R score was 41 (35-43), while the total median MRC score was 88 (84-90), indicating mild-moderate level functional impairment in the PLS cohort (Table 7.1). Bladder dysfunction was evident in 29% of PLS patients, while none of the PLS patients exhibited sensory dysfunction (Table 7.1).

	PLS	**HSP**	**ALS**
Mean age of disease onset (SEM, years)	58 (3.3)	39 (3.0)	57 (1.1)
Mean disease duration (SEM, months)	85.5 (14)	244.4 (32.7)	15.6 (1.9)
Clinical features (%)			
-Bulbar dysfunction	64	0	37
-Urinary urgency	29	69	0
-Sensory symptoms	0	92	0
Median MRC sum score (IQR)	88 (84-90)	90 (90-90)	84 (79-88)
UMN score (IQR)	14 (14-15)	14 (14-15)	12 (9-13)

Table 7.1. Clinical features for the 14 primary lateral sclerosis (PLS), 82 amyotrophic lateral sclerosis (ALS) and 13 hereditary spastic paraparesis (HSP) patients. The mean age of disease onset was significantly greater for PLS patients. The Medical Research Council (MRC) sum score (see Methods) was comparable between PLS and HSP patients, as was the upper motor neuron (UMN) score, indicating a comparable degree of functional impairment and clinical upper motor neuron dysfunction. All data are expressed as mean ± standard error of the mean (SEM) or median (interquartile range, IQR).

The hereditary spastic paraparesis cohort was clinically characterized by a slowly evolving progressive spastic paraparesis with a similar degree of UMN dysfunction (median UMN score 14, 14-15) when compared to the PLS cohort. There was a moderate degree of functional impairment as indicated by a median SPRS score of 17 (IQR 11-24), while the muscle strength appeared to be preserved (Table 7.1). In contrast to PLS, HSP patients exhibited a significantly younger age of symptom onset (39 ± 3.0 years, Table 7.1, $P < 0.0001$), with the mean disease duration being significantly longer (244.4 ± 32.7 months, $P < 0.001$). In addition, bladder dysfunction (69%) and sensory abnormalities (92%) were more frequent in the HSP cohort, while bulbar dysfunction was not evident in HSP.

Prior to undertaking cortical excitability studies, the degree of peripheral disease burden was assessed. The CMAP amplitude (PLS 9.0 ± 0.8 mV; HSP 11.0 ± 1.0mV; ALS 6.9±0.5mV; controls 9.9 ± 0.5 mV, $F = 8.5$, $P < 0.001$) and NI (PLS 2.2 ± 0.3; HSP 2.2 ± 0.3; ALS 1.2 ± 0.2; controls 2.3 ± 0.1, $F = 13.4$, $P < 0.001$) were similar in the PLS and HSP cohorts and comparable to normal controls, but were significantly greater when compared to the ALS cohort. Taken together, these findings confirmed preserved lower motor neuron function in the PLS and HSP cohorts.

Cortical excitability

Transcranial magnetic stimulation studies disclosed a significant increase in the frequency of motor cortex inexcitability, defined as a resting or active motor threshold > 95% of maximal stimulator output, in PLS patients. Specifically, the motor cortex was inexcitable in 71% of PLS and 24% of ALS patients, while a "normal" level of motor cortex excitability was evident in the HSP patients ($x^2=37$, $P<0.0001$, Figure 7.1A). In the remaining four PLS patients, threshold tracking TMS studies disclosed a significantly increased RMT (PLS 74.5

± 6.4%, 95% confidence interval [CI] 55.3-60.9%, Figure 7.1B). There was no significant difference in RMT between HSP and ALS patients and controls (RMT $_{HSP}$ 52.0 ± 2.2%; RMT $_{CONTROLS}$ 58.1±1.4%, P<0.05, RMT $_{ALS}$ 56.8±1.1%, Figure 7.1B).

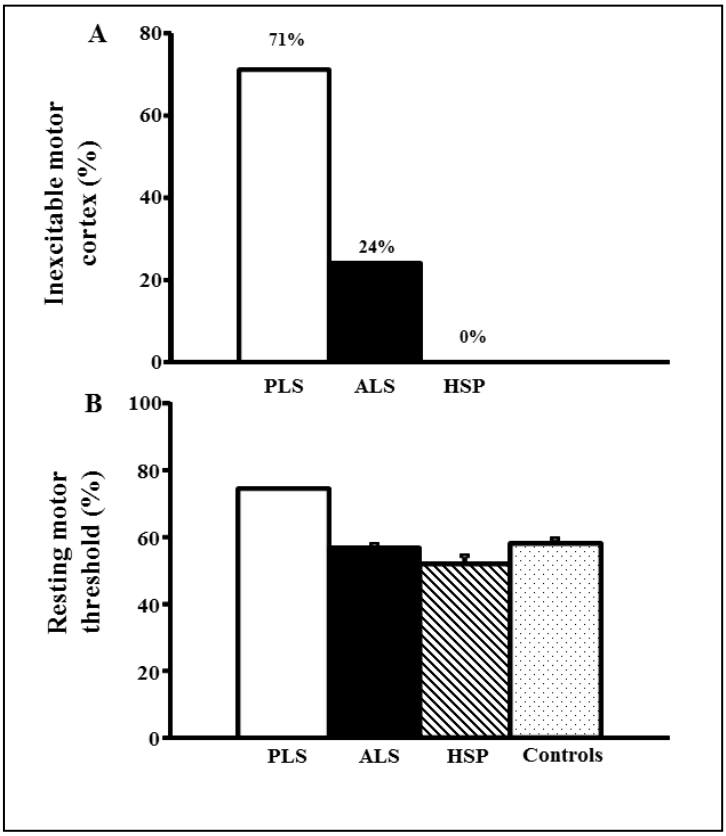

Figure 7.1. **(A)** The frequency of motor cortex inexcitability was more frequent in primary lateral sclerosis (PLS) patients when compared to amyotrophic lateral sclerosis (ALS) and hereditary spastic paraparesis (HSP) patients. **(B)** The resting motor threshold was significantly increased in PLS patients. ****P < 0.0001.

Paired pulse TMS was utilized to assess short interval intracortical inhibition and intracortical facilitation, both biomarkers of motor cortical function (39). Short interval intracortical inhibition was reduced in PLS (0.26%, -3.8 to 1.4%, 95% CI 9.7-13.9%, Figure 7.2A) and ALS phenotypes (-0.15%, -3.6 to 7.0%, P < 0.01, Figure 7.2A) when compared to HSP 7.0% (6.8 to 10.1%) and controls 12.0% (7.3 to 15.4%).

Following SICI, a period of intracortical facilitation develops between ISI of 10-30 ms (568). Intracortical facilitation was increased in PLS (-5.6%, -8.5 to -5.3%, 95% CI -2.5 to -0.7%, Figure 7.2B) and ALS (-3.2%, -6.6 to -0.5%, P < 0.01, Figure 7.2B) phenotypes when compared to HSP (-0.17%, -0.80 to 1.0%, P < 0.01, Figure 7.2B) and healthy controls (-0.70%, -3.1 to 2.7%, P < 0.01, Figure 7.2B). Importantly, ICF was comparable between PLS and ALS cohorts (Figure 7.2B).

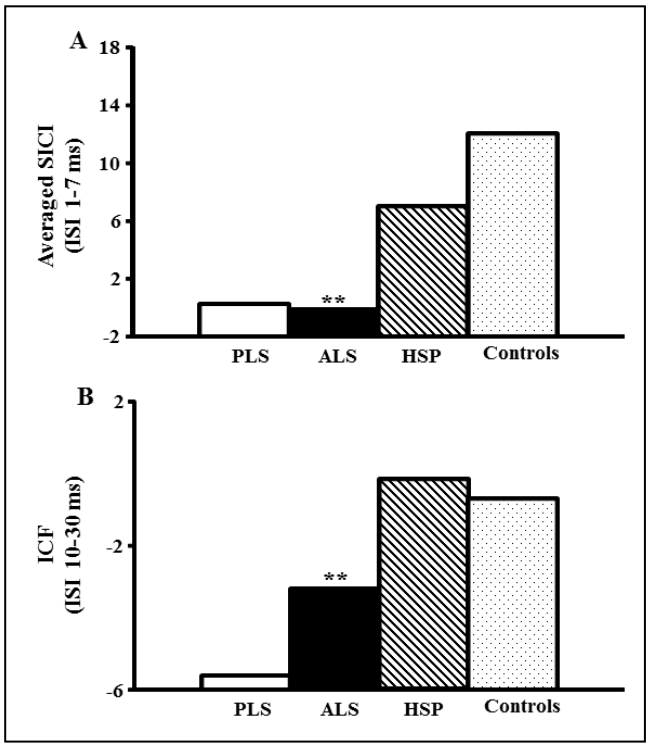

Figure 7.2. (A) Averaged short interval intracortical inhibition (SICI) between interstimulus interval (ISI) 1-7 ms was significantly reduced in primary lateral sclerosis (PLS) and amyotrophic lateral sclerosis (ALS) patients when compared to hereditary spastic paraparesis (HSP) patients and controls. **(B)** Intracortical facilitation (ICF), between ISI of 10-30 ms, was significantly increased in PLS and ALS patients. **P < 0.01.

Single-pulse TMS studies the CSP duration was reduced in PLS (CSP $_{PLS}$ 172.2 ± 5.4 ms, 95% CI 206.4-222 ms, Figure 7.3) and ALS patients when compared to the HSP cohort and healthy controls (CSP $_{ALS}$ 178.1±5.1ms CSP $_{HSP}$ 202.1±7.9ms; CSP $_{CONTROLS}$ 214.2±3.9ms, F = 13.5, P < 0.001, Figure 7.3). In contrast, while there was a trend for the MEP amplitude to be increased in the PLS (30.0 ± 7.8%, 95% CI 19-28.6%) and ALS phenotypes when compared to HSP and controls, this difference was not significant (MEP $_{ALS}$ 31.0±2.1%; MEP $_{HSP}$ 22.5±2.8%; MEP $_{CONTROLS}$ 23.8±2.4%, F = 1.6, P = 0.18). Surprisingly, central motor conduction time was comparable between groups (CMT $_{PLS}$ 6.9±0.6 ms; CMT $_{ALS}$ 6.0±0.1ms; CMT $_{HSP}$ 6.2±0.3ms; CMT $_{CONTROLS}$ 5.5±0.3ms).

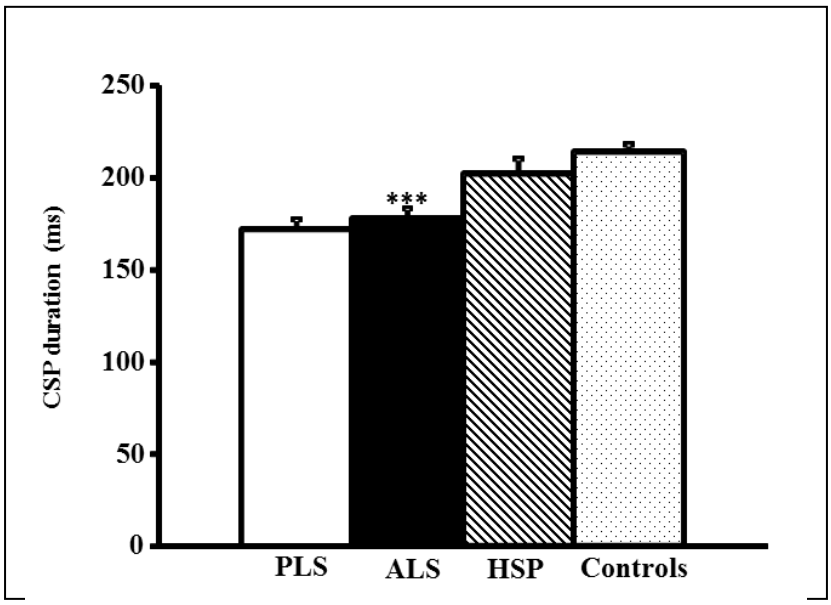

Figure 7.3. The cortical silent period (CSP) duration was significantly reduced in primary lateral sclerosis (PLS) and amyotrophic lateral sclerosis (ALS) patients when compared to hereditary spastic paraparesis (HSP) patients and controls.***P< 0.001

Discussion

The findings in the present establish that cortical dysfunction was an intrinsic feature across the ALS and PLS, with motor cortex inexcitability predominant in the PLS phenotype. In contrast, cortical hyperexcitability was the predominant feature in the ALS phenotype, heralded by a marked reduction in short interval intracortical inhibition and CSP duration along with an increase in intracortical facilitation. By comparison, cortical excitability was preserved in hereditary spastic paraplegia, despite a comparable degree of clinical upper motor neuron dysfunction. These findings suggest that cortical dysfunction appears to be an important pathophysiological process across the MND phenotypes, with the PLS and ALS phenotypes forming a pathophysiological continuum. In addition, the findings in the present study underscore the potential utility of the threshold tracking TMS technique in differentiating PLS from the potential mimic disorder HSP.

Pathophysiological processes underlying the MND phenotypes

Neuropathological studies in PLS have reported marked neuronal degeneration in the primary motor cortex, prefrontal cortex and corticospinal tracts (70, 565). Ubiquitin-positive and hyaline inclusions have also been observed in the frontal cortex and anterior horn cells, although the motor neuron population in the spinal cord and hypoglossal nucleus appear relatively preserved. Similar neuropathological abnormalities have been documented in ALS, characterized by degeneration of inhibitory cortical neurons (188), although the extent of neuronal degeneration, particularly Betz cell loss, seems less prominent (70, 565). Separately, neuroimaging studies have established cortical abnormalities in both ALS and PLS phenotypes, characterized by cortical atrophy along with reduction in the N-acetylaspartate/creatinine ratio, fluorodeoxyglucose and [(11) C]-flumazenil binding and cerebral blood flow underscoring the neuropathological findings (70, 569, 570).

The TMS abnormalities evident in the PLS and ALS phenotypes most likely relate to the underlying pathology of the corticomotoneuronal system, although the extent and nature of the dysfunction seems to be different between the phenotypes. Importantly, the frequency of motor cortex inexcitability was significantly greater in the PLS phenotype. Given that resting motor threshold may reflect the density of corticomotoneuronal projections onto spinal motor neurons as well as excitability of large motor cortical neurons (Betz cells) (39), the findings in the present study may reflect a greater degree of neurodegeneration within the motor cortex (Betz cells) and corticospinal tracts in the PLS phenotype.

In contrast, cortical hyperexcitability was the predominant TMS feature in the ALS phenotype and was characterized by marked reduction of SICI and CSP duration along with an increase in ICF. While features of cortical hyperexcitability were also evident in PLS, their frequency was less when compared to the ALS cohort, being evident in 28% of PLS subjects. Given that the TMS parameters are modulated by GABAergic inhibitory cortical circuits located within the motor cortex and glutamatergic activity (39, 396), the findings in the present study suggests that glutamate excitoxicity and cortical disinhibition form the pathophysiological basis in the ALS phenotype. A similar pathophysiological process was also evident in a proportion of PLS patients, thereby suggesting that the ALS and PLS phenotypes represent a pathophysiological continuum. While the finding of increased resting motor threshold in the PLS phenotype could potentially argue against the notion of a pathophysiological continuum, this finding could be accounted for by a greater degree of corticomotoneuronal degeneration in the PLS phenotype, a notion supported by previous TMS studies [28-30].

Importantly, the TMS differences between ALS and PLS, may in part account for the discordant rate of neurodegeneration of spinal and bulbar motor neurons. Motor neuronal degeneration in ALS was postulated to be mediated via an anterograde glutamate mediated excitotoxic process (24). Given that cortical hyperexcitability was not a prominent feature in the current PLS cohort, the relative sparing of spinal and bulbar motor neurons in PLS may argue against the existence of significant glutamate excitotoxicity. Alternatively, it could also be argued that motor neurons in PLS patients may be less susceptible to the toxic effects of glutamate. Specifically, a number of molecular features may render motor neurons more vulnerable to glutamate toxicity, including expression of glutamate receptors that are more permeable to influx of Ca^{2+} ions (197, 198, 200, 201), a reduced capacity to buffer intracellular Ca^{2+} (203), and an inability to regulate intracellular calcium (204). As such, the motor neurons in PLS patients may lack these harmful factors or alternatively may have evolved specific defence processes against the deleterious effects of glutamate excitoxicity, although this notion remains speculative and needs to be further verified in future studies.

In contrast to findings in the PLS and ALS phenotypes, cortical function remained preserved in HSP despite a comparable degree of clinical UMN dysfunction. These discordant findings likely reflect differences in the underlying neuropathology, whereby a length dependent dying-back axonopathy of the corticospinal tracts seems to predominate in HSP (571). While more extensive neuropathological abnormalities have been reported in complicated forms of HSP, including thinning of the corpus callosum, degeneration within the thalamus, cerebral white matter, substantia nigra, motor cortex and the cerebellum (572, 573), the neuroanatomy of the motor cortex and corticomotoneuronal system seems to be preserved in the pure UMN phenotype of *spastin* related HSP (574). Importantly, findings from the present study suggest

that HSP is a unique disease entity that involves the upper motor neurons, with a spinal predominant pathophysiological process.

Diagnostic utility of threshold tracing TMS in differentiating the clinical phenotype

In addition to providing pathophysiological insights, the present study has established potential utility of the threshold tracking TMS technique in differentiating PLS from HSP. Specific clinical features, including age of onset, mild sensory symptoms, urinary urgency and bulbar dysfunction have been proposed as diagnostic aids in differentiating PLS and HSP (66, 70, 575). A substantial clinical overlap, however, has been reported between the PLS and HSP phenotypes, limiting the diagnostic utility of these clinical features (78, 576). In addition, a family history of HSP has also been proposed as a potential diagnostic aid, although apparently sporadic forms of HSP have been reported (577). The present study has established marked differences in cortical excitability between PLS and HSP, with absence of overlap in TMS abnormalities, thereby underscoring the utility of the threshold tracking TMS technique as a diagnostic aid in differentiating PLS from HSP in a clinical setting.

Chapter 8

CORTICAL CONTRIBUTIONS TO THE FLAIL LEG SYNDROME: PATHOPHYSIOLOGICAL INSIGHTS

Summary

Having established that cortical hyperexcitability reliably underscores upper motor neuron dysfunction across the MND/ALS phenotypes, we wanted to explore whether cortical hyperexcitability formed the pathophysiological basis for the flail leg syndrome (FL), an atypical ALS variant, with predominant lower motor neuron findings. Cortical excitability studies were undertaken on 18 FL patents, using the threshold tracking transcranial magnetic stimulation (TMS) technique, and results were compared to healthy controls, upper and lower limb-onset ALS as well as bulbar-onset and the flail arm variant ALS. Cortical hyperexcitability was a feature of FL and was heralded by a significant reduction of short interval intracortical inhibition (FL 7.2±1.8%; controls 13.2±0.8%, $P<0.01$) and cortical silent period (CSP) duration (FL 181.7±10.8ms; controls 209.8±3.4ms; $P<0.05$) along with an increase in motor evoked potential amplitude (FL 29.2±5.1%; controls 18.9±1.2%, $P < 0.05$). The degree of cortical hyperexcitability was comparable between FL and other ALS phenotypes, defined by site of disease onset. In addition, the CSP duration correlated with biomarkers of peripheral neurodegeneration in FL. Cortical hyperexcitability is a feature of the flail leg syndrome, being comparable to other ALS phenotypes. Importantly, cortical hyperexcitability correlates with neurodegeneration, and as such may contribute to the underlying pathophysiology in FL.

Introduction

The flail leg (FL) syndrome, also referred to as leg amyotrophic diplegia (84) or pseudopolyneuritic variant of amyotrophic lateral sclerosis (ALS), is considered to be an atypical variant of ALS, first described in the early 20th century . Clinically, the FL syndrome is characterised by a predominant lower motor neuron phenotype with absent or subtle upper motor neuron (UMN) signs, with disease remaining confirmed to the lower limbs for a prolonged period (84, 87, 88). The median survival for the FL phenotype has been reported to be 90 months (84, 88), suggesting a more favourable prognosis when compared to the typical ALS phenotype. Importantly, there appears to be a heterogeneity of the FL phenotype, with some studies reporting a greater degree of UMN dysfunction and shorter survival, approximating the disease course to more classical ALS (89). While it has been suggested that the clinical heterogeneity is best explained by differences in definition of the FL phenotype, with inadvertent inclusion of classical ALS phenotypes (84), the underlying pathophysiological mechanisms remain to be clarified.

The pathophysiological processes underlying the various ALS phenotypes appear to be multifactorial, with a complex interaction of molecular and genetic mechanisms (47, 48). Cortical hyperexcitability has been established as an intrinsic process in sporadic and familial forms of ALS, occurring at the early stages of the disease and linked to peripheral neurodegeneration (183, 185, 510). In addition, cortical hyperexcitability has been identified even in atypical ALS phenotypes, including the flail arm variant ALS (FA), where there is a general paucity of upper motor neuronal features on clinical examination (240, 578). Specifically, despite the absence of UMN signs, cortical hyperexcitability appeared to be a

uniform finding in FA and was comparable to the classical ALS phenotype. Given the similarities in the natural history between FL and FA, and that LMN dysfunction predominates in both phenotypes (88, 240, 579), it would seem plausible that cortical dysfunction may also contribute to development of the flail leg syndrome, perhaps forming the pathophysiological basis of the clinical heterogeneity evident in FL.

Cortical excitability can be assessed non-invasively by utilising threshold tracking transcranial magnetic stimulation (TMS) techniques (329). Single pulse TMS studies have reported prolongation of central motor conduction time in FL (580), which was commensurate with findings in classical ALS phenotypes, thereby suggesting the presence of subclinical UMN dysfunction, a finding underscored by pathological studies documenting degeneration of the corticospinal tracts (581, 582). The issue, however, of whether cortical hyperexcitability was evident in FL syndrome, and whether it was a uniform finding across the FL phenotype remains to be elucidated. Consequently, the present study has attempted to better define the phenotype of flail limb presentations. In addition, cortical excitability has been assessed in the FL phenotype, in order to determine whether differences in cortical hyperexcitability were evident in the FL syndrome.

Methods

This prospective study recruited patients with the FL phenotype, which was defined according to the following criteria: (i) lower motor neuron disorder of the lower limbs that is characterised by progressive distal onset wasting and weakness; (ii) confined to lower limbs for at least 12 months; (iii) brisk tendon reflexes or pathological reflexes, such as the extensor plantar response

or Hoffman sign, could be present in patients with the flail leg pattern of muscle wasting and weakness as outlined in point 1; (iv) absence of hypertonia or clonus (88). The clinical and neurophysiological findings in the flail leg syndrome ALS patients were compared with other ALS subgroups, including 23 lower limb-onset and 43 upper limb-onset ALS patients, as well as 8 the flail arm variant ALS (240), and 48 bulbar-onset ALS patients. The Awaji diagnostic criteria was applied in the flail leg syndrome and typical ALS patients (6). Specifically, needle EMG testing was undertaken in all ALS patients in at least three regions (upper limb, lower limb, bulbar or thoracic) and lower motor neuron dysfunction was defined according to the Awaji criteria (6), including the presence of chronic neurogenic changes together with fibrillation potentials/positive sharp waves or fasciculations. EMG abnormalities had to be evident in at least 2 muscles innervated by different nerves and nerve roots in the spinal region, or one muscle in the bulbar/thoracic region. The assessment of upper motor neuron dysfunction remained clinically based. All patients provided written informed consent to the procedures approved by the Western Sydney Local Health District and South East Sydney Area Health Service Human Research Ethics Committees.

At assessment, all patients underwent conventional neurophysiological testing to exclude mimic disorders according to established techniques (514). Demographic data was collected from all patients and included age, gender, handedness, disease duration (months), region of onset, use of Riluzole. Patients were also clinically staged using the revised amyotrophic lateral sclerosis functional rating scale (ALSFRS-R) (495) and the Medical Research Council (MRC) score for assessing muscle strength from the following muscle groups bilaterally: shoulder abduction, elbow flexion and extension, wrist dorsiflexion, finger abduction and thumb abduction, hip

flexion, knee extension and ankle dorsiflexion, yielding a total score of 90. Upper motor neuron (UMN) function was assessed by a dedicated UMN score(497), which ranged from 0 (no UMN signs) to 16 (widespread UMN signs).

Cortical function was assessed by applying a 90 mm circular coil (Magstim, UK) to the vertex of the cranium, with the ensuing motor evoked potential (MEP) responses recorded over the right abductor pollicis brevis (APB) muscle, according to a previously reported technique (329). A threshold tracking paradigm was utilised, whereby a target MEP response of 0.2 mV (±20%) was tracked (329). Resting motor threshold (RMT) was defined as the stimulus intensity required to generate and maintain the target MEP response. **A *paired-pulse threshold tracking*** paradigm**,** with subthreshold condition stimulus set to 70% RMT, was utilised to determine the short interval intracortical inhibition (SICI) and intracortical facilitation (ICF) as previously described (329). ***Single pulse TMS*** was utilized to determine the maximal MEP amplitude (mV), cortical silent period (CSP) duration (ms) and central motor conduction time (CMCT), with details of the technique described previously (329).

Formal assessment of the lower motor neuronal system was also undertaken in the same sitting. compound muscle action potential (CMAP) was recorded over the APB, first dorsal interosseous and the abductor digit minimi muscles according to previously established techniques (13). The resultant baseline-peak CMAP amplitude (mV), onset latency (ms), minimum F-wave latency and F-wave frequency were measured.

Recordings of the CMAP and MEP responses were amplified and filtered (3Hz-3 kHz) using a Nicolet-Biomedical EA-2 amplifier (Viking Select version 11.1.0, Natus, Madison, USA) and sampled at 10 kHz using a 16-bit data acquisition card (National Instruments PCI-MIO-16E-4). Data acquisition and stimulation delivery were controlled by QTRACS software (version 16/02/2009, © Professor Hugh Bostock, Institute of Neurology, Queen Square, London, UK).

Statistical analysis

Cortical excitability results were compared to 60 healthy controls (mean age 50.8±1.3 years, 33 males, 27 females, range 28-73 years). All data were tested for normality using the Shapiro-Wilk test prior to analysis. Analysis of variance (ANOVA) with Bonferroni post hoc analysis was used for multiple comparisons between normally distributed variables while the Kruskal-Wallis test was used for variables without normal distribution. Student t-test or Mann-Whitney U test was used for comparisons between groups. A probability (P) value of <0.05 was considered statistically significant. Results were expressed as mean ± standard error of the mean (SEM) or median (interquartile range).

Results

Clinical features

From a cohort of 140 consecutive ALS patients, studied over a four year period until June 2015, 18 FL syndrome patients were identified comprising 12.9% of the total ALS cohort (Table 8.1).

	FL	ALS_{LL}	ALS_{UL}	FA	Bulbar
NUMBER (%TOTAL)	18(12.4)	27(18.6)	44(30.3)	8(5.5)	48(33.1)
AGE(YEARS) SEM	64 1.9	57.5 2.2	56.1 2.1	60.1 3.1	62.6 1.7
GENDER(M:F)	8:10	17:10	27:20	5:3	27:21
Disease Duration at TMS testing [months(IQR)]	17.5 (10.5-24)	11 (6-20)	9 (6-15)	12.5 (8.8-33)	12 (8-19)
Disease Duration at census date [months (IQR)]	38 (24-53)	29 (19-41)	26 (18-32.8)	52 (23-69)	31 (19-42)
ALSFRS-R (maximum 48)	41.5 (4.-44)	40 (35.3-42.8)	43 (39-46)	44.5 (42-46.3)	42 (37.3-44)
MRC LL (maximum 30) P value	22.5 (17-25.5) (<0.001)	25 (20.3-27.8)	30 (28-30)	30 (30-30)	30 (30-30)
MRC UL (maximum 60) P value	60 (58-60) (<0.001)	53.5 (47.3-60)	52 (47-56)	42 (31.3-49.3)	58 (56-60)
MRC APB (maximum 5) P value	5 (5-5) (<0.05)	4 (4-5)	4 (4-5)	4.5 (3.8-5)	5 (4-5)
MRC SUM (maximum 90)	80.5 (76.8-83.8)	79 (70.3-82.8)	81 (75-85.3)	72 (61.3-79.3)	89 (84-90)
UMN SCORE (maximum 16) P Value	9 (1.3-12) (<0.01)	11 (8.8-12)	12 (10-12)	5.5 (0-10.5)	12 (8.3-14)

Table 8.1. Demographic characteristics of 18 patients with flail leg (FL) syndrome is summarised and compared with four other amyotrophic lateral sclerosis (ALS) phenotypes including lower limb onset ALS (ALS_{LL}), upper limb onset ALS(ALS_{LL}), flail arm variant ALS (FA) and bulbar onset classic ALS (Bulbar). Significant differences in characteristics between ALS_{FL} and other phenotypes are explained below. The degree of functional disability, as indicated by the amyotrophic lateral sclerosis functional rating scale-revised (ALSFRS-R) was comparable between different ALS phenotypes. Lower limb muscle strength, as measured by the Medical Research Council (MRC) score was significantly lower in FL patients when compared to upper limb onset, bulbar onset and flail arm variant ALS phenotypes ($P < 0.001$), but comparable to lower limb onset ALS. Upper limb strength, as measured by the MRC score (MRC UL) was significantly higher in FL when compared to flail arm variant, upper and lower limb onset ALS phenotypes but not bulbar onset ALS ($P < 0.001$). The abductor pollicis brevis (APB) strength was significantly higher in FL and bulbar onset ALS phenotypes when compared to the other three ALS phenotypes ($P < 0.05$).The upper motor neuron (UMN) score significantly lower in FL patients when compared to bulbar and upper limb onset ALS ($P< 0.01$), but comparable to lower limb onset ALS and flail arm variant ALS.

The flail limb phenotype was characterised by progressive distal onset weakness and wasting of the lower limbs in all patients, which was confined to the lower limbs for at least 12 months (Table 8.1). UMN signs became evident in 78% while absent UMN signs were noted in 22% of flail leg syndrome patients. Importantly, the median UMN score was significantly lower in flail leg syndrome patients when compared to bulbar and upper limb onset ALS ($\chi^2 = 19.2$, df 4, $P < 0.01$, Table 8.1), and none of the flail leg syndrome patients exhibited pathological reflexes, spasticity or clonus. At the time of assessment, 9 (50%) flail leg syndrome patients were classified as Awaji "possible", and 3 (17%) as Awaji probable. Six (33%) patients did not exhibit upper motor neuron signs and were best categorised as a progressive muscular atrophy phenotype.

Evidence of disease spread to other regions was documented in 56% (N=10) of flail leg syndrome patients at a median time of 29.5 (25.3-38.3) months after symptom onset. The next

region of spread included bilateral upper limbs in 4 patients, right upper limb in 3, left upper limb in 2 and respiratory system in one patient. Importantly, UMN signs were significantly less prominent in flail leg syndrome patients that remained localised to the lower limbs ($UMN_{Localised}$ 1.5 [0-10]; UMN_{Spread} 11 [8.3-13], $P < 0.05$). The median survival during the follow-up period (June 30 2015) was significantly longer in the flail leg syndrome cohort when compared to the other ALS phenotypes ($\chi^2 = 24.9$, $P < 0.001$, Table 8.1). Importantly, 5 (28%) flail leg syndrome patients died during the study period, with median survival being 39 (22-44) months. Importantly, UMN signs were significantly more prevalent in the flail leg syndrome patients that died (UMN_{DEAD} 12 [10-12.5]; UMN_{ALIVE} 2 [0-10.5], $Z=-2.1$, $P < 0.05$).

The degree of functional disability, as assessed by the ALSFRS-R score, was similar between flail leg syndrome patients and other ALS phenotypes ($\chi^2 = 8.4$, df 4, $P = 0.08$, Table 8.1). As expected, the degree of lower limb muscle strength was significantly lower in flail leg syndrome patients when compared to upper limb onset, bulbar onset and flail arm variant ALS phenotypes, but comparable to lower limb onset ALS ($\chi^2 = 67.7$, df 4, $P < 0.001$, Table 8.1). In contrast, upper limb strength was relatively preserved in flail leg syndrome patients, with the MRC upper limb scores being significantly higher in flail leg syndrome when compared to flail arm variant, upper and lower limb onset ALS phenotypes ($\chi^2 = 41.7$, df 4, $P < 0.001$, Table 8.1), but was comparable to bulbar onset ALS (Table 8.1). In keeping with higher upper limb MRC scores, the APB strength was significantly higher in flail leg syndrome and bulbar onset ALS phenotypes when compared to the other three ALS phenotypes ($\chi^2 = 11.8$, df 4, $P < 0.05$, Table 8.1).

Diagnostic studies: Magnetic resonance imaging studies of the brain and spinal cord were normal in all patients as were the following laboratory investigations: basic biochemistry, haematology, vasculitic screen (anti-nuclear antibody, extractable nuclear antibody, anti-neutrophil cytoplasmic antibody and angiotensin converting enzyme), immunoelectrophoeresis, anti-ganglioside antibodies (GM1, GQ1b), Kennedys disease genetic testing (male patients only), thyroid function studies, paraneoplastic screen, infective (human immunodeficiency virus, hepatitis-B, hepatitis C and syphilis) and coeliac disease serology. Cerebrospinal fluid (CSF) analysis was undertaken in 5 flail leg syndrome patients and did not reveal any abnormality. Nerve conduction studies (NCS) excluded conduction block and other features of nerve demyelination in all patients. The tibial and common peroneal nerve motor CMAP responses were reduced in all patients, while median and ulnar nerve motor NCS were normal. Sensory responses were normal throughout.

The CMAP amplitude from the target APB muscle in flail leg syndrome patients was 8.0±0.8mV and was comparable to healthy controls (10.4±0.4mV, P=0.13). In contrast, the CMAP amplitude from APB muscles, was significantly reduced in other ALS phenotypes when compared to healthy controls (Table 8.2).

	FL	ALS_{LL}	ALS_{UL}	FA	Bulbar	Control
Mean CMAP*	8.0	7.0	6.6	5.0	6.8	10.4
(SEM)	0.8	1.1	0.5	0.8	0.5	0.4
P value		(<0.01)	(<0.01)	(<0.01)	(<0.01)	
Mean SICI (%)	7.2	3.6	2.4	1.6	1.9	13.2
(SEM)	1.8	1.3	1.4	3.1	1.3	0.8
P value	(<0.01)					
CSP duration	181.7	189.0	186.5	182.5	180.5	209.8
(ms) (SEM)	10.8	8.8	7.5	9.8	6.8	3.4
P Value	(<0.05)					
MEP Amplitude	29.2	36.8	29.8	34.4	36.1	18.9
(SEM)	5.1	3.2	3.5	5.4	3.7	1.2
P Value	(<0.05)					
CMCT (ms)	6.7	6.5	6.6	6.4	6.7	5.6
(SEM)	0.5	0.4	0.3	0.4	0.3	0.2
P value	(<0.001)					
RMT (%)	59.3	54.8	56.0	60.1	57.7	58.9
(SEM)	2.0	2.2	1.3	3.1	1.5	1.0

Table 8.2. The neurophysiological findings in the flail leg (FL) syndrome and other amyotrophic lateral sclerosis (ALS) phenotypes. The mean compound muscle action potential amplitude (CMAP*, mV) was significantly reduced in other ALS phenotypes, including lower limb onset (ALS_{LL}), upper limb onset (ALS_{UL}) and flail arm variant ALS (FA), but not the FL syndrome when compared to healthy controls. Mean short interval intracortical inhibition (SICI) and cortical silent period (CSP) duration were significantly reduced in FL when compared to controls, but were comparable to other ALS phenotypes. The motor evoked potential (MEP) amplitude, expressed as percentage of the corresponding CMAP amplitude, was significantly increased in FL when compared to healthy controls but comparable to other ALS phenotypes. Central motor conduction time (CMCT) was prolonged in FL when compared to healthy controls, but comparable to other ALS phenotypes. Resting motor threshold (RMT) was similar across all groups. Data is expressed as mean ± standard error of mean (SEM).

Cortical Function

At the time of cortical excitability testing, the median disease duration in flail leg syndrome patients was 17.5 (10.5-24) months and was longer when compared to other ALS phenotypes, although this was not significantly different (P =0.18, Table 8.1). The motor cortex was inexcitable in one flail leg syndrome patient (6%) and consequently, cortical excitability studies were undertaken in 17 flail leg syndrome patients.

Short interval intracortical inhibition was significantly reduced in flail leg syndrome patients when compared to healthy controls (FL 7.2±1.8%; controls 13.2 ± 0.8%, P<0.01, Figure 8.1A). Importantly, although SICI was higher in flail leg syndrome when compared to other ALS phenotypes, this difference was not significant (P=0.30, Figure 8.1B, Table 8.2). Subgroup analysis disclosed a significant reduction of SICI in flail leg syndrome patients with evident UMN signs compared to those without UMN signs ($SICI_{UMN>1}$ 6.0±2.0%; $SICI_{UMN=0}$ 10.9±0.8%, P<0.05, Figure 8.2A). In addition, SICI was lower in flail leg syndrome patients that died during the follow up period ($SICI_{DIED}$ 3.3±3.2%; $SICI_{ALIVE}$ 8.5±2.2%, P<0.05 Figure 8.2B). There was no significant difference in ICF between flail leg syndrome patients and healthy controls (F=1.4, df 5, P=0.21, Figure 8.1A, Table 8.2).

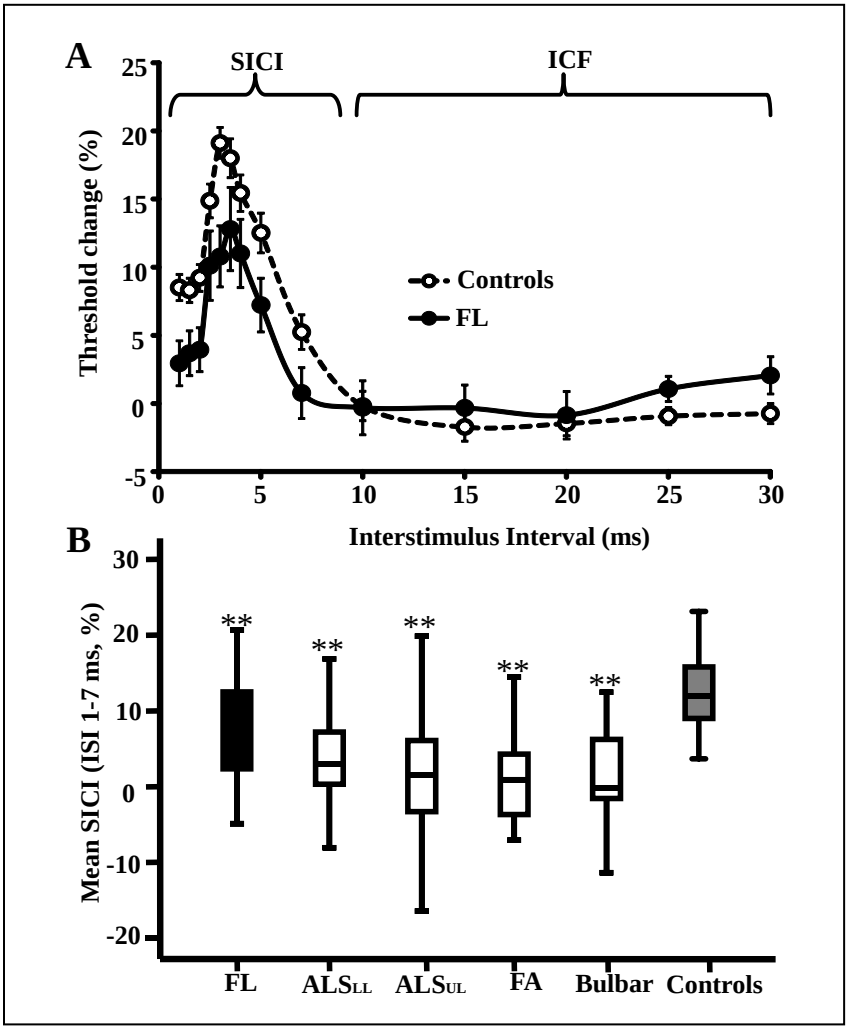

Figure 8.1. (A) Short interval intracortical inhibition (SICI) was significantly reduced in the flail leg (FL) syndrome when compared to controls. There was no significant difference in intracortical facilitation (ICF) between groups. **(B)** Mean short interval intracortical inhibition (SICI), between interstimulus interval 1-7 ms, was significantly reduced in flail leg (FL) syndrome when compared to healthy controls, but was comparable to other amyotrophic lateral sclerosis (ALS) phenotypes including lower limb onset (AL_{LL}), upper limb onset (AL_{UL}), flail arm variant ALS (FA) and bulbar onset ALS.

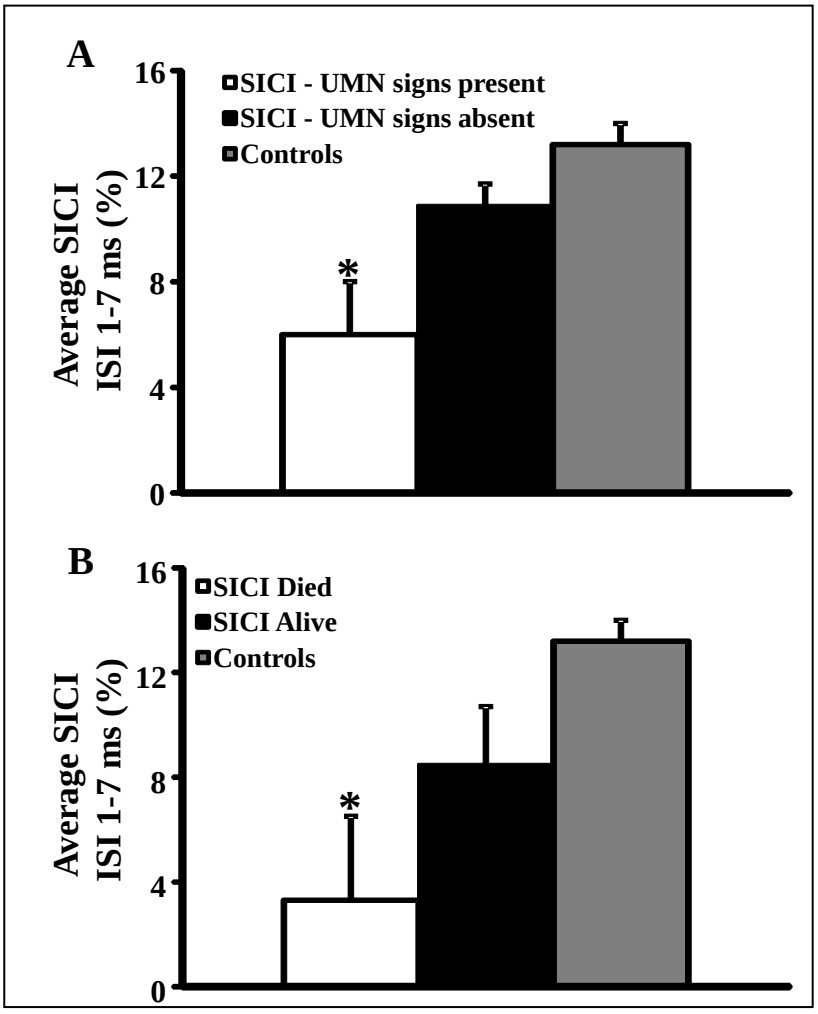

Figure 8.2. Short interval intracortical inhibition (SICI), between interstimulus interval (ISI) 1-7 ms was significantly reduced in flail leg syndrome (FL) patients with **(A)** prominent upper motor neuron (UMN) signs and **(B)** in patients that had died during the follow up period. *P < 0.05.

Single pulse TMS disclosed a significant reduction of the cortical silent period (CSP) duration in flail leg syndrome patients when compared to healthy controls (FL 181.7±10.8ms; controls 209.8±3.4ms; $P<0.05$, Figure 8.3A). Importantly, the reduction in CSP duration was only evident in flail leg patients with UMN signs ($FL_{UMN=0}$ 206.5 ±13.9 ms; $FL_{UMN>1}$ 161 ±10.0 ms, $F=13.6$, $P < 0.001$, Fig 8.3B). In contrast, there was no significant difference in CSP duration between flail leg syndrome patients and other ALS phenotypes ($F=0.11$, df 4, $P=0.98$, Figure 8.3A, Table 8.2). The CSP duration was significantly correlated with the CMAP amplitude ($R=0.42$, $P < 0.05$), suggesting that a reduction in CSP duration, and thereby cortical hyperexcitability, was linked with the process of neurodegeneration.

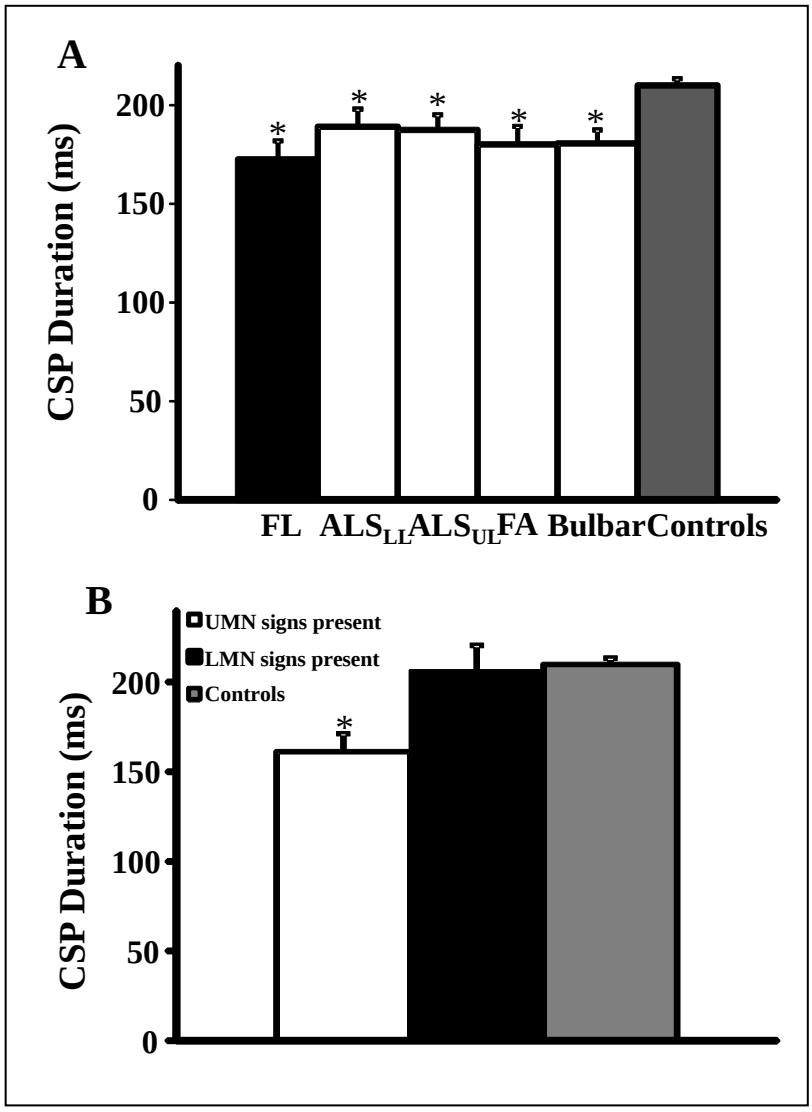

Figure 8.3. (A) The cortical silent period (CSP) duration was significantly reduced in in flail leg (FL) syndrome when compared to healthy controls, but was comparable to other amyotrophic lateral sclerosis (ALS) phenotypes including lower limb onset (AL_{LL}), upper limb onset (AL_{UL}), flail arm variant ALS (FA) and bulbar onset ALS. (B) The CSP duration was significantly reduced in FL patients with upper motor neuron (UMN) signs. *P<0.05.

Of further relevance, the MEP amplitude was significantly increased in flail leg syndrome patients when compared to healthy controls (FL 29.2 ± 5.1%; controls 18.9 ± 1.2%, $P < 0.05$, Figure 8.4A), but similar to other ALS phenotypes ($F=1.3$, df 4, $P=0.26$, Figure 8.4B, Table 8.2). Interestingly, the MEP amplitude significantly correlated with the UMN score (Rho = 0.47, $P < 0.05$, Fig 8.3B). As previously reported (583), the central motor conduction time was significantly longer in flail leg syndrome patients when compared to healthy controls (FL 6.7±0.5 ms; controls 5.6 ± 0.2 ms, $P<0.05$), but comparable to other ALS phenotypes ($P=0.98$, Table 8.2). The CMCT was comparable in flail leg syndrome patients with and without UMN sign ($P=0.24$). In contrast, there was no significant differences in the resting motor threshold between FL patients and other ALS phenotypes or healthy controls ($P=0.44$, Table 8.2).

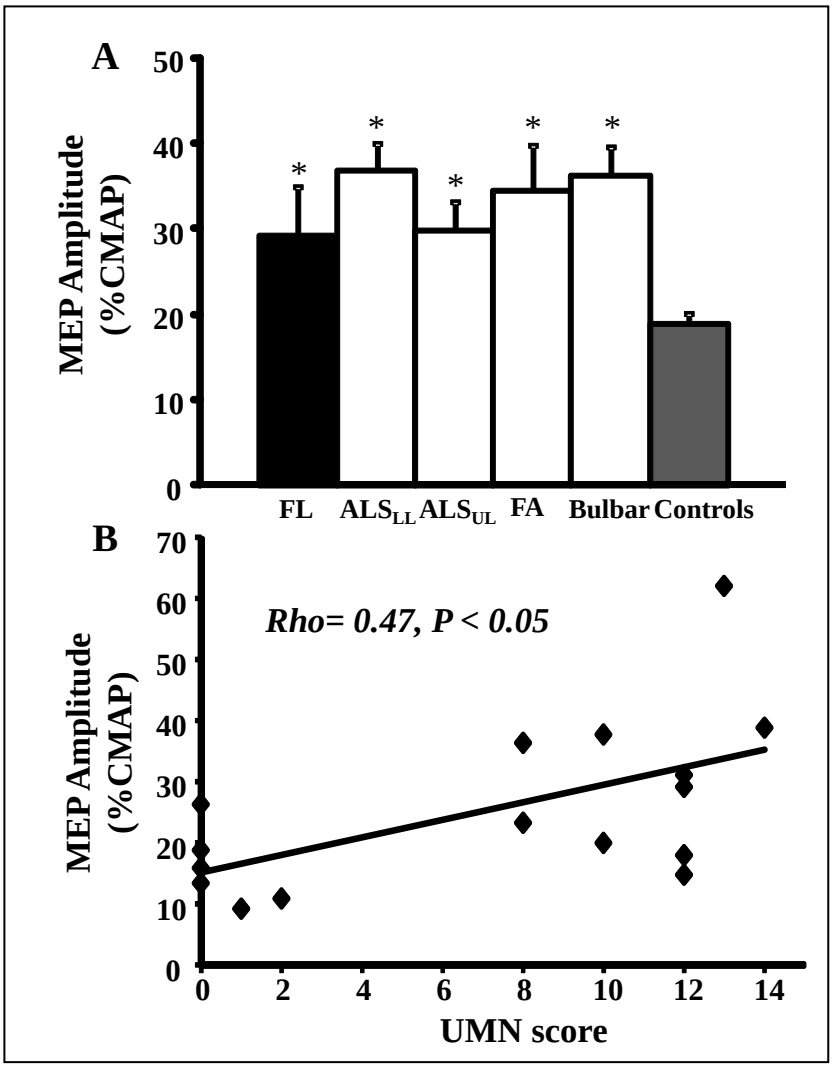

Figure 8.4. (A) The motor evoked potential amplitude (MEP) was significantly increased in FL syndrome when compared to healthy controls, but was comparable to other ALS phenotypes including AL_{LL}, AL_{UL}, FA and bulbar onset ALS. (B) The MEP amplitude was significantly correlated with the upper motor neuron (UMN) score. *P < 0.05.

Discussion

The findings in the present study suggest that the flail leg syndrome is a heterogeneous phenotype, characterised by the core clinical features of regional restriction of muscle wasting and weakness, and relatively prolonged survival. Importantly, the degree of upper motor neuronal abnormalities varied within the flail leg syndrome phenotype, whereby prominent UMN signs were evident in 78% of cases, and the absence of UMN signs was associated with a more favourable prognosis. In addition, cortical hyperexcitability, as heralded by a significant reduction of short interval intracortical inhibition, was only evident in the flail leg syndrome patients exhibiting UMN signs, with the degree of cortical hyperexcitability comparable to other ALS phenotypes. In contrast, cortical excitability appeared to be preserved in flail leg syndrome patients with absent UMN signs, despite a prolonged central motor conduction time in the entire cohort. Taken together, the present findings imply heterogeneity of the clinical phenotype and underlying pathophysiological processes, with cortical dysfunction evident in flail leg syndrome patients exhibiting UMN signs, resembling that seen in the classical ALS phenotypes.

Flail leg phenotype

The definition of the FL syndrome has varied between different studies leading to uncertainties in diagnosis and prognosis (88, 89, 579, 584). Specifically, while some studies have mandated the restriction of disease to the lower limbs for at least 12 months and allowed pathological reflexes to evolve during this period, others have defined the flail leg syndrome as a pure LMN disorder confined to the lower limbs for at least 24 months (84). Consequently, differences in

prognosis have varied between studies, with some reporting prolonged survival (84, 88, 579), while others have documented a shorter survival that was commensurate with typical forms of ALS (89). The differences in survival were attributed to inadvertent recruitment of lower limb onset ALS patients (84). In contrast, others have failed to establish a significant association between the presence of UMN signs and survival in the FL syndrome (88).

In the present study, UMN signs were evident in most flail leg syndrome patients, despite the characteristic phenotype of distal muscle weakness and wasting confined to the lower limbs for at least 12 months. Importantly, the degree of clinical UMN dysfunction appeared to be associated with increased mortality, supporting the importance of UMN dysfunction in FL pathogenesis, and in keeping with previous studies reporting a higher mortality in progressive muscular atrophy phenotypes developing UMN signs (585).

FL syndrome and pathophysiology

Cortical hyperexcitability is an intrinsic process in ALS, including atypical phenotypes such as the flail arm variant (183, 185, 240, 510), and is linked to lower motor neuron degeneration (184, 185, 187). In the present study, cortical hyperexcitability, as heralded by a significant reduction of SICI, was a feature in the flail leg syndrome patients exhibiting UMN signs, and was comparable to other ALS phenotypes. In contrast, the degree of cortical excitability was preserved in flail leg patients exhibiting the clinically pure LMN phenotype. Importantly, the mortality rate in the flail leg cohort exhibiting features of cortical hyperexcitability was significantly higher (Fig. 8.3B), suggesting a heterogeneity of the underlying pathophysiological processes. At a pathophysiological level, TMS features of cortical hyperexcitability appear to be

mediated by degeneration of parvalbumin positive inhibitory cortical interneurons acting via $GABA_A$ receptors (188), as well as glutamate excitoxicity (224, 379), which therefore could form the pathophysiological basis in the flail leg cohort exhibiting UMN signs.

In addition to reduction of SICI, there was a significant reduction in CSP duration along with an increase in the MEP amplitude, which was more prominent in flail leg patients with UMN signs. Given that the CSP duration is mediated by cortical inhibitory circuits distinct to those mediating SICI (369), and the MEP amplitude reflects cortical output (39), the findings provide further support for a pathophysiological importance of cortical hyperexcitability in flail leg patients with UMN signs and underscore the presence of heterogeneity in the flail leg syndrome.

A potential limitation of the present study relates to measurement of cortical excitability from the APB muscle rather than the more affected lower limb muscles. The main reason for assessing cortical excitability form the APB muscle was a technical one, with resting motor thresholds being significantly higher in lower limb muscles and therefore limiting a reliable recording of SICI (39). Future application of threshold tracking TMS to lower limb muscles may be of importance by potentially disclosing that cortical hyperexcitability is a focal finding related to the region of onset.

Separately, spinal cord abnormalities, as heralded by prolonged central motor conduction time, were a uniform finding in the flail leg syndrome, and were in keeping with previous TMS studies documenting prolonged CMCT despite an absence of pyramidal signs (583). Given that CMCT reflects conduction along the corticospinal tracts (39), the present findings would imply a

dysfunction of the pyramidal tracts, perhaps reflecting the pathological findings of extensive degeneration of myelinated fibers in the lateral corticospinal tracts (586). Consequently, the combination of cortical hyperexcitability along with prolonged CMCT could reflect a more extensive pathophysiological process in the flail leg syndrome phenotypes exhibiting UMN signs. Identifying factors that govern the differences in the pathophysiological processes across the flail leg phenotype could be of therapeutic significance, with strategies aimed at modulating these putative factors resulting in restricted disease and prolonged survival.

SUMMARY

AND

CONCLUSIONS

This thesis encompasses work undertaken to improve on the current diagnostic criteria in amyotrophic lateral sclerosis (ALS), whilst also utilising a novel transcranial magnetic stimulation (TMS) technique to gain insights into cortical dysfunction, and thereby understand pathophysiological mechanism underlying ALS. In ***chapter 1*** an individual patient data (IPD) analysis was undertaken on the currently published diagnostic studies in ALS, looking at the Awaji and revised El Escorial criteria (EEC). The IPD analysis revealed the Awaji criteria to be more sensitive than the EEC. We proposed a new 'laboratory supported Awaji criteria', which was more sensitive than the existing Awaji criteria. In our analysis of the published studies to date, all the studies were single center by design, with some retrospective in nature. Furthermore in the published studies there was a lack of specificity data, confounding the interpretation of the findings from the primary studies.

Therefore in ***chapter 2*** we designed the first prospective multicenter study to further evaluate the two diagnostic criteria. Our study revealed that both diagnostic criteria were highly specific (99.5%), with the Awaji criteria being more sensitive across the bulbar and limb subgroups of ALS. By loosening the current Awaji criteria to 'possible', there was an improvement in the sensitivity of the criteria, without a significant loss of specificity. One of the limitation of both diagnostic criteria, was the lack of an objective biomarker of upper motor neuron (UMN) dysfunction.

We then utilised a novel threshold tracking TMS technique, in ***chapter 3,*** where we identified cortical dysfunction heralded as cortical hyperexcitability, being evident early in the ALS disease

process. Cortical hyperexcitability was a useful biomarker of UMN dysfunction, and when used in combination with the Awaji criteria, there was an improvement in the diagnostic accuracy, with 88% of Awaji possible patients having evidence of cortical dysfunction.

While this study revealed cortical hyperexcitability to be a useful biomarker of cortical dysfunction, the study was not performed according the 'Standards for reporting of diagnostic accuracy' (STARD) criteria, the 'gold standard' for diagnostic tests. Subsequently a multicenter prospective study was undertaken in ***chapter 4***. In this study utilising threshold tracking TMS testing, the averaged short interval intracortical inhibition (SICI) was the most robust diagnostic biomarker when plotted on receiver operating characteristic curves. Furthermore by using biomarkers of cortical dysfunction, it was possible to reliably differentiate ALS from similar mimic disorders.

Having established that cortical hyperexcitability was an early and specific biomarker in ALS, we explored whether the same process of cortical hyperexcitability was evident in the most common familial form of ALS, the c9orf72 gene expansion. In ***chapter 5***, our study revealed that cortical hyperexcitability was uniform across both sporadic and familial ALS. Thereby suggesting that irrespective of the underlying aetiology in ALS, cortical hyperexcitability appears to be a universal finding. Furthermore, whilst affected individuals with familial ALS had evidence of cortical hyperexcitability, asymptomatic carriers had normal cortical functioning, thereby suggesting that the c9orf72 gene expansion may be risk factor in developing ALS, but other triggers may exist that result in the expression of the gene.

Given that cortical dysfunction is similar in familial and sporadic ALS, we then used axonal excitability testing in ***chapter 6***, to explore peripheral nervous system abnormalities. Using mathematical modelling we identified an increase in persistent Na^+ conductances along with reduced K^+ currents to best explain the changes in axonal excitability in familial ALS secondary to the c9orf72 gene expansion. Furthermore, similar to finding normal cortical functioning in asymptomatic carriers in chapter 5, we found that asymptomatic carriers had normal findings on axonal excitability testing.

In ***chapter 7 and 8*** we aimed to evaluate whether cortical hyperexcitability was a universal findings across the ALS phenotypes. In ***chapter 7***, we investigated an UMN predominant form of ALS, primary lateral sclerosis (PLS) and a similar condition which can often mimic PLS, hereditary spastic paraparesis (HSP). We established that PLS patients more often had an inexcitable motor cortex on TMS testing, while patients with ALS had features of cortical hyperexcitability. Conversely in HSP, cortical function was "normal", arguing for the presence of disparate pathophysiological processes and suggesting that TMS can be utilised as a diagnostic biomarker in differentiating PLS from HSP.

In ***chapter 8*** we explored whether cortical hyperexcitability was a feature in the clinically lower motor neuron phenotype of ALS, the flail-leg syndrome. Importantly, cortical hyperexcitability was evident in a subgroup of flail leg syndrome patients, being comparable to sporadic and familial ALS cohorts. Interestingly, cortical excitability was preserved in the flail leg syndrome patients with a pure LMN phenotype. Taken together, these findings suggest heterogeneity of the disease process in ALS, particularly the atypical ALS variants such as the flail leg syndrome.

Understanding the factors that govern these discordant pathophysiological findings could be of therapeutic significance in ALS.

Future Directions

Cortical hyperexcitability appears to be an early and specific biomarker, preceding the development of LMN dysfunction in ALS. Future studies will utilise threshold tracking TMS technique to explore whether the development of cortical hyperexcitability occurs prior to onset of disease in specific body regions, such as cranial and lumbosacral regions. These studies will assist in identifying the pattern of disease spread in ALS, thereby probing whether corticomotoneurons act as a conduit for ALS progression in a non-contiguous manner. The studies will be undertaken on a cohort of sporadic ALS patients in a longitudinal manner, with ongoing review of patients every 6 months. In addition to utilising TMS derived cortical excitability markers, we will also be utilising 'Motor Unit Number Estimation' techniques, to quantitatively evaluate lower motor neuron loss over time.

In addition, further longitudinal studies will be undertaken on c9orf72 gene expansion asymptomatic carriers from chapter 4 and 5, to identify if cortical and peripheral markers of dysfunction can be seen prior to disease conversion in the asymptomatic carrier cohort. Our research group has already identified similar findings in longitudinal studies of SOD-1 mutation carriers, whereby cortical hyperexcitability was an early phenomenon preceding the onset of clinically evident disease.

Of further relevance, the role of corticomotoneurons in ALS pathogenesis will be further investigated by combing threshold tracking TMS techniques with sophisticated MRI neuroimaging. Specifically, cross-sectional and longitudinal studies will be undertaken on sporadic ALS patients and c9orf72 expansion carriers. The corticomotoneuronal function will be assessed by utilising cortical thickness analysis, resting state networks, 'connectomics' and sodium coil imaging in concert with TMS studies, in order to establish the timing and site of disease onset, along with patterns of disease spread. Ultimately, such an approach will shed further light on ALS pathogenesis, with the hope of uncovering novel therapeutic targets.

GLOSSARY OF ABBREVIATIONS

ALS	amyotrophic lateral sclerosis
ALSFRS-R	amyotrophic lateral sclerosis functional rating scale-revised
AMPA	α amino 3 hydroxy 5 methyl 4 isoxazole proprionic acid
ANOVA	analysis of variance
APB	abductor pollicis brevis
ATP	adenosine tri phosphate
CMAP	compound muscle action potential
CMCT	central motor conduction time
CSP	cortical silent period
DAP	depolarizing after depolarization
DNA	deoxyribonucleic acid
EMG	electromyography
FTD	frontotemporal dementia
FUS	fused in sarcoma
GABA	gamma amino butyric acid
ICF	intracortical facilitation
ITPR	inositol 1,4,5-triphosphate receptor
I/V	current threshold relationship
KD	Kennedy's Disease
LA	latent addition
LICI	long interval intracortical inhibition

LMN	lower motor neuron
MEP	motor evoked potential
MMNCB	multifocal motor neuropathy with conduction block
MND	motor neuron disease
MRC	Medical Research Council
MT	motor threshold
MUNE	motor unit number estimation
MUP	motor unit potential
NCS	nerve conduction study
NI	neurophysiological index
NMDA	N-methyl, D-aspartate receptor
PBP	progressive bulbar palsy
PLS	primary lateral sclerosis
PMA	progressive muscular atrophy
PSW	positive sharp waves
RMT	resting motor threshold
RNA	ribonucleic acid
ROC	receiver operating characteristic
RRP	relative refractory period
SDTC	strength duration time constant
SICI	short-interval intracortical inhibition
SMA	spinal muscular atrophy
SOD	superoxide dismutase

SR	stimulus response curve
STARD	standards for reporting of diagnostic accuracy
TARDBP	transactive region deoxyribonucleic acid binding protein
TEd	threshold electrotonus depolarising
TEh	threshold electrotonus hyperpolarising
TMS	transcranial magnetic stimulation
UMN	upper motor neuron

References

1. Charcot J, Joffroy A. Deux cas d'atrophie musculaire progressive avec lesion de la substance grise et des faisceaux antero-lateraux de la moelle epiniere. Arch Physiol Neurol Pathol. 1869;2:744-54.
2. McDermott CJ, Shaw PJ. Diagnosis and management of motor neurone disease. Bmj. 2008;336(7645):658-62.
3. Chancellor AM, Slattery JM, Fraser H, Swingler RJ, Holloway SM, Warlow CP. The prognosis of adult-onset motor neuron disease: a prospective study based on the Scottish Motor Neuron Disease Register. J Neurol. 1993;240(6):339-46.
4. del Aguila MA, Longstreth WT, Jr., McGuire V, Koepsell TD, van Belle G. Prognosis in amyotrophic lateral sclerosis: a population-based study. Neurology. 2003;60(5):813-9.
5. Australian Institute of Health and Welfare http://www.aihw.gov.au/ [cited 2015 09/11/2015].
6. de Carvalho M, Dengler R, Eisen A, England JD, Kaji R, Kimura J, et al. Electrodiagnostic criteria for diagnosis of ALS. Clin Neurophysiol. 2008;119(3):497-503.
7. Logroscino G, Beghi E, Zoccolella S, Palagano R, Fraddosio A, Simone IL, et al. Incidence of amyotrophic lateral sclerosis in southern Italy: a population based study. J Neurol Neurosurg Psychiatry. 2005;76(8):1094-8.
8. Rowland LP. Diagnosis of amyotrophic lateral sclerosis. J Neurol Sci. 1998;160 Suppl 1:S6-24.
9. Talbot K. Motor neurone disease. Postgrad Med J. 2002;78(923):513-9.
10. Rocha JA, Reis C, Simoes F, Fonseca J, Mendes Ribeiro J. Diagnostic investigation and multidisciplinary management in motor neuron disease. J Neurol. 2005;252(12):1435-47.
11. Kuwabara S, Sonoo M, Komori T, Shimizu T, Hirashima F, Inaba A, et al. Dissociated small hand muscle atrophy in amyotrophic lateral sclerosis: frequency, extent, and specificity. Muscle Nerve. 2008;37(4):426-30.
12. Wilbourn AJ. The “split hand syndrome”. Muscle Nerve. 2000;23(1):138.
13. Menon P, Kiernan MC, Yiannikas C, Stroud J, Vucic S. Split-hand index for the diagnosis of amyotrophic lateral sclerosis. Clin Neurophysiol. 2013;124(2):410-6.
14. Menon P, Bae JS, Mioshi E, Kiernan MC, Vucic S. Split-hand plus sign in ALS: Differential involvement of the flexor pollicis longus and intrinsic hand muscles. Amyotroph Lateral Scler. 2012.
15. Gubbay SS, Kahana E, Zilber N, Cooper G, Pintov S, Leibowitz Y. Amyotrophic lateral sclerosis. A study of its presentation and prognosis. J Neurol. 1985;232(5):295-300.
16. Lechtzin N, Rothstein J, Clawson L, Diette GB, Wiener CM. Amyotrophic lateral sclerosis: evaluation and treatment of respiratory impairment. Amyotroph Lateral Scler Other Motor Neuron Disord. 2002;3(1):5-13.
17. Houseman G, Kelley M. Early respiratory insufficiency in the ALS patient: a case study. J Neurosci Nurs. 2005;37(4):216-8.
18. Scelsa SN, Yakubov B, Salzman SH. Dyspnea-fasciculation syndrome: early respiratory failure in ALS with minimal motor signs. Amyotroph Lateral Scler Other Motor Neuron Disord. 2002;3(4):239-43.

19. Czaplinski A, Strobel W, Gobbi C, Steck AJ, Fuhr P, Leppert D. Respiratory failure due to bilateral diaphragm palsy as an early manifestation of ALS. Medical Science Monitor. 2003;9(5):CS34-6.
20. Hanagasi HA, Gurvit IH, Ermutlu N, Kaptanoglu G, Karamursel S, Idrisoglu HA, et al. Cognitive impairment in amyotrophic lateral sclerosis: evidence from neuropsychological investigation and event-related potentials. Brain Res Cogn Brain Res. 2002;14(2):234-44.
21. Abrahams S, Goldstein LH, Simmons A, Brammer M, Williams SC, Giampietro V, et al. Word retrieval in amyotrophic lateral sclerosis: a functional magnetic resonance imaging study. Brain. 2004;127(Pt 7):1507-17.
22. Abrahams S, Leigh P, Goldstein L. Cognitive change in ALS: a prospective study. Neurology. 2005;64:1222 - 6.
23. Ringholz GM, Appel SH, Bradshaw M, Cooke NA, Mosnik DM, Schulz PE. Prevalence and patterns of cognitive impairment in sporadic ALS. Neurology. 2005;65(4):586-90.
24. Eisen A, Kim S, Pant B. Amyotrophic lateral sclerosis (ALS): a phylogenetic disease of the corticomotoneuron? Muscle Nerve. 1992;15:219-24.
25. Kiernan M. Motor neuron disease: a Pandora's box. Med J Aust. 2003;178:311-2.
26. de Carvalho M, Swash M. Nerve conduction studies in amyotrophic lateral sclerosis. Muscle Nerve. 2000;23:344-52.
27. Iijima M, Arasaki K, Iwamoto H, Nakanishi T. Maximal and minimal motor nerve conduction velocities in patients with motor neuron diseases: correlation with age of onset and duration of illness. Muscle Nerve. 1991;14(11):1110-5.
28. Daube JR. Electrodiagnostic studies in amyotrophic lateral sclerosis and other motor neuron disorders. Muscle Nerve. 2000;23(10):1488-502.
29. Eisen A, Swash M. Clinical neurophysiology of ALS. Clin Neurophysiol. 2001;112(12):2190-201.
30. Costa J, Swash M, de Carvalho M. Awaji criteria for the diagnosis of amyotrophic lateral sclerosis:a systematic review. Arch Neurol. 2012;69(11):1410-6.
31. Li TM, Day SJ, Alberman E, Swash M. Differential diagnosis of motoneurone disease from other neurological conditions. Lancet. 1986;2(8509):731-3.
32. Bostock H, Sharief MK, Reid G, Murray NMF. Axonal ion channel dysfunction in amyotrophic lateral sclerosis. Brain. 1995;118(1):217-25.
33. Horn S, Quasthoff S, Grafe P, Bostock H, Renner R, Schrank B. Abnormal axonal inward rectification in diabetic neuropathy. Muscle Nerve. 1996;19(10):1268-75.
34. Mogyoros I, Kiernan M, Burke D, Bostock H. Strength-duration properties of sensory and motor axons in amyotrophic lateral sclerosis. Brain. 1998;121:851-9.
35. Kanai K, Kuwabara S, Misawa S, Tamura N, Ogawara K, Nakata M, et al. Altered axonal excitability properties in amyotrophic lateral sclerosis: impaired potassium channel function related to disease stage. Brain. 2006;129:953-62.
36. Roth G. Fasciculations and their F-response. Localisation of their axonal origin. J Neurol Sci. 1984;63(3):299-306.
37. Miller TM, Layzer RB. Muscle cramps. Muscle Nerve. 2005;32:431-42.
38. Swash M. Why are upper motor neuron signs difficult to elicit in amyotrophic lateral sclerosis? J Neurol Neurosurg Psychiatry. 2012;83(6):659-62.

39. Vucic S, Ziemann U, Eisen A, Hallett M, Kiernan MC. Transcranial magnetic stimulation and amyotrophic lateral sclerosis: pathophysiological insights. J Neurol Neurosurg Psychiatry. 2013;84:1161-70.
40. Eisen A, Shytbel W, Murphy K, Hoirch M. Cortical magnetic stimulation in amyotrophic lateral sclerosis. Muscle Nerve. 1990;13(2):146-51.
41. Caramia MD, Cicinelli P, Paradiso C, Mariorenzi R, Zarola F, Bernardi G, et al. 'Excitability changes of muscular responses to magnetic brain stimulation in patients with central motor disorders. Electroencephalogr Clin Neurophysiol. 1991;81:243-50.
42. Eisen A, Pant B, Stewart H. Cortical excitability in amyotrophic lateral sclerosis: a clue to pathogenesis. Can J Neurol Sci. 1993;20:11-6.
43. Desiato MT, Caramia MD. Towards a neurophysiological marker of amyotrophic lateral sclerosis as revealed by changes in cortical excitability. Electroencephalogr Clin Neurophysiol. 1997;105(1):1-7.
44. Magistris MR, Rosler KM, Truffert A, Myers JP. Transcranial stimulation excites virtually all motor neurons supplying the target muscle. A demonstration and a method improving the study of motor evoked potentials. Brain 1998;121 437-50.
45. Zanette G, Tamburin S, Manganotti P, Refatti N, Forgione A, Rizzuto N. Different mechanisms contribute to motor cortex hyperexcitability in amyotrophic lateral sclerosis. Clin Neurophysiol. 2002;113(11):1688-97.
46. Komissarow L, Rollnik JD, Bogdanova D, Krampfl K, Khabirov FA, Kossev A, et al. Triple stimulation technique (TST) in amyotrophic lateral sclerosis. Clin Neurophysiol. 2004;115(2):356-60.
47. Vucic S, Rothstein JD, Kiernan MC. Advances in treating amyotrophic lateral sclerosis: insights from pathophysiological studies. Trends Neurosci. 2014;37(8):433-42.
48. Kiernan MC, Vucic S, Cheah BC, Turner MR, Eisen A, Hardiman O, et al. Amyotrophic lateral sclerosis. Lancet. 2011;377(9769):942-55.
49. Brooks B, Miller R, Swash M, Munsat T. El Escorial revisited: revised criteria for the diagnosis of amyotrophic lateral sclerosis. Amyotroph Lateral Scler Other Motor Neuron Disord. 2000;1:293 - 9.
50. Brooks B. El Escorial World Federation of Neurology criteria for the diagnosis of amyotrophic lateral sclerosis. Subcommittee on Motor Neuron Diseases/Amyotrophic Lateral Sclerosis of the World Federation of Neurology Research Group on Neuromuscular Diseases and the El Escorial "Clinical limits of amyotrophic lateral sclerosis" workshop contributors. J Neurol Sci. 1994;124(Suppl):96 - 107.
51. Chio A. ISIS Survey: an international study on the diagnostic process and its implications in amyotrophic lateral sclerosis. J Neurol. 1999;246 Suppl 3:1-5.
52. Douglass CP, Kandler RH, Shaw PJ, McDermott CJ. An evaluation of neurophysiological criteria used in the diagnosis of motor neuron disease. J Neurol Neurosurg Psychiatry. 2010;81(6):646-9.
53. de Carvalho M, Swash M. Awaji diagnostic algorithm increases sensitivity of El Escorial criteria for ALS diagnosis. Amyotroph Lateral Scler. 2009;10(1):53-7.
54. Boekestein WA, Kleine BU, Hageman G, Schelhaas HJ, Zwarts MJ. Sensitivity and specificity of the 'Awaji' electrodiagnostic criteria for amyotrophic lateral sclerosis: Retrospective comparison of the Awaji and revised El Escorial criteria for ALS. Amyotroph Lateral Scler. 2010;11:497-501.

55. Schrooten M, Smetcoren C, Robberecht W, Van Damme P. Benefit of the Awaji diagnostic algorithm for amyotrophic lateral sclerosis: A prospective study. Ann Neurol. 2011;70(1):79-83.
56. Okita T, Nodera H, Shibuta Y, Nodera A, Asanuma K, Shimatani Y, et al. Can Awaji ALS criteria provide earlier diagnosis than the revised El Escorial criteria? J Neurol Sci. 2011;302(1–2):29-32.
57. Chen A, Weimer L, Brannagan T, 3rd, Colin M, Andrews J, Mitsumoto H, et al. Experience with the Awaji Island modifications to the ALS diagnostic criteria. Muscle Nerve. 2010;42(5):831-2.
58. Krarup C. Lower motor neuron involvement examined by quantitative electromyography in amyotrophic lateral sclerosis. Clin Neurophysiol. 2011;122(2):414-22.
59. Gawel M, Kuzma-Kozakiewicz M, Szmidt-Salkowska E, Kamińska A. Are we really closer to improving the diagnostic sensitivity in ALS patients with Awaji criteria? Amyotroph Lateral Scler Frontotemporal Degener. 2014;15(3-4):257-61.
60. Higashihara M, Sonoo M, Imafuku I, Fukutake T, Kamakura K, Inoue K, et al. Fasciculation potentials in amyotrophic lateral sclerosis and the diagnostic yield of the Awaji algorithm. Muscle Nerve. 2012;45(2):175-82.
61. Jang J-S, Bae JS. AWAJI criteria are not always superior to the previous criteria: A meta-analysis. Muscle Nerve. 2015;51(6):822-9.
62. de Carvalho M, Costa J, Swash M. Comment on: The Awaji criteria are not always superior to the previous criteria: A meta-analysis. Muscle Nerve. 2015:n/a-n/a.
63. Ludolph A, Drory V, Hardiman O, Nakano I, Ravits J, Robberecht W, et al. A revision of the El Escorial criteria - 2015. Amyotroph Lateral Scler Frontotemporal Degener. 2015:1-2.
64. Erb WH. Uber einen wenig bekannten spinalen Symptomencomplex. Berliner Klinische Wochenschrift. 1875;12:357-9.
65. Charcot JM. Scle'rose des cordons latdraux de la moelle gpiniere chez une femme hysterique, atteinte

de contracture permanente des quatre membres. Bulletin et Mimoires de la Sociili Midicale des Hopitaux de Paris, Second series. 1865;2:24-42.
66. Gordon PH, Cheng B, Katz IB, Pinto M, Hays AP, Mitsumoto H, et al. The natural history of primary lateral sclerosis. Neurology. 2006;66(5):647-53.
67. Tartaglia MC, Rowe A, Findlater K, Orange JB, Grace G, Strong MJ. Differentiation between primary lateral sclerosis and amyotrophic lateral sclerosis: examination of symptoms and signs at disease onset and during follow-up. Archives of Neurology. 2007;64(2):232-6.
68. Tomik B, Zur KA, Szczudlik A. Pure primary lateral sclerosis--Case reports. Clinical Neurology & Neurosurgery. 2008;110(4):387-91.
69. Singer MA, Statland JM, Wolfe GI, Barohn RJ. Primary lateral sclerosis. Muscle & Nerve. 2007;35(3):291-302.
70. Pringle CE, Hudson AJ, Munoz DG, Kiernan JA, Brown WF, Ebers GC. Primary lateral sclerosis. Clinical features, neuropathology and diagnostic criteria. Brain. 1992;115 (Pt 2):495-520.
71. Gastaut JL, Bartolomei F. Mills' syndrome: ascending (or descending) progressive hemiplegia: a hemiplegic form of primary lateral sclerosis? Journal of Neurology, Neurosurgery & Psychiatry. 1994;57(10):1280-1.

72. Gordon PH, Cheng B, Katz IB, Mitsumoto H, Rowland LP. Clinical features that distinguish PLS, upper motor neuron-dominant ALS, and typical ALS. Neurology. 2009;72(22):1948-52.
73. Bäumer D, Butterworth R, Menke RAL, Talbot K, Hofer M, Turner MR. Progressive hemiparesis (Mills syndrome) with aphasia in amyotrophic lateral sclerosis. Neurology. 2014;82(5):457-8.
74. Tartaglia MC, Laluz V, Rowe A, Findlater K, Lee DH, Kennedy K, et al. Brain atrophy in primary lateral sclerosis. Neurology. 2009;72(14):1236-41.
75. Peretti-Viton P, Azulay JP, Trefouret S, Brunel H, Daniel C, Viton JM, et al. MRI of the intracranial corticospinal tracts in amyotrophic and primary lateral sclerosis. Neuroradiology. 1999;41(10):744-9.
76. Kuipers-Upmeijer J, de Jager AEJ, Hew JM, Snoek JW, van Weerden TW. Primary lateral sclerosis: clinical, neurophysiological, and magnetic resonance findings. J Neurol Neurosurg Psychiatry. 2001;71(5):615-20.
77. Ulug AM, Grunewald T, Lin MT, Kamal AK, Filippi CG, Zimmerman RD, et al. Diffusion tensor imaging in the diagnosis of primary lateral sclerosis. Journal of Magnetic Resonance Imaging. 2004;19(1):34-9.
78. Le Forestier N, Maisonobe T, Piquard A, Rivaud S, Crevier-Buchman L, Salachas F, et al. Does primary lateral sclerosis exist? A study of 20 patients and a review of the literature. Brain. 2001;124(Pt 10):1989-99.
79. Konagaya M, Sakai M, Matsuoka Y, Konagaya Y, Hashizume Y. Upper motor neuron predominant degeneration with frontal and temporal lobe atrophy. Acta Neuropathologica. 1998;96(5):532-6.
80. Sugihara H, Horiuchi M, Kamo T, Fujisawa K, Abe M, Sakiyama T, et al. A case of primary lateral sclerosis taking a prolonged clinical course with dementia and having an unusual dendritic ballooning. Neuropathology. 1999;19(1):77-84.
81. Mochizuki A, Komatsuzaki Y, Iwamoto H, Shoji S. Frontotemporal dementia with ubiquitinated neuronal inclusions presenting with primary lateral sclerosis and parkinsonism: clinicopathological report of an autopsy case. Acta Neuropathologica. 2004;107(4):377-80.
82. Tan CF, Kakita A, Piao YS, Kikugawa K, Endo K, Tanaka M, et al. Primary lateral sclerosis: a rare upper-motor-predominant form of amyotrophic lateral sclerosis often accompanied by frontotemporal lobar degeneration with ubiquitinated neuronal inclusions? Report of an autopsy case and a review of the literature. Acta Neuropathologica. 2003;105(6):615-20.
83. Beal MF, Richardson EP, Jr. Primary lateral sclerosis: a case report. Archives of Neurology. 1981;38(10):630-3.
84. Dimachkie MM, Muzyka IM, Katz JS, Jackson C, Wang Y, McVey AL, et al. Leg Amyotrophic Diplegia: Prevalence and Pattern of Weakness at US Neuromuscular Centers. J Clin Neuromusc Dis. 2013;15(1):7-12.
85. Visser J, van den Berg-Vos RM, Franssen H, van den Berg LH, Wokke JH, de Jong JM, et al. Disease course and prognostic factors of progressive muscular atrophy. Arch Neurol. 2007;64(4):522-8.
86. Ince PG, Evans J, Knopp M, Forster G, Hamdalla HH, Wharton SB, et al. Corticospinal tract degeneration in the progressive muscular atrophy variant of ALS. Neurology. 2003;60(8):1252-8.

87. Patrikios JS. Contribution à l'étude des formes cliniques et de l'anatomie pathologique de la sclérose latérale amyotrophique: Faculté de médecine; 1918.
88. Wijesekera LC, Mathers S, Talman P, Galtrey C, Parkinson MH, Ganesalingam J, et al. Natural history and clinical features of the flail arm and flail leg ALS variants. Neurology. 2009;72(12):1087-94.
89. Chio A, Calvo A, Moglia C, Mazzini L, Mora G, group Ps. Phenotypic heterogeneity of amyotrophic lateral sclerosis: a population based study. J Neurol, Neurosurg & Psychiatry. 2011;82(7):740-6.
90. Andersen PM, Al-Chalabi A. Clinical genetics of amyotrophic lateral sclerosis: what do we really know? Nat Rev Neurol. 2011;7(11):603-15.
91. Gros-Louis F, Gaspar C, Rouleau GA. Genetics of familial and sporadic amyotrophic lateral sclerosis. Biochim Biophys Acta. 2006;1762:956-72.
92. Pasinelli P, Brown RH. Molecular biology of amyotrophic lateral sclerosis: insights from genetics. Nat Rev Neurosci. 2006;7(9):710-23.
93. Patel SA, Maragakis NJ. Amyotrophic lateral sclerosis: pathogenesis, differential diagnoses, and potential interventions. J Spinal Cord Med. 2002;25(4):262-73.
94. Neusch C, Bahr M, Schneider-Gold C. Glia cells in amyotrophic lateral sclerosis: new clues to understanding an old disease? Muscle Nerve. 2007;35(6):712-24.
95. Gonzalez de Aguilar JL, Echaniz-Laguna A, Fergani A, Rene F, Meininger V, Loeffler JP, et al. Amyotrophic lateral sclerosis: all roads lead to Rome. J Neurochem. 2007;101(5):1153-60.
96. Vucic S, Kiernan M. Pathophysiology of degeneration in familial amyotrophic lateral sclerosis. Curr Mol Med. 2009;9:255-72.
97. Renton Alan E, Majounie E, Waite A, Simón-Sánchez J, Rollinson S, Gibbs JR, et al. A Hexanucleotide Repeat Expansion in C9ORF72 Is the Cause of Chromosome 9p21-Linked ALS-FTD. Neuron. 2011;72:257-68.
98. DeJesus-Hernandez M, Mackenzie Ian R, Boeve Bradley F, Boxer Adam L, Baker M, Rutherford Nicola J, et al. Expanded GGGGCC Hexanucleotide Repeat in Noncoding Region of C9ORF72 Causes Chromosome 9p-Linked FTD and ALS. Neuron. 2011;72:245-56.
99. Chiò A, Borghero G, Restagno G, Mora G, Drepper C, Traynor BJ, et al. Clinical characteristics of patients with familial amyotrophic lateral sclerosis carrying the pathogenic GGGGCC hexanucleotide repeat expansion of C9ORF72. Brain. 2012;135(3):784-93.
100. Majounie E, Renton AE, Mok K, Dopper EGP, Waite A, Rollinson S, et al. Frequency of the C9orf72 hexanucleotide repeat expansion in patients with amyotrophic lateral sclerosis and frontotemporal dementia: a cross-sectional study. The Lancet Neurology. 2012;11(4):323-30.
101. Al-Sarraj S, King A, Troakes C, Smith B, Maekawa S, Bodi I, et al. P62 positive, TDP-43 negative, neuronal cytoplasmic and intranuclear inclusions in the cerebellum and hippocampus define the pathology of C9orf72-linked FTLD and MND/ALS. Acta Neuropathologica. 2011;122(6):691-702.
102. Boeve BF, Boylan KB, Graff-Radford NR, DeJesus-Hernandez M, Knopman DS, Pedraza O, et al. Characterization of frontotemporal dementia and/or amyotrophic lateral sclerosis associated with the GGGGCC repeat expansion in C9ORF72. Brain. 2012;135(3):765-83.

103. van Rheenen W, van Blitterswijk M, Huisman MH, Vlam L, van Doormaal PT, Seelen M, et al. Hexanucleotide repeat expansions in C9ORF72 in the spectrum of motor neuron diseases. Neurology. 2012;79(9):878-82.
104. Gijselinck I, Van Mossevelde S, van der Zee J, Sieben A, Engelborghs S, De Bleecker J, et al. The C9orf72 repeat size correlates with onset age of disease, DNA methylation and transcriptional downregulation of the promoter. Mol Psychiatry. 2015.
105. Snowden JS, Harris J, Richardson A, Rollinson S, Thompson JC, Neary D, et al. Frontotemporal dementia with amyotrophic lateral sclerosis: a clinical comparison of patients with and without repeat expansions in C9orf72. Amyotroph Lateral Scler Frontotemporal Degener. 2013;14(3):172-6.
106. Devenney E, Vucic S, Hodges JR, Kiernan MC. Motor neuron disease-frontotemporal dementia: a clinical continuum. Expert Rev Neurother. 2015;15(5):509-22.
107. Taylor LJ, Brown RG, Tsermentseli S, Al-Chalabi A, Shaw CE, Ellis CM, et al. Is language impairment more common than executive dysfunction in amyotrophic lateral sclerosis? J Neurol Neurosurg Psychiatry. 2013;84(5):494-8.
108. Boxer AL, Mackenzie IR, Boeve BF, Baker M, Seeley WW, Crook R, et al. Clinical, neuroimaging and neuropathological features of a new chromosome 9p-linked FTD-ALS family. Journal of Neurology, Neurosurgery & Psychiatry. 2011;82(2):196-203.
109. Pearson JP, Williams NM, Majounie E, Waite A, Stott J, Newsway V, et al. Familial frontotemporal dementia with amyotrophic lateral sclerosis and a shared haplotype on chromosome9p. Journal of Neurology. 2011;258(4):647-55.
110. Whitwell JL, Weigand SD, Boeve BF, Senjem ML, Gunter JL, DeJesus-Hernandez M, et al. Neuroimaging signatures of frontotemporal dementia genetics: C9ORF72, tau, progranulin and sporadics. Brain. 2012;135(3):794-806.
111. Ling S-C, Polymenidou M, Cleveland DonÂ W. Converging Mechanisms in ALS and FTD: Disrupted RNA and Protein Homeostasis. Neuron. 2013;79(3):416-38.
112. Ciura S, Lattante S, Le Ber I, Latouche M, Tostivint H, Brice A, et al. Loss of function of C9orf72 causes motor deficits in a zebrafish model of Amyotrophic Lateral Sclerosis. Ann Neurol. 2013:doi: 10.1002/ana.23946.
113. Mori K, Lammich S, Mackenzie IR, Forne I, Zilow S, Kretzschmar H, et al. hnRNP A3 binds to GGGGCC repeats and is a constituent of p62-positive/TDP43-negative inclusions in the hippocampus of patients with C9orf72 mutations. Acta Neuropathol. 2013;125(3):413-23.
114. Donnelly Christopher J, Zhang P-W, Pham Jacqueline T, Heusler Aaron R, Mistry Nipun A, Vidensky S, et al. RNA Toxicity from the ALS/FTD C9ORF72 Expansion Is Mitigated by Antisense Intervention. Neuron. 2013;80(2):415-28.
115. Ash Peter EA, Bieniek Kevin F, Gendron Tania F, Caulfield T, Lin W-L, DeJesus-Hernandez M, et al. Unconventional Translation of C9ORF72 GGGGCC Expansion Generates Insoluble Polypeptides Specific to c9FTD/ALS. Neuron. 2013;77(4):639-46.
116. Simón-Sánchez J, Dopper EGP, Cohn-Hokke PE, Hukema RK, Nicolaou N, Seelaar H, et al. The clinical and pathological phenotype of C9ORF72 hexanucleotide repeat expansions. Brain. 2012;135(3):723-35.
117. Mahoney CJ, Beck J, Rohrer JD, Lashley T, Mok K, Shakespeare T, et al. Frontotemporal dementia with the C9ORF72 hexanucleotide repeat expansion: clinical, neuroanatomical and neuropathological features. Brain. 2012;135(3):736-50.

118. Boeve BF, Boylan KB, Graff-Radford NR, DeJesus-Hernandez M, Knopman DS, Pedraza O, et al. Characterization of frontotemporal dementia and/or amyotrophic lateral sclerosis associated with the GGGGCC repeat expansion in C9ORF72. Brain. 2012;135(Pt 3):765-83.
119. Josephs KA, Dickson DW. Hippocampal sclerosis in tau-negative frontotemporal lobar degeneration. Neurobiology of Aging. 2009;28(11):1718-22.
120. Sreedharan J, Blair IP, Tripathi VB, Hu X, Vance C, Rogelj B, et al. TDP-43 mutations in familial and sporadic amyotrophic lateral sclerosis. Science. 2008;319(5870):1668-72.
121. Vance C, Rogelj B, Hortobagyi T, De Vos KJ, Nishimura AL, Sreedharan J, et al. Mutations in FUS, an RNA processing protein, cause familial amyotrophic lateral sclerosis type 6. Science. 2009;323(5918):1208-11.
122. Daoud H, Valdmanis PN, Kabashi E, Dion P, Dupré N, Camu W, et al. Contribution of TARDBP mutations to sporadic amyotrophic lateral sclerosis. J Med Genet. 2009;46(2):112-4.
123. Kwiatkowski TJ, Jr., Bosco DA, Leclerc AL, Tamrazian E, Vanderburg CR, Russ C, et al. Mutations in the FUS/TLS gene on chromosome 16 cause familial amyotrophic lateral sclerosis. Science. 2009;323(5918):1205-8.
124. Xu Y-F, Zhang Y-J, Lin W-L, Cao X, Stetler C, Dickson D, et al. Expression of mutant TDP-43 induces neuronal dysfunction in transgenic mice. Molecular Neurodegeneration. 2011;6(1):73.
125. Wils H, Kleinberger G, Janssens J, Pereson S, Joris G, Cuijt I, et al. TDP-43 transgenic mice develop spastic paralysis and neuronal inclusions characteristic of ALS and frontotemporal lobar degeneration. Proc Natl Acad Sci USA. 2010;107:3858 - 63.
126. Xu Y, Gendron T, Zhang Y, Lin W, D'Alton S, Sheng H, et al. Wild-type human TDP-43 expression causes TDP-43 phosphorylation, mitochondrial aggregation, motor deficits, and early mortality in transgenic mice. J Neurosci. 2010;30:10851 - 9.
127. Igaz L, Kwong L, Lee E, Chen-Plotkin A, Swanson E, Unger T, et al. Dysregulation of the ALS-associated gene TDP-43 leads to neuronal death and degeneration in mice. J Clin Invest. 2011;121:726 - 38.
128. Shan X, Chiang P, Price D, Wong P. Altered distributions of Gemini of coiled bodies and mitochondria in motor neurons of TDP-43 transgenic mice. Proc Natl Acad Sci USA. 2010;107:16325 - 30.
129. Swarup V, Phaneuf D, Bareil C, Robertson J, Rouleau G, Kriz J, et al. Pathological hallmarks of amyotrophic lateral sclerosis/frontotemporal lobar degeneration in transgenic mice produced with TDP-43 genomic fragments. Brain. 2011;134:2610 - 26.
130. Tsai K, Yang C, Fang Y, Cho K, Chien W, Wang W, et al. Elevated expression of TDP-43 in the forebrain of mice is sufficient to cause neurological and pathological phenotypes mimicking FTLD-U. J Exp Med. 2010;207:1661 - 73.
131. Wegorzewska I, Bell S, Cairns N, Miller T, Baloh R. TDP-43 mutant transgenic mice develop features of ALS and frontotemporal lobar degeneration. Proc Natl Acad Sci USA. 2009;106:18809 - 14.
132. Van Deerlin VM, Leverenz JB, Bekris LM, Bird TD, Yuan W, Elman LB, et al. TARDBP mutations in amyotrophic lateral sclerosis with TDP-43 neuropathology: a genetic and histopathological analysis. Lancet Neurol. 2008;7(5):409-16.

133. Wu LS, Cheng WC, Shen CK. Targeted depletion of TDP-43 expression in the spinal cord motor neurons leads to the development of amyotrophic lateral sclerosis-like phenotypes in mice. J Biol Chem. 2012;287(33):27335-44.
134. Iguchi Y, Katsuno M, Niwa J-i, Takagi S, Ishigaki S, Ikenaka K, et al. Loss of TDP-43 causes age-dependent progressive motor neuron degeneration. Brain. 2013;136(5):1371-82.
135. Shelkovnikova TA, Peters OM, Deykin AV, Connor-Robson N, Robinson H, Ustyugov AA, et al. Fused in Sarcoma (FUS) Protein Lacking Nuclear Localization Signal (NLS) and Major RNA Binding Motifs Triggers Proteinopathy and Severe Motor Phenotype in Transgenic Mice. J Biol Chem. 2013;288(35):25266-74.
136. Murakami T, Yang SP, Xie L, Kawano T, Fu D, Mukai A, et al. ALS mutations in FUS cause neuronal dysfunction and death in Caenorhabditis elegans by a dominant gain-of-function mechanism. Hum Mol Genet. 2012;21(1):1-9.
137. Dewey CM, Cenik B, Sephton CF, Dries DR, Mayer P, Good SK, et al. TDP-43 Is Directed to Stress Granules by Sorbitol, a Novel Physiological Osmotic and Oxidative Stressor. Mol Cell Biol. 2011;31(5):1098-108.
138. Liu-Yesucevitz L, Bilgutay A, Zhang YJ, Vanderweyde T, Citro A, Mehta T, et al. Tar DNA binding protein-43 (TDP-43) associates with stress granules: analysis of cultured cells and pathological brain tissue. PLoS One. 2010;5(10):e13250.
139. Ito D, Seki M, Tsunoda Y, Uchiyama H, Suzuki N. Nuclear transport impairment of amyotrophic lateral sclerosis-linked mutations in FUS/TLS. Ann Neurology. 2011;69(1):152-62.
140. Bosco DA, Lemay N, Ko HK, Zhou H, Burke C, Kwiatkowski TJ, et al. Mutant FUS proteins that cause amyotrophic lateral sclerosis incorporate into stress granules. Hum Mol Genet. 2010;19(21):4160-75.
141. Colombrita C, Zennaro E, Fallini C, Weber M, Sommacal A, Buratti E, et al. TDP-43 is recruited to stress granules in conditions of oxidative insult. J Neurochem. 2009;111(4):1051-61.
142. Andersson M, Stahlberg A, Arvidsson Y, Olofsson A, Semb H, Stenman G, et al. The multifunctional FUS, EWS and TAF15 proto-oncoproteins show cell type-specific expression patterns and involvement in cell spreading and stress response. BMC Cell Biology. 2008;9(1):37.
143. Bentmann E, Haass C, Dormann D. Stress granules in neurodegeneration – lessons learnt from TAR DNA binding protein of 43 kDa and fused in sarcoma. FEBS J. 2013;280(18):4348-70.
144. Dormann D, Rodde R, Edbauer D, Bentmann E, Fischer I, Hruscha A, et al. ALS-associated fused in sarcoma (FUS) mutations disrupt Transportin-mediated nuclear import. EMBO J. 2010;29(16):2841-57.
145. Dewey CM, Cenik B, Sephton CF, Johnson BA, Herz J, Yu G. TDP-43 aggregation in neurodegeneration: are stress granules the key? Brain Res. 2012;1462:16-25.
146. Deng H-X, Chen W, Hong S-T, Boycott KM, Gorrie GH, Siddique N, et al. Mutations in UBQLN2 cause dominant X-linked juvenile and adult-onset ALS and ALS/dementia. Nature. 2011;477(7363):211-5.
147. van Es MA, Veldink JH, Saris CGJ, Blauw HM, van Vught PWJ, Birve A, et al. Genome-wide association study identifies 19p13.3 (UNC13A) and 9p21.2 as susceptibility loci for sporadic amyotrophic lateral sclerosis. Nat Genet. 2009;41(10):1083-7.
148. Cox LE, Ferraiuolo L, Goodall EF, Heath PR, Higginbottom A, Mortiboys H, et al. Mutations in CHMP2B in lower motor neuron predominant amyotrophic lateral sclerosis (ALS). PLoS One. 2010;5(3):e9872.

149. Chow CY, Landers JE, Bergren SK, Sapp PC, Grant AE, Jones JM, et al. Deleterious Variants of FIG4, a Phosphoinositide Phosphatase, in Patients with ALS. Am J Hum Gen. 2009;84(1):85-8.
150. Chen HJ, Anagnostou G, Chai A, Withers J, Morris A, Adhikaree J, et al. Characterization of the properties of a novel mutation in VAPB in familial amyotrophic lateral sclerosis. J Bio Chem. 2010;285(51):40266-81.
151. Johnson JO, Mandrioli J, Benatar M, Abramzon Y, Van Deerlin VM, Trojanowski JQ, et al. Exome Sequencing Reveals VCP Mutations as a Cause of Familial ALS. Neuron. 2010;68(5):857-64.
152. Fecto F, Yan J, Vemula SP, Liu E, Yang Y, Chen W, et al. SQSTM1 mutations in familial and sporadic amyotrophic lateral sclerosis. Arch Neurol. 2011;68(11):1440-6.
153. Del Bo R, Tiloca C, Pensato V, Corrado L, Ratti A, Ticozzi N, et al. Novel optineurin mutations in patients with familial and sporadic amyotrophic lateral sclerosis. Journal of Neurology, Neurosurgery and Psychiatry. 2011;82(11):1239-43.
154. Al-Chalabi A, Calvo A, Chio A, Colville S, Ellis CM, Hardiman O, et al. Analysis of amyotrophic lateral sclerosis as a multistep process: a population-based modelling study. Lancet Neurol. 2014;13(11):1108-13.
155. Eisen A, Kiernan M, Mitsumoto H, Swash M. Amyotrophic lateral sclerosis: a long preclinical period? J Neurol Neurosurg Psychiatry. 2014;85(11):1232-8.
156. Boillee S, Vande Velde C, Cleveland DW. ALS: a disease of motor neurons and their nonneuronal neighbors. Neuron. 2006;52:39-59.
157. Mancuso R, Navarro X. Amyotrophic lateral sclerosis: Current perspectives from basic research to the clinic. Prog Neurobiol. 2015;133:1-26.
158. Saba L, Viscomi MT, Caioli S, Pignataro A, Bisicchia E, Pieri M, et al. Altered Functionality, Morphology, and Vesicular Glutamate Transporter Expression of Cortical Motor Neurons from a Presymptomatic Mouse Model of Amyotrophic Lateral Sclerosis. Cereb Cortex. 2015.
159. Watkins JC, Evans RH. Excitatory amino acid transmitters. Annu Rev Pharmacol Toxicol. 1981;21:165-204.
160. Heath PR, Shaw PJ. Update on the glutamatergic neurotransmitter system and the role of excitotoxicity in amyotrophic lateral sclerosis. Muscle Nerve. 2002;26(4):438-58.
161. Dong H, Zhang P, Song I, Petralia RS, Liao D, Huganir RL. Characterization of the glutamate receptor-interacting proteins GRIP1 and GRIP2. J Neurosci. 1999;19(16):6930-41.
162. Vandenberg RJ. Molecular pharmacology and physiology of glutamate transporters in the central nervous system. Clin Exp Pharmacol Physiol. 1998;25(6):393-400.
163. Laake JH, Slyngstad TA, Haug FM, Ottersen OP. Glutamine from glial cells is essential for the maintenance of the nerve terminal pool of glutamate: immunogold evidence from hippocampal slice cultures. J Neurochem. 1995;65(2):871-81.
164. Simeone TA, Sanchez RM, Rho JM. Molecular biology and ontogeny of glutamate receptors in the mammalian central nervous system. J Child Neurol. 2004;19(5):343-60.
165. MacDermott AB, Mayer ML, Westbrook GL, Smith SJ, Barker JL. NMDA-receptor activation increases cytoplasmic calcium concentration in cultured spinal cord neurones. Nature. 1986;321(6069):519-22.
166. Kutsuwada T, Kashiwabuchi N, Mori H, Sakimura K, Kushiya E, Araki K, et al. Molecular diversity of the NMDA receptor channel. Nature. 1992;358(6381):36-41.

167. Meguro H, Mori H, Araki K, Kushiya E, Kutsuwada T, Yamazaki M, et al. Functional characterization of a heteromeric NMDA receptor channel expressed from cloned cDNAs. Nature. 1992;357(6373):70-4.
168. Michaelis EK. Molecular biology of glutamate receptors in the central nervous system and their role in excitotoxicity, oxidative stress and aging. Prog Neurobiol. 1998;54(4):369-415.
169. Monyer H, Sprengel R, Schoepfer R, Herb A, Higuchi M, Lomeli H, et al. Heteromeric NMDA receptors: molecular and functional distinction of subtypes. Science. 1992;256(5060):1217-21.
170. Ishii T, Moriyoshi K, Sugihara H, Sakurada K, Kadotani H, Yokoi M, et al. Molecular characterization of the family of the N-methyl-D-aspartate receptor subunits. J Biol Chem. 1993;268(4):2836-43.
171. Watanabe M, Inoue Y, Sakimura K, Mishina M. Distinct spatio-temporal distributions of the NMDA receptor channel subunit mRNAs in the brain. Ann N Y Acad Sci. 1993;707:463-6.
172. Watanabe M, Inoue Y, Sakimura K, Mishina M. Distinct distributions of five N-methyl-D-aspartate receptor channel subunit mRNAs in the forebrain. J Comp Neurol. 1993;338(3):377-90.
173. Watanabe M, Mishina M, Inoue Y. Distinct distributions of five NMDA receptor channel subunit mRNAs in the brainstem. J Comp Neurol. 1994;343(4):520-31.
174. Watanabe M, Mishina M, Inoue Y. Distinct spatiotemporal expressions of five NMDA receptor channel subunit mRNAs in the cerebellum. J Comp Neurol. 1994;343(4):513-9.
175. Ciabarra AM, Sevarino KA. An anti-chi-1 antibody recognizes a heavily glycosylated protein in rat brain. Brain Res Mol Brain Res. 1997;46(1-2):85-90.
176. Nishi M, Hinds H, Lu HP, Kawata M, Hayashi Y. Motoneuron-specific expression of NR3B, a novel NMDA-type glutamate receptor subunit that works in a dominant-negative manner. J Neurosci. 2001;21(23):RC185.
177. Chatterton JE, Awobuluyi M, Premkumar LS, Takahashi H, Talantova M, Shin Y, et al. Excitatory glycine receptors containing the NR3 family of NMDA receptor subunits. Nature. 2002;415(6873):793-8.
178. Dingledine R, Borges K, Bowie D, Traynelis SF. The glutamate receptor ion channels. Pharmacol Rev. 1999;51(1):7-61.
179. Heath P, Shaw P. Update on the glutamatergic neurotransmitter system and the role of excitotoxicity in amyotrophic lateral sclerosis. Muscle Nerve. 2002;26:438 - 58.
180. Lerma J. Roles and rules of kainate receptors in synaptic transmission. Nature Reviews Neuroscience. 2003;4(6):481-95.
181. Desiato M, Bernardi, G, Hagi, AH, Boffa L, Caramia, MD. Transcranial magnetic stimulation of motor pathways directed to muscles supplied by cranial nerves in ALS. Clin Neurophysiol. 2002;113:132-40.
182. Prout AJ, Eisen A. The cortical silent period and ALS. Muscle Nerve. 1994;17:217-23.
183. Vucic S, Kiernan MC. Novel threshold tracking techniques suggest that cortical hyperexcitability is an early feature of motor neuron disease. Brain. 2006;129:2436-46.
184. Vucic S, Kiernan MC. Upregulation of persistent sodium conductances in familial ALS. J Neurol Neurosurg Psychiatry. 2010;81(2):222-7.
185. Vucic S, Nicholson GA, Kiernan MC. Cortical hyperexcitability may precede the onset of familial amyotrophic lateral sclerosis. Brain. 2008;131:1540-50.

186. Blair IP, Williams KL, Warraich ST, Durnall JC, Thoeng AD, Manavis J, et al. FUS mutations in amyotrophic lateral sclerosis: clinical, pathological, neurophysiological and genetic analysis. J Neurol Neurosurg Psychiatry. 2009.
187. Menon P, Kiernan MC, Vucic S. Cortical hyperexcitability precedes lower motor neuron dysfunction in ALS. Clinical Neurophysiol. 2015;126:803-9.
188. Nihei K, McKee AC, Kowall NW. Patterns of neuronal degeneration in the motor cortex of amyotrophic lateral sclerosis patients. Acta Neuropathologica. 1993;86:55-64.
189. Foerster BR, Callaghan BC, Petrou M, Edden RA, Chenevert TL, Feldman EL. Decreased motor cortex gamma-aminobutyric acid in amyotrophic lateral sclerosis. Neurology. 2012;78(20):1596-600.
190. Ionov ID. Survey of ALS-associated factors potentially promoting Ca(2+) overload of motor neurons. Amyotroph Lateral Scler. 2007;8(5):260-5.
191. Rothstein JD, Jin L, Dykes-Hoberg M, Kuncl RW. Chronic inhibition of glutamate uptake produces a model of slow neurotoxicity. Proc Natl Acad Sci U S A. 1993;90(14):6591-5.
192. Rothstein JD, Van Kammen M, Levey AI, Martin LJ, Kuncl RW. Selective loss of glial glutamate transporter GLT-1 in amyotrophic lateral sclerosis. Ann Neurol. 1995;38(1):73-84.
193. Trotti D, Rolfs A, Danbolt NC, Brown RH, Jr., Hediger MA. SOD1 mutants linked to amyotrophic lateral sclerosis selectively inactivate a glial glutamate transporter. Nat Neurosci. 1999;2(9):848.
194. Boston-Howes W, Gibb SL, Williams EO, Pasinelli P, Brown RH, Jr., Trotti D. Caspase-3 cleaves and inactivates the glutamate transporter EAAT2. J Biol Chem. 2006;281(20):14076-84.
195. Gibb SL, Boston-Howes W, Lavina ZS, Gustincich S, Brown RH, Jr., Pasinelli P, et al. A Caspase-3-cleaved Fragment of the Glial Glutamate Transporter EAAT2 Is Sumoylated and Targeted to Promyelocytic Leukemia Nuclear Bodies in Mutant SOD1-linked Amyotrophic Lateral Sclerosis. J Biol Chem. 2007;282(44):32480-90.
196. Rothstein JD, Patel S, Regan MR, Haenggeli C, Huang YH, Bergles DE, et al. Beta-lactam antibiotics offer neuroprotection by increasing glutamate transporter expression. Nature. 2005;433(7021):73-7.
197. Kawahara Y, Ito K, Sun H, Aizawa H, Kanazawa I, Kwak S. Glutamate receptors: RNA editing and death of motor neurons. Nature. 2004;427(6977):801.
198. Kwak S, Kawahara Y. Deficient RNA editing of GluR2 and neuronal death in amyotropic lateral sclerosis. J Mol Med. 2005;83(2):110-20.
199. Takuma H, Kwak S, Yoshizawa T, Kanazawa I. Reduction of GluR2 RNA editing, a molecular change that increases calcium influx through AMPA receptors, selective in the spinal ventral gray of patients with amyotrophic lateral sclerosis. Ann Neurol. 1999;46(6):806-15.
200. Van Damme P, Braeken D, Callewaert G, Robberecht W, Van Den Bosch L. GluR2 deficiency accelerates motor neuron degeneration in a mouse model of amyotrophic lateral sclerosis. J Neuropathol Exp Neurol. 2005;64(7):605-12.
201. Van Damme P, Van Den Bosch L, Van Houtte E, Callewaert G, Robberecht W. GluR2-dependent properties of AMPA receptors determine the selective vulnerability of motor neurons to excitotoxicity. J Neurophysiol. 2002;88(3):1279-87.
202. Cox L, Kirby J, Shaw P. Pathogenesis of motor neurone disease. In: Kiernan M, editor. The Motor Neurone Disease Handbook. Sydney: Australasian Medical Publishing Company Limited

2007. p. 26-55.
203. Ince P, Stout N, Shaw P, Slade J, Hunziker W, Heizmann CW, et al. Parvalbumin and calbindin D-28k in the human motor system and in motor neuron disease. Neuropathol Appl Neurobiol. 1993;19(4):291-9.
204. van Es MA, Van Vught PW, Blauw HM, Franke L, Saris CG, Andersen PM, et al. ITPR2 as a susceptibility gene in sporadic amyotrophic lateral sclerosis: a genome-wide association study. Lancet Neurol. 2007;6:869-77.
205. Choe CU, Ehrlich BE. The inositol 1,4,5-trisphosphate receptor (IP3R) and its regulators: sometimes good and sometimes bad teamwork. Sci STKE. 2006;2006(363):re15.
206. Amendola J, Durand J. Morphological differences between wild-type and transgenic superoxide dismutase 1 lumbar motoneurons in postnatal mice. J Comp Neurol. 2008;511(3):329-41.
207. Quinlan KA. Links between Electrophysiological and Molecular Pathology of Amyotrophic Lateral Sclerosis. Integ Comp Biol. 2011;51(6):913-25.
208. Choi DW. Ionic dependence of glutamate neurotoxicity. J Neurosci. 1987;7(2):369-79.
209. Shaw P, Kuncl R. Current concepts in the pathogenesis of ALS. In: WR K, editor. Motor Neuron Disease. Lodon: WB Saunders; 2002. p. 37-73.
210. Stys PK. Anoxic and ischemic injury of myelinated axons in CNS white matter: from mechanistic concepts to therapeutics. J Cereb Blood Flow Metab. 1998;18(1):2-25.
211. Miller RJ, Murphy SN, Glaum SR. Neuronal Ca2+ channels and their regulation by excitatory amino acids. Ann N Y Acad Sci. 1989;568:149-58.
212. Meldrum B, Garthwaite J. Excitatory amino acid neurotoxicity and neurodegenerative disease. Trends Pharmacol Sci. 1990;11(9):379-87.
213. Regan RF, Panter SS, Witz A, Tilly JL, Giffard RG. Ultrastructure of excitotoxic neuronal death in murine cortical culture. Brain Res. 1995;705(1-2):188-98.
214. Bondy SC, Lee DK. Oxidative stress induced by glutamate receptor agonists. Brain Res. 1993;610(2):229-33.
215. Lees GJ. Contributory mechanisms in the causation of neurodegenerative disorders. Neuroscience. 1993;54(2):287-322.
216. Maher P, Davis JB. The role of monoamine metabolism in oxidative glutamate toxicity. J Neurosci. 1996;16(20):6394-401.
217. Bensimon G, Lacomblez L, Meininger V. A controlled trial of riluzole in amyotrophic lateral sclerosis. ALS/Riluzole Study Group. N Engl J Med. 1994;330:585-91.
218. Gurney ME, Cutting FB, Zhai P, Doble A, Taylor CP, Andrus PK, et al. Benefit of vitamin E, riluzole, and gabapentin in a transgenic model of familial amyotrophic lateral sclerosis. Ann Neurol. 1996;39(2):147-57.
219. Gurney ME, Fleck TJ, Himes CS, Hall ED. Riluzole preserves motor function in a transgenic model of familial amyotrophic lateral sclerosis. Neurology. 1998;50(1):62-6.
220. Lacomblez L, Bensimon G, Leigh PN, Guillet P, Meininger V. Dose-ranging study of riluzole in amyotrophic lateral sclerosis. Amyotrophic Lateral Sclerosis/Riluzole Study Group II. Lancet. 1996;347:1425-31.
221. Cheah B, Vucic S, Krishnan A, Kiernan M. Riluzole, neuroprotection and amyotrophic lateral sclerosis. Current medicinal chemistry. 2010;17(18):1942-59.
222. Wainger BJ, Cudkowicz ME. Cortical Hyperexcitability in Amyotrophic Lateral Sclerosis: C9orf72 Repeats. JAMA neurology. 2015:1-3.

223. Saxena S, Roselli F, Singh K, Leptien K, Julien J-P, Gros-Louis F, et al. Neuroprotection through Excitability and mTOR Required in ALS Motoneurons to Delay Disease and Extend Survival. Neuron. 2013;80(1):80-96.
224. Vucic S, Lin CS-Y, Cheah BC, Murray J, Menon P, Krishnan AV, et al. Riluzole exerts central and peripheral modulating effects in amyotrophic lateral sclerosis. Brain. 2013;136(5):1361-70.
225. Lemon RN, Griffiths J. Comparing the function of the corticospinal system in different species: organizational differences for motor specialization? Muscle Nerve. 2005;32(3):261-79.
226. Armand J. The origin, course and terminations of corticospinal fibers in various mammals. Prog Brain Res. 1982;57:329-60.
227. Eisen AA, Shtybel W. AAEM minimonograph #35: Clinical experience with transcranial magnetic stimulation. Muscle Nerve. 1990;13(11):995-1011.
228. Eisen A, Kuwabara S. The split hand syndrome in amyotrophic lateral sclerosis. J Neurol, Neurosurg Psychiatry. 2012;83:399-403.
229. Menon P, Kiernan MC, Vucic S. Appearance, phenomenology and diagnostic utility of the split hand in amyotrophic lateral sclerosis. Neurodeg Dis Manag. 2011;1(6):457-62.
230. Menon P, Kiernan MC, Vucic S. ALS pathophysiology: Insights form the split-hand phenomenon. Clin neurophysiol. 2013:doi:pii: S1388-2457(13)00994-2. 10.1016.
231. Menon P, Kiernan MC, Vucic S. Cortical excitability differences in hand muscles follow a split-hand pattern in healthy controls. Muscle Nerve. 2013:doi: 10.1002/mus.24072.
232. Bae JS, Menon P, Mioshi E, Kiernan MC, Vucic S. Cortical excitability differences between flexor pollicis longus and APB. Neurosci Lett. 2013;541:150-4.
233. Turner MR, Wicks P, Brownstein CA, Massagli MP, Toronjo M, Talbot K, et al. Concordance between site of onset and limb dominance in amyotrophic lateral sclerosis. J Neurol Neurosurg Psychiatry. 2011;82(8):853-4.
234. Devine MS, Kiernan MC, Heggie S, McCombe PA, Henderson RD. Study of motor asymmetry in ALS indicates an effect of limb dominance on onset and spread of weakness, and an important role for upper motor neurons. Amyotroph Lateral Scler Frontotemporal Degener. 2014;15(7-8):481-7.
235. Lillo P, Hodges JR. Frontotemporal dementia and motor neurone disease: overlapping clinic-pathological disorders. J Clin Neurosci. 2009;16(9):1131-5.
236. Neumann M, Sampathu DM, Kwong LK, Truax AC, Micsenyi MC, Chou TT, et al. Ubiquitinated TDP-43 in Frontotemporal Lobar Degeneration and Amyotrophic Lateral Sclerosis. Science. 2006;314(5796):130-3.
237. Vucic S, Cheah BC, Yiannikas C, Kiernan MC. Cortical excitability distinguishes ALS from mimic disorders. Clin Neurophysiol. 2011;122:1860-6.
238. Vucic S, Kiernan MC. Cortical excitability testing distinguishes Kennedy's disease from amyotrophic lateral sclerosis. Clin Neurophysiol. 2008;119:1088-96.
239. Vucic S, Nicholson GA, Kiernan MC. Cortical excitability in hereditary motor neuronopathy with pyramidal signs: comparison with ALS. J Neurol Neurosurg Psychiatry. 2010;81(1):97-100.
240. Vucic S, Kiernan MC. Abnormalities in cortical and peripheral excitability in flail arm variant amyotrophic lateral sclerosis. J Neurol Neurosurg Psychiatry. 2007;78:849-52.
241. Williamson TL, Cleveland DW. Slowing of axonal transport is a very early event in the toxicity of ALS-linked SOD1 mutants to motor neurons. Nat Neurosci. 1999;2(1):50-6.

242. Gould TW, Buss RR, Vinsant S, Prevette D, Sun W, Knudson CM, et al. Complete dissociation of motor neuron death from motor dysfunction by Bax deletion in a mouse model of ALS. J Neurosci. 2006;26(34):8774-86.
243. Pagani MR, Reisin RC, Uchitel OD. Calcium signaling pathways mediating synaptic potentiation triggered by amyotrophic lateral sclerosis IgG in motor nerve terminals. J Neurosci. 2006;26(10):2661-72.
244. Pun S, Santos AF, Saxena S, Xu L, Caroni P. Selective vulnerability and pruning of phasic motoneuron axons in motoneuron disease alleviated by CNTF. Nat Neurosci. 2006;9(3):408-19.
245. Fischer LR, Culver DG, Tennant P, Davis AA, Wang M, Castellano-Sanchez A, et al. Amyotrophic lateral sclerosis is a distal axonopathy: evidence in mice and man. Exp Neurol. 2004;185(2):232-40.
246. Miller RG, Jackson CE, Kasarskis EJ, England JD, Forshew D, Johnston W, et al. Practice parameter update: The care of the patient with amyotrophic lateral sclerosis: multidisciplinary care, symptom management, and cognitive/behavioral impairment (an evidence-based review): report of the Quality Standards Subcommittee of the American Academy of Neurology. Neurology. 2009;73(15):1227-33.
247. Turner MR, Kiernan MC, Leigh PN, Talbot K. Biomarkers in amyotrophic lateral sclerosis. Lancet Neurol. 2009;8:94-109.
248. Vucic S, Burke D, Kiernan MC. Diagnosis of motor neuron disease. In: Kiernan MC, editor. The Motor Neuron Disease Handbook. Sydney: Australasian Medical Publishing Company Limited; 2007. p. 89-115.
249. Eisen A, Weber M. The motor cortex and amyotrophic lateral sclerosis. Muscle Nerve. 2001;24(4):564-73.
250. Gowers WR. Manual of Diseases of the Nervous System. London: Churchill; 1886-88.
251. Kiernan J, Hudson A. Changes in sizes of cortical and lower motor neurons in amyotrophic lateral sclerosis. Brain. 1991(114):843-53.
252. Pamphlett R, Kril J, Hng T. Motor neuron disease: a primary disorder of corticomotoneurons? . Muscle Nerve 1995(18):314-8.
253. Gowers W. A Manual of Diseases of the Nervous System: spinal cord and nerves. London: Churchill; 1888. p. 356-81.
254. Flament D, Goldsmith P, Buckley CJ, Lemon RN. Task dependence of responses in first dorsal interosseous muscle to magnetic brain stimulation in man. J Physiol. 1993;464:361-78.
255. Ravits J, Paul P, Jorg C. Focality of upper and lower motor neuron degeneration at the clinical onset of ALS. Neurology. 2007;68(19):1571-5.
256. Boillee S, Vande Velde C, Cleveland DW. ALS: a disease of motor neurons and their nonneuronal neighbors. Neuron. 2006;52(1):39-59.
257. Chung MJ, Suh YL. Ultrastructural changes of mitochondria in the skeletal muscle of patients with amyotrophic lateral sclerosis. Ultrastruct Pathol. 2002;26(1):3-7.
258. Higgins CM, Jung C, Xu Z. ALS-associated mutant SOD1G93A causes mitochondrial vacuolation by expansion of the intermembrane space and by involvement of SOD1 aggregation and peroxisomes. BMC Neurosci. 2003;4:16.
259. Kirkinezos IG, Bacman SR, Hernandez D, Oca-Cossio J, Arias LJ, Perez-Pinzon MA, et al. Cytochrome c association with the inner mitochondrial membrane is impaired in the CNS of G93A-SOD1 mice. J Neurosci. 2005;25(1):164-72.

260. Lederer CW, Torrisi A, Pantelidou M, Santama N, Cavallaro S. Pathways and genes differentially expressed in the motor cortex of patients with sporadic amyotrophic lateral sclerosis. BMC Genomics. 2007;8:26.
261. Xu Z, Jung C, Higgins C, Levine J, Kong J. Mitochondrial degeneration in amyotrophic lateral sclerosis. J Bioenerg Biomembr. 2004;36(4):395-9.
262. Mancuso R, Navarro X. Amyotrophic lateral sclerosis: Current perspectives from basic research to the clinic. Prog Neurobiol. 2015;133:1-26.
263. Dugan LL, Choi DW. Excitotoxicity, free radicals, and cell membrane changes. Ann Neurol. 1994;35:S17-21.
264. Bowling AC, Beal MF. Bioenergetic and oxidative stress in neurodegenerative diseases. Life Sci. 1995;56(14):1151-71.
265. Kong J, Xu Z. Massive mitochondrial degeneration in motor neurons triggers the onset of amyotrophic lateral sclerosis in mice expressing a mutant SOD1. J Neurosci. 1998;18(9):3241-50.
266. Comi GP, Bordoni A, Salani S, Franceschina L, Sciacco M, Prelle A, et al. Cytochrome c oxidase subunit I microdeletion in a patient with motor neuron disease. Ann Neurol. 1998;43(1):110-6.
267. Fujita K, Yamauchi M, Shibayama K, Ando M, Honda M, Nagata Y. Decreased cytochrome c oxidase activity but unchanged superoxide dismutase and glutathione peroxidase activities in the spinal cords of patients with amyotrophic lateral sclerosis. J Neurosci Res. 1996;45(3):276-81.
268. Jung C, Higgins CM, Xu Z. Mitochondrial electron transport chain complex dysfunction in a transgenic mouse model for amyotrophic lateral sclerosis. J Neurochem. 2002;83(3):535-45.
269. Bilsland LG, Nirmalananthan N, Yip J, Greensmith L, Duchen MR. Expression of mutant SOD1G93A in astrocytes induces functional deficits in motoneuron mitochondria. J Neurochem. 2008;107(5):1271-83.
270. Damiano M, Starkov AA, Petri S, Kipiani K, Kiaei M, Mattiazzi M, et al. Neural mitochondrial Ca2+ capacity impairment precedes the onset of motor symptoms in G93A Cu/Zn-superoxide dismutase mutant mice. J Neurochem. 2006;96(5):1349-61.
271. Jaiswal M, Zech W-D, Goos M, Leutbecher C, Ferri A, Zippelius A, et al. Impairment of mitochondrial calcium handling in a mtSOD1 cell culture model of motoneuron disease. BMC Neuroscience. 2009;10(1):64.
272. Nguyen KT, GarcÃa-ChacÃ³n LE, Barrett JN, Barrett EF, David G. The Î¨m depolarization that accompanies mitochondrial Ca2+ uptake is greater in mutant SOD1 than in wild-type mouse motor terminals. Proc Nat Acad Sci USA. 2009;106(6):2007-11.
273. Li Q, Vande Velde C, Israelson A, Xie J, Bailey AO, Dong M-Q, et al. ALS-linked mutant superoxide dismutase 1 (SOD1) alters mitochondrial protein composition and decreases protein import. Proc Nat Acad Sci USA. 2010;107(49):21146-51.
274. MacAskill AF, Atkin TA, Kittler JT. Mitochondrial trafficking and the provision of energy and calcium buffering at excitatory synapses. Eur J Neurosci. 2010;32(2):231-40.
275. MacAskill AF, Rinholm JE, Twelvetrees AE, Arancibia-Carcamo IL, Muir J, Fransson A, et al. Miro1 Is a Calcium Sensor for Glutamate Receptor-Dependent Localization of Mitochondria at Synapses. Neuron. 2009;61(4):541-55.
276. Bilsland LG, Sahai E, Kelly G, Golding M, Greensmith L, Schiavo G. Deficits in axonal transport precede ALS symptoms in vivo. Proc Natl Acad Sci U S A. 2010;107(47):20523-8.

277. Cheah BC, Kiernan MC. Dexpramipexole, the R(+) enantiomer of pramipexole, for the potential treatment of amyotrophic lateral sclerosis. IDrugs. 2010;13(12):911-20.
278. Cudkowicz M, Bozik ME, Ingersoll EW, Miller R, Mitsumoto H, Shefner J, et al. The effects of dexpramipexole (KNS-760704) in individuals with amyotrophic lateral sclerosis. Nat Med. 2011;17:1652-56.
279. Cudkowicz ME, van den Berg LH, Shefner JM, Mitsumoto H, Mora JS, Ludolph A, et al. Dexpramipexole versus placebo for patients with amyotrophic lateral sclerosis (EMPOWER): a randomised, double-blind, phase 3 trial. The Lancet Neurology. 2013;12(11):1059-67.
280. Bozik ME, Mitsumoto H, Brooks BR, Rudnicki SA, Moore DH, Zhang B, et al. A post hoc analysis of subgroup outcomes and creatinine in the phase III clinical trial (EMPOWER) of dexpramipexole in ALS. Amyotrop Lateral Scler Frontotemporal Degener. 2014;15(5-6):406-13.
281. Rosen DR, Siddique T, Patterson D, Figlewicz DA, Sapp P, Hentati A, et al. Mutations in Cu/Zn superoxide dismutase gene are associated with familial amyotrophic lateral sclerosis. Nature. 1993;362(6415):59-62.
282. Andersen P. Amyotrophic lateral sclerosis genetics with Mendelian inheritance. In: Brown Jr R, Swash M, Pasinelli P, editors. Amyotrophic Lateral Sclerosis. 2nd ed. London: Informa Healthcare; 2006. p. 187-207.
283. Bruijn LI, Miller TM, Cleveland DW. Unraveling the mechanisms involved in motor neuron degeneration in ALS. Annu Rev Neurosci. 2004;27:723-49.
284. Liu R, Althaus JS, Ellerbrock BR, Becker DA, Gurney ME. Enhanced oxygen radical production in a transgenic mouse model of familial amyotrophic lateral sclerosis. Ann Neurol. 1998;44(5):763-70.
285. Beckman JS, Koppenol WH. Nitric oxide, superoxide, and peroxynitrite: the good, the bad, and ugly. Am J Physiol. 1996;271(5 Pt 1):1424-37.
286. Mitsumoto H, Santella RM, Liu X, Bogdanov M, Zipprich J, Wu HC, et al. Oxidative stress biomarkers in sporadic ALS. Amyotroph Lateral Scler. 2008;9(3):177-83.
287. Andrus PK, Fleck TJ, Gurney ME, Hall ED. Protein oxidative damage in a transgenic mouse model of familial amyotrophic lateral sclerosis. J Neurochem. 1998;71(5):2041-8.
288. Gurney ME, Pu H, Chiu AY, Dal Canto MC, Polchow CY, Alexander DD, et al. Motor neuron degeneration in mice that express a human Cu,Zn superoxide dismutase mutation. Science. 1994;264(5166):1772-5.
289. Prudencio M, Hart PJ, Borchelt DR, Andersen PM. Variation in aggregation propensities among ALS-associated variants of SOD1: Correlation to human disease. Hum Mol Genet. 2009;18(17):3217-26.
290. Orrell RW, Lane RJ, Ross M. A systematic review of antioxidant treatment for amyotrophic lateral sclerosis/motor neuron disease. Amyotroph Lateral Scler. 2008;9(4):195-211.
291. Sato T, Nakanishi T, Yamamoto Y, Andersen PM, Ogawa Y, Fukada K, et al. Rapid disease progression correlates with instability of mutant SOD1 in familial ALS. Neurology. 2005;65(12):1954-7.
292. Bruijn LI, Houseweart MK, Kato S, Anderson KL, Anderson SD, Ohama E, et al. Aggregation and motor neuron toxicity of an ALS-linked SOD1 mutant independent from wild-type SOD1. Science. 1998;281(5384):1851-4.
293. Sasaki S, Iwata M. Impairment of fast axonal transport in the proximal axons of anterior horn neurons in amyotrophic lateral sclerosis. Neurology. 1996;47(2):535-40.

294. Borchelt DR, Wong PC, Becher MW, Pardo CA, Lee MK, Xu ZS, et al. Axonal transport of mutant superoxide dismutase 1 and focal axonal abnormalities in the proximal axons of transgenic mice. Neurobiol Dis. 1998;5(1):27-35.
295. Kieran D, Hafezparast M, Bohnert S, Dick JR, Martin J, Schiavo G, et al. A mutation in dynein rescues axonal transport defects and extends the life span of ALS mice. J Cell Biol. 2005;169(4):561-7.
296. Beers DR, Henkel JS, Xiao Q, Zhao W, Wang J, Yen AA, et al. Wild-type microglia extend survival in PU.1 knockout mice with familial amyotrophic lateral sclerosis. Proc Natl Acad Sci U S A. 2006;103(43):16021-6.
297. Henkel JS, Beers DR, Wen S, Rivera AL, Toennis KM, Appel JE, et al. Regulatory T-lymphocytes mediate amyotrophic lateral sclerosis progression and survival. EMBO Mol Med. 2013;5(1):64-79.
298. Zhao W, Beers D, Appel S. Immune-mediated Mechanisms in the Pathoprogression of Amyotrophic Lateral Sclerosis. J Neuroimmune Pharmacol. 2013;8(4):888-99.
299. Atkin JD, Farg MA, Turner BJ, Tomas D, Lysaght JA, Nunan J, et al. Induction of the unfolded protein response in familial amyotrophic lateral sclerosis and association of protein-disulfide isomerase with superoxide dismutase 1. J Biol Chem. 2006;281(40):30152-65.
300. Atkin JD, Farg MA, Walker AK, McLean C, Tomas D, Horne MK. Endoplasmic reticulum stress and induction of the unfolded protein response in human sporadic amyotrophic lateral sclerosis. Neurobiol Dis. 2008;30(3):400-7.
301. Li W, Lee M-H, Henderson L, Tyagi R, Bachani M, Steiner J, et al. Human endogenous retrovirus-K contributes to motor neuron disease. Sci Transl Medicine. 2015;7(307):307ra153-307ra153.
302. Boillee S, Yamanaka K, Lobsiger CS, Copeland NG, Jenkins NA, Kassiotis G, et al. Onset and progression in inherited ALS determined by motor neurons and microglia. Science. 2006;312:1389-92.
303. Nagai M. Rats expressing human cytosolic copper-zinc superoxide dismutase transgenes with amyotrophic lateral sclerosis: associated mutations develop motor neuron disease. J Neurosci. 2001;21:9246-54.
304. Haidet-Phillips AM, Hester ME, Miranda CJ, Meyer K, Braun L, Frakes A, et al. Astrocytes from familial and sporadic ALS patients are toxic to motor neurons. Nat Biotech. 2011;29(9):824-8.
305. Yamanaka K, Chun SJ, Boillee S, Fujimori-Tonou N, Yamashita H, Gutmann DH, et al. Astrocytes as determinants of disease progression in inherited amyotrophic lateral sclerosis. Nat Neurosci. 2008;11(3):251-3.
306. Lino MM, Schneider C, Caroni P. Accumulation of SOD1 mutants in postnatal motoneurons does not cause motoneuron pathology or motoneuron disease. J Neurosci. 2002;22(12):4825-32.
307. Pramatarova A, Laganiere J, Roussel J, Brisebois K, Rouleau GA. Neuron-specific expression of mutant superoxide dismutase 1 in transgenic mice does not lead to motor impairment. J Neurosci. 2001;21(10):3369-74.
308. Gong YH, Parsadanian AS, Andreeva A, Snider WD, Elliott JL. Restricted expression of G86R Cu/Zn superoxide dismutase in astrocytes results in astrocytosis but does not cause motoneuron degeneration. J Neurosci. 2000;20(2):660-5.

309. Ferraiuolo L, Higginbottom A, Heath PR, Barber S, Greenald D, Kirby J, et al. Dysregulation of astrocyte-motoneuron cross-talk in mutant superoxide dismutase 1-related amyotrophic lateral sclerosis. Brain. 2011;134(Pt 9):2627-41.
310. Barker AT, Jalinous R, Freeston IL. Non-invasive magnetic stimulation of human motor cortex. Lancet. 1985;1(8437):1106-7.
311. Rossini PM, Barker AT, Berardelli A, Caramia MD, Caruso G, Cracco RQ, et al. Non-invasive electrical and magnetic stimulation of the brain, spinal cord and roots: basic principles and procedures for routine clinical application. Report of an IFCN committee. Electroencephalogr Clin Neurophysiol. 1994;91(2):79-92.
312. Chen R, Cros D, Curra A, Di Lazzaro V, Lefaucheur JP, Magistris MR, et al. The clinical diagnostic utility of transcranial magnetic stimulation: report of an IFCN committee. Clin Neurophysiol. 2008;119:504-32.
313. Abdeen MA, Stuchly MA. Modeling of magnetic field stimulation of bent neurons. IEEE Trans Biomed Eng. 1994;41(11):1092-5.
314. Mills K. Magnetic stimulation and central conduction time. Eisen A, editor. Amsterdam: Elsevier B.V.; 2004. 283-93 p.
315. Patton HD, Amassian VE. Single and multiple-unit analysis of cortical stage of pyramidal tract activation. J Neurophysiol. 1954;17(4):345-63.
316. Di Lazzaro V, Profice P, Ranieri F, Capone F, Dileone M, Oliviero A, et al. I-wave origin and modulation. Brain Stim. 2012;5(4):512-25.
317. Rudiak D, Marg E. Finding the depth of magnetic brain stimulation: a re-evaluation. Electroencephalogr Clin Neurophysiol. 1994;93(5):358-71.
318. Kaneko K, Fuchigami Y, Morita H, Ofuji A, Kawai S. Effect of coil position and stimulus intensity in transcranial magnetic stimulation on human brain. J Neurol Sci. 1997;147(2):155-9.
319. Di Lazzaro V, Oliviero A, Profice P, Saturno E, Pilato F, Insola A, et al. Comparison of descending volleys evoked by transcranial magnetic and electric stimulation in conscious humans. Electroencephalography and Clinical Neurophysiology/Electromyography and Motor Control. 1998;109(5):397-401.
320. Werhahn KJ, Fong JK, Meyer BU, Priori A, Rothwell JC, Day BL, et al. The effect of magnetic coil orientation on the latency of surface EMG and single motor unit responses in the first dorsal interosseous muscle. Electroencephalogr Clin Neurophysiol. 1994;93(2):138-46.
321. Kaneko K, Kawai S, Fuchigami Y, Morita H, Ofuji A. The effect of current direction induced by transcranial magnetic stimulation on the corticospinal excitability in human brain. Electroencephalogr Clin Neurophysiol. 1996;101(6):478-82.
322. Sakai K, Ugawa Y, Terao Y, Hanajima R, Furubayashi T, Kanazawa I. Preferential activation of different I waves by transcranial magnetic stimulation with a figure-of-eight-shaped coil. Exp Brain Res. 1997;113(1):24-32.
323. Di Lazzaro V, Oliviero A, Mazzone P, Pilato F, Saturno E, Dileone M, et al. Generation of I waves in the human: spinal recordings. Supplements to Clinical Neurophysiology. 2003;56:143-52.
324. Di Lazzaro V, Oliviero A, Pilato F, Mazzone P, Insola A, Ranieri F, et al. Corticospinal volleys evoked by transcranial stimulation of the brain in conscious humans. Neurological Research. 2003;25(2):143-50.

325. Day BL, Dressler D, Maertens de Noordhout A, Marsden CD, Nakashima K, Rothwell JC, et al. Electric and magnetic stimulation of human motor cortex: surface EMG and single motor unit responses. J Physiol (Lond). 1989;412:449-73.
326. Ziemann U, Rothwell JC. I-waves in motor cortex. J Clin Neurophysiol. 2000;17(4):397-405.
327. Rossini PM, Berardelli A, Deuschl G, Hallett M, Maertens de Noordhout AM, Paulus W, et al. Applications of magnetic cortical stimulation. The International Federation of Clinical Neurophysiology. Electroencephalogr Clin Neurophysiol Suppl. 1999;52:171-85.
328. Fisher RJ, Nakamura Y, Bestmann S, Rothwell JC, Bostock H. Two phases of intracortical inhibition revealed by transcranial magnetic threshold tracking. Exp Brain Res. 2002;143:240-8.
329. Vucic S, Howells J, Trevillion L, Kiernan MC. Assessment of cortical excitability using threshold tracking techniques. Muscle Nerve. 2006;33:477-86.
330. Groppa S, Oliviero A, Eisen A, Quartarone A, Cohen LG, Mall V, et al. A practical guide to diagnostic transcranial magnetic stimulation: report of an IFCN committee. Clin Neurophysiol. 2012;123(5):858-82.
331. Brouwer B, Ashby P. Corticospinal projections to upper and lower limb spinal motoneurons in man. Electroencephalogr Clin Neurophysiol. 1990;76(6):509-19.
332. Chen R, Tam A, Butefisch C, Corwell B, Ziemann U, Rothwell JC, et al. Intracortical inhibition and facilitation in different representations of the human motor cortex. J Neurophysiol. 1998;80(6):2870-81.
333. Macdonell RA, Shapiro BE, Chiappa KH, Helmers SL, Cros D, Day BJ, et al. Hemispheric threshold differences for motor evoked potentials produced by magnetic coil stimulation. Neurology. 1991;41(9):1441-4.
334. Triggs WJ, Calvanio R, Levine M. Transcranial magnetic stimulation reveals a hemispheric asymmetry correlate of intermanual differences in motor performance. Neuropsychologia. 1997;35(10):1355-63.
335. Amassian VE, Stewart M, Quirk GJ, Rosenthal JL. Physiological basis of motor effects of a transient stimulus to cerebral cortex. Neurosurgery. 1987;20(1):74-93.
336. Epstein CM, Schwartzberg DG, Davey KR, Sudderth DB. Localizing the site of magnetic brain stimulation in humans. Neurology. 1990;40(4):666-70.
337. Di Lazzaro V, Oliviero A, Profice P, Pennisi MA, Pilato F, Zito G, et al. Ketamine increases human motor cortex excitability to transcranial magnetic stimulation. Journal of Physiology. 2003;547(Pt 2):485-96.
338. Ziemann U. TMS and drugs. Clin Neurophysiol. 2004(115):1717-29.
339. Mavroudakis N, Caroyer JM, Brunko E, Zegers de Beyl D. Effects of diphenylhydantoin on motor potentials evoked with magnetic stimulation. Electroencephalogr Clin Neurophysiol. 1994;93(6):428-33.
340. Boroojerdi B, Battaglia F, Muellbacher W, Cohen LG. Mechanisms influencing stimulus-response properties of the human corticospinal system. Clin Neurophysiol. 2001;112(5):931-7.
341. Rossini PM, Desiato M, Lavaroni F, Caramia M. Brain excitability and electroencephalographic activation: non-invasive evaluation in healthy humans via transcranial magnetic stimulation. Brain Research. 1991;567(1):111-9.
342. Attarian S, Azulay JP, Lardillier D, Verschueren A, Pouget J. Transcranial magnetic stimulation in lower motor neuron diseases. Clin Neurophysiol. 2005;116:35-42.

343. Berardelli A, Inghilleri M, Cruccu G, Mercuri B, Manfredi M. Electrical and magnetic transcranial stimulation in patients with corticospinal damage due to stroke or motor neurone disease. Electroencephalogr Clin Neurophysiol. 1991;81(5):389-96.
344. de Carvalho M, Turkman A, Swash M. Motor responses evoked by transcranial magnetic stimulation and peripheral nerve stimulation in the ulnar innervation in amyotrophic lateral sclerosis: the effect of upper and lower motor neuron lesion. J Neurol Sci. 2003;210(1-2):83-90.
345. Miscio G, Pisano F, Mora G, Mazzini L. Motor neuron disease: usefulness of transcranial magnetic stimulation in improving the diagnosis. Clin Neurophysiol. 1999;110(5):975-81.
346. Triggs WJ, Macdonell RA, Cros D, Chiappa KH, Shahani BT, Day BJ. Motor inhibition and excitation are independent effects of magnetic cortical stimulation. Annals of Neurol. 1992;32(3):345-51.
347. Triggs WJ, Menkes D, Onorato J, Yan RS, Young MS, Newell K, et al. Transcranial magnetic stimulation identifies upper motor neuron involvement in motor neuron disease. Neurology. 1999;53:605-11.
348. Urban P, Wicht S, Hopf H. Sensitivity of transcranial magnetic stimulation of cortico-bulbar vs. cortico-spinal tract involvement in ALS. J Neurol. 2001;248(248):850-5.
349. Kohara N, Kaji R, Kojima Y, Mills KR, Fujii H, Hamano T, et al. Abnormal excitability of the corticospinal pathway in patients with amyotrophic lateral sclerosis: a single motor unit study using transcranial magnetic stimulation. Electroencephalogr Clin Neurophysiol. 1996;101(1):32-41.
350. Mills KR, Nithi KA. Corticomotor threshold is reduced in early sporadic amyotrophic lateral sclerosis. Muscle Nerve. 1997;20:1137-41.
351. Hirota N, Eisen A, Weber M. Complex fasciculations and their origin in amyotrophic lateral sclerosis and Kennedy's disease. Muscle Nerve. 2000;23:1872-5.
352. Di Lazzaro V, Restuccia D, Oliviero A, Profice P, Ferrara L, Insola A, et al. Magnetic transcranial stimulation at intensities below active motor threshold activates intracortical inhibitory circuits. Exp Brain Res. 1998;119:265-8.
353. Devanne H, Lavoie BA, Capaday C. Input-output properties and gain changes in the human corticospinal pathway. Exp Brain Res. 1997;114(2):329-38.
354. Ziemann U. Cortical threshold and excitability measurements. In: Eisen A, editor. Clinical Neurophysiology of Motor Neuron Diseases Handbook of Clinical Neurophysiology. Amsterdam: Elsevier; 2004. p. 317-35.
355. Hess CW, Mills KR, Murray NM, Schriefer TN. Magnetic brain stimulation: central motor conduction studies in multiple sclerosis. Ann Neurol. 1987;22(6):744-52.
356. Paulus W, Classen J, Cohen LG, Large CH, Di Lazzaro V, Nitsche M, et al. State of the art: Pharmacologic effects on cortical excitability measures tested by transcranial magnetic stimulation. Brain Stimul. 2008;1(3):151-63.
357. Vucic S, Cheah BC, Yiannikas C, Vincent A, Kiernan MC. Corticomotoneuronal function and hyperexcitability in acquired neuromyotonia. Brain. 2010;133(9):2727-33.
358. Mills K. Magnetic stimulation and central conduction time. In: A E, editor. Clinical Neurophysiology of Motor Neuron Diseases Handbook of Clinical Neurophysiology. Amsterdam: Elsevier; 2004. p. 283-93.
359. Claus D. Central motor conduction: method and normal results. Muscle Nerve. 1990;13(12):1125-32.

360. Mills KR, Murray NM. Electrical stimulation over the human vertebral column: which neural elements are excited? Electroencephalogr Clin Neurophysiol. 1986;63(6):582-9.
361. Mills KR. The natural history of central motor abnormalities in amyotrophic lateral sclerosis. Brain 2003;126:2558-66.
362. Eisen A, Entezari-Taher M, Stewart H. Cortical projections to spinal motoneurons: changes with aging and amyotrophic lateral sclerosis. Neurology. 1996;46(5):1396-404.
363. Cantello R, Gianelli M, Civardi C, Mutani R. Magnetic brain stimulation: the silent period after the motor evoked potential. Neurology. 1992;42(10):1951-9.
364. Inghilleri M, Berardelli A, Cruccu G, Manfredi M. Silent period evoked by transcranial stimulation of the human cortex and cervicomedullary junction. J Physiol (Lond). 1993;466:521-34.
365. Triggs WJ, Kiers L, Cros D, Fang J, Chiappa KH. Facilitation of magnetic motor evoked potentials during the cortical stimulation silent period. Neurology. 1993;43(12):2615-20.
366. Cantello R, Gianelli M, Civardi C, Mutani R. Magnetic brain stimulation: the silent period after the motor evoked potential. Neurology. 1992;42:1951-9.
367. Connors BW, Malenka RC, Silva LR. Two inhibitory postsynaptic potentials, and GABAA and GABAB receptor-mediated responses in neocortex of rat and cat. J Physiol (Lond). 1988;406:443-68.
368. Siebner HR, Dressnandt J, Auer C, Conrad B. Continuous intrathecal baclofen infusions induced a marked increase of the transcranially evoked silent period in a patient with generalized dystonia. Muscle Nerve. 1998;21(9):1209-12.
369. Werhahn KJ, Kunesch E, Noachtar S, Benecke R, Classen J. Differential effects on motorcortical inhibition induced by blockade of GABA uptake in humans. J Physiol (Lond). 1999;517:591-7.
370. Kornau H-C. GABAB receptors and synaptic modulation. Cell and tissue research. 2006;326(2):517-33.
371. Wu LG, Saggau P. Presynaptic inhibition of elicited neurotransmitter release. Trends Neurosci. 1997;20(5):204-12.
372. Takahashi T, Kajikawa Y, Tsujimoto T. G-Protein-coupled modulation of presynaptic calcium currents and transmitter release by a GABAB receptor. J Neurosci. 1998;18(9):3138-46.
373. Filippov AK, Couve A, Pangalos MN, Walsh FS, Brown DA, Moss SJ. Heteromeric assembly of GABA(B)R1 and GABA(B)R2 receptor subunits inhibits Ca(2+) current in sympathetic neurons. J Neurosci. 2000;20(8):2867-74.
374. Priori A, Berardelli A, Inghilleri M, Accornero N, Manfredi M. Motor cortical inhibition and the dopaminergic system. Pharmacological changes in the silent period after transcranial brain stimulation in normal subjects, patients with Parkinson's disease and drug-induced parkinsonism. Brain. 1994;117:317-23.
375. Ziemann U, Bruns D, Paulus W. Enhancement of human motor cortex inhibition by the dopamine receptor agonist pergolide: evidence from transcranial magnetic stimulation. Neurosci Lett. 1996;208(3):187-90.
376. Siciliano G, Manca ML, Sagliocco L, Pastorini E, Pellegrinetti A, Sartucci F, et al. Cortical silent period in patients with amyotrophic lateral sclerosis. J Neurol Sci. 1999;169(1-2):93-7.
377. Wittstock M, Wolters A, Benecke R. Transcallosal inhibition in amyotrophic lateral sclerosis. Clin Neurophysiol. 2007;118(2):301-7.

378. Kujirai T, Caramia MD, Rothwell JC, Day BL, Thompson PD, Ferbert A, et al. Corticocortical inhibition in human motor cortex. J Physiol (Lond). 1993;471:501-19.
379. Hanajima R, Ugawa Y, Terao Y, Sakai K, Furubayashi T, Machii K, et al. Paired-pulse magnetic stimulation of the human motor cortex: differences among I waves. J Physiol (Lond). 1998;509:607-18.
380. Nakamura H, Kitagawa H, Kawaguchi Y, Tsuji H. Intracortical facilitation and inhibition after transcranial magnetic stimulation in conscious humans. J Physiol (Lond). 1997;498:817-23.
381. Di Lazzaro V, Oliviero A, Meglio M, Cioni B, Tamburrini G, Tonali P, et al. Direct demonstration of the effect of lorazepam on the excitability of the human motor cortex. Clin Neurophysiol. 2000;111(5):794-9.
382. Bormann J. Electrophysiology of GABAA and GABAB receptor subtypes. Trends Neurosci. 1988;11(3):112-6.
383. Macdonald RL, Olsen RW. GABAA receptor channels. Annu Rev Neurosci. 1994;17:569-602.
384. Mohler H. GABA(A) receptor diversity and pharmacology. Cell Tissue Res. 2006;326(2):505-16.
385. Barnard EA, Skolnick P, Olsen RW, Mohler H, Sieghart W, Biggio G, et al. International Union of Pharmacology. XV. Subtypes of gamma-aminobutyric acidA receptors: classification on the basis of subunit structure and receptor function. Pharmacol Rev. 1998;50(2):291-313.
386. Rudolph U, Mohler H. GABA-based therapeutic approaches: GABAA receptor subtype functions. Curr Opin Pharmacol. 2006;6(1):18-23.
387. Di Lazzaro V, Pilato F, Dileone M, Profice P, Ranieri F, Ricci V, et al. Segregating two inhibitory circuits in human motor cortex at the level of GABAA receptor subtypes: A TMS study. Clin Neurophysiol. 2007;118(10):2207-14.
388. Stefan K, Kunesch E, Benecke R, Classen J. Effects of riluzole on cortical excitability in patients with amyotrophic lateral sclerosis. Ann Neurol. 2001;49:536-9.
389. Schwenkreis P, Liepert J, Witscher K, Fischer W, Weiller C, Malin JP, et al. Riluzole suppresses motor cortex facilitation in correlation to its plasma level. A study using transcranial magnetic stimulation. Exp Brain Res. 2000;135(3):293-9.
390. Ziemann U, Tergau F, Bruns D, Baudewig J, Paulus W. Changes in human motor cortex excitability induced by dopaminergic and anti-dopaminergic drugs. Electroencephalogr Clin Neurophysiol. 1997;105(6):430-7.
391. Ilic TV, Korchounov A, Ziemann U. Complex modulation of human motor cortex excitability by the specific serotonin re-uptake inhibitor sertraline. Neurosci Lett. 2002;319:116-20.
392. Ziemann U, Rothwell JC, Ridding MC. Interaction between intracortical inhibition and facilitation in human motor cortex. J Physiol (Lond). 1996;496:873-81.
393. Kiers L, Cros D, Chiappa KH, Fang J. Variability of motor potentials evoked by transcranial magnetic stimulation. Electroencephalogr Clin Neurophysiol. 1993;89:415-23.
394. Vucic S, Cheah BC, Krishnan AV, Burke D, Kiernan MC. The effects of alterations in conditioning stimulus intensity on short interval intracortical inhibition. Brain Res. 2009(1273das): 39-47.
395. Vucic S, Cheah BC, Kiernan MC. Dissecting the Mechanisms Underlying Short-Interval Intracortical Inhibition Using Exercise. Cereb Cortex. 2011(21):1639-44.

396. Ziemann U, Lonnecker S, Steinhoff BJ, Paulus W. The effect of lorazepam on the motor cortical excitability in man. Exp Brain Res. 1996(109):127-35.
397. Ilic TV, Meintzschel F, Cleff U, Ruge D, Kessler KR, Ziemann U. Short-interval paired-pulse inhibition and facilitation of human motor cortex: the dimension of stimulus intensity. J Physiol (Lond). 2002;545(Pt 1):153-67.
398. Di Lazzaro V, Pilato F, Dileone M, Ranieri F, Ricci V, Profice P, et al. GABAA receptor subtype specific enhancement of inhibition in human motor cortex. J Physiol. 2006;575(Pt 3):721-6.
399. Hanajima R, Furubayashi T, Iwata NK, Shiio Y, Okabe S, Kanazawa I, et al. Further evidence to support different mechanisms underlying intracortical inhibition of the motor cortex. Exp Brain Res. 2003;151(4):427-34.
400. Roshan L, Paradiso GO, Chen R. Two phases of short-interval intracortical inhibition. Exp Brain Res. 2003;151(3):330-7.
401. Hanajima R, Ugawa Y, Terao Y, Ogata K, Kanazawa I. Ipsilateral cortico-cortical inhibition of the motor cortex in various neurological disorders J Neurol Sci 1996(140):109-16.
402. Yokota T, Yoshino A, Inaba A, Saito Y. Double cortical stimulation in amyotrophic lateral sclerosis. J Neurol Neurosurg Psychiatry. 1996;61:596-600.
403. Ziemann U, Winter M, Reimers CD, Reimers K, Tergau F, Paulus W. Impaired motor cortex inhibition in patients with amyotrophic lateral sclerosis. Evidence from paired transcranial magnetic stimulation. Neurology. 1997;49(5):1292-8.
404. Sommer M, Tergau F, Wischer S, Reimers CD, Beuche W, Paulus W. Riluzole does not have an acute effect on motor thresholds and the intracortical excitability in amyotrophic lateral sclerosis. J Neurol. 1999;246 Suppl 3:III22-6.
405. Blair IP, Williams KL, Warraich ST, Durnall JC, Thoeng AD, Manavis J, et al. FUS mutations in amyotrophic lateral sclerosis: clinical, pathological, neurophysiological and genetic analysis. J Neurol Neurosurg Psychiatry. 2010;81:1286-8.
406. Nihei K, McKee AC, Kowall NW. Patterns of neuronal degeneration in the motor cortex of amyotrophic lateral sclerosis patients. Acta Neuropathologica. 1993;86(1):55-64.
407. Vucic S, Cheah BC, Kiernan MC. Defining the mechanisms that underlie cortical hyperexcitability in amyotrophic lateral sclerosis. Exp Neurol. 2009;220:177-82.
408. Bostock H, Cikurel K, Burke D. Threshold tracking techniques in the study of human peripheral nerve. Muscle Nerve. 1998;21(2):137-58.
409. Burke D, Kiernan MC, Bostock H. Excitability of human axons. Clin Neurophysiol. 2001;112:1575-85.
410. Bostock H, Sharief MK, Reid G, Murray NM. Axonal ion channel dysfunction in amyotrophic lateral sclerosis. Brain 1995;118:217-25.
411. Kiernan M, Burke D. Threshold electrotonus in the assessment of Motor Neuron Disease. In: Daube J, Mauguiere F, editors. Handbook of Clinical Neurophysiology. Amsterdam: Elsevier; 2004. p. 359-66.
412. Mogyoros I, Kiernan MC, Burke D, Bostock H. Ischemic resistance of cutaneous afferents and motor axons in patients with amyotrophic lateral sclerosis. Muscle Nerve. 1998;21(12):1692-700.
413. Vucic S, Kiernan MC. Axonal excitability properties in amyotrophic lateral sclerosis. Clin Neurophysiol. 2006;117:1458-66.

414. Baker M, Bostock H. Depolarization changes the mechanism of accommodation in rat and human motor axons. J Physiol (Lond). 1989;411:545-61.
415. Bostock H, Burke D, Hales JP. Differences in behaviour of sensory and motor axons following release of ischaemia. Brain. 1994;117(Pt 2):225-34.
416. Mogyoros I, Kiernan MC, Burke D, Bostock H. Excitability changes in human sensory and motor axons during hyperventilation and ischaemia. Brain. 1997;120(Pt 2):317-25.
417. Grosskreutz J, Lin C, Mogyoros I, Burke D. Changes in excitability indices of cutaneous afferents produced by ischaemia in human subjects. J Physiol (Lond). 1999;518(Pt 1):301-14.
418. Grosskreutz J, Lin CS, Mogyoros I, Burke D. Ischaemic changes in refractoriness of human cutaneous afferents under threshold-clamp conditions. J Physiol (Lond). 2000;523:807-15.
419. Bostock H. The strength-duration relationship for excitation of myelinated nerve: computed dependence on membrane parameters. J Physiol (Lond). 1983;341:59-74.
420. Mogyoros I, Kiernan MC, Burke D. Strength-duration properties of human peripheral nerve. Brain. 1996;119(2):439-47.
421. Mogyoros I, Lin C, Dowla S, Grosskreutz J, Burke D. Strength-duration properties and their voltage dependence at different sites along the median nerve. Clin Neurophysiol. 1999;110(9):1618-24.
422. Weiss G. Sur la possibilité de rendre comparables entre eux les appareils servant l'excitation électrique. Arch Ital Biol. 1901;35:413-46.
423. Bostock H, Rothwell JC. Latent addition in motor and sensory fibres of human peripheral nerve. J Physiol (Lond). 1997;498(Pt 1):277-94.
424. French CR, Sah P, Buckett KJ, Gage PW. A voltage-dependent persistent sodium current in mammalian hippocampal neurons. J Gen Physiol. 1990;95:1139-57.
425. Crill WE. Persistent sodium current in mammalian central neurons. Annu Rev Physiol. 1996;58:349-62.
426. Catterall WA. From ionic currents to molecular mechanisms: the structure and function of voltage-gated sodium channels. Neuron. 2000;26(1):13-25.
427. Catterall WA, Goldin AL, Waxman SG. International Union of Pharmacology. XLVII. Nomenclature and structure-function relationships of voltage-gated sodium channels. Pharmacol Rev. 2005;57:397-409.
428. Baker MD, Bostock H. Inactivation of macroscopic late Na+ current and characteristics of unitary late Na+ currents in sensory neurons. J Neurophysiol. 1998;80:2538-49.
429. Catterall WA. Voltage-gated sodium channels at 60: structure, function and pathophysiology. J Physiol. 2012;590(11):2577-89.
430. Goldin AL. Resurgence of sodium channel research. Annu Rev Physiol. 2001;63:871-94.
431. Brown AM, Schwindt PC, Crill WE. Different voltage dependence of transient and persistent Na+ currents is compatible with modal-gating hypothesis for sodium channels. J Neurophysiol. 1994;71:2562-5.
432. Chen Y, Yu FH, Surmeier DJ, Scheuer T, Catterall WA. Neuromodulation of Na+ channel slow inactivation via cAMP-dependent protein kinase and protein kinase C. Neuron. 2006;49(3):409-20.
433. Carr DB, Day M, Cantrell AR, Held J, Scheuer T, Catterall WA, et al. Transmitter modulation of slow, activity-dependent alterations in sodium channel availability endows neurons with a novel form of cellular plasticity. Neuron. 2003;39(5):793-806.

434. Brismar T. Electrical properties of isolated demyelinated rat nerve fibres. Acta Physiol Scand. 1981;113(2):161-6.
435. Mogyoros I, Kiernan MC, Gracies JM, Burke D. The effect of stimulus duration on the latency of submaximal nerve volleys. Muscle Nerve. 1996;19(10):1354-6.
436. Kiernan MC, Krishnan AV, Lin CS, Burke D, Berkovic SF. Mutation in the Na+ channel subunit SCN1B produces paradoxical changes in peripheral nerve excitability. Brain. 2005;128(Pt 8):1841-6.
437. Kuo JJ, Siddique T, Fu R, Heckman CJ. Increased persistent Na(+) current and its effect on excitability in motoneurones cultured from mutant SOD1 mice. J Physiol (Lond). 2005;563(Pt 3):843-54.
438. Kanai K, Kuwabara S, Arai K, Sung JY, Ogawara K, Hattori T. Muscle cramp in Machado-Joseph disease: altered motor axonal excitability properties and mexiletine treatment. Brain. 2003;126:965-73.
439. Shibuya K, Misawa S, Nasu S, Sekiguchi Y, Mitsuma S, Beppu M, et al. Split hand syndrome in amyotrophic lateral sclerosis: different excitability changes in the thenar and hypothenar motor axons. J Neurol Neurosurg Psychiatry. 2013;84(9):969-72.
440. Stys PK, Waxman SG, Ransom BR. Na(+)-Ca2+ exchanger mediates Ca2+ influx during anoxia in mammalian central nervous system white matter. Ann Neurol. 1991;30(3):375-80.
441. Stys PK, Sontheimer H, Ransom BR, Waxman SG. Noninactivating, tetrodotoxin-sensitive Na+ conductance in rat optic nerve axons. Proc Natl Acad Sci U S A. 1993;90(15):6976-80.
442. Bostock H, Baker M. Evidence for two types of potassium channel in human motor axons in vivo. Brain Research. 1988;462(2):354-8.
443. Kiernan MC, Burke, D. Threshold electronus and the assessment of nerve excitability in amyotrophic lateral sclerosis. In: Eisen A, editor. Clinical Neurophysiology of Motor Neuron Diseases. Amsterdam: Elsevier; 2004. p. 359-66.
444. Kiernan MC, Burke D, Andersen KV, Bostock H. Multiple measures of axonal excitability: a new approach in clinical testing. Muscle Nerve. 2000;23(3):399-409.
445. Kiernan MC, Lin CS, Andersen KV, Murray NM, Bostock H. Clinical evaluation of excitability measures in sensory nerve. Muscle Nerve. 2001;24(7):883-92.
446. Krishnan AV, Lin CS, Park SB, Kiernan MC. Axonal ion channels from bench to bedside: a translational neuroscience perspective. Prog Neurobiol. 2009;89(3):288-313.
447. Pape HC. Queer current and pacemaker: the hyperpolarization-activated cation current in neurons. Annu Rev Physiol. 1996;58:299-327.
448. Yu FH, Yarov-Yarovoy V, Gutman GA, Catterall WA. Overview of molecular relationships in the voltage-gated ion channel superfamily. Pharmacol Rev. 2005;57:387-95.
449. Judge SI, Bever CT, Jr. Potassium channel blockers in multiple sclerosis: neuronal Kv channels and effects of symptomatic treatment. Pharmacol Ther. 2006;111:224-59.
450. Baker M, Bostock H, Grafe P, Martius P. Function and distribution of three types of rectifying channel in rat spinal root myelinated axons. J Physiol (Lond). 1987;383:45-67.
451. Gordon TR, Kocsis JD, Waxman SG. Evidence for the presence of two types of potassium channels in the rat optic nerve. Brain Res. 1988;447(1):1-9.
452. Safronov BV, Bischoff U, Vogel W. Single voltage-gated K+ channels and their functions in small dorsal root ganglion neurones of rat. J Physiol (Lond). 1996;493:393-408.

453. Safronov BV, Kampe K, Vogel W. Single voltage-dependent potassium channels in rat peripheral nerve membrane. J Physiol (Lond). 1993;460:675-91.
454. Roper J, Schwarz JR. Heterogeneous distribution of fast and slow potassium channels in myelinated rat nerve fibres. J Physiol (Lond). 1989;416:93-110.
455. Chiu SY, Ritchie JM. On the physiological role of internodal potassium channels and the security of conduction in myelinated nerve fibres. Proc R Soc Lond B Biol Sci. 1984;220(1221):415-22.
456. Kiernan MC, Bostock H. Effects of membrane polarization and ischaemia on the excitability properties of human motor axons. Brain. 2000;123:2542-51.
457. Kiernan MC, Guglielmi JM, Kaji R, Murray NM, Bostock H. Evidence for axonal membrane hyperpolarization in multifocal motor neuropathy with conduction block. Brain. 2002;125(Pt 3):664-75.
458. Kiernan MC, Walters RJ, Andersen KV, Taube D, Murray NM, Bostock H. Nerve excitability changes in chronic renal failure indicate membrane depolarization due to hyperkalaemia. Brain. 2002;125(Pt 6):1366-78.
459. Krishnan AV, Kiernan MC. Altered nerve excitability properties in established diabetic neuropathy. Brain. 2005;128(Pt 5):1178-87.
460. Krishnan AV, Phoon RK, Pussell BA, Charlesworth JA, Bostock H, Kiernan MC. Altered motor nerve excitability in end-stage kidney disease. Brain. 2005;128(Pt 9):2164-74.
461. Krishnan AV, Phoon RK, Pussell BA, Charlesworth JA, Bostock H, Kiernan MC. Neuropathy, axonal Na(+)/K(+) pump function and activity-dependent excitability changes in end-stage kidney disease. Clin Neurophysiol. 2006.
462. Krishnan AV, Phoon RK, Pussell BA, Charlesworth JA, Kiernan MC. Sensory nerve excitability and neuropathy in end stage kidney disease. J Neurol Neurosurg Psychiatry. 2006;77(4):548-51.
463. Park SB, Lin CS-Y, Krishnan AV, Goldstein D, Friedlander ML, Kiernan MC. Oxaliplatin-induced neurotoxicity: changes in axonal excitability precede development of neuropathy. Brain. 2009;132(10):2712-23.
464. Mayer M, Westbrook G. A voltage-clamp analysis of inward (anomalous) rectification in mouse spinal sensory ganglion neurones. The Journal of physiology. 1983;340(1):19-45.
465. Pape H-C. Queer current and pacemaker: the hyperpolarization-activated cation current in neurons. Annual Review of Physiology. 1996;58(1):299-327.
466. Jan LY, Jan YN. Voltage-gated and inwardly rectifying potassium channels. The Journal of physiology. 1997;505(2):267-82.
467. Baker M, Bostock H, Grafe P, Martius P. Function and distribution of three types of rectifying channel in rat spinal root myelinated axons. The Journal of physiology. 1987;383(1):45-67.
468. Bader C, Bertrand D. Effect of changes in intra-and extracellular sodium on the inward (anomalous) rectification in salamander photoreceptors. The Journal of physiology. 1984;347(1):611-31.
469. Bayliss DA, Viana F, Bellingham MC, Berger AJ. Characteristics and postnatal development of a hyperpolarization-activated inward current in rat hypoglossal motoneurons in vitro. Journal of Neurophysiology. 1994;71(1):119-28.

470. Vagg R, Mogyoros I, Kiernan MC, Burke D. Activity-dependent hyperpolarization of human motor axons produced by natural activity. The Journal of physiology. 1998;507(3):919-25.
471. Kaji R, Bostock H, Kohara N, Murase N, Kimura J, Shibasaki H. Activity-dependent conduction block in multifocal motor neuropathy. Brain. 2000;123(8):1602-11.
472. Cappelen-Smith C, Kuwabara S, Lin CSY, Mogyoros I, Burke D. Activity-dependent hyperpolarization and conduction block in chronic inflammatory demyelinating polyneuropathy. Annals of neurology. 2000;48(6):826-32.
473. Kiernan MC, Lin CSY, Burke D. Differences in activity-dependent hyperpolarization in human sensory and motor axons. The Journal of physiology. 2004;558(1):341-9.
474. Lin CS, Kuwabara S, Cappelen-Smith C, Burke D. Responses of human sensory and motor axons to the release of ischaemia and to hyperpolarizing currents. The Journal of physiology. 2002;541(3):1025-39.
475. Hodgkin A, Huxley A. A quantitative descirption of membrane current and its application to conduction and excitation in nerve. J Physiol (Lond). 1952(117):500-44.
476. Scholz A, Reid G, Vogel W, Bostock H. Ion channels in human axons. J Neurophysiol. 1993;70:1274-9.
477. Burke D, Kiernan M, Mogyoros I, Bostock H. Susceptibility to conduction block: differences in the biophysical properties of cutaneous afferents and motor axons. Physiology of ALS and Related Diseases. 1997:43-53.
478. Kiernan MC, Cikurel K, Bostock H. Effects of temperature on the excitability properties of human motor axons. Brain. 2001;124(4):816-25.
479. Barrett EF, Barrett JN. Intracellular recording from vertebrate myelinated axons: mechanism of the depolarizing afterpotential. J Physiol (Lond). 1982;323:117-44.
480. McIntyre CC, Richardson AG, Grill WM. Modeling the excitability of mammalian nerve fibers: influence of afterpotentials on the recovery cycle. J Neurophysiol. 2002;87(2):995-1006.
481. Jonas P, Brau ME, Hermsteiner M, Vogel W. Single-channel recording in myelinated nerve fibers reveals one type of Na channel but different K channels. Proc Natl Acad Sci U S A. 1989;86:7238-42.
482. Vabnick I, Shrager P. Ion channel redistribution and function during development of the myelinated axon. J Neurobiol. 1998;37(1):80-96.
483. Reid G, Scholz A, Bostock H, Vogel W. Human axons contain at least five types of voltage-dependent potassium channel. J Physiol (Lond). 1999;518:681-96.
484. Barrett EF, Barrett JN. Intracellular recording from vertebrate myelinated axons: mechanism of the depolarizing afterpotential. The Journal of physiology. 1982;323(1):117-44.
485. Krishnan AV, Phoon RK, Pussell BA, Charlesworth JA, Bostock H, Kiernan MC. Altered motor nerve excitability in end-stage kidney disease. Brain. 2005;128(9):2164-74.
486. Ziemann U, Lönnecker S, Steinhoff B, Paulus W. Effects of antiepileptic drugs on motor cortex excitability in humans: a transcranial magnetic stimulation study. Annals of neurology. 1996;40(3):367-78.
487. Ziemann U, Tergau F, Bruns D, Baudewig J, Paulus W. Changes in human motor cortex excitability induced by dopaminergic and anti-dopaminergic drugs. Electroencephalography and Clinical Neurophysiology/Electromyography and Motor Control. 1997;105(6):430-7.
488. Ziemann U. Pharmacology of TMS. Clin Neurophysiol. 2003(56):226-31.

489. Fisher R, Nakamura Y, Bestmann S, Rothwell J, Bostock H. Two phases of intracortical inhibition revealed by transcranial magnetic threshold tracking. Experimental Brain Research. 2002;143(2):240-8.
490. Di Lazzaro V, Oliviero A, Profice P, Ferrara L, Saturno E, Pilato F, et al. The diagnostic value of motor evoked potentials. Clinical Neurophysiology. 1999;110(7):1297-307.
491. Mills K, Murray N, Hess C. Magnetic and electrical transcranial brain stimulation: physiological mechanisms and clinical applications. Neurosurgery. 1987;20(1):164-8.
492. Cantello R, Gianelli M, Civardi C, Mutani R. Magnetic brain stimulation The silent period after the motor evoked potential. Neurology. 1992;42(10):1951-.
493. Bostock H, Baker M. Evidence for two types of potassium channel in human motor axons in vivo. Brain Research. 1988;462(2):354-8.
494. Bostock H, Rothwell J. Latent addition in motor and sensory fibres of human peripheral nerve. The Journal of physiology. 1997;498(Pt 1):277-94.
495. Cedarbaum JM, Stambler N, Malta E, Fuller C, Hilt D, Thurmond B, et al. The ALSFRS-R: a revised ALS functional rating scale that incorporates assessments of respiratory function. BDNF ALS Study Group (Phase III). J Neurol Sci. 1999;169:13-21.
496. O'Brien MD. Aid to the examination of the peripheral nervous system. 4 ed. London: W.B.Saunders; 2004. p. 1-3.
497. Turner MR, Cagnin A, Turkheimer FE, Miller CC, Shaw CE, Brooks DJ, et al. Evidence of widespread cerebral microglial activation in amyotrophic lateral sclerosis: an [11C](R)-PK11195 positron emission tomography study. Neurobiol Dis. 2004;15(3):601-9.
498. Brooks BR, Miller RG, Swash M, Munsat TL. El Escorial revisited: revised criteria for the diagnosis of amyotrophic lateral sclerosis. Amyotroph Lateral Scler. 2000;1:293-9.
499. Aggarwal S, Cudkowicz M. ALS drug development: reflections from the past and a way forward. Neurotherapeutics. 2008;5(4):516-27.
500. Whiting P, Rutjes A, Reitsma J, Bossuyt P, Kleijnen J. The development of QUADAS: a tool for the quality assessment of studies of diagnostic accuracy included in systematic reviews. BMC Medical Research Methodology. 2003;3(1):25.
501. Macaskill P, Gatsonis C, Deeks J, Harbord R, Takwoingi Y. Chapter 10: Analysing and Presenting Results http://srdta.cochrane.org/: The Cochrane Collaboration; 2010.
502. Noto YI, Misawa S, Kanai K, Shibuya K, Isose S, Nasu S, et al. Awaji ALS criteria increase the diagnostic sensitivity in patients with bulbar onset. Clin Neurophysiol. 2012;123:382-5.
503. Misawa S, Noto Y, Shibuya K, Isose S, Sekiguchi Y, Nasu S, et al. Ultrasonographic detection of fasciculations markedly increases diagnostic sensitivity of ALS. Neurology. 2011;77(16):1532-7.
504. Geevasinga N, Menon P, Yiannikas C, Kiernan MC, Vucic S. Diagnostic utility of cortical excitability studies in amyotrophic lateral sclerosis. Eur J Neurol. 2014;21:1451-7.
505. Bresch S, Delmon E, Soriani MH, Desnuelle C. Electrodiagnostic criteria for early diagnosis of bulbar-onset ALS: a comparison of El Escorial, revised El Escorial and Awaji algorithm. Rev Neurol (Paris). 2014;170:134-9.
506. Nzwalo H, de Abreu D, Swash M, Pinto S, de Carvalho M. Delayed diagnosis in ALS: The problem continues. J Neurol Sci. 2014;343(1–2):173-5.
507. Benatar M, Tandan R. The Awaji criteria for the diagnosis of amyotrophic lateral sclerosis: Have we put the cart before the horse? Muscle Nerve. 2011;43(4):461-3.

508. Stewart LA, Parmar MKB. Meta-analysis of the literature or of individual patient data: is there a difference? The Lancet. 1993;341(8842):418-22.
509. Jeng GT, Scott JR, Burmeister LF. A comparison of meta-analytic results using literature vs individual patient data: Paternal cell immunization for recurrent miscarriage. JAMA. 1995;274(10):830-6.
510. Menon P, Geevasinga N, Yiannikas C, Howells J, Kiernan M, Vucic S. The sensitivity and specificity of threshold-tracking transcranial magnetic stimulation for the diagnosis of amyotrophic lateral sclerosis: a prospective study Lancet Neurol. 2015;14:478-84.
511. Brooks BR. El Escorial World Federation of Neurology criteria for the diagnosis of amyotrophic lateral sclerosis. Subcommittee on Motor Neuron Diseases/Amyotrophic Lateral Sclerosis of the World Federation of Neurology Research Group on Neuromuscular Diseases and the El Escorial "Clinical limits of amyotrophic lateral sclerosis" workshop contributors. J Neurol Sci. 1994;124 Suppl:96-107.
512. Traynor BJ, Alexander M, Corr B, Frost E, Hardiman O. Effect of a multidisciplinary amyotrophic lateral sclerosis (ALS) clinic on ALS survival: a population based study, 1996-2000. J Neurol Neurosurg Psychiatry. 2003;74:1258-61.
513. Cedarbaum J, Stambler N, Malta E, Fuller C, Hilt D, Thurmond B, et al. The ALSFRS-R: a revised ALS functional rating scale that incorporates assessments of respiratory function. Journal of the Neurological Sciences. 1999;169(1-2):13-21.
514. Siao P, Cros D, Vucic S. Practical approach to electromyography. New York: Demos Medical Publishing; 2011.
515. Aggarwal SP, Zinman L, Simpson E, McKinley J, Jackson KE, Pinto H, et al. Safety and efficacy of lithium in combination with riluzole for treatment of amyotrophic lateral sclerosis: a randomised, double-blind, placebo-controlled trial. Lancet Neurol. 2010;9(5):481-8.
516. O'Brien MD. Aid to the examination of the peripheral nervous system. London: W.B.Saunders; 2004. p. 1-3.
517. Mills KR. The natural history of central motor abnormalities in amyotrophic lateral sclerosis. Brain. 2003;126:2558-66.
518. Lemon RN. What drives corticospinal output? F1000 Biol Rep. 2010;2:51.
519. Bossuyt PM, Reitsma JB, Bruns DE, Gatsonis CA, Glasziou PP, Irwig LM, et al. The STARD Statement for Reporting Studies of Diagnostic Accuracy: Explanation and Elaboration. Clin Chem. 2003;49(1):7-18.
520. Bensimon G, Lacomblez L, Delumeau JC, Bejuit R, Truffinet P, Meininger V. A study of riluzole in the treatment of advanced stage or elderly patients with amyotrophic lateral sclerosis. J Neurol. 2002;249(5):609-15.
521. Lomen-Hoerth C, Murphy J, Langmore S, Kramer JH, Olney RK, Miller B. Are amyotrophic lateral sclerosis patients cognitively normal? Neurology. 2003;60(7):1094-7.
522. Donnelly Christopher J, Zhang P-W, Pham Jacqueline T, Haeusler Aaron R, Mistry Nipun A, Vidensky S, et al. RNA Toxicity from the ALS/FTD C9ORF72 Expansion Is Mitigated by Antisense Intervention. Neuron. 2013;80(2):415-28.
523. Wainger Brian J, Kiskinis E, Mellin C, Wiskow O, Han Steve SW, Sandoe J, et al. Intrinsic Membrane Hyperexcitability of Amyotrophic Lateral Sclerosis Patient-Derived Motor Neurons. Cell Rep. 2014;7(1):1-11.

524. Turner MR, Hardiman O, Benatar M, Brooks BR, Chio A, de Carvalho M, et al. Controversies and priorities in amyotrophic lateral sclerosis. The Lancet Neurology. 2013;12(3):310-22.
525. Turner MR, Kiernan MC. Does interneuronal dysfunction contribute to neurodegeneration in amyotrophic lateral sclerosis? Amyotrophic Lateral Sclerosis. 2012;13(3):245-50.
526. Ramesh TM, Shaw PJ, McDearmid J. A zebrafish model exemplifies the long preclinical period of motor neuron disease. J Neurol Neurosurg Psychiatry. 2014;85(11):1288-9.
527. Williams KL, Fifita JA, Vucic S, Durnall JC, Kiernan MC, Blair IP, et al. Pathophysiological insights into ALS with C9ORF72 expansions. J Neurol, Neurosurg & Psychiatry. 2013.
528. Nakata M, Kuwabara S, Kanai K, Misawa S, Tamura N, Sawai S, et al. Distal excitability changes in motor axons in amyotrophic lateral sclerosis. Clin Neurophysiol. 2006;117(7):1444-8.
529. Tamura N, Kuwabara S, Misawa S, Kanai K, Nakata M, Sawai S, et al. Increased nodal persistent Na+ currents in human neuropathy and motor neuron disease estimated by latent addition. Clin Neurophysiol. 2006;117:2451-8.
530. Bostock H, Sharief MK, Reid G, Murray NM. Axonal ion channel dysfunction in amyotrophic lateral sclerosis. Brain. 1995;118:217-25.
531. Kiernan M, Burke D. Threshold electrotonus and the assessment of nerve excitability in amyotrophic lateral sclerosis. In: Eisen A, editor. Clinical Neurophysiology of Motor Neuron Diseases. 4. Amsterdam: Elsevier; 2004. p. 359-66.
532. Menon P, Kiernan MC, Vucic S. ALS pathophysiology: Insights from the split-hand phenomenon. Clinical Neurophysiology. 2014;125(1):186-93.
533. Shibuya K, Misawa S, Nasu S, Sekiguchi Y, Mitsuma S, Beppu M, et al. Split hand syndrome in amyotrophic lateral sclerosis: different excitability changes in the thenar and hypothenar motor axons. Journal of Neurology, Neurosurgery & Psychiatry. 2013.
534. Mogyoros I, Kiernan MC, Burke D. Strength-duration properties of human peripheral nerve. Brain. 1996;119(Pt 2):439-47.
535. Mogyoros I, Kiernan MC, Burke D. Strength-duration properties of sensory and motor axons in carpal tunnel syndrome. Muscle Nerve. 1997;20(4):508-10.
536. Mogyoros I, Lin CS, Kuwabara S, Cappelen-Smith C, Burke D. Strength-duration properties and their voltage dependence as measures of a threshold conductance at the node of Ranvier of single motor axons. Muscle Nerve. 2000;23(11):1719-26.
537. Cedarbaum JM, Stambler N, Malta E, Fuller C, Hilt D, Thurmond B, et al. The ALSFRS-R: a revised ALS functional rating scale that incorporates assessments of respiratory function. BDNF ALS Study Group (Phase III). J Neurol Sci. 1999;169(1-2):13-21.
538. Medical Research Council. Aid to the examination of the peripheral nervous system. London: Her Majesty's Stationary Office; 1976. 1-2 p.
539. Mioshi E, Dawson K, Mitchell J, Arnold R, Hodges JR. The Addenbrooke's Cognitive Examination Revised (ACE-R): a brief cognitive test battery for dementia screening. Int J Geriatr Psychiatry. 2006;21(11):1078-85.
540. de Carvalho M, Swash M. Nerve conduction studies in amyotrophic lateral sclerosis. Muscle Nerve. 2000;23(3):344-52.

541. Farrar MA, Vucic S, Lin CS, Park SB, Johnston HM, du Sart D, et al. Dysfunction of axonal membrane conductances in adolescents and young adults with spinal muscular atrophy. Brain. 2011;134(Pt 11):3185-97.
542. Kiernan MC, Isbister GK, Lin CS, Burke D, Bostock H. Acute tetrodotoxin-induced neurotoxicity after ingestion of puffer fish. Ann Neurol. 2005;57(3):339-48.
543. Bostock H, Baker M, Reid G. Changes in excitability of human motor axons underlying post-ischaemic fasciculations: evidence for two stable states. J Physiol. 1991;441:537-57.
544. Bostock H, Sharief MK, Reid G, Murray NM. Axonal ion channel dysfunction in amyotrophic lateral sclerosis. Brain. 1995;118 (Pt 1):217-25.
545. Farrar MA, Park SB, Lin CS-Y, Kiernan M. Evolution of peripheral nerve function in humans: novel insights from motor nerve excitability. The Journal of Physiology. 2013;591(1):273-86.
546. Schwarz JR, Reid G, Bostock H. Action potentials and membrane currents in the human node of Ranvier. Pflugers Arch. 1995;430(2):283-92.
547. Bostock H, Rothwell JC. Latent addition in motor and sensory fibres of human peripheral nerve. J Physiol. 1997;498 (Pt 1):277-94.
548. Howells J, Trevillion L, Bostock H, Burke D. The voltage dependence of I(h) in human myelinated axons. J Physiol. 2012;590(Pt 7):1625-40.
549. Kiernan MC, Cikurel K, Bostock H. Effects of temperature on the excitability properties of human motor axons. Brain. 2001;124(Pt 4):816-25.
550. Eisen A. Clinical electrophysiology of the upper and lower motor neuron in amyotrophic lateral sclerosis. Sem Neurol. 2001;21:141-54.
551. Baker MD, Bostock H. Low-threshold, persistent sodium current in rat large dorsal root ganglion neurons in culture. J Neurophysiol. 1997;77(3):1503-13.
552. Nakata M, Baba H, Kanai K, Hoshi T, Sawai S, Hattori T, et al. Changes in Na(+) channel expression and nodal persistent Na(+) currents associated with peripheral nerve regeneration in mice. Muscle Nerve. 2008;37(6):721-30.
553. Cheah BC, Lin CSY, Park SB, Vucic S, Krishnan AV, Kiernan MC. Progressive axonal dysfunction and clinical impairment in amyotrophic lateral sclerosis. Clin Neurophysiol.123(12):2460-7.
554. Kanai K, Shibuya K, Sato Y, Misawa S, Nasu S, Sekiguchi Y, et al. Motor axonal excitability properties are strong predictors for survival in amyotrophic lateral sclerosis. J Neurol, Neurosurg & Psychiatry. 2012;83(7):734-8.
555. Stys PK. Axonal degeneration in multiple sclerosis: is it time for neuroprotective strategies? Ann Neurol. 2004;55(5):601-3.
556. Stys PK. General mechanisms of axonal damage and its prevention. J Neurol Sci. 2005;233:3-13.
557. Stys PK. Sodium channel blockers as neuroprotectants in neuroinflammatory disease: a double-edged sword. Ann Neurol. 2007;62(1):3-5.
558. Waxman SG. Axonal conduction and injury in multiple sclerosis: the role of sodium channels. Nat Rev Neurosci. 2006;7:932-41.
559. Roth G. The origin of fasciculations. Ann Neurol. 1982;12(6):542-7.
560. Mills KR. Characteristics of fasciculations in amyotrophic lateral sclerosis and the benign fasciculation syndrome. Brain 2010;133(11):3458-69.

561. de Carvalho M, Swash M. Fasciculation potentials and earliest changes in motor unit physiology in ALS. Journal of Neurology, Neurosurgery & Psychiatry. 2013.
562. de Carvalho M, Swash M. Cramps, muscle pain, and fasciculations: not always benign? Neurology. 2004;63(4):721-3.
563. Vucic S, Rothstein JD, Kiernan MC. Advances in treating amyotrophic lateral sclerosis: Insights from pathophysiological studies. Trends Neurosci. 2014:doi: 10.1016/j.tins.
564. Strong MJ, Gordon PH. Primary lateral sclerosis, hereditary spastic paraplegia and amyotrophic lateral sclerosis: discrete entities or spectrum? Amyotroph Later Scler. 2005;6(1):8-16.
565. Singer MA, Statland JM, Wolfe GI, Barohn RJ. Primary lateral sclerosis. Muscle Nerve. 2007;35(3):291-302.
566. Schule R, Holland-Letz T, Klimpe S, Kassubek J, Klopstock T, Mall V, et al. The Spastic Paraplegia Rating Scale (SPRS): a reliable and valid measure of disease severity. Neurology. 2006;67(3):430-4.
567. Mills KR, Murray NM. Electrical stimulation over the human vertebral column: which neural elements are excited? Electroencephalogr Clin Neurophysiol. 1986;63:582-9.
568. Vucic S, Cordato DJ, Yiannikas C, Schwartz RS, Shnier RC. Utility of magnetic resonance imaging in diagnosing ulnar neuropathy at the elbow. Clin Neurophysiol. 2006;117(3):590-5.
569. Le Forestier N, Maisonobe T, Spelle L, Lesort A, Salachas F, Lacomblez L, et al. Primary lateral sclerosis: further clarification. J Neurol Sci. 2001;185(2):95-100.
570. Turner MR, Agosta F, Bede P, Govind V, Lulé D, Verstraete E. Neuroimaging in amyotrophic lateral sclerosis. Biomark Med. 2012;6(3):319-37.
571. Deluca GC, Ebers GC, Esiri MM. The extent of axonal loss in the long tracts in hereditary spastic paraplegia. Neuropathol Appl Neurobiol. 2004;30(6):576-84.
572. Kuru S, Sakai M, Konagaya M, Yoshida M, Hashizume Y. Autopsy case of hereditary spastic paraplegia with thin corpus callosum showing severe gliosis in the cerebral white matter. Neuropathology. 2005;25(4):346-52.
573. Nomura H, Koike F, Tsuruta Y, Iwaki A, Iwaki T. Autopsy case of autosomal recessive hereditary spastic paraplegia with reference to the muscular pathology. Neuropathology. 2001;21(3):212-7.
574. Behan WM, Maia M. Strumpell's familial spastic paraplegia: genetics and neuropathology. J Neurol Neurosurg Psychiatry. 1974;37(1):8-20.
575. Fink JK. Progressive Spastic Paraparesis: Hereditary Spastic Paraplegia and Its Relation to Primary and Amyotrophic Lateral Sclerosis. Semin Neurol. 2001;21(02):199-208.
576. Brugman F, Veldink JH, Franssen H, de Visser M, de Jong JM, Faber CG, et al. Differentiation of hereditary spastic paraparesis from primary lateral sclerosis in sporadic adult-onset upper motor neuron syndromes. Arch Neurol. 2009;66(4):509-14.
577. Brugman F, Scheffer H, Schelhaas HJ, Nillesen WM, Wokke JH, van de Warrenburg BP, et al. Seipin/BSCL2 mutation screening in sporadic adult-onset upper motor neuron syndromes. J Neurol. 2009;256(5):824-6.
578. Geevasinga N, Menon P, Sue CM, Kumar KR, Ng K, Yiannikas C, et al. Cortical excitability changes distinguish the motor neuron disease phenotypes from hereditary spastic paraplegia. Eur J Neurol. 2015;22(5):826-31, e57-8.

579. Talman P, Forbes A, Mathers S. Clinical phenotypes and natural progression for motor neuron disease: analysis from an Australian database. Amyotrophic Lateral Sclerosis. 2009;10(2):79-84.
580. Kachi T, Sobue G, Yamada T, Tamura T, Ando K. [Central motor conduction time in the pseudopolyneuritic form of amyotrophic lateral sclerosis]. Rinsho shinkeigaku= Clinical neurology. 1991;31(9):1029-31.
581. Terao S, Sobue G, Hashizume Y, Mukai E, Mitsuma T. A clinicopathological study of the somatic motor efferents in the pseudopolyneuritic form of amyotrophic lateral sclerosis. Rinsho Shinkeigaku. 1991;31(2):163-9.
582. Kobayashi Z, Tsuchiya K, Arai T, Yokota O, Watabiki S, Ishizu H, et al. Pseudopolyneuritic form of ALS revisited: clinical and pathological heterogeneity. Neuropathology. 2010;30(4):372-80.
583. Kachi T, Sobue G, Yamada T, Tamura T, Ando K. Central motor conduction time in the pseudopolyneuritic form of amyotrophic lateral sclerosis. Rinsho Shinkeigaku. 1991;31(9):1029-31.
584. Desiato M, Bernardi G, Hagi AH, Boffa L, Caramia MD. Transcranial magnetic stimulation of motor pathways directed to muscles supplied by cranial nerves in ALS. Clin Neurophysiol. 2002;113:132-40.
585. Van den Berg-Vos RM, Visser J, Kalmijn S, Fischer K, de Visser M, de Jong V, et al. A long-term prospective study of the natural course of sporadic adult-onset lower motor neuron syndromes. Arch Neurol. 2009;66(6):751-7.
586. Terao S-i, Sobue G, Hashizume Y, Mitsuma T, Takahashi A. Disease-specific patterns of neuronal loss in the spinal ventral horn in amyotrophic lateral sclerosis, multiple system atrophy and X-linked recessive bulbospinal neuronopathy, with special reference to the loss of small neurons in the intermediate zone. J Neurol. 1994;241(4):196-203.